

A Contribution to the Synthesis of Cannabinoids

A THESIS SUBMITTED TO THE GRADUATE DIVISION OF THE
UNIVERSITY OF HAWAI'I AT MĀNOA IN PARTIAL FULFILLMENT OF THE
REQUIREMENTS FOR THE DEGREE OF

Master of Science
in
Chemistry

November 2016


By
David Francis Michael Gilles

Thesis Committee:

Marcus A. Tius, Chairperson
Thomas Hemscheidt
Matthew Cain

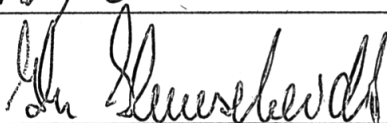
We certify that we have read this thesis and that, in our opinion, it is satisfactory in scope and quality as a thesis for the degree of Master of Science in Chemistry.

THESIS COMMITTEE



Chairperson





Acknowledgments

I preface this section by saying this is the only portion of my thesis that has been edited by myself alone. Fortunately, I waited to write this section until after I had learned just how shitty a writer I am, and had time to improve my vocabulary and the precision of my language.

As I am poised to defend this thesis I am reminded of the words of Mr. Marley: “Good friends we have, oh, good friends we’ve lost... Along the way. In this great future, you can’t forget your past.” Therefore, I ko’u no’ono’o ‘ana i ka noho ‘ana i kēia mokupuni nani maoli nō, i O’ahu, ho’opiha ‘ia au e nā hali’a aloha. Like nā ‘ike a me nā hana Hawai’i me nā aupuni mō’ī ea’e; pohihihi ‘o Hawai’i akā pa’a nō ia i nā mo’olelo o nā kūpuna. Ola au me kēia mau ‘ike waiwai o nā kūpuna: ‘o pono, kuleana a me aloha nā mea nui. Ola au i ke ola pono me ke aloha a me ke kuleana i ha’awai mai ai ia’u. Nui ka mahalo i nā kumu i a’o ia’u i kēia mau ‘ike waiwai. I Hawai’i nei, ‘o ke aloha ka mea nui, ‘o ke aloha ka mea mua: aloha ‘āina, aloha kekahi i kekahi, a aloha iho. Na ko’u mau hoa aloha a me ko’u ‘ohana i aloha nui ia’u i kēia wā kula laeo’o a aloha nui au iā lākou- ku’u ipo kekahi. I ka’u ‘ike i ke ānuenue ‘o Hawai’i, he mea ho’omana’o ia ia’u - ‘a’ohe hana nui i ke alu ‘ia. ‘O kēia ka ‘ōlelo no’eau na’u e pūlama i ka’u holomua ‘ana. Aloha.¹¹¹

I have had the honor of reading a number of theses published from the bowels of Bilger Addition, specifically from the Tius group. One thing that stands out is how grateful students are for the patience and guidance that Dr. Tius provides. Admittedly, this was always something that aroused suspicion as a fledgling chemist who still dreaded the inevitable and unwavering Saturday group meeting, but as I am at the apex of this process I see the truth in the sentiments that echo through the theses of old. Although there is an internal shitspark that has driven me to accomplish the work described within this thesis, Dr. Tius has been an Aztec fire dancer - beautifully manipulating my shitspark into a monumental shitfire storm which has accomplished more than I thought possible just a few years ago. I cannot express in words how grateful I am to Dr. Tius. Marc has been an excellent mentor and staunch confidant during my tenure in graduate school. He has helped me with countless personal trials either through discussion or example. As a mentor Marc is demanding, fair, forgiving, patient and most of all perhaps a man of his word who truly wants the best for his students. Marcus, in my opinion, may be the definition of success — his work is his love, and everyday he makes great effort to achieve perfection as a teacher, a chemist, and a mentor. I aim to be as fortunate as him someday, and with his lessons I undoubtedly will be.

I would like to acknowledge all the friends I have, and all the friends I lost during these past years. *They* say you work hard for friends and harder for enemies and I think graduate school at UH gives you plenty of reasons to work hard. *They* also say birds of a shitfeather flock together, and I would not be in a position to graduate without the support and encouragement of my fellow shitbirds, especially Josh Gurr, Julie Cramer, Charles Holjencin, Samson Souza,

Hope Sartain, Giacomo Mazzotti, Ram Nuepane, Stephen Parish, Steve Tobin, and those whom I am legally obligated not to mention — but who's deeds still give me inspiration.

I would also like to thank past and present cannabinoid chemists in the Tius group and abroad for excellent inspiration and guidance which helped in the development of this thesis. A very special thanks is given to Dr. Thanh Chi Ho and Dr. Xiaojun Huang (Tyler). I am most fond of these two, and am most grateful to for the time we shared and my initial laboratory training.

There is also a large number of professionals whom I have had the pleasure of working with and who's council has been invaluable. Dr. Francisco Lopez-Tapia and Dr. Christine Brotherton-Pleiss are irreplaceable resources for discussing the perils and mechanisms of organic chemistry and I am grateful to have worked alongside them. I'm also glad, and impressed, that they have outlasted my time in the lab. Dr. Walt Niemczura and especially Wesley Yoshida have been facets of the the first floor of Bilger Addition, and their expertise in NMR has been extremely valuable and has aided my work.

And where would anyone in the department be without Glo — Thank you Glo for making spending money so fun 🌧️💰👓.

I would like to thank other members of my committee: Dr. Thomas Hemscheidt and Dr. Matthew Cain. Your time and guidance, however infrequent, was much appreciated. This goes double for the lack of sucrose found on your words.

At long last I would finally like acknowledge the love and support I have received from Stephanie Hentschel everyday. I started graduate school with merely an interest in learning more about the fascinating science of chemistry (and as a means to continue living in Hawai'i) and as graduate school took over my life Stephanie was always there with her patience and flexibility to accommodate the demands; the moody days or weeks of unsuccessful reactions; the inside jokes that arise from observing and teaching the next generation of chemists; the often awkward conversation of those devoted to chemistry; and the cobwebs in my wallet brought on by meager wages and alcohol abuse — the latter two should soon be ameliorated. Stephanie is an infinite reservoir of love, thoughtfulness, and support that shares no equal, and has encouraged me through all the work I am to describe herein. This thesis is dedicated to you... My ku'u ipo.



Abstract

Chapter 1. Cannabis, Cannabinoids, and the Endocannabinoid System. A brief background on the discovery and pharmacology of cannabinoids and of cannabinoid receptors is described. This is complemented by a summary and comparison of the cannabinoid receptor affinities of various cannabinoid ligands, and a discussion of ligand binding assays, structure activity relationships, and ligand assisted protein structure experiments, and how data from these ligand evaluation methods guide rational ligand design. Additionally, early approaches developed for the production of synthetic cannabinoids are presented and discussed as they relate to the research conducted in the Tius group.

Chapter 2. The Total Synthesis of Ketocannabinoids Revisited. The early impediment which stalled the synthesis of target cannabinoid ligands but provided a side project that culminated in the abbreviated synthesis of ketocannabinoids is discussed. Prior published work describing the previous syntheses of ketocannabinoids is presented and the challenges encountered during their improvements are described. Notably, improvements herein are applicable to the synthesis of classical, non-classical, and hybrid cannabinoid classes, and have been demonstrated through the total synthesis of enantioenriched nabilone — a highly potent cannabinoid ligand in its own right, and whose racemate is a FDA approved pharmaceutical ingredient and arguably the most iconic ketocannabinoid.

Chapter 3. The Total Synthesis of C-9 and C-11 Functionalized Classical Cannabinoids. The total synthesis of a series of C-9 and C-11 functionalized tricyclic classical cannabinoids derived from enantioenriched nabilone is described. The synthesis of target ligands was performed primarily using simple functional group manipulations and relied upon a divergent nucleophilic displacement of organiodide intermediates. Of note are the simple reaction conditions, and benign reagents employed for these transformations. Challenges encountered during the synthesis of the eight target ligands are described as well as the

solutions employed to overcome them. The pharmacological evaluation of target ligands is now charged to our collaborators at Northeastern University — the results of which will be published following completion.

Table of Contents

Acknowledgments	3
Abstract	5
Table of Contents	7
List of Abbreviations	9
<u>Chapter 1. Cannabis, Cannabinoids, and the Endocannabinoid System</u>	14
Characteristic Terpenes found within <i>Cannabis sativa L.</i>	18
Mechoulam's Total Synthesis of (-)- Δ^9 -THC.....	22
Currently FDA Approved Cannabinoids.....	23
Discovery of the Cannabinoid Receptors.....	24
Discovery of the Endocannabinoid System	27
Ligand Binding Assays of Cannabinoid Ligands.....	27
Ligand Assisted Protein Structure Experiment.....	29
Serpentine Representation of hCB ₂	30
Definitions of the Different Cannabinoid Classes.....	31
Cannabinoid Pharmacophores and the Affects of their Manipulation	33
Targeted Cannabinoid Ligands to be Prepared	41/42
Early Synthetic Approaches to Tricyclic Cannabinoids Related to Target Ligands	43
<u>Chapter 2. The Total Synthesis of Ketocannabinoids Revisited</u>	49
Synthesis of Advanced Intermediate Triflate.....	50
Introduction of a New Project.....	51
Synthetic Targets.....	52
Analysis of Ketocannabinoids and Common Terpenic Reaction Partners.....	53
Examples of 1,4-Addition to Apoverbenone.....	56

Previous Syntheses of Apoverbenone.....	58
Attempts at the One-step Dehydrogenation of Nopinone.....	60
Attempts at the Two-step Dehydrogenation of Nopinone.....	62
Initial Attempts at Lewis Acid Catalyzed 1,4-Addition to Apoverbenone.....	65
Successful Conjugate Addition to Apoverbenone.....	66
Total Synthesis of (-)-Nabilone using Vanadyl Triflate.....	69
Extraction of Phloroglucinol Using Hot Water.....	72
Total Synthesis of (-)-Nabilone using <i>p</i> -Toluenesulfonic Acid.....	74
<u>Chapter 3. The Total Synthesis of C-9 and C-11 Functionalized Classical</u>	
Cannabinoids.....	80
Introduction.....	81
Retrosynthetic Analysis of C-11 Series..	83
Synthetic Work to Intermediate C-11 Halide	84
Synthesis of Three C-11 Target Ligands	87
Retrosynthetic Analysis of a C-11 Aldoxime	89
Reductive Amination and Dehydration of C-11 Aldehyde.....	93
Retrosynthetic Analysis of C-9 Series	95
Synthesis of Two C-9 Target Ligands.....	97
Reductive Amination and Isothiocyanation of (-)-Nabilone.....	98
Conclusion	99
<u>Experimental</u>.....	101
<u>Appendix I.</u> Spectra for Selected Compounds in Chapters 2 and 3.....	145
<u>Appendix II:</u> References and Notes.....	188

List of Abbreviations

[α]	specific rotation
Å	Angstrom
Ac	acetyl
AIDS	acquired immunodeficiency syndrome
app	apparent
aq	aqueous
BC	Before Christ
br	broadened
Bn	benzyl
BINAP	2,2'-bis(diphenylphosphino)-1,1'-binaphthyl
<i>ca.</i>	circa (approximately)
cAMP	cyclic adenosine monophosphate
calcd	calculated
cat.	catalytic
°C	degrees Celsius
CB ₁	cannabinoid receptor 1
CB ₂	cannabinoid receptor 2
log	logarithm
cm ⁻¹	reciprocal centimeters
CNS	central nervous system
δ (ppm)	chemical shift (parts per million)
d	day(s) (length of reaction time)
d	doublet

dba	dibenzylideneacetone
dd	doublet of doublets
ddd	doublet of doublet of doublets
dddd	doublet of doublet of doublet of doublets
DPPA	diphenylphosphoryl azide (diphenylphosphorazidate)
dppf	1,1'-bis(diphenylphosphino)ferrocene
dt	doublet of triplets
DMAP	4-(dimethylamino)pyridine
DMF	<i>N,N</i> -dimethylformamide
DMP	Dess-Martin periodinane
DMSO	dimethyl sulfoxide
dr	diastereomeric ratio
EI	electron impact
e.g.	exempli gratia (for the sake of example)
ELSD	evaporative light scattering detector
ESI	electrospray ionization
EtOAc	ethyl acetate
g	gram(s)
GPCR(s)	G-protein-coupled receptor(s)
GPR18	G-protein-coupled receptor 18
GPR55	G-protein-coupled receptor 55
GPR119	G-protein-coupled receptor 119
h	hour(s)
HHC	hexahydrocannabinol(s)
HMPA	hexamethylphosphoric acid triamide

HOBT	1-hydroxybenzotriazole
HPLC	high performance liquid chromatography
HRMS	high resolution mass spectrum
Hz	hertz
<i>i</i> -	iso
IBX	<i>o</i> -iodoxybenzoic acid
IC ₅₀	half maximal inhibitory concentration
IR	infrared
Pr	propyl
<i>J</i>	coupling constant
K _i	absolute inhibition constant
K _D	dissociation constant
<i>L</i> -	levorotation
LAPS	ligand-assisted protein structure
LC	liquid chromatography
LDA	lithium diisopropylamide
m	multiplet
<i>m</i> -	meta
<i>m</i> -CPBA	<i>meta</i> -chloroperbenzoic acid
M	molar (concentration)
M+	molecular ion
MHz	megahertz
min	minute(s)
mm Hg	millimeters of mercury
mg	milligram(s)

mL	milliliter(s)
mmol	millimole(s)
MOM	methoxymethyl
mp	melting point
Ms	methanesulfonyl
μL	microliter(s)
MS	mass spectrometry; or molecular sieves
<i>m/z</i>	mass to charge ratio
<i>n</i> -	normal
NaHMDS	sodium <i>bis</i> (trimethylsilyl)amide
NAG	northern aliphatic group
nm	nanometers
nM	nanomolar
N	normal (concentration)
NMR	nuclear magnetic resonance
Ns	2-nitrobenzenesulfonyl
<i>o</i> -	ortho
O.N.	overnight
<i>p</i> -	para
<i>p</i> -TsOH·H ₂ O	<i>p</i> -toluenesulfonic acid monohydrate
Ph	phenyl
PH	phenolic hydroxyl
PhNTf ₂	<i>N</i> -phenylbistrifluoromethanesulfonimide
Pyr	pyridine
q	quartet

<i>R</i>	rectus
<i>rac</i>	racemic
rt	room temperature
s	second(s)
s	singlet
<i>s</i> -	secondary
<i>S</i>	sinister
SAH	southern aliphatic hydroxyl
SAR	structure – activity relationships
SC	side chain
SM	starting material
<i>t</i> -	tertiary
TFAA	trifluoroacetic anhydride
TBS	<i>t</i> -butyldiphenylsilyl
td	triplet of doublets
TEA	triethylamine
THC	tetrahydrocannabinol
THF	tetrahydrofuran
TLC	thin layer chromatography
TBS	<i>tert</i> -butyldimethylsilyl
TMS	trimethylsilyl
Ts	toluenesulfonyl
UV	ultraviolet
wt.	weight

Chapter 1

Cannabis, Cannabinoids,
and The Endocannabinoid System

Cannabis sativa L. from the Latin *canna*, meaning reed, *bis* — in twos, and the adjective *sativa* for sown or cultivated, was aptly named.¹ For millennia, cannabis has been cultivated for its abundant and uniquely useful fiber, flowers and seeds, and ancient pottery displaying cannabis fiber imprints have been found dating back as far as 10,000 years.² While *Cannabis sativa* L. has three known species — *sativa*, *indica*, and *ruderalis* — it is most commonly referred to by colloquial terms depending on the resource for which it is grown; hemp for fiber and seeds, or marijuana for flowers (**Figure 1**).

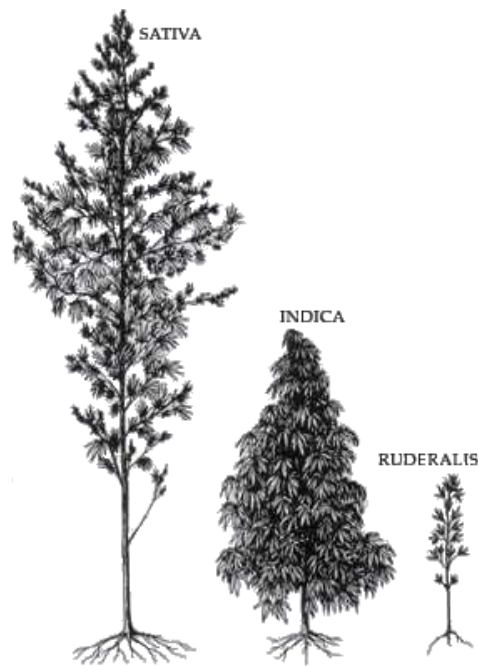


Figure 1: Depictions of the Species of *Cannabis sativa* L.

Ancient China is often referred to as *the land of silk and hemp*, and for good reason. The Chinese domesticated wild hemp and uncovered the utility of its fiber around 2800 BC.³ After proper retting,^{4a} hemp fiber was pressed to make the first paper, braided into yarn, and the yarn was then used for clothes, ropes, and bowstrings. Due to hemp's short agricultural cycle, its

fiber was readily available, and as an export helped ancient China develop into a super power. Although hemp grew naturally in many parts of Asia and India, it was not cultivated and used throughout the world until the pioneering work of the Chinese.⁵ Many countries relied upon hemp for its low cost and high strength especially for sailing canvas, rope and paper by which the written word could be spread. Hemp was brought to the Americas in the early 1600s^{6a} and was such a valuable export to England, and necessity for colonial living that ‘must grow’ taxes were enacted in Jamestown in 1619. Massachusetts and Connecticut followed this precedent in 1631 and 1632, respectively.^{6a} With technological advances in the harvest and retting of hemp, the potential uses for this fiber were all but limited by human imagination.^{4b} Cultivation of hemp in the United States, however, was outlawed in the 1930s and has only recently begun to resurge.^{6b}

Cannabis sativa’s other cultivar, marijuana, also has deep roots in celestial China. Between the legends of Fu Hsi, Shen Nung, and Huang Ti, as well as writings and artifacts of the time, historians claim marijuana has been ingested for medicinal and spiritual purposes as early as 2800 BC.^{3,5} This is further supported by a recent excavation which discovered 3 pounds of preserved marijuana in the Yanghai Tombs of the Gobi Desert dating 700 BC.⁷ Marijuana’s incorporation in traditional chinese medicine has been well documented and appears with extensive detail in the oldest known copies of *The Pen Ts’ao*’, dating 50 AD. Marijuana’s utility in chinese medicine was highlighted by its analgesic use — in combination with wine — during challenging abdominal surgeries performed by Hua T’o in the second century AD.⁵

Preparations of marijuana differ by country and time period, but traditionally the flowers of a marijuana plant are smoked or ingested, combined with other spices and ingredients into a paste such as bhang, or suspended in alcohol as tinctures. Similar preparations can be applied to the clays and creams of hashish and charas, which are the compiled resinous deposits found on the leaves and flowers of marijuana.^{8,9}

The dispersion of marijuana from central Asia followed much the same trend as hemp, and as its use spread, so did the conjecture that marijuana palliated earaches, bladder infections, memory issues, palpitating hearts, insomnia and numerous other ailments. This led to the widespread use of marijuana leading into the 19th century despite the fact that little was known about its mechanism of action. Conventional bioassays of the 1800s involved administration of marijuana to dogs, resulting in ataxia for active extracts and tinctures.¹⁰ Although canine ataxia was consistent with central nervous system (CNS) activation, little else regarding what was in cannabis, or how it worked could be determined using the tools available.

Journals and communications in the mid 1800s report physicians observing assorted, and sometimes contradictory results upon marijuana administration. The variation of results was later traced back to the country and species from which the particular hashish or marijuana extracts were produced.¹¹ Although *C. indica*, the second species of *Cannabis sativa* L., had been recognized by the late 1700s due to its differing shape, foliage, flowering and region of growth, this may have been the first distinction of the two by their medicinal qualities.¹¹ Furthermore, this hinted at the complex combination and natural variation of biologically active constituents within cannabis.¹² In fact, modern techniques of separation and isolation^{13a} applied to marijuana have resulted in the discovery of more than 420 small molecules produced by cannabis. Many of these are terpenes known for their aroma and medicinal utility, and are characteristically found in other plants (**Figure 2**).¹²

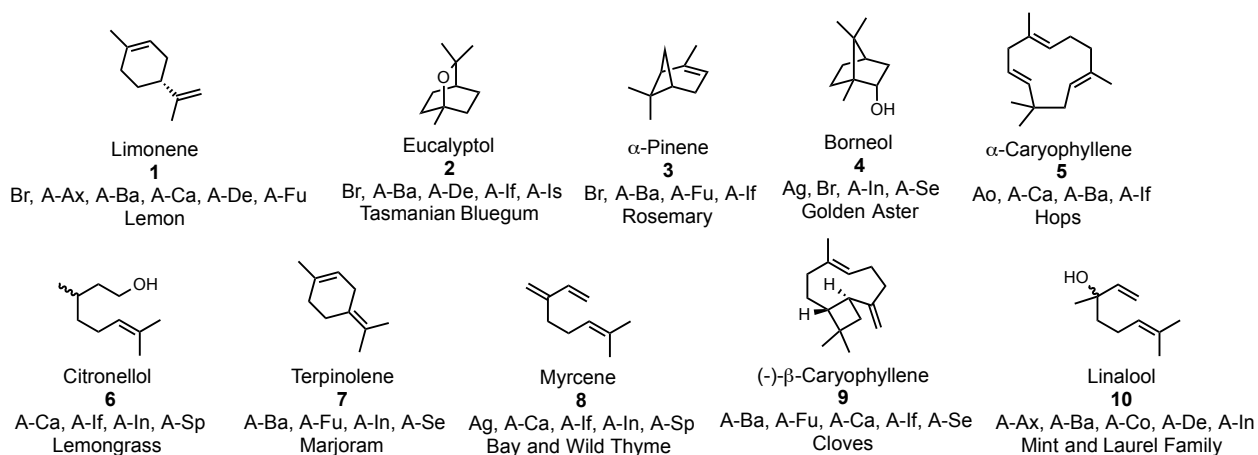


Figure 2: Therapeutic Uses and Common Origin of Major Terpenes Within Cannabis Flower
Note; **A:**Anti, **Br.:** Bronchodilator, **Ba.:**Bacterial, **If.:**Inflammatory, **Fu.:**Fungal, **Se.:**Septic,
Ca.:Cancer, **Is.:**Ischemic, **De.:**Depressant, **In.:**Insomnia, **Sp.:**Spasmodic, **Ao.:**Anorectic,
Ax.:Anxiety, **Co.:**Convulsive, **Ag.:**Analgesic

By 1899, interest in the active principles of cannabis led Wood and coworkers to distill alcoholic charas extracts under reduced pressure.¹³ This distillation produced a crude red oil, named cannabinol that was subjected to degradation studies to determine its structure. A single component was isolated and characterized as $C_{21}H_{25}O_2$, and was shown to contain a hydroxyl group. Cannabinol (CBN) thus became the first known compound intrinsically produced by cannabis, or phytocannabinoid described.¹⁴ Unfortunately, the complexity of the original charas was not detected by Wood's experiments and cannabinol would remain the only known component of cannabis for thirty years. Moreover, the active components of charas were not carried forward following distillation, which was confirmed by the greatly diminished biological activity of the red oil. Limited by the tools of the 19th century, little progress was made to further determine the components within marijuana. Ignorance of the identity of cannabis' active components put the medical field in contention during the following decades, debating the precise utility of cannabis and which species, *indica* or *sativa*, held more promise.^{11,15}

Despite the International Opium Convention of 1925,¹⁶ which put forth sanctions that led to the Marihuana Tax Act of 1937 and eventual ban of cannabis,^{6a} research of the illicit plant accelerated in the early 20th century. Cahn, in 1931, repeated the distillation of charas and isolation of CBN, and was able to propose structure **11** (**Figure 3**).¹⁷ Given the relative consistency of patient testimonials on the use of charas, and charas tinctures, as well as analytical data on cannabiniol, cannabis was presumed to have only one active component.¹⁸ However, Cahn's isolated compound did not produce the characteristic ataxia in dogs, as the original charas had.¹⁹ The mild activity of CBN surprised Cahn and his contemporaries, but the structure he outlined helped guide synthetic efforts that would eventually elucidate the structure of CBN and other phytocannabinoids.

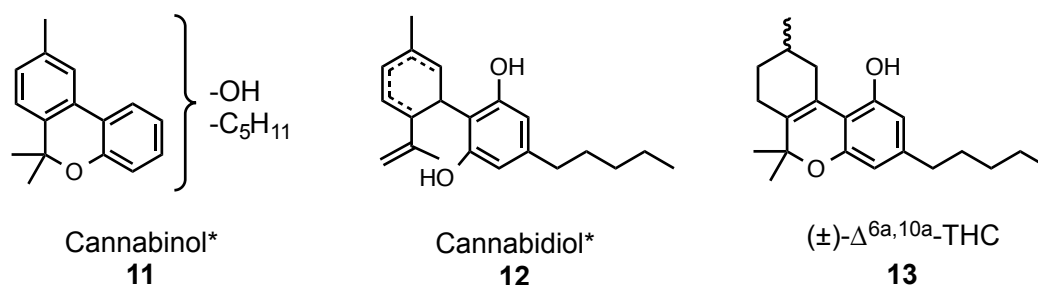


Figure 3: Proposed Structure of CBN*, CBD*, and Racemic Δ^{6a,10a}-THC

Following an uneventful decade, collaborative efforts by Levane, Todd and Adams in the early 1940s found other major constituents in marijuana.²⁰ Using partial synthesis and isolation techniques, cannabidiol (**12**; CBD*) was discovered from cannabis extracts. Through hydrogenation, two olefins were confirmed from isolated CBD* although degradation studies could not determine the position of the internal double bond. Moreover, circular dichroism experiments revealed cannabidiol extracts to be non-racemic, further complicating its

elucidation because of the potential presence of three chiral centers. Additionally, treatment of extracted cannabidiol with pyridine hydrochloride by Adams and coworkers resulted in the formation of a 'tetrahydrocannabinol' many times more potent than cannabinol or cannabidiol in canine bioassays.^{20e} This 'tetrahydrocannabinol' could also be found within charas extracts although its structure eluded its discoverers. Apace with this work, synthesis of biologically active racemic $\Delta^{6a,10a}$ -tetrahydrocannabinol (**13**; **Figure 3**) was described, and when dehydrogenated with sulfur, cannabinol was obtained. Furthermore, when extracted cannabidiol was treated with acid to provide the elusive 'tetrahydrocannabinol' and *then* oxidized, analytically pure CBN was obtained. These experiments confirmed Cahn's proposed dibenzopyran fragment (**11**) while fully elucidating the correct structure of cannabinol (**15**; **Figure 4**).^{20a,c}

Levane, upon the re-inspection of the 100-lb lump of charas that help to discover cannabidiol and the 'tetrahydrocannabinol', found that CBN was the resulting product of spontaneous decomposition. The transformation of the active constituents of charas to the inactive CBN was confirmed by prolonged exposure of charas to air or refluxing its alcoholic extracts.¹⁸ This discovery supported previous observations of declining biological activity in aging charas, hashish, marijuana, and their corresponding tinctures.²¹

The tools of the 1940s were unable to confirm the position of the double bonds, or the orientation of stereocenters within cannabidiol or the related 'tetrahydrocannabinol'.^{20d} As such, further characterization of CBD and 'tetrahydrocannabinol' was prevented until nuclear magnetic resonance (NMR) was available in the late 1950s. Following this, Mechoulam and Gaoni published a seminal paper in 1964, incorporating ¹H NMR spectroscopy into their structure elucidation. This account detailed the purification of hashish by chromatography which allowed for the isolation and characterization of three major compounds: cannabidiol **14**, cannabinol **15**, and — for the first time — Δ^9 -tetrahydrocannabinol (Δ^9 -THC, **16**; **Figure 4**).²² After administration of the three purified components of hashish to canines, Δ^9 -THC resulted in

characteristic ataxia comparable to that of the pre-purified hashish. Isolated cannabidiol and cannabinol did not produce the same CNS activation when administered to canines, thus Δ^9 -THC was identified as the major psychoactive constituent of cannabis.

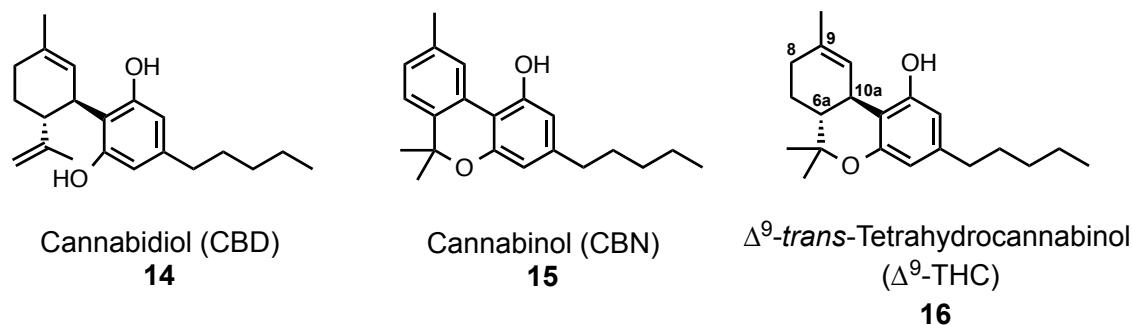
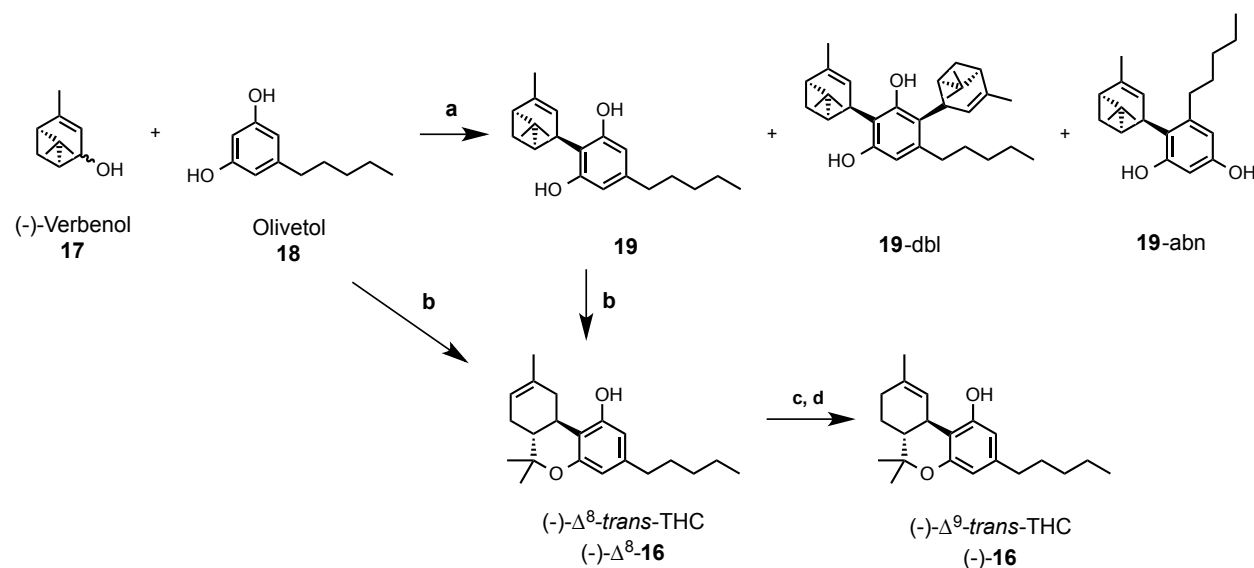


Figure 4: Constituents Within Hashish Confirmed by ^1H NMR

A year after the correct structures of **14** and **16** were described, the first total synthesis of racemic *trans*- Δ^9 -THC and CBD was carried out by condensation of olivetol and citral.²³ A synthesis which replaced citral with (-)-verbenol (**17**) followed two years later, and provided enantioenriched *trans*- Δ^9 -THC and CBD (**Scheme 1**).²⁴ The key step in this synthesis was the Brønsted acid condensation which resulted in a mixture of the desired **19**, as well as double (**19-dbl**) and abnormal (**19-abn**) addition to the aromatic ring (**a**; **Scheme 1**). The production of byproducts was later determined to be a feature of all condensations using **18**, resulting from the non-bulky *n*-pentyl chain which allows *ortho*-substitution to take place. This can be ameliorated by the one-pot condensation and *in-situ* cyclobutane ring opening of **19**, leading directly to the unnatural and thermodynamically more stable Δ^8 olefinic isomer ((-)- Δ^8 -**16**, **b**; **Scheme 1**). Isomerization of the alkene was accomplished by treatment of (-)- Δ^8 -THC with hydrogen chloride to form the C-9 tertiary halide, followed by dehydrohalogenation with sodium hydride to afford a primarily (-)- Δ^9 -THC ((-)-**16**, **c**, **d**; **Scheme 1**).

This synthesis afforded (-)-**16** in 19% overall yield using simple material and, crucially, avoided the challenging and lengthy extractions from hashish, charas, or marijuana flowers. This synthesis could be modified to produce CBD and CBN, and made it unnecessary to produce active cannabinoids from marijuana, a process that was (and is) limited by plant to plant variations in production and was challenged by the legal status of cannabis that complicated its procurement. The availability of synthetic Δ^9 -THC in its naturally occurring isomer was of particular interest to biologists and physicians attempting to determine marijuana's role and mode of action within humans. Moreover, the synthesis described by Mechoulam allowed for rapid production of synthetic analogues which could be used to further determine the role of marijuana.



Scheme 1: Stereospecific Synthesis of (-)- Δ^9 -trans-THC, (-)-**16**^a

^aReagents and Conditions: (a) *p*-TsOH·H₂O; (b) BF₃·OEt₂; (c) HCl(g), ZnCl₂ cat.; (d) NaH

Though the Controlled Substance Act of 1970 categorized cannabis as a Schedule I narcotic with "...high potential for abuse... [and] no currently accepted medical use",²⁵ clinical

trials of cannabis and Δ^9 -THC were burgeoning. Investigations of the benefits of marijuana for the treatment of alcohol dependence, glaucoma, asthma, epilepsy, cancer and chemotherapy related pain and nausea, appetite regulation, the gain or loss of weight, as well as depression took place throughout the 1970s.²⁶ Despite the social pressure engendered by the often beneficial results revealed by these studies, federal courts have consistently ruled that cannabis containing (-)- Δ^9 -THC remain a Schedule I narcotic in the US.

Perhaps influenced by the growing data from clinical trials, countries around the world began incorporating synthetic Δ^9 -THC and its analogues into their modern pharmacopeia. The utility of both (-)- Δ^9 -THC and its analogue nabilone (**20**) could not be refuted by the US for long, and were given FDA approval in 1985 for chemotherapy related nausea under the trade names Marinol® and Cesamet® (**Figure 5**).²⁸

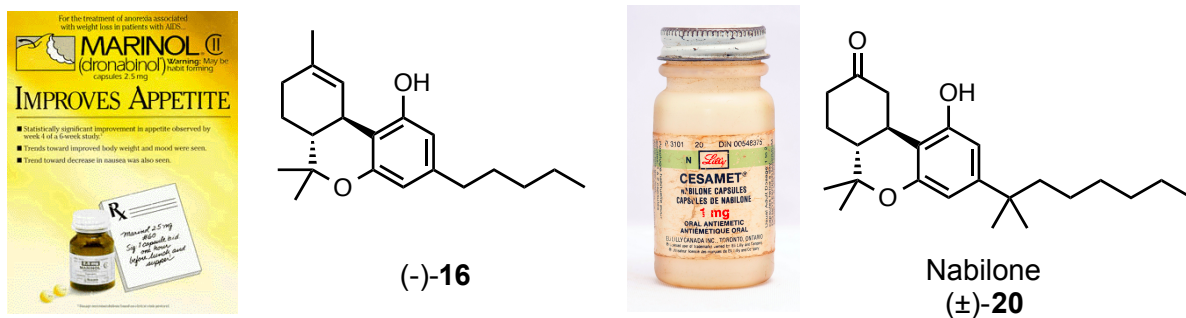


Figure 5: Currently Approved FDA Cannabinoids

At the time Marinol and Cesamet were approved for prescription use, cannabimimetic activity, or the potency of cannabis, was still measured by the traditional bioassays in dogs, monkeys and mice.¹⁰ Characteristic results from these bioassays were consistently observed, but biologists worked fervently through the 1980s to determine a less cumbersome bioassay to

evaluate the cannabimimetic activity in humans. Prior to 1984 it had been generally accepted, given the lipophilicity of cannabinoid structures and experimental evidence, that cannabinoids interact with cell membranes in a non specific manner.²⁹ This was challenged in 1984 by the work of Howlett, with material provided by Pfizer, that showed that potent synthetic cannabinoids inhibited adenylyl cyclase in neuroblastoma cells, suggesting the involvement of a guanosine-protein coupled receptor (GPCR).³⁰ In 1988, Devane in a collaboration with Howlett, showed the concentration dependent displacement of a highly potent radiolabelled cannabinoid [³H]-CP-55,940 (**21**; **Figure 6**) by Δ⁹-THC in a ligand binding assay (LBA). This confirmed a specific binding site on a protein within rat brain tissue.³¹ Further confirmation of the first cannabinoid receptor (CB₁) was given when Matsuda cloned and expressed this GPCR from rat brain in 1990,³¹ followed by the expression of human CB₁ in 1991 by Gerard.³² In 1993 Munro found, cloned and expressed a second cannabinoid receptor (CB₂) within a preparation of a human promyelocytic leukaemic cell line (HL60).³³

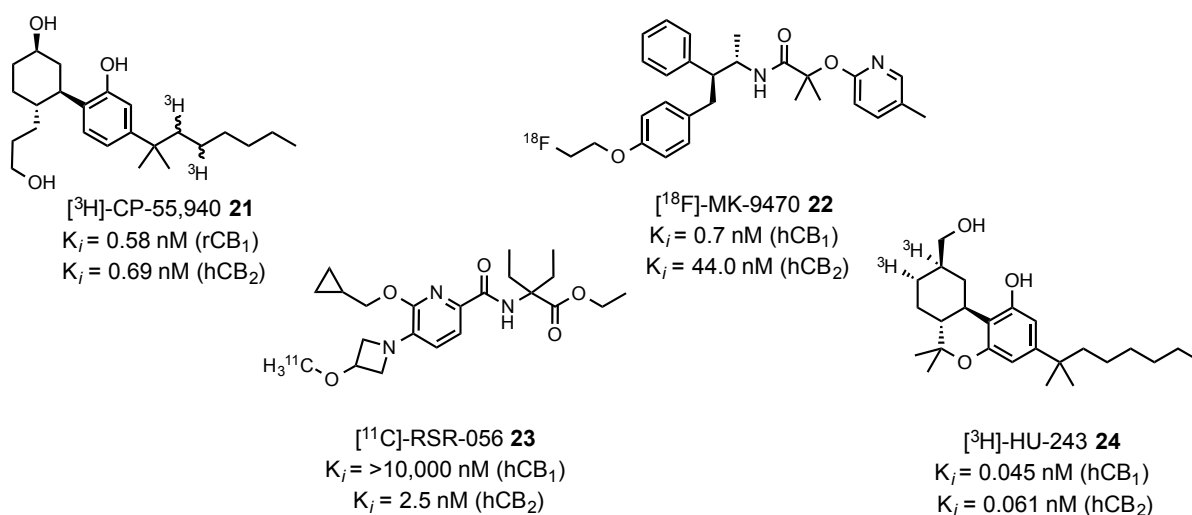


Figure 6: Radiolabelled High Affinity and Selective Tracer Cannabinoids

Note: h = human recombinant; r = rat

Following the discovery of CB₁ and CB₂, positron emission tomography (PET) was used to determine the anatomical distribution of the cannabinoid receptors. During a PET scan, a highly potent, selective, and radiolabelled cannabinoid *tracer*, such as **22** or **23** (**Figure 6**),³⁴ is administered intravenously. As tracers move through the bloodstream, the positrons emitted from radioactive isotopes are recorded and plotted. Overlay of a PET scan with computed tomography (CT) scans can then give a detailed tissue localization of positrons and therefore cannabinoid receptors.³⁵ The highest concentrations of CB₁ reside in the brain, specifically the cerebral cortex, hippocampus, cerebellum, striatum, globus pallidus, and substantia nigra — organs linked to the CNS, which is consistent with the observed cannabis and Δ⁹-THC induced psychotropic effects. This receptor is also distributed, albeit at lower concentrations, in the gastrointestinal tract, pancreas, testis, uterus, prostate, eyes, lungs, kidney, adipose tissue, and heart^{34a,35a} In a complementary fashion, CB₂ is only expressed in the brain during times of inflammation and at homeostasis is found in peripheral tissue, with high concentrations in the spleen, tonsils, immune cells, and thymus.^{34b} Very recently CB₂ has also been expressed in hippocampal principal cells.^{35c}

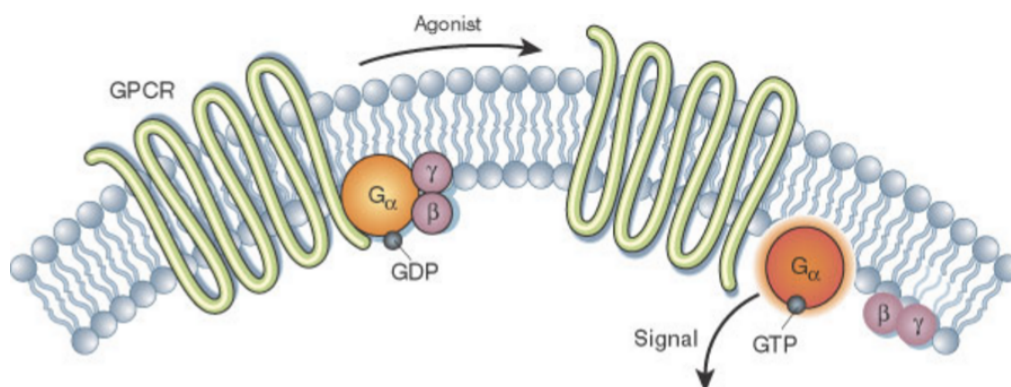


Figure 7: Agonist Activation of G_α of a Membrane Bound GPCR³⁷

Note: Activation of G_α and Release G_{βγ} Complex Lead to Distinct Downstream Effectors

Although the dissemination of cannabinoid receptors is quite different, both are GPCRs, exemplified by coupling to the subunits (G_α , G_β , G_γ) of a heterotrimeric guanosine protein, as well as the typical seven transmembrane α -helices weaving through the cell membrane (**Figure 7**).

Comparison of the amino acid sequences of CB₁ and CB₂ revealed a 44% overall, and 68% transmembrane or intracellular domain homology.³⁸ Moreover, the activation of either of these receptors by an agonist (a chemical that binds and activates a receptor to elicit a biological response) is accompanied by regulation of adenylyl cyclase. This is often observed by the regulation of cyclic adenosine monophosphate, or cAMP^{37a} and mitogen-activated proteins (MAPs), as well as the modulation of ion channels. The regulations resulting from CB₁ and CB₂ activation differ slightly,³⁸ and are modified by variations in the agonistic functionality of the cannabinoids or ligands that bind to the receptors. Cannabimimetic activity is then dependent on receptor affinity *and* whether a ligand is a full, partial, neutral, inverse, or irreversible agonist (**Figure 8**).³⁹

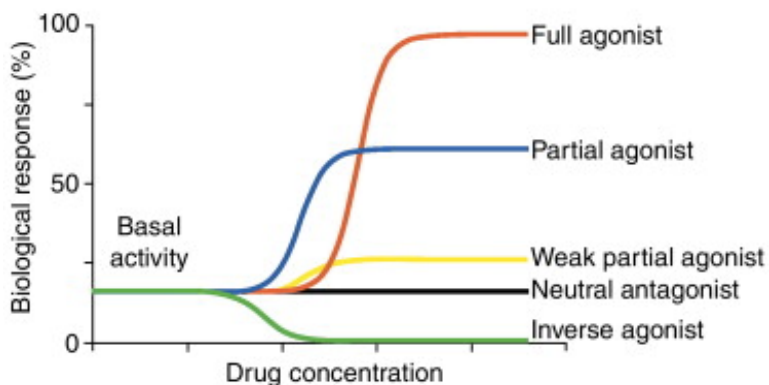


Figure 8: Depictions of Ligand Definitions According to Biological Activity
Note: Basal Activity is the Physiological Response in the Absence of a Ligand³⁹

Contemporaneously with studies that discovered CB₂, an experiment was reported in which radioligand [³H]-HU-243 (**24**; **Figure 6**) was displaced by an endogenous molecule within porcine brain. After fractionation and chromatography of 4.5 kilograms of brain, 0.6 milligrams of arachidonylethanolamine **25** (AEA) was recovered, and linked to this observation (**Figure 9**).⁴⁰ Competitive binding of endogenous, or internally biosynthesized, molecules to CB₁ was unexpected, but led to the first understanding of the existence of the endocannabinoid system (ECS). The ECS is composed of both CB₁ and CB₂, as well as the endogenous ligands, enzymes responsible for ligand metabolism, and perhaps even unidentified components.⁴¹

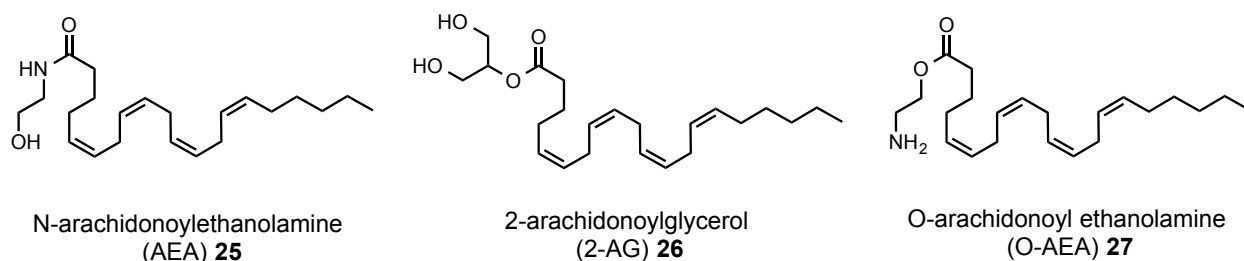


Figure 9: Various Endogenous Cannabinoids

While understanding of the ECS continues to grow, this vast lipid signaling network has been shown to regulate many aspects of embryonic development and homeostasis including immunity and inflammation, apoptosis and carcinogenesis, neuroprotection and neural plasticity, pain and emotional memory, as well as hunger, feeding, metabolism, nociception, energy balance, and cardiovascular health.⁴² Given the diversity of functions that the ECS helps regulate, cannabinoid ligands have been developed to interrogate the selective activation of these functions. To this end, preparation of novel ligands with a high level of receptor specificity and affinity has been of paramount importance for the development of drugs which influence these systems.

Ligand binding assays (LBAs) have aided in the design of new diverse and selective cannabinoids. A typical LBA uses radiolabelled cannabinoids such as [³H]-CP-55,940 or [³H]-HU-243 (**21**, **24**; **Figure 6**) called substrates, with known agonistic activity that are bound to a cannabinoid receptor. After complexation, a potential inhibitor of the radioligand — a yet unexamined cannabinoid ligand — is then introduced to the substrate-receptor complex in various concentrations. The amount of ligand incorporation, or substrate inhibition is measured by the resulting discharge of tritium labelled material. The concentration that results in a 50% reduction of substrate incorporation is designated as the IC₅₀ for the inhibitor or ligand.⁴³ Since the binding potential between radiolabelled substrates varies, the absolute inhibition constant, K_i, is derived using the Cheng-Prusoff equation (**Equation 1**).

$$(1) \quad K_i = IC_{50}/(1+[L]/K_D)$$

Equation 1: Determination of Absolute Inhibition Constant

Note; [L]: Fixed concentration of radioligand, K_D: Half maximal activation of receptor by radioligand

Even though the Cheng-Prusoff equation is only applicable if the substrate and ligand bind competitively to the same site, the resulting absolute inhibition constant is directly comparable to other ligands.⁴⁴ The process of using LBAs, though useful to determine the potency associated with a ligand, is cumbersome due to the inherent post-synthesis evaluation of ligands which leads to a type of hypothesis based methodology for targeted ligand design. For a more logical development of ligands, based on the receptor binding pockets and structural and chemical requirements for their activation, crystal structures of the cannabinoid receptors are necessary.

Since CB₁ and CB₂ are both GPCRs, crystallization of these proteins presents a challenge. Of the hundreds of diverse guanosine-protein coupled receptors known, there exist only a handful of accurate crystal structures. The challenge associated with the crystallization of GPCRs comes from their structural conformation, and more importantly, the conformation of their ligand binding pocket, which is dependent upon the cell membrane in which they reside.⁴⁵ This dependency often results in rapid conformational changes and denaturation of the protein outside of the cell membrane. This issue can usually be avoided with ligand-protein co-crystallization, but attempts to use this technique on the cannabinoid receptors has resulted in significant conformational changes.^{44a} Currently, attempts to crystallize the cannabinoid receptors are being performed with an appropriately truncated version of the proteins, potentially allowing greater stability and rigidity outside the cell membrane *without* conformational changes.⁴⁶

The crystallization issues surrounding the cannabinoid receptors have prompted the development of the ligand-assisted protein structure (LAPS) technique by Makriyannis and coworkers.⁴⁷ This experimental technique is used to obtain information about the key amino acid residues that interact with ligands. Complexation of high affinity ligands with a cannabinoid receptor, followed by covalent attachment of the ligand to the receptor, mediated by one or more reactive functional groups on the ligand, is followed by enzymatic degradation of the covalent ligand-receptor complex, resulting in the fragmentation of the protein to a number of peptides. Analysis and sequencing by mass spectrometry can then identify amino acid sites that interact with the complexed ligand. Using the primary amino acid sequence the location of the ligand binding pocket can then be determined by systematically exchanging labile amino acid residues with unreactive alternatives through site directed protein mutagenesis, the result of a series of cysteine exchanges are shown in **Figure 10**.⁴⁷

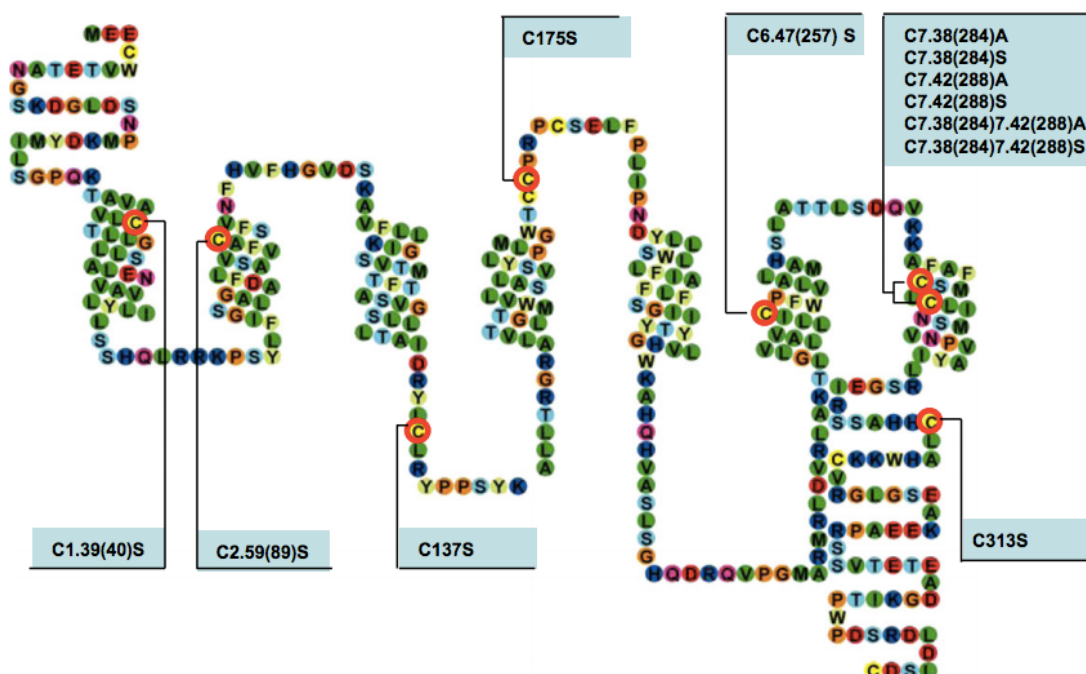


Figure 10: Serpentine Representation of Site-directed Mutagenesis Performed on hCB₂^{47c}
Note: Transmembrane Cysteine Residues Subjected to Mutation are Circle in Red

Although LAPS is challenging and does not reveal three dimensional information of the binding pocket, data obtained is used for computer modeling of the ligand-receptor complex and complemented by a ligand's structure activity relationship (SAR). Through analysis of a ligand, taking into account the 3-dimensional structure, electron density, covalent or polar functionality, steric bulk, and flexibility, as well as comparing changes in receptor affinity, SARs can help determine which feature of the ligand is responsible for a change in biological activity. This can then be combined with data obtained from LAPS, making rational drug or cannabinoid design a more systematic and logical process.

The design of unique and interesting cannabinoids is nothing new, and even before LBAs, LAPSs, SARs, and the discovery of the endocannabinoid system, rational interpretation of empirical data was used to guide the production of synthetic cannabinoid analogues. The

identification of pharmacophores, or structural features required for cannabimimetic activity, began in the 1940s with observations of cannabinoid analogues exhibiting various levels of potency. These pharmacophores were more easily interrogated in the 1970s, after the introduction of NMR and definitive structural elucidation of marijuana's active components.^{20e, 55,56} Guided by the traditional bioassays, and then by more advanced CB₁ and CB₂ ligand binding assays, distinct cannabinoid pharmacological properties have been described, and are defined within the different classes of structurally distinct cannabinoids.

Initially, cannabinoids were defined as intrinsically produced compounds obtained from marijuana, hemp, or their extracts, but now have been subsumed into the much larger context of the endocannabinoid system. A cannabinoid, defined by contemporary standards, is a compound with direct or indirect activation of one or both cannabinoid receptors. Categorized by source, there exist endogenous, synthetic, and phytocannabinoids for those prepared by the body, the human, or the plant, respectively (**Figure 11**).¹⁴

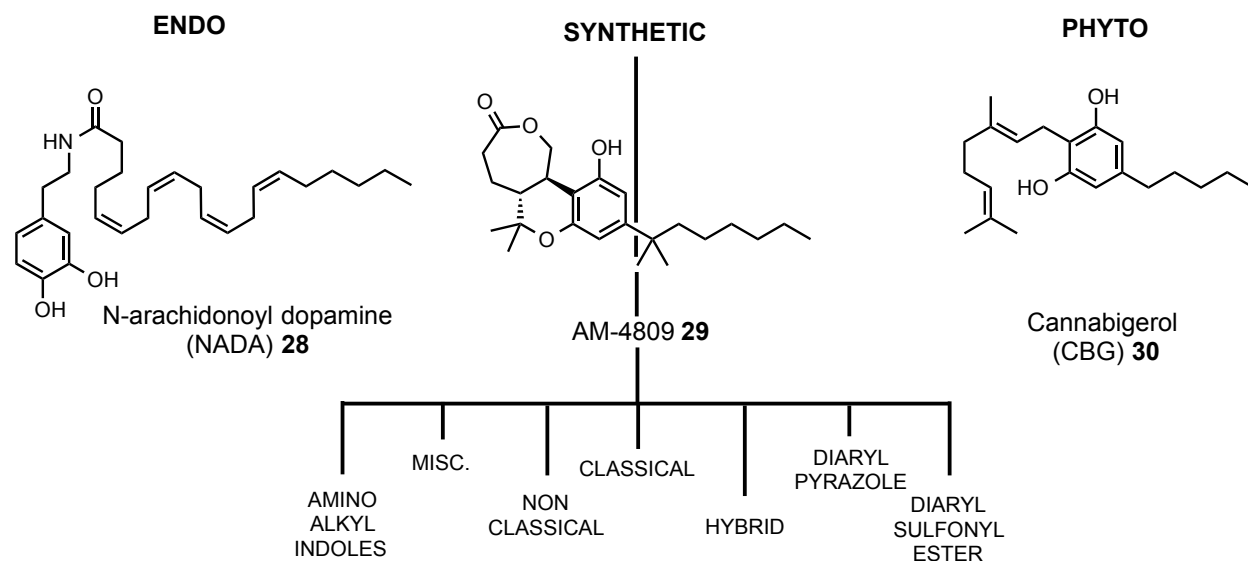


Figure 11: Classes of Cannabinoids

Since phyto- or endocannabinoids can be produced synthetically, classes based on source are not mutually exclusive. Additionally, each class contains direct ligands that bind to CB₁ or CB₂ as well as indirect ligands that influence cannabimimetic activity in some other manner, i.e. interfere with degradation pathways.¹⁴ Furthermore, ligands can interact at either allosteric or orthosteric binding sites of a cannabinoid receptor leading to various agonistic properties, creating further distinctions between cannabinoids. Subsequently, due to the large number of synthetic cannabinoids in production and being examined as novel drugs, synthetic cannabinoids have been split into sub-classes based on familiar structural features.

A number of synthetic cannabinoid classes, that bear little to no obvious structural homology with (-)-**16**, were developed by pharmaceutical companies and will be described only briefly.⁴⁸ Diarylpyrazoles represent a structural motif researched by Sanofi-Aventis.⁴⁹ Rimonabant, (**31**; **Figure 12**) is a ligand belonging to this class, and shows extremely high receptor affinity and selectivity toward CB₁. Aminoalkyl indole compounds, such as Pravadoline **32** were initially developed by Sterling-Winthrop to take advantage of the dispersion of CB₂ throughout peripheral tissue, and act as non-steroidal anti-inflammatory drugs.⁵⁰ Diarylsulfonyl ester **33** was developed by Bayer for analgesic and neuroprotective effects,⁵¹ and Japan Tobacco Company developed **34** and a number of other similar cannabinoids that act as CB₂ selective agonists.⁵²

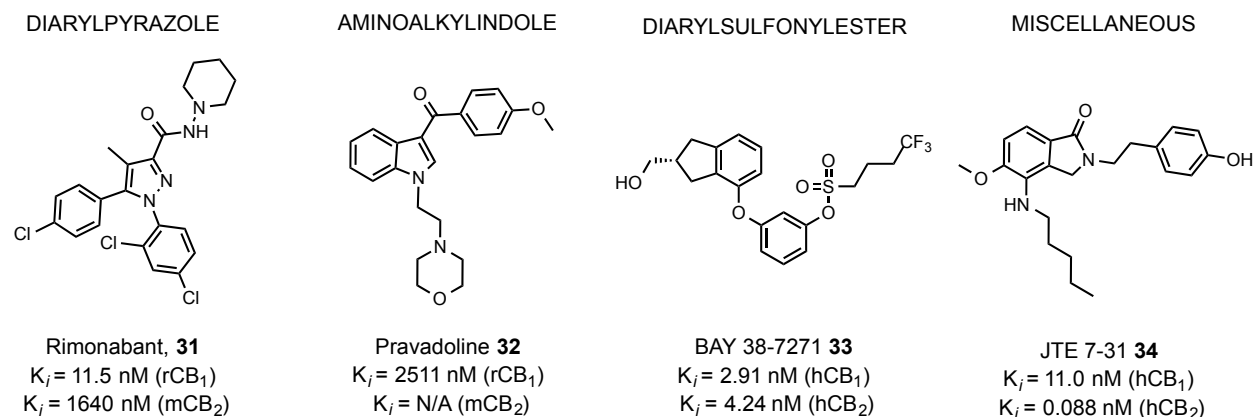


Figure 12: Structurally Diverse Synthetic Cannabinoids

Classical cannabinoids, like Δ^9 -THC, are the most recognizable class of synthetic (or phyto) cannabinoids, and are characterized by their chromane core and ABC ring system (**Figure 13**). Closely related are the non-classical and hybrid cannabinoids. Non-classical cannabinoids are defined by the open pyran B ring, typified by **36**. The open bicyclic system of non-classical analogues can then be equipped with differing functionality at carbon atoms 6a and 6. Although synthetic non-classical cannabinoids appear peculiar, they are structurally related to cannabidiol (CBD, **14**; **Figure 4**). Hybrid cannabinoids were originally described in the context of combining non-classical functionality at C-6a into a classical tricyclic skeleton.⁵⁴ This work produced the first classical/ non-classical (CC/NCC) hybrid cannabinoids, but subsequent work has explored the combination of classical cannabinoids with aminoalkyl indoles.^{54e} Classical/non-classical hybrid cannabinoid **35** exemplifies its class, with functionality extending from C-6 of the classical B ring (**Figure 13**). These three sub-classes of phyto-inspired synthetic cannabinoids share three pharmacophores: the *northern aliphatic group*, *phenolic hydroxyl*, and lipophilic or *C-3 side chain*.

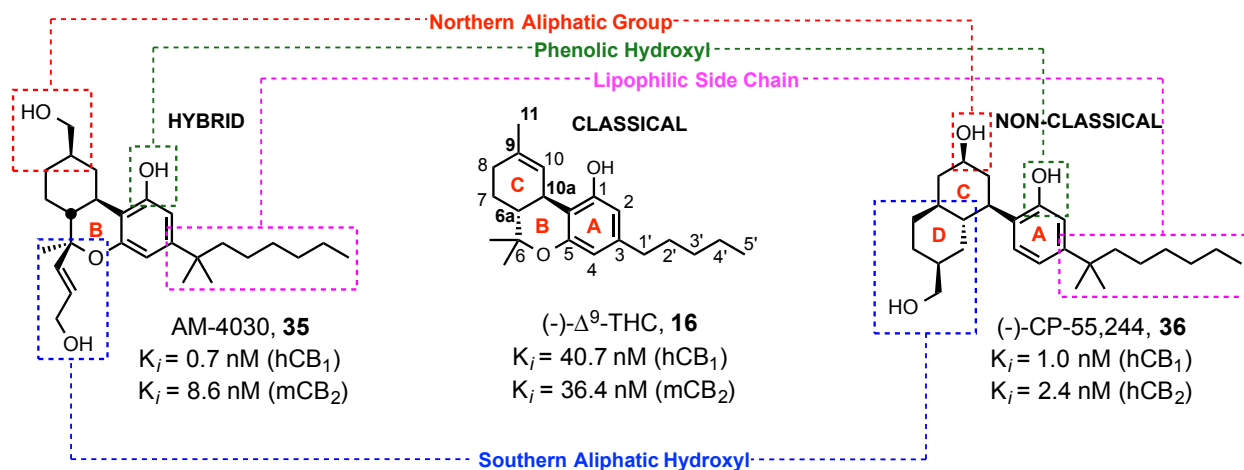


Figure 13: Pharmacophores of Classical, Non-Classical, and CC/NCC Hybrid Cannabinoids

Note: Dibenzopyran Nomenclature Shown for (-)-**16**

The *southern aliphatic hydroxyl* group is a feature shared amongst non-classical and some hybrid analogues and refers to functionality at C-6a, or C-6, other than the classical *gem*-dimethyl. The *hydroxyl* term was added after optimization of receptor affinity at Pfizer determined that an alkyl chain at C-6a with a hydroxyl group at the terminal carbon potentiated the ligand binding (Compare **38**, **39**; **Figure 14**).⁵³

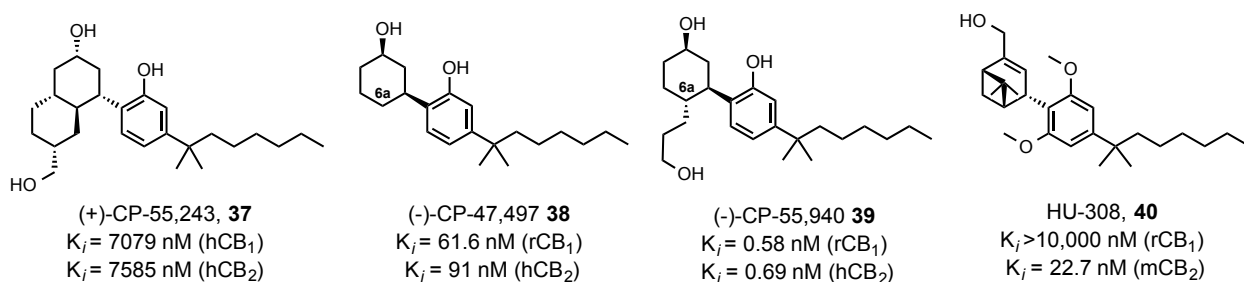


Figure 14: Various Non-Classical Cannabinoids

In the 1990s, Tius and coworkers complemented the work done at Pfizer related to **39**, and explored the conformational requirements of a southern aliphatic hydroxyl group.⁵⁴ By

also influences the potency of ligands. Interestingly, the naturally abundant Δ^9 isomers show diminished receptor affinity compared to their Δ^8 and Δ^{11} isomers (**49, 50, 51**; **Figure 16**).

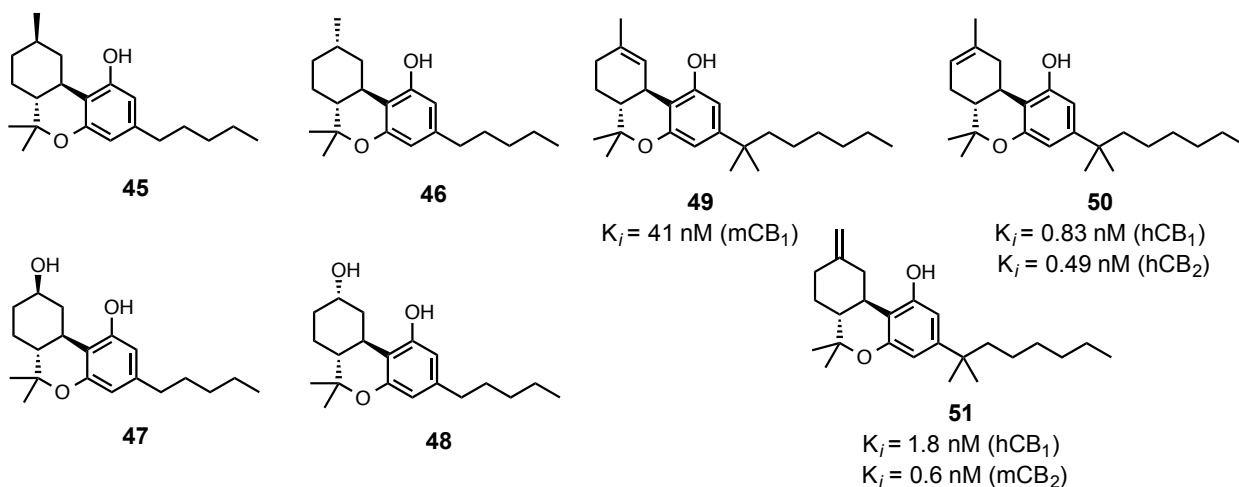


Figure 16: Illustrations of Stereochemistry at C9 and Alkene Position of Northern Aliphatic Group

A crucial feature that influences cannabimimetic activity is the BC ring junction stereochemistry. Although the B ring feature is absent in non-classical analogues, the absolute configuration at carbon atoms 6a and 10a is critical to receptor affinity in all non-classical, hybrid, and classical cannabinoids — as illustrated by the comparison of HU-210 with enantiomer HU-211 (**52, 53**; **Figure 17**).⁵⁷

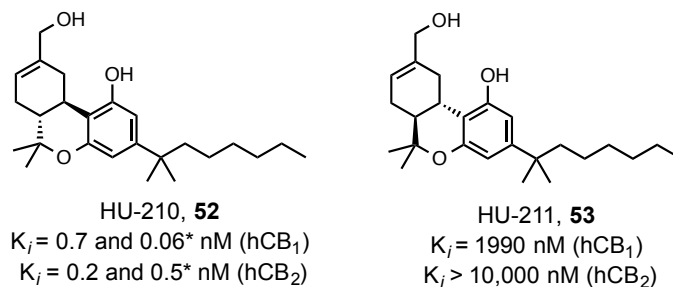


Figure 17: Illustrations of Ring Junction Stereochemistry^{57b}

The phenolic functionality at C-1 is another common pharmacophore and key to CB₁ receptor affinity. Removing or masking the phenolic hydroxyl functionality greatly reduces or abolishes ligand binding to CB₁, as a comparison of **54**, **56**, and **49** with **55**, **57** and **58**, respectively, demonstrates. (**Figure 18**).^{58,59} Interestingly, affinity to CB₂ is only slightly affected by these changes. This illustrates a major difference in the binding pockets of the two cannabinoid receptors, and serves as a basis for the development of CB₂ selective ligands.⁶⁰

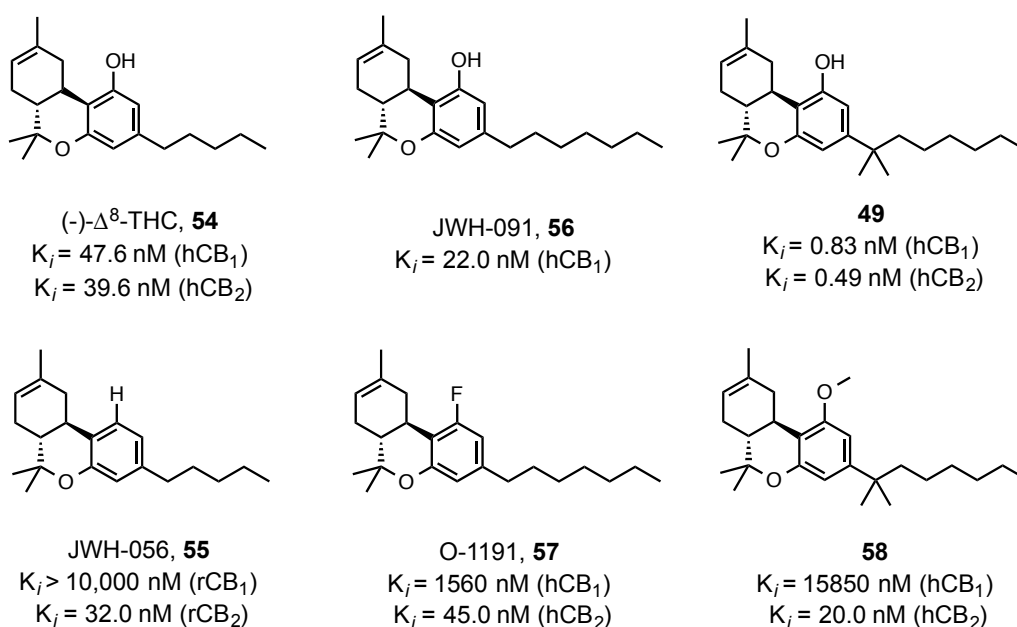


Figure 18: Replacement of Phenolic Hydroxyl and Effects on Receptor Affinity

The C-3 side chain has been extensively examined in classical, non-classical and hybrid cannabinoids, and may be the most manipulated of all the pharmacophores. The relative flexibility, length, steric bulk, electronic properties, and functional groups present have all been scrutinized and **Figure 19** serves as an abbreviated representation of the published results. Manipulations of the C-3 side chain can reveal the complexity of the cannabinoid binding pocket, but lipophilic substitution here is often accompanied by high receptor affinity.

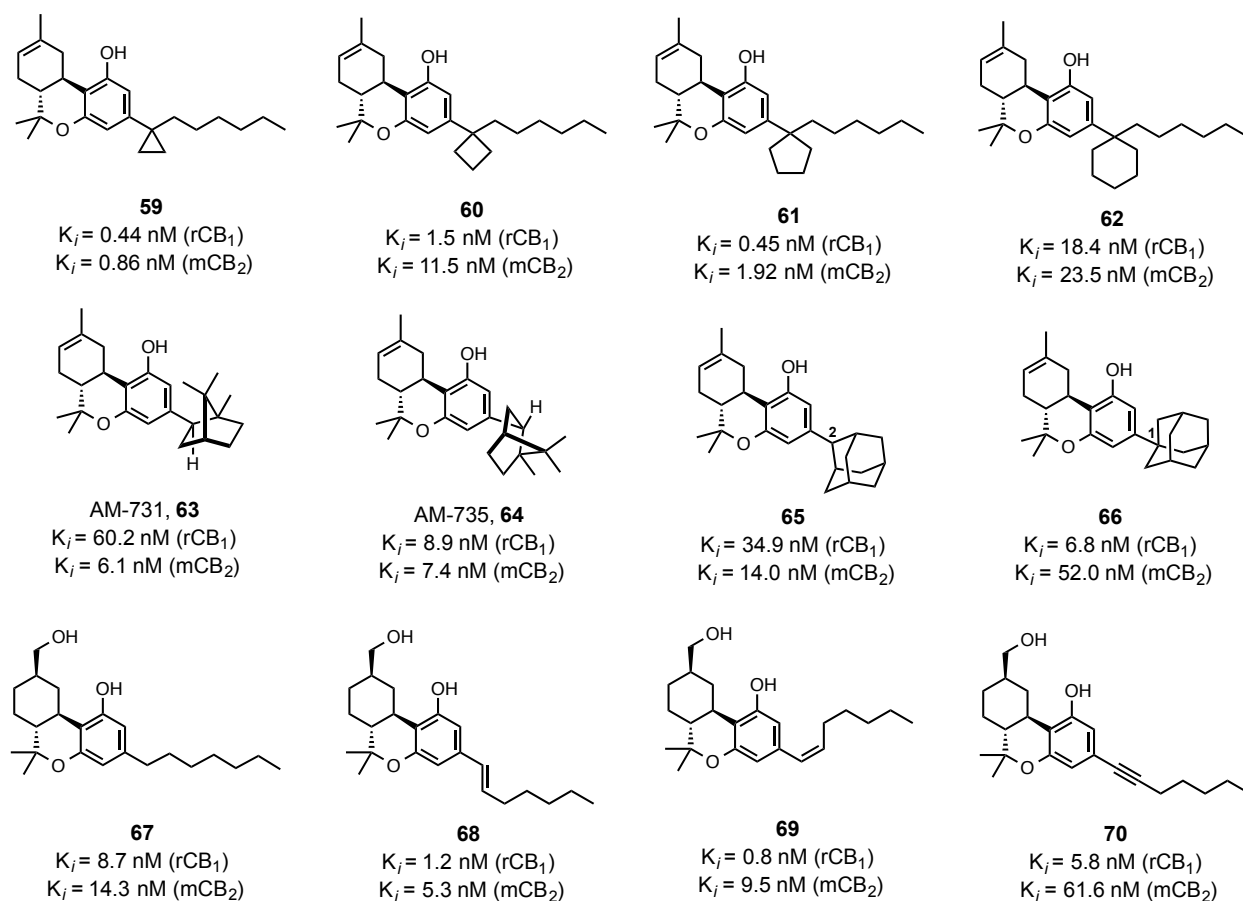


Figure 19: Increased Bulk and Unsaturation at C1' of Classical Cannabinoids

Expanding on the discovery by Adams that a dimethylheptyl side chain, as in **49**, potentiated ligand binding, a series of compounds were prepared to determine the trend between steric bulk at C-1' and receptor affinity (**59 - 62**; **Figure 19**). Increasing the bulk throughout this series modulated receptor affinity, but no drastic change or trend in potency related to C-1' bulk was borne out in the subsequent ligand binding assays (**Figure 19**).^{61a}

Following the pharmacological evaluation of **62**, the steric bulk at C-1' required for receptor activation was probed, and led to the isobornyl and bornyl derivatives **63** and **64**, respectively (**Figure 19**).^{61b} Because the large caged structures were well tolerated by CB₁ and CB₂ binding pockets, adamantyl derivatives connected at C-2 (**65**) or C-1 (**66**) were synthesized

and evaluated (**Figure 19**). Not only were the adamantyl side chains tolerated but considerable receptor selectivity was exhibited by **66**, however, the selectivity was the reverse of what had been noted for **63**.^{61c} The high receptor affinity, selectivity, and relative ease of synthesis has led to the preference for C-1 adamantyl side chains over their C-2 isomers.

The specificity of the cannabinoid receptor's binding domain is highlighted when changes to the electronics and conformational flexibility of the lipophilic side chain are made. Unsaturation between C-1' and C-2' as in **68** and **69** leads to increased receptor affinity, and receptor selectivity is also modulated by either a *cis* or *trans* alkene at this position, however, no further increase in potency is noted when C-1' and C-2' are joined by a triple bond, as illustrated by alkyne **70** (**Figure 19**).⁶²

Targeted covalent inhibitors (TCIs) represent an interesting development in cannabinoid ligands. These high affinity ligands are designed in parallel with LAPS experiments, and are equipped with reactive functional groups. Once a TCI is bound to a cannabinoid receptor, the reactive group comes in proximity to certain amino acid residues in or around the receptor's binding site. By exploiting the reactivity of proximal amino acids, covalent bonds between the cannabinoid receptor and the labile functionality of a receptor bound ligand can then be formed. This is followed by LAPS experiments and site directed mutagenesis to determine precisely which amino acids form the covalent bonds, and in turn the approximate position of the binding pocket within the receptor protein. Installation of reactive functionality on various positions of a high affinity TCI scaffold can then probe and target different amino acid residues along the cannabinoid receptor sequence.⁶³ Two major types of covalently activated cannabinoids have been employed as TCIs; those bearing electrophilic or photoactivatable functionality.

The most common electrophilic functional group used is an isothiocyanate (-NCS), which has previously been applied to the study of opioid,⁶⁴ NMDA,⁶⁵ and benzodiazepine⁶⁶ receptors. Isothiocyanates react quite slowly with water, but under physiological conditions react to form

covalent bonds with thiol, hydroxyl, or amine nucleophiles. Such is the case for **71**, which was the first CB₂ selective covalent probe that led to the discovery of cysteine C6.47(247) as a critical amino acid adjacent to the CB₂ binding pocket (**Figures 10; 20**).⁶⁷

Photoactivatable probes contain functionality with latent reactivity which permits them to access a binding pocket prior to activation. Following equilibration to form a ligand-receptor complex and photo-irradiation, reactions occur between the ligand and proximal amino acid residues. Photoactivatable probes have been used in the study of muscarine,^{68a} serotonin,^{68b} retinal receptors,^{68c} and azides (-N₃) are a commonly used photoactivatable moiety due to their ease of preparation and stability in the absence of light. Azides provide access, upon irradiation, to highly reactive intermediates which can be intercepted with a wide range of amino acid residues (**72, 74; Figure 20**).⁶⁹

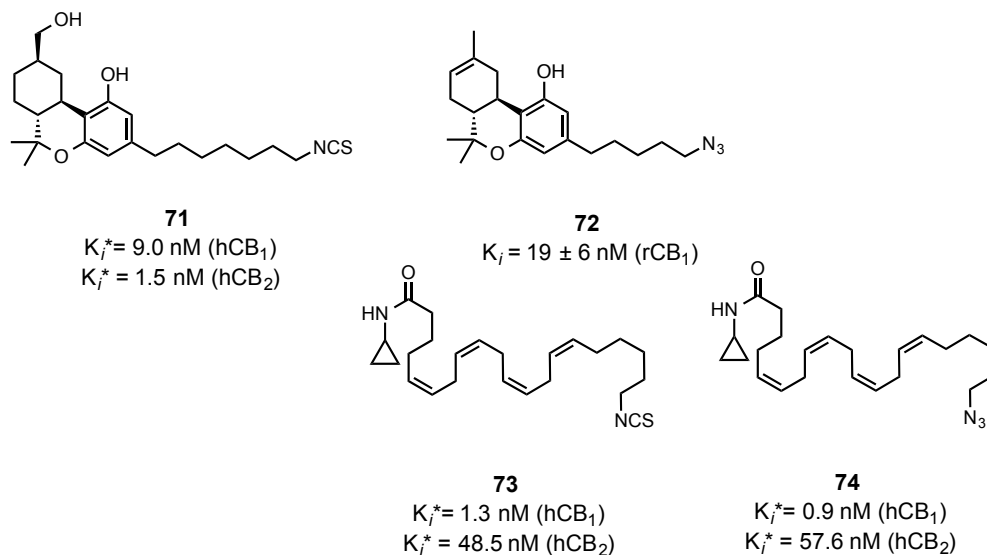


Figure 20: Covalent Inhibitors of The Cannabinoid Receptors

Ogawa prepared a number of classical cannabinoids (**77 - 81**) equipped with isothiocyanate, azide, and cyano (-CN) functionality at C-3' of an adamantyl side chain to be used as targeted covalent inhibitors (**Figure 21**).⁷⁰ Isothiocyanate and azide functional groups

confer high affinity whereas precursor amine **75** is inactive at the cannabinoid receptors. Moreover all analogues in this series show markedly higher CB₂ affinity than the unsubstituted **76**, and binding for both receptors was further potentiated when the reactive functional group was separated from the adamantyl core by a methylene group, as in **78**, **80**, and **82**. Additionally, **77** - **82** function as agonists for CB₁, but interestingly **77**, **78**, and **82** act as inverse agonists at CB₂. It is also observed that **80** and **82** are irreversible agonists, making them ideal candidates for LAPS studies. These irreversible agonists are also being employed in attempts to co-crystallize ligand-receptor complexes.⁷⁰

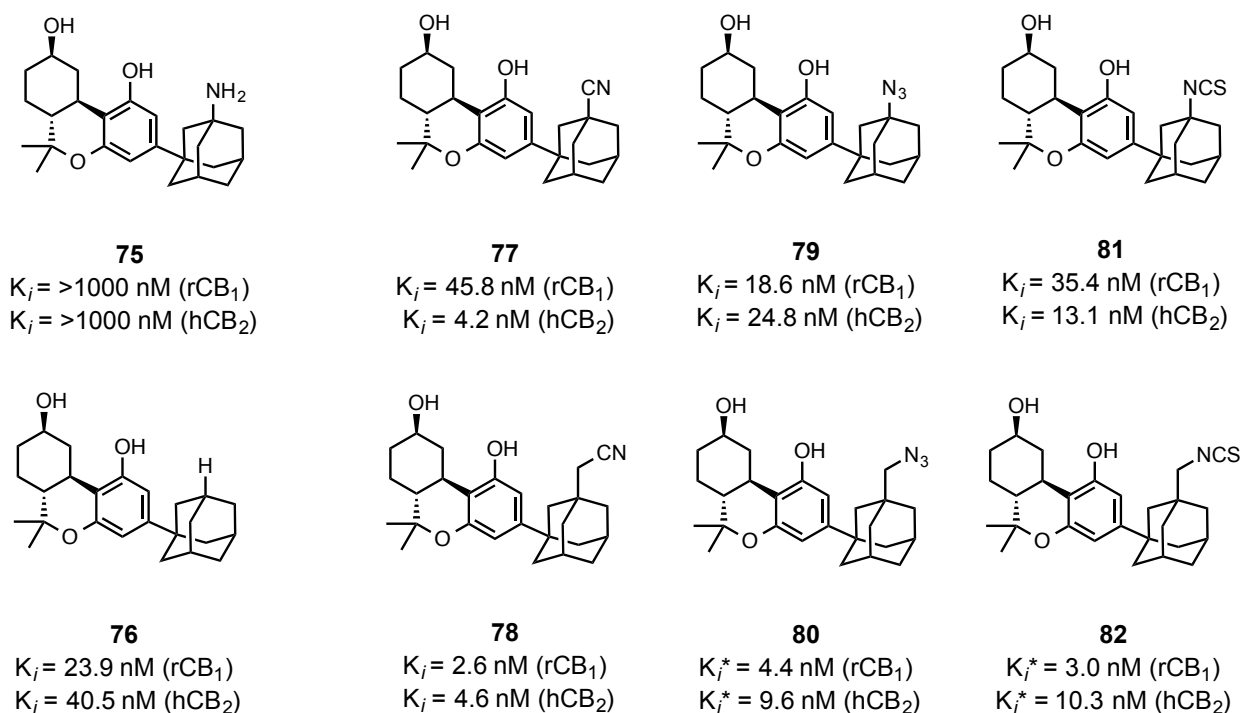


Figure 21: Classical Cannabinoid Targeted Covalent Inhibitors
Note: K_i^{*} represents apparent K_i for irreversible agonists

Spurred by the potency, agonism, and potential uses for Ogawa's ligands in LAPS and co-crystallization experiments, this thesis describes the preparation and evaluation of similar covalent probes appended at C-9 or C-11 of a classical cannabinoid scaffold (**83** - **90**; **Figure**

22). In addition to azide, cyano, and isothiocyanate functionality, nitrate esters which can be regarded as nitric oxide (NO) generators, putatively responsible for the so-called endothelial derived relaxation factor,⁷¹ have also been prepared and their pharmacology has been examined.

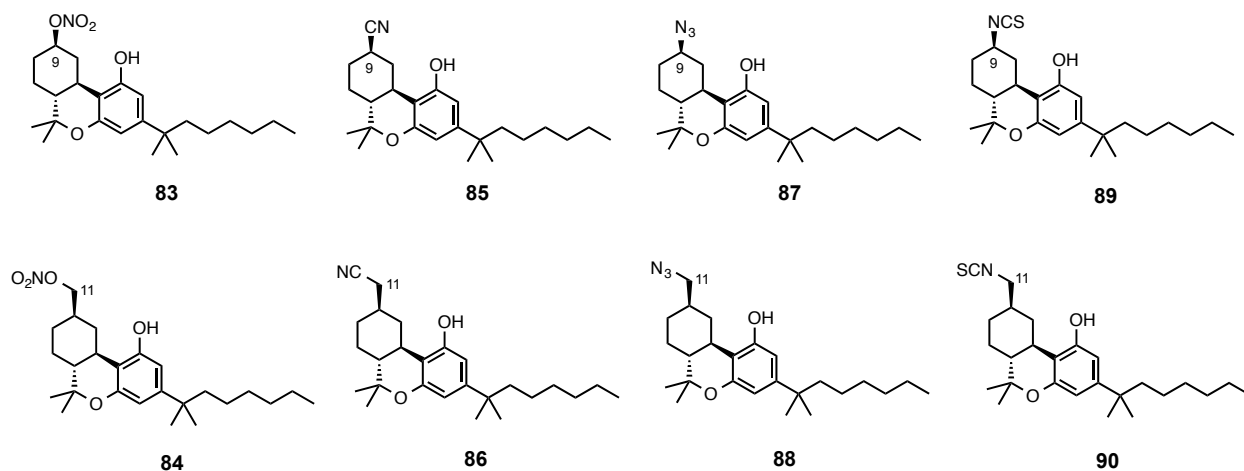
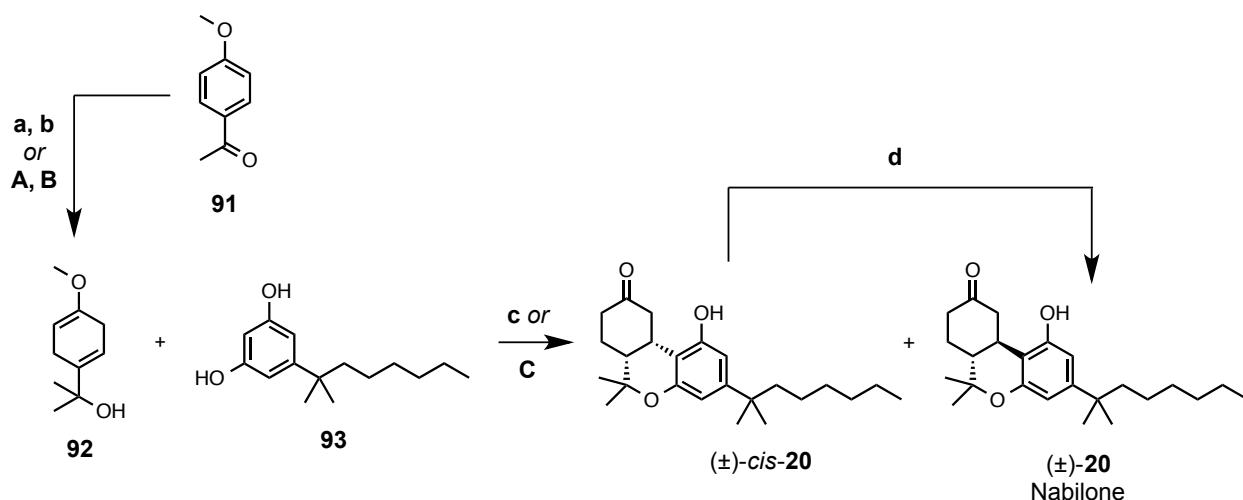


Figure 22: Cannabinoid Receptor Probes Described in Chapter 3

The synthesis of classical cannabinoids has come a long way since the work of Todd and Adams, and many clever approaches have been applied to the production of these simple tricyclic molecules. Tetrahydrocannabinol (**16**) has been prepared by means of Brønsted or Lewis acid catalyzed condensation, lithio-anion or cuprate additions, cycloaddition reactions, and even Claisen rearrangements as the key step.⁷² Recently a stereodivergent catalytic synthesis has been performed to allow selective access to the four stereoisomers of **16**.⁷³ Many of these pathways however suffer from: unsatisfactory yields; formation of C-2 and C-4 regioisomers upon terpene condensation with olivetol (see **19-dbl**, **19-abn**; **Scheme 1**); ring junction isomers at C-10a and C-6a, other than the naturally occurring *R, R* (**c**, **Scheme 2**); and difficulty avoiding the C-9 double bond isomerization to the thermodynamically more stable Δ^8 -

position (**b**, **Scheme 1**). Even after decades of synthetic effort, no single synthesis has appropriately addressed all of these issues;⁷⁴ however, **83** — **90** share a common synthetic intermediate, **20**, for which an effective, albeit flawed, synthesis was described nearly forty years ago (**Schemes 2, 3**).



Scheme 2: Total Synthesis of Racemic Nabilone^a

^aReagents and Conditions: (**a**) MeMgBr, Et₂O, 35 °C, 3 h; 94%; (**b**) Li⁰, NH₃(l), -78° C; 56% from **91**; (**c**) SnCl₄, CH₂Cl₂, 0 °C, 7 h; 89% (4.5:1 *cis:trans*); (**d**) AlCl₃, CH₂Cl₂, 0 °C, 4 h; 92% (**A**) MeMgCl, THF, 10 °C then Δ, 4.5 h; 94%; (**B**) Li⁰, NH₃(g), *t*-BuOH, THF, -10 °C; 58%; (**C**) Tf₂O, ~30/1 v/v CH₂Cl₂/H₂O, -20 °C to 0 °C; 83% (exclusively *cis*)

Note: **A, B, C** represent modifications as of 2010^{ref.76}

The synthesis of racemic and optically active nabilone was originally described in great detail by Archer and coworkers at Eli Lilly Company (**Scheme 2, 3**).⁷⁵ Racemic **20** was produced in four steps, starting from the achiral *p*-methoxy acetophenone or acetanisole **91**. Standard methyl Grignard addition followed by a slightly modified Birch reduction afforded tertiary alcohol **92** in 56% over two steps (**a, b**; **Scheme 2**). The critical condensation and cyclization reaction was performed using a large excess of SnCl₄ which was added to a mixture of **92** and dimethylheptyl resorcinol (**93**; **c**; **Scheme 2**). The initial attempts at this powerful

transformation produced low yields, but when water was used in addition to tin tetrachloride the yield of *cis*- and *trans*-(\pm)-**20** improved dramatically to 89%. Although water improved the yield of the condensation/annulation, this reaction lacked stereospecificity, which led to the formation of both *cis* and *trans* nabilone as well as their enantiomers. The complex reaction mixture was simplified by treatment with aluminum chloride in a separate step, which led to the isomerization of racemic *cis*-nabilone to its epimer *trans*-nabilone, (\pm)-**20**, in 93% yield. These four steps provided *trans*-nabilone in 45% overall yield from *p*-methoxy acetophenone (**Scheme 2**).⁷⁵

The use of large quantities of tin tetrachloride near the end of the synthesis of (\pm)-**20** is somewhat problematic. Removal of tin salt emulsions are difficult and have created experimental complications during extraction, and as racemic nabilone is intended for human consumption, the risk of tin exposure is a concern to patients as Cesamet® is often administered two or three times a day throughout the entirety of a chemotherapy cycle, greatly increasing the likelihood of tin exposure if it remains present in *trans*-nabilone.^{79b} Moreover, regulatory bodies such as the United States Food and Drug Administration (FDA), have stringent quality control guidelines for active pharmaceutical ingredients (APIs). Although tin is a Class 3 element based upon its generally low toxicity and likelihood of exposure, its inorganic salts have been linked to anemia and chromosomal damage in rats.^{79a}

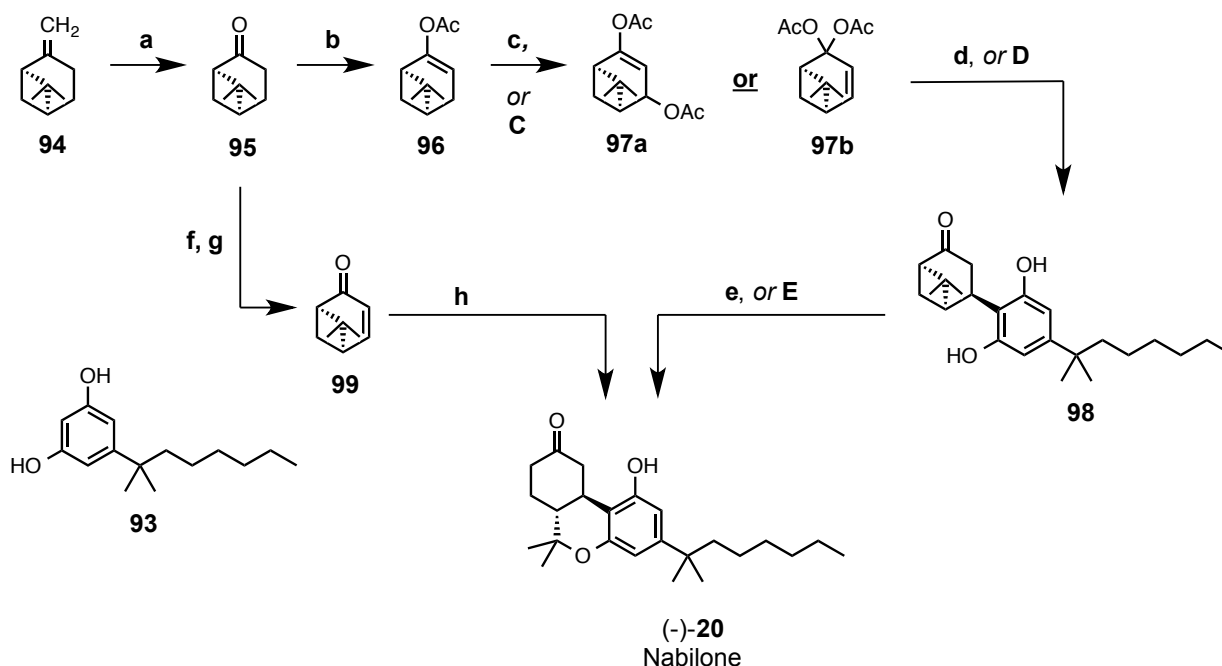
To avoid the risk of tin exposure entirely, the synthesis of racemic **20** has been amended most recently by the replacement of tin tetrachloride with triflic anhydride (**C**; **Scheme 2**). As was found by Archer when employing tin tetrachloride, the yield of the annulation/condensation using triflic anhydride could also be improved by the introduction of water to this reaction, a 3:1 mol ratio with **93** being optimal. Presumably the *in situ* generation of triflic acid is responsible for the improved yield, interestingly though, using triflic acid at the outset of annulation or triflic anhydride with a lower ratio of water (1:1 mol:mol with **93**) reduced the yield of the intermediate (\pm)-*cis*-**20** from 83% to 65% or 72%, respectively.⁷⁶ Also described in the modified synthesis of

(±)-**20** is a useful adaptation to the classic Birch reduction, in which gaseous ammonia is bubbled through the reaction medium at -10 °C to produce **92**, avoiding the use of a preparative scale -78 °C reactor as well as the risks associated with large quantities of liquid ammonia (**B**; **Scheme 2**). With these modifications, the synthesis of (±)-**20** can be performed without the use of heavy metal reagents, while increasing the overall yield by 9% on a 300 gram scale (**Scheme 2**).⁷⁶

The production of (±)-nabilone is useful, as Cesamet is administered as a racemate of *trans*-nabilone, however, for the interrogation of CB₁ and CB₂, the pharmacological properties of new ligands and their agonistic potential with the cannabinoid receptors there is a need for enantiomerically enriched material to ensure optimum ligand binding and receptor potentiation, rendering a synthesis which provides racemic **20** unsuitable for the production of synthetic cannabinoids used in biological assays. Therefore an enantioselective synthesis of (-)-**20** is the preferred method for the assembly of target ligands **83** - **90**.

Although Archer and coworkers described a number of methods for the synthesis of optically active nabilone, two were especially successful and both start from enantioenriched, inexpensive (-)-β-pinene (**94**; **Scheme 3**).⁷⁵ An impressively brief, four-step synthesis of (-)-nabilone from **94** was developed (**a**, **f**, **g**, **h**; **Scheme 3**), however, the overall yield was unserviceable, providing less than 10% of (-)-**20**. The low yield (-)-nabilone from this route was presumed to be caused by the poor reactivity of apoverbenone **99**, which led chemists to generate synthetic equivalents **97a** or **97b**. Diacetates **97** are very reactive, rendering them unstable at elevated temperatures, which contributes to the low yield of either **97a** or **97b** following vacuum distillation (**c**; **Scheme 3**). Moreover the ease with which **97a** or **97b** decompose at elevated temperatures requires their condensation with **93** to be carried out at ambient temperature lest they decompose to **99** (**d**; **Scheme 3**). After four hours at room temperature, exposure of either diacetate to a mixture of *p*-toluenesulfonic acid (*p*-TsOH) and

dimethylheptyl resorcinol produced **98**, which was isolated in 70% yield after trituration with hexanes (**d**; **Scheme 3**). Further treatment of the white crystals of **98** with *p*-TsOH in refluxing chloroform led to a 2:1 *cis:trans* mixture of (-)-**20** in 92% yield. Although *cis*-nabilone could be isomerized in a separate step to the *trans* (-)-**20** in 70% yield by treatment with aluminum chloride, a one step conversion to (-)-**20** was more practical, and treatment of **98** with tin tetrachloride provided *trans*-nabilone in 84% yield (**e**; **Scheme 3**). The five transformations from **94**, leading through either diacetate (**97a** or **97b**), that eventuate in the isolation of (-)-**20**, were originally performed in 21% overall yield and the synthesis was deemed by Archer and his contemporaries as the most convenient preparation of (-)-nabilone (**a, b, c, d, e**; **Scheme 3**).



Scheme 3: Total Synthesis of Optically Active Nabilone^a

^aReagents and Conditions: (**a**) O_3 , $\text{CH}_3\text{OH}/\text{CH}_2\text{Cl}_2$, -78°C , ii. Me_2S , -78°C to rt; 89%; (**b**) isopropenyl acetate, *p*-TsOH \cdot H $_2$ O, reflux, 6 h; (**c**) $\text{Pb}(\text{OAc})_4$, PhH, reflux; 2 h; 41% of **97b**; 18 h; 39% **97a**; yield from **95**; (**d**) **93**, *p*-TsOH \cdot H $_2$ O, CHCl_3 , rt; 70%; (**e**) SnCl_4 , CHCl_3 , rt, 16 h; 84%; (**f, g**) Bromination followed by dehydrobromination; (**h**) **93**, AlCl_3 , CH_2Cl_2 , 0°C to rt, 72 h; 16%; (**C**) $\text{Pb}(\text{OAc})_4$, PhH, gentle reflux; 2 h; (**D**) crude **97a/b**, **93**, *p*-TsOH \cdot H $_2$ O, CHCl_3 , rt; 96 h; 76% from **96**; (**E**) TMSOTf, $\text{CH}_2\text{Cl}_2/\text{CH}_3\text{NO}_2$, 0°C to rt, 3 h; 73%

Note: **C, D, E** represent improvements as of 2014^{ref77}

This synthesis of enantioenriched nabilone, just as the original synthesis of racemic **20**, leaves something to be desired — *c'est-à-dire* a high throughput synthesis void of heavy metal reagents. The use of SnCl₄ for the annulation of **98** to (-)-**20** introduces the same problem as the condensation/annulation of **92** with dimethylheptyl resorcinol during the synthesis of racemic nabilone, but unfortunately at the final step of the synthetic route (**93**, **c**; **Scheme 2**). This problem is exacerbated by the other heavy metal reagent employed to provide enantioenriched nabilone: lead tetraacetate. Organic lead compounds, when exposed to air, are known to undergo fairly rapid degradation to form persistent inorganic lead compounds which can be difficult to remove during purification. Moreover, *plumbum* is designated as a Class 1 element, with no known biological function in humans, and the exposure to lead can cause adverse neurological, reproductive, developmental, immune, cardiovascular and renal health effects. The dangers associated with lead compounds have led to FDA allowable levels of exposure 100 times more strict than those of tin.⁷⁹ The strict guidelines for pharmaceuticals and the likelihood of lead contamination in samples of (-)-nabilone may be why Cesamet® is produced and administered as a racemate, as the production of (±)-**20** does not require the use of the diacetates or lead during its synthesis.

Fortunately, the Eli Lilly synthesis of optically active nabilone has been repeatedly used over the last four decades, during which time chemists have addressed some issues encountered during the preparation of (-)-**20**. The state-of-the-art synthesis of (-)-nabilone was most recently used in 2014, during the production of **29** which features a lactone in the C ring and defines a new cannabinergic chemotype.⁷⁷ The major modifications as of 2014 include: (1) oxidation of **96** at the lowest temperature possible to avoid the decomposition of the diacetates **97**; (2) use of crude **97** for condensation, which avoids the need for distillation; (3) supplanting SnCl₄ with TMSOTf, to avoid the use of this heavy metal reagent (**C**, **D**, **E**; **Scheme 3**).⁷⁴ These three major modifications resulted in an increase in the overall yield from 21% to 28% from

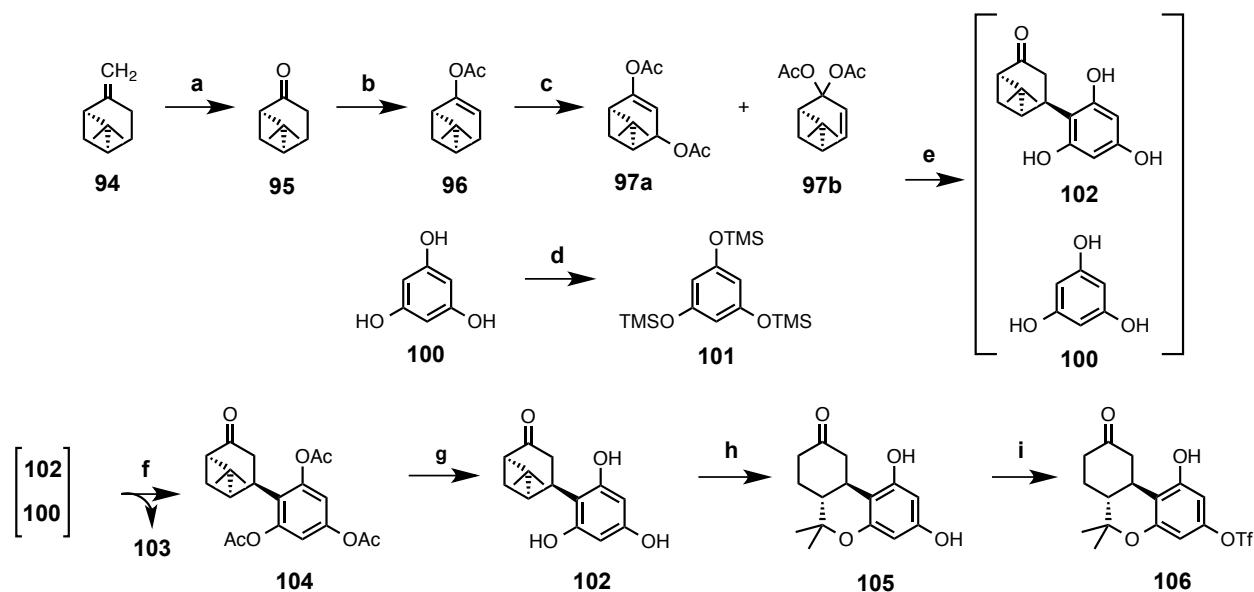
commercially available **94**.⁷⁷ Unfortunately the use of superstoichiometric lead tetraacetate is still necessary for the production of the diacetates, and no attempts to replace this toxic reagent have been reported. Furthermore, since the diacetates are required for an acceptable overall yield of (-)-nabilone, the unfortunate use of lead tetraacetate detracts from all the currently published syntheses of (-)-nabilone.

The straightforward and reproducible synthesis of (-)-nabilone, the groundbreaking activity and utility associated with its C-9 ketone, and the pharmaceutical success of its racemate, have encouraged chemists to derivatize the tricyclic cannabinoid core in hopes of discovering another molecule to add to the medical armamentarium. Moreover the skeleton of (-)-**20** provides a cannabinoid framework well suited for late stage development of new cannabinergic chemotypes and functionalized inhibitors while ensuring that biological activity is retained. For these reasons, the strategy that was developed in 1977 by Archer and coworkers for the synthesis of optically active nabilone has arguably been the most widely applied for the preparation of classical, non-classical, and hybrid cannabinoids. This is where my work began.

Chapter 2

The Total Synthesis of Ketocannabinoids Revisited

Work toward the targeted cannabinoid ligands featured in **Figure 22 (Chapter 1)** began as many synthetic projects do: Providing aid to a fellow graduate student on an analogous system. Assisting at this time Thanh Chi Ho for the synthesis of triflate **106**, the author prepared diacetates **97**, performed their condensation with persilylated phloroglucinol **101**, and cyclized trihydroxyphenyl **102** to **105** (**c, e, h; Scheme 4**).



Scheme 4: Synthesis of Advanced Intermediate Triflate **106^a**

^aReagents and Conditions: (a) O₃, CH₃OH/CH₂Cl₂, -78 °C, ii. Me₂S, -78 °C to rt; 89%; (b) isopropenyl acetate, *p*-TsOH·H₂O, reflux, 6 h; (c) Pb(OAc)₄, PhH, reflux, 2.5 h; 71% from **95**; (d) Et₃N, TMSCl, THF, 0 °C to rt, 3 h (e) *p*-TsOH·H₂O, CHCl₃/Me₂CO, 0 °C to rt, 2 h; (f) Ac₂O, Pyr, DMAP, CH₂Cl₂, rt, 12 h; chromatography; (g) KOH, CH₃OH, 0 °C, 2 h; 64% from **97** (h) TMSOTf, CH₃NO₂, 0 °C, 2.5 h; 95%; (i) PhNTf₂, Et₃N, CH₂Cl₂, rt, 14 h; 84%

Originally outlined in 2010 by Dixon and coworkers for the late stage attachment of heteroadamantyl side chains,⁷⁸ the synthesis to tricyclic intermediate **106** according to the process outlined in **Scheme 4** is perhaps the most versatile route to cannabinoid analogues. The pathway to **106** represents a modification to the Eli Lilly synthesis of enantioenriched

nabilone (**Scheme 3; Chapter 1**), and takes advantage of the regioselective triflation of **105** that was developed in this group (**i; Scheme 4**). This synthesis was the first to combine functionality at C-9 with a C-3 triflate which enables late stage introduction of the side chain, as well as providing a synthetic handle for manipulations at the northern aliphatic region.

Although useful, this route is both complicated and simplified by its aromatic component (**100; Scheme 4**). Phloroglucinol has limited solubility in CHCl_3 , the typical solvent previously used for the condensation of **97** with resorcinols. This problem was overcome by using persilylated phloroglucinol **101**, as well as a mixed solvent system which included minimal amounts of acetone. Controlling the regiochemistry of the Friedel-Crafts addition was greatly simplified by using the C_3 symmetric **101**, as abnormal addition is not an issue (see **19-abn; Scheme 1; Chapter 1**). However phloroglucinol is strongly activated toward electrophilic attack, allowing double addition to take place (see **19-dbl; Scheme 1; Chapter 1**). This is suppressed by using a two-fold excess of the aromatic fragment. However, the presence of excess **100** at the end of the reaction is problematic, due to its similar chromatographic mobility with **102**. This made it necessary to peracetylate the mixture of **100** and **102** so as to separate the resulting acetates by chromatography (**f; Scheme 4**). This process unfortunately added two steps to the synthesis of **106**, but does provide intermediate **104** which is appropriate for long term storage, in contrast to **102**, which can oxidize quite rapidly to quinone derivatives when exposed to air (**Scheme 4**).⁷⁸

Soon after work toward **106** began, lead tetraacetate, which is vital for the synthesis of **97**, came under short supply. Due to the reserve of oxidant becoming increasingly precious, work toward the synthesis of **106** was suspended. Thus a side project began, the *stóchos* of which was to devise a synthesis leading to optically active intermediates **107** — **109** that did not require the use of lead tetraacetate (**Figure 23**). The success of this project would expedite work toward targeted ligands **83** — **90** (**Figure 22; Chapter 1**), as well as abolish the toxic

heavy metal reagent that was a persistent relic of the oxidants available to chemists in 1977. Initial synthetic planning was guided by aspirations of an *ideal synthesis* which were enunciated by Hendrickson, Wender, and Gaich.⁸⁰ These aspirations were further invigorated by the opportunity to contribute to a general synthetic route that uses innocuous reagents for the preparation of diverse and new cannabinoid ligands for the investigation of CB₁ and CB₂.

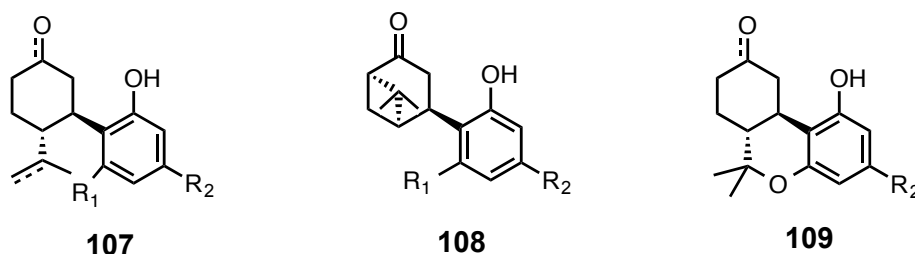


Figure 23: Optically Active General Intermediates **107 - 109**

Note: R₁ = -OH, -H; R₂ = -OH, -Alkyl, etc.

Since chemists began synthesizing cannabinoids, many dozens of synthetic routes have been described. The need for a synthetic handle at C-9 narrowed the scope of the literature reviewed to focus on routes that produced C-9 ketocannabinoids. The first synthesis of a ketocannabinoid related to **107** — **109** was described in 1966 by Fahrenholtz and coworkers.^{81a} Fahrenholtz's work utilized a ketocannabinoid as an intermediate to selectively produce racemic Δ^8 - or Δ^9 -THC, and although noteworthy, this synthesis and its subsequent improvements^{81b} are not enantioselective. Fahrenholtz's work was repeated during the total synthesis of racemic nabilone by Archer, but the synthetic route was difficult to scale up, as was the separation of stereoisomers. Another strategy for the preparation of ketocannabinoids which expanded upon the Mechoulam synthesis of enantioenriched Δ^9 -THC was described during the total synthesis of nabilone (**Scheme 1**). By starting with (-)-verbenol, Archer provided an alternate method to (-)-nabilone, but this route suffered from a low yielding photolysis reaction and was complicated

by the late stage ozonolysis that introduced the C-9 ketone. The challenges encountered during the preparation of ketocannabinoids using the strategies of Fahrenholtz and Mechoulam were overcome by utilizing oxygenated terpenes, which led to the preferred routes previously outlined for the synthesis of (-)-nabilone (**Scheme 2, 3; Chapter 1**).⁷⁵

The strategies examined during the preparation of racemic and enantioenriched nabilone have been a valuable resource for subsequent syntheses of C-9 ketocannabinoids. Based on those strategies, and related work, two things are clear: 1. the introduction of the oxygen at C-9 should come early in the synthetic route and 2. asymmetry, without the use of asymmetry inducing ligands and/or catalysts, is most efficiently introduced by means of an enantioenriched terpene. This has led chemists to the common retrosynthetic disconnection of the C-10a — C-11 bond which fragments **107** into enantioenriched monoterpene **A** and aromatic fragment **B** (**Figure 24**).⁷²

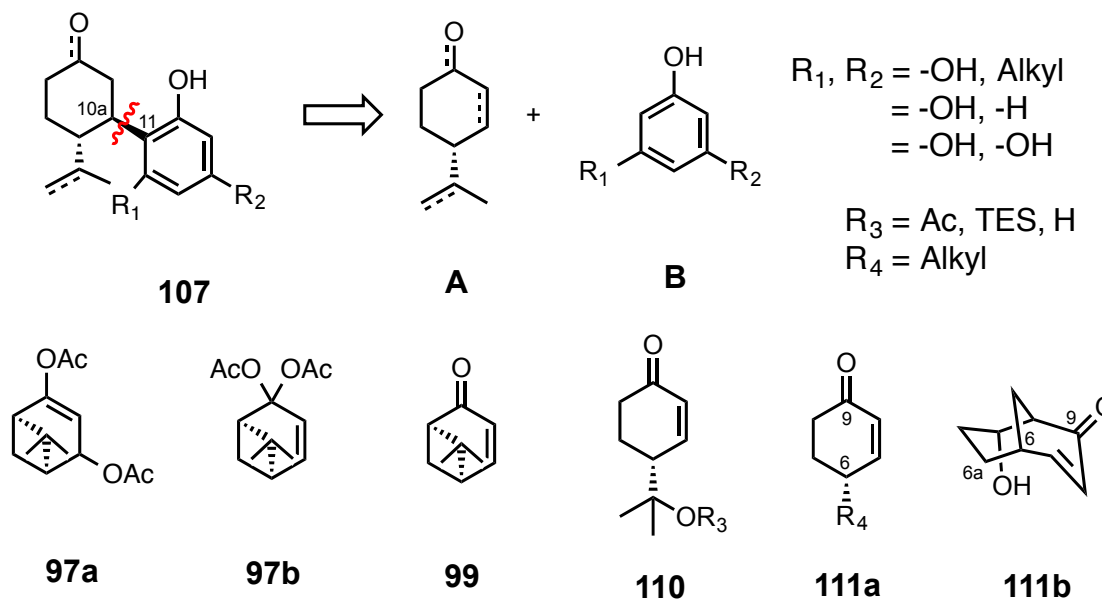


Figure 24: Retrosynthetic Disconnection of Representative Ketocannabinoid **107** and Common Oxygenated Terpenic Reaction Partners

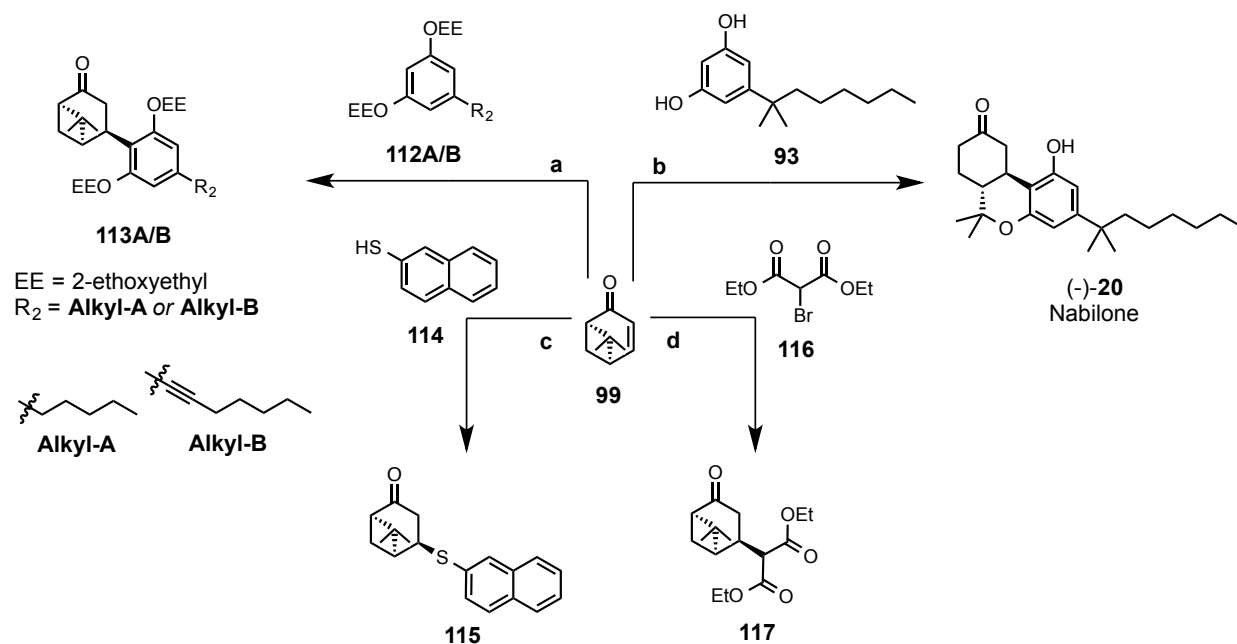
This disconnection greatly simplifies the synthesis of bi- or tricyclic ketocannabinoids, and depending upon the C-3 alkyl group of the desired ligand, the aromatic fragment **B** can be chosen from a wide range of phenols ($R_1 = -H$, $R_2 = -Alkyl$) and resorcinols ($R_1 = -OH$, $R_2 = -Alkyl$), or phloroglucinol ($R_1 = R_2 = -OH$; **B**; **Figure 24**). The achiral and planar reaction partner **B** has been combined with **A**, an oxygenated terpene, or terpene-derived partner such as the ones shown at the bottom of **Figure 24**. Any of the enantioenriched terpene-derived enones **110** ($R_3 = Ac$ or TES or H) enables the synthesis of optically active tricyclic cannabinoids. Enone **110** ($R_3 = Ac$) was most conveniently prepared by Razdan starting from bicyclic nopinone (**95**) in two steps using $BF_3 \cdot OEt_2$ and zinc acetate ($Zn(OAc)_2$) followed by a Saegusa oxidation as modified by Tsuji with allyl ethyl carbonate in the presence of $Pd(OAc)_2$, DPPE, and Bu_3SnOMe with an overall yield of 61%. The large γ substituent of **110** provides good facial selectivity during conjugate addition, and the products resulting from the condensation of **110** ($R = Ac$) with aromatic compounds are often further derivitized to provide Δ^9 -C-11 oxygenated cannabinoids. Similarly, silylated enone **110** ($R_3 = TES$) or the unprotected tertiary alcohol **110** ($R_3 = H$) provide comparable facial selectivity during the conjugate addition to its β -carbon, and can readily be cyclized to the classical tricyclic cannabinoid skeleton. However, the tertiary alcohol **110** ($R_3 = H$) or its silylated counterpart **110** ($R_3 = TES$) are prepared from **110** ($R_3 = Ac$) in two or three additional steps with an overall yield of 44% or 37%, respectively. Enone **111a** is most conveniently prepared from enantioenriched perillaldehyde, however this limits γ -substitution to isopropenyl, or isopropenyl derived alkyl substituents at R_4 . The isopropenyl group is large enough to direct conjugate addition to the natural *trans* configuration but *n*-alkyl substituents at this position lack the bulk to enforce stereoselectivity. The desire for a stereospecific condensation with **111a** ($R_4 = n$ -alkyl) led Itagaki and coworkers to prepare the masked synthetic equivalent **111b** for the preparation of nonclassical cannabinoids such as (-)-CP-55,940 (**Figure 24**).^{72c} While the caged bicycle **111b** has potential to enable the expedient

synthesis of non-classical cannabinoids, its utility for the preparation of other cannabinoid classes presents a challenge, as the formation of the dihydrobenzopyran is not possible without functionality at C-6a (**Figure 24**). Moreover, while **111b** can be prepared from commercially available 4-hydroxy cinnamate in six straightforward manipulations and provides nearly enantiopure **111b**, the overall yield is 37%.^{71d} The difficulty in procuring **110** or **111**, preparing them enantioselectively, and their variable utility in the preparation of the bi- or tricyclic cannabinoid core have led to the choice of **97** or **99** for most enantioselective ketocannabinoid syntheses.

A distinct advantage of using either the diacetates **97** or enone **99** comes from the *gem*-dimethyl substituent of the cyclobutane ring, which enforces complete facial selectivity during condensation to provide the general intermediate **108** (**Figure 23**). Moreover, subsequent intramolecular cyclobutane ring opening of **108** can be performed to furnish *either* the dihydrobenzopyran classical cannabinoid skeleton as seen in **109** *or* an isopropenyl group at C-6a, depicted by general intermediate **107**, which allows functionalization of the non-classical bicyclic scaffold, all the while maintaining the *R* absolute stereochemistry at C-6a (**Figure 23**). Additionally, the synthesis of either the diacetates or apoverbenone from nopinone is more concise than the syntheses of **110** or **111**.

Although both apoverbenone (**99**) and the diacetates (**97**) have been used to produce C-9 ketocannabinoids, the use of **99** as a terpenic unit has often been hampered by its lack of reactivity.^{72,74,75} A synthetic equivalent of **97** that retains its reactivity and precludes the use of lead tetraacetate would solve the problem of using this toxic reagent, however, devising a three step route to an enantioenriched equivalent of **97**, which is more reactive than **99**, and leads to stereospecific condensation was a challenge. An alternative chiral, non-racemic equivalent of **97** that was not derived from **97** or enone **99** was difficult to imagine which prompted a closer look at the previous syntheses of ketocannabinoids.

As described for the synthesis of optically active nabilone, **99** was combined with resorcinol **93** by the action of aluminum chloride (**b**; **Scheme 5**). Although AlCl_3 is an extremely reactive Lewis acid, and even though the yield of this step was minuscule, this experiment provided a precedent for a successful Lewis acid mediated conjugate addition to apoverbenone. Because low reactivity has been associated with apoverbenone, Lewis acids have always been used to activate it toward conjugate addition during ketocannabinoid syntheses. Moreover, the 1,4-addition of resorcinols with non-bulky C-5 side chains to apoverbenone has required higher order aryl cuprates as well as Lewis acids to obtain high yields of intermediate cannabinoids (**113**; **a**; **Scheme 5**).^{82c} Scouring the literature for other perhaps less cumbersome methods for conjugate addition to **99** provided two published reports, only one of which had been utilized for the synthesis of cannabinoids (**c**, **d**; **Scheme 5**).



Scheme 5: Representative Examples of Conjugate Addition to Apoverbenone^a

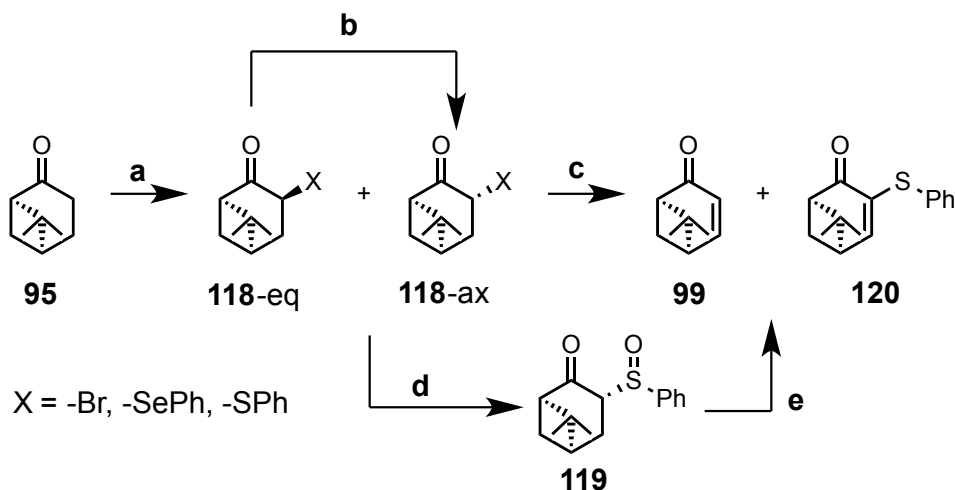
^aReagents and Conditions: (**a**) $n\text{-BuLi}$, **112A** or **112B**, THF, $\text{LiCuCN}(\text{imidazole})$; to cuprate add 1/1 **99**/ $\text{BF}_3 \cdot \text{Et}_2\text{O}$, THF, -78°C , 66% of **113A**, 55% of **113B**; (**b**) **93**, AlCl_3 , CH_2Cl_2 , 0°C to rt, 72 h; 16%; (**c**) **114**, cathodic electrolysis conditions, 0.02-0.05 F/mol; unreported yield; (**d**) **116**, In^0 , TMSCl , THF, 0.5 h, rt; unreported yield.

Diester **117** was used by Moore and coworkers for the production of heteroaromatic and pyridyl non-classical cannabinoids ligands.^{82b,c} Although this method is presumably well suited for the preparation of these particular ligands it uses exotic indium metal to perform the 1,4-addition and the yield associated with this method is not mentioned. Similarly the yield of the electrochemically^{82f} catalyzed 1,4-addition to **99** was not reported. The scarceness of published examples as well as the elaborate experimental conditions necessary for successful conjugate addition to **99** further reinforced the impression that apoverbenone is a poor Michael acceptor.

It was curious that conjugate addition to **99** appeared to be such a challenge for chemists, as all manner of enones are widely used as Michael acceptors. Given the similarity between **97** and **99** a nucleophilic conjugate addition to apoverbenone should be possible under similar conditions. Because **97** easily decomposes to apoverbenone, the presence of **99** in reaction mixtures was thought to be responsible for the low yields and long reaction times of Brønsted acid catalyzed Michael additions to **97**.^{72a,74,75,77} However, the precedent of aluminum chloride which sufficiently polarized **99** for 1,4-addition, prompted us to investigate a wider panel of Lewis acids, including ones that were unknown in the 1970s, but which could similarly activate apoverbenone. Before Lewis acids could be screened however, a more convenient route to apoverbenone was necessary.

Contemporary procedures that furnish apoverbenone start with ketone **95** and are addition-elimination methods that take advantage of the fact that nopinone can only enolize to form a single enolate that does not violate Bredt's Rule. Although useful, the addition is often non-selective, and provides an unequal mixture of diastereomers in favor of equatorial α -substitution. These diastereomers are not separated but isomerized in a separated step to afford the axial α -substituent which is antiperiplanar to one of the β -hydrogen atoms to facilitate elimination. Additionally, noxious or toxic reagents, two or more steps, and high temperatures are required to produce enone **99** via the reported pathways.⁸³

The need for **99** with high optical purity led Grimshaw and Grimshaw to extensively study and improve upon the known methods for the preparation of apoverbenone in 1972. Their work has been replicated a number of times in the last forty years and involves the bromination and dehydrobromination of nopinone to obtain **99** in 70% overall yield (**Route 1**; **Scheme 6**).^{84a} Purification and recrystallization of intermediate α -bromoketone (**118-ax**, X = Br) prior to dehydrobromination provided **99** with high optical purity following elimination. This route, although fairly straightforward is encumbered by the need to isomerize **118-eq** to **118-ax** (X = Br) with alumina so as to facilitate elimination, and by the variability of the radical bromination which can produce between 58% and 81% yield of **118** (X = Br). This inconsistency in yield is presumably due to the formation of α,α -dibromide compounds which often lead to the decomposition of **118** (X = Br).^{83,85}



Scheme 6: Classical Conversions of Nopinone to Apoverbenone^a

^aReagents and Conditions: **Route 1:** (a) NBS, CCl₄, benzoyl peroxide, reflux, 3 h; **118** (X = -Br); (b) Al₂O₃; 58% two steps; (c) **118-ax** (X = -Br), Li₂CO₃, LiBr, DMSO, 150 °C, 60 h; 74%; **Route 2:** (a) (PhSe)₂, SeO₂, MsOH; 87% of **118-ax** (X = -SePh); (c) 7.5% H₂O₂, then pyridine, CH₂Cl₂; 70%; **Route 3:** (a) LDA, PhSSO₂Ph, THF; 97%; 85:15 **118-eq**: **118-ax** (X = -SPh); (d) Using purified **118-eq** or **118-ax** or **118** (X = -SPh), *m*-CPBA, CH₂Cl₂; 99% 2:1 diastereomeric sulfoxides (e) K₂CO₃, PhMe, 120 °C, 4 h; 93%.

In 1993 Kato and coworkers described an alternate route to **99** using an addition-elimination approach. Phenylselenenylation of nopinone **95**, followed by selenoxide fragmentation provides apoverbenone in 63% overall yield (**Route 2; Scheme 6**).⁸⁶ The use of toxic and expensive selenenyl compounds for this transformation was unattractive to us in the context of the broader synthetic revision that was underway. Kato, noted that this reagent choice was not optimal, and disclosed a further improvement for the preparation of **99** five years later. This route proceeded by way of sulfenylation, isomerization, oxidation, and dehydrosulfenylation of nopinone to furnish **99** in 89% overall yield (**Route 3; Scheme 6**). Although a competing Pummerer rearrangement to form **120** was reported during dehydrosulfenylation, this could be avoided by proper purification of intermediate **119** and the reagents required for its final transformation to apoverbenone.⁸³ While these addition-elimination methods have merit, the problems associated with them discouraged their use.

Methods to dehydrogenate aliphatic ketones to enones in a single step, either by the use of stoichiometric oxidants, or catalytically, have been developed extensively in the years following Kato's work, yet their application to ketone **95** had not been described.⁸⁷ Moreover, ever since Nicolaou and coworkers in 2002 described the use of *o*-iodoxybenzoic acid (IBX, **122; Figure 25**) as an oxidant that can be tuned to convert aliphatic ketones either to enones or dienones, IBX has been commonly used for desaturating ketones. Additionally, IBX is cheap, easily handled, and effective under mild conditions and could lead to **99** directly from nopinone in a single step without the need for heavy metal reagents. Therefore, IBX was our first choice for the attempted one step transformation of **95** to **99**.⁸⁷

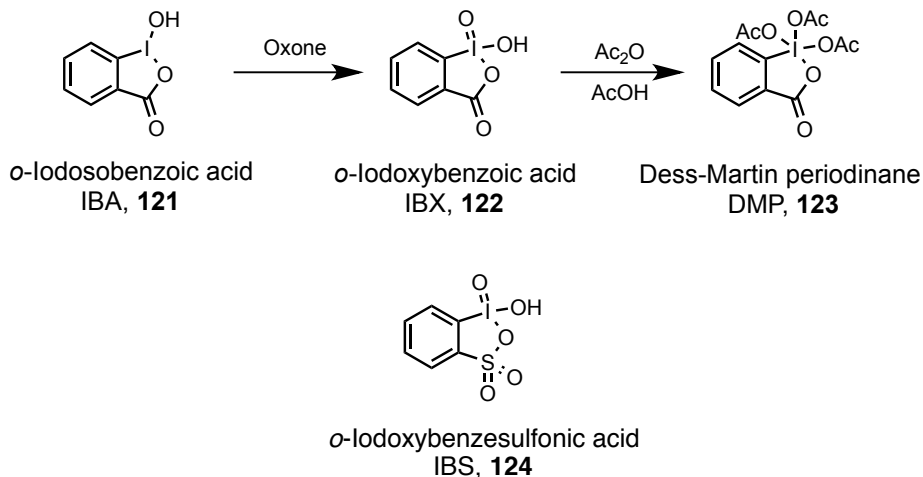
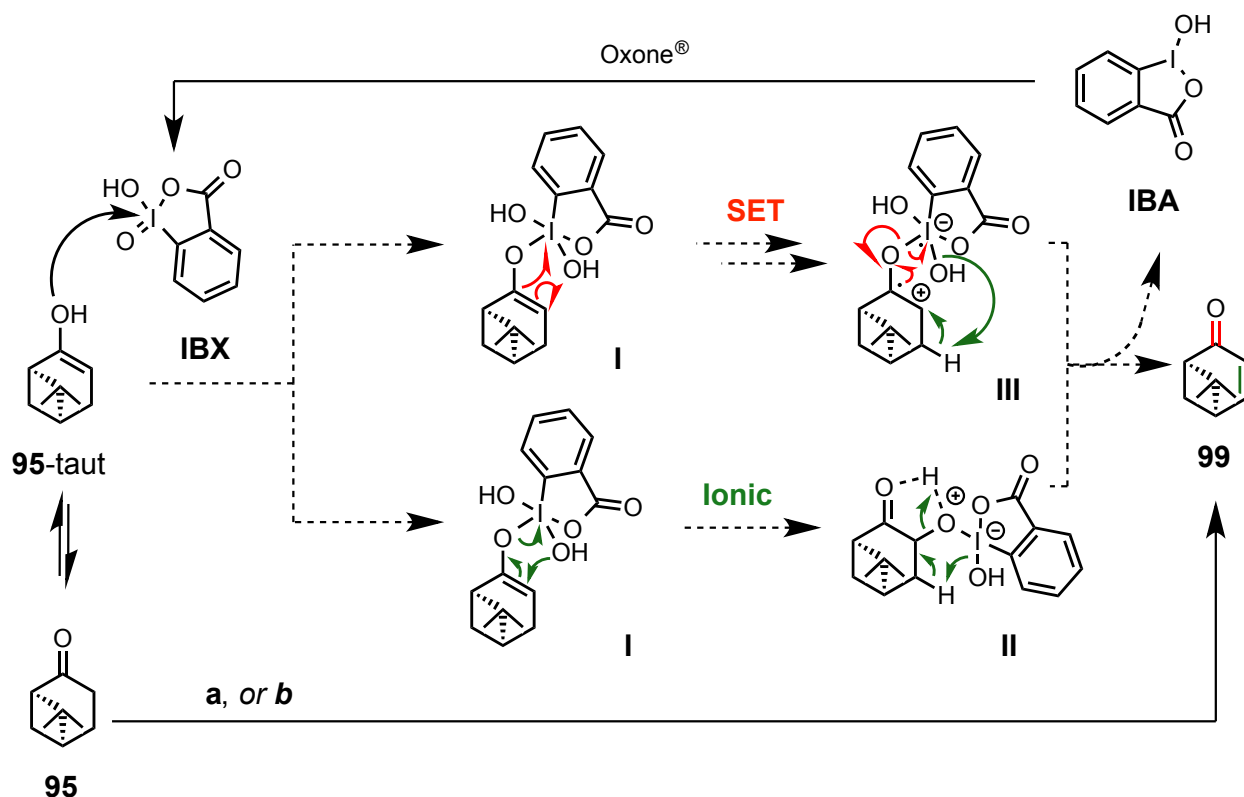


Figure 25: Common Hypervalent Iodide Species

After extensive efforts we were unable to perform dehydrogenation of nopinone using a sub-stoichiometric loading of IBX with Oxone[®] as the stoichiometric oxidant. Complete dehydrogenation of nopinone to apoverbenone using an IBX and Oxone[®] system was only achieved through the use of four equivalents of **122**, and although this represented a one step procedure, it provided an unacceptable 20% yield of **99** (**a**; **Scheme 7**). It is unclear where the material loss occurred during the dehydrogenation with IBX. Initially it was suspected that the volatility of **99** led to the decreased yield, but this was discounted when following dehydrogenation, purified **99** was concentrated with a gentle stream of nitrogen to provide similar yields to those obtained when concentration took place under reduced pressure. Suspecting that decomposition of **95** and/or **99** was taking place as a result of the use of superstoichiometric IBX and Oxone[®], we looked for a more reactive I^V reagent which could be used catalytically for this dehydrogenation.

Recently *o*-iodoxybenzenesulfonic acid (IBS, **124**; **Figure 25**), has been described by Ishihara and coworkers as a more reactive alternative to *o*-iodoxybenzoic acid.⁸⁸ In an attempt to overcome the sluggish dehydrogenation to apoverbenone by IBX, **124** was employed for the

transformation of **95** to **99**. This was also not successful, and full conversion to **99** was not accomplished during our screening of this reagent (**b**; **Scheme 7**). This result was a stark contrast to the positive control, which provided cyclohexenone from cyclohexanone in 89% yield when the latter was treated with 5 mol% IBS and stoichiometric Oxone[®] in nitromethane.



Scheme 7: Proposed Mechanism for the Dehydrogenation of Nopinone Using IBX, and One Step Dehydrogenation to Apoverbenone Using I^V Species^a

^aReagents and Conditions: **(a)** IBX, DMSO, 80 °C, 20%; **(b)** IBS, Oxone, CH₃NO₂, 80 °C, 48 h, 80% conversion

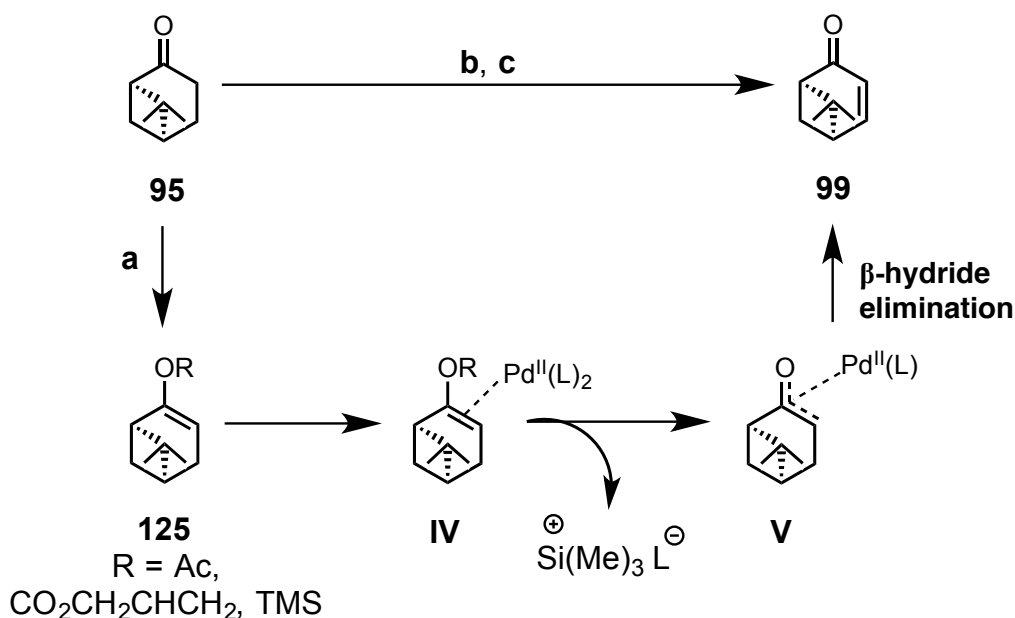
Reported examples of the dehydrogenation of ketones that use hypervalent iodine reagents have all been on substrates that are relatively more conformationally flexible and less hindered than ketone **95**. Mechanistically, the dehydrogenation of nopinone using IBX (or IBS) has been proposed to proceed through either an ionic or single electron transfer (SET) pathway

beginning with the complexation of the enol tautomer of **95** followed by proton transfer (**Scheme 7**). Additionally, during the oxidation of alcohols with IBX (postulated as an ionic mechanism), the rate-limiting step has been shown to be the *hypervalent twisting* of intermediate IBX-substrate complexes. This twisting is a coordinated motion of intermediates such as **II** and **III** driven by the necessity to generate the more stable and planar form of the byproduct IBA, **121**, which is obtained after a successful oxidation (**Scheme 7**).^{87h} Although the analogous study of the rate-limiting step during the dehydrogenation of ketones has yet to be reported, it follows that the bridged dimethyl cyclobutane ring of **95** may severely hinder the necessary rotation of intermediates **II** or **III**, resulting in the unsatisfactory yields.

An unfortunate and complicating aspect of the one step dehydrogenation of **95** to **99** stems from the similarity of the starting material's physical properties with those of apoverbenone. The chromatographic mobilities of **95** and **99** are so similar that a one step procedure can't be monitored by thin layer chromatography (TLC), requiring the inconvenient use of ¹H NMR, MS, or IR to assess its progress. Furthermore, if the dehydrogenation was incomplete, the isolation enone **99** by flash chromatography or distillation provided negligible separation — entraining ketone starting material within the product. The failure of the iodine reagents to produce **99** in acceptable yield led us to examine two step procedures for the oxidation of **95**.

The first thought for a two step process was a Saegusa-Ito oxidation that proceeded through enol ester or a trialkylsilyl enol ether of **95** (**125**; **Scheme 8**). Modifications to the standard Saegusa oxidation by Tsuji could be applied to acetate **125** (R = Ac; **Scheme 8**; also **96**; **Scheme 4**). However, this modification requires the use of tributyltin methoxide to provide the tin enolate intermediate (**IV**, R = SnBu₃), which is necessary for transmetallation with a π -allylpalladium complex generated *in situ* to afford intermediate **V** (L = allyl) which subsequently undergoes the desired β -hydride elimination (**Scheme 8**). Even though this method would use

the mono-acetate **96** that had been prepared in our group, the application of a toxic tin reagent was unattractive. An alternative modification, also by Tsuji, employs an allyl enol carbonate (**125**; R = CO₂CH₂CHCH₂) to generate the same intermediate **V** (L = allyl) without the use of tributyltin methoxide. This method has been used to prepare enones in good yields, and **125** (R = CO₂CH₂CHCH₂) would presumably be isolable and possess much different chromatographic mobility than that of **95** or **99**, allowing for a straightforward stepwise oxidation.



Scheme 8: Saegusa-Ito Oxidation of Nopinone^a

^aReagents and Conditions: (a) see text; (b) LDA, TMSCl, -78 °C to 0 °C, 1 h; [provides crude **125** (R = TMS)] (c) cat. Pd(OAc)₂, DMSO, O₂, rt, 36 h; 85% from **95**

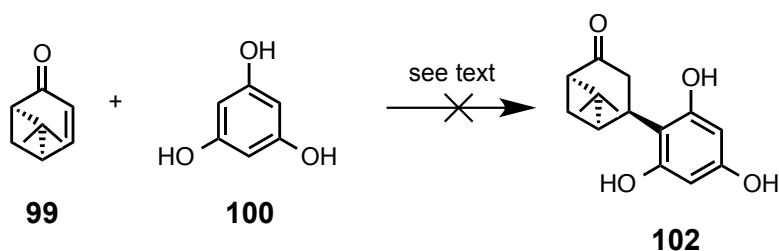
Treatment of **95** with LDA followed by allyl chloroformate provided **125** (R = CO₂CH₂CHCH₂) in 92% yield after chromatography. However, boiling **125** (R = CO₂CH₂CHCH₂) in acetonitrile with stoichiometric palladium acetate and 1,2-*bis*-(diphenylphosphino)ethane (dppe) produced no observable enone **99**, and the majority of allyl enol carbonate was recovered from the reaction unchanged. This failure was peculiar, given the substrate scope

presented by Tsuji and success of the positive control, which afforded cyclohexenone in 76% overall yield from cyclohexanone. However, recovery of allyl enol carbonate **125** ($R = \text{CO}_2\text{CH}_2\text{CHCH}_2$) was not altogether unexpected following the unsuccessful dehydrogenation of **95** using iodine reagents. The recovery of **125** ($R = \text{CO}_2\text{CH}_2\text{CHCH}_2$) after its attempted oxidation suggested that intermediate **IV** was forming either reversibly or not at all, and that under these conditions the coordination of palladium to provide intermediate **V** was not occurring (**Scheme 8**). This led us to trap the enolate of **95** as a silyl enol ether (**125**; $R = \text{TMS}$), which has been shown to form oxa- π -allylpalladium complexes such as **V** ($L = \text{OAc}$) under mild conditions, which following dehydrosilylation affords enones in excellent yields.⁸⁹

Silyl enol ether **125** ($R = \text{TMS}$) was prepared by the treatment of nopinone with LDA followed by trimethylsilyl chloride in nearly quantitative yield (**a**; **Scheme 8**). In order to avoid heating **125** ($R = \text{TMS}$) and aspiring to use only catalytic palladium, the modifications to the Saegusa reaction that were described by Larock and coworkers were applied.^{89c} Replication of Larock's method by treatment of **125** ($R = \text{TMS}$) with palladium acetate in dimethylsulfoxide under an atmosphere of oxygen at ambient temperature provided **99**. The amount of $\text{Pd}(\text{OAc})_2$ could be decreased to 2.5 mol%, however this led to the recovery of *ca.* 10% of unreacted **95** as judged by ^1H NMR. For the most cost effective dehydrosilylation of **125** ($R = \text{TMS}$) a catalyst loading of 10 mol% was determined to be optimal (**b**; **Scheme 8**). Under these conditions apoverbenone was produced in 85% yield over two steps with minimal recovery of nopinone ($\sim 4\%$ as judged by ^1H NMR). Additionally, the optical purity of **99** obtained through the Saegusa-Ito oxidation was comparable to that obtained by Grimshaw's procedure, with the discrepancy presumably caused by both the optical purity of our commercially sourced (-)- β -pinene (96% ee) as well as unreacted **95** which inversely bends polarized light ($[\alpha]^{20}_{\text{D}} +311.0^\circ$ (*c* 2.4, CHCl_3) [lit. $[\alpha]^{25}_{\text{D}} +319^\circ$ (*c* 2.4% in CHCl_3)]).⁸⁴ Application of the Saegusa-Ito oxidation did not reduce the total number of steps to **99**, however, this method is high yielding, mild, catalytic, and easily

monitored by TLC. Moreover, **99** is formed from intermediate **125** (R = TMS) without the need for purification, isomerization, sulfoxide formation (as in the dehydrosulfenylation which affords **119**) or extreme heat, superseding the previously described processes which provide apoverbenone.

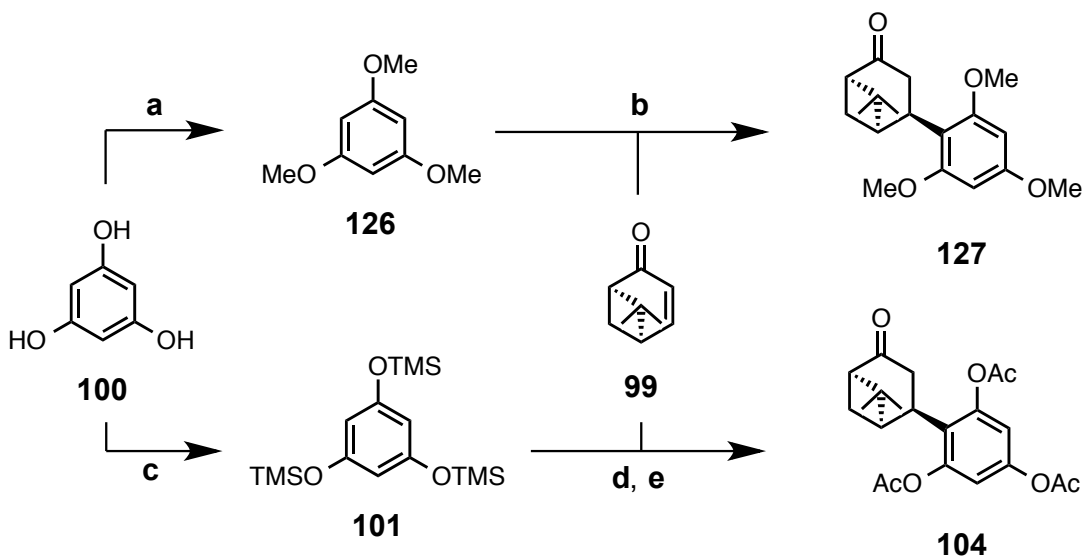
With apoverbenone in hand, various methods were screened to determine its potential as a Michael acceptor. To improve the likelihood of success, initial attempts at conjugate addition employed the highly activated, electron rich nucleophile phloroglucinol (**100**). Additionally, the first Lewis acids screened were scandium triflate ($\text{Sc}(\text{OTf})_3$) and ytterbium triflate ($\text{Yb}(\text{OTf})_3$), which were chosen for their non-nucleophilic counter ion. Unfortunately the mixture of **99**, **100**, and either Lewis acid in a variety of solvents and at a number of different temperatures did not result in conjugate addition (**Scheme 9**).⁹⁰ Conjugate addition of phloroglucinol to enones has been shown to be catalyzed under basic conditions, however, subjecting **100** to sodium hydride (NaH) in THF followed by the introduction of apoverbenone to the reaction mixture was unsuccessful for the preparation of **102**.



Scheme 9: Initial Attempts to Prepare **102** Through The Michael Addition of Apoverbenone

The permethyl ether of phloroglucinol (**126**) has also been used for the conjugate addition to enones, but this nucleophile has required the use of the unusual amphoteric Lewis acid-Lewis base, vanadyl triflate ($\text{VO}(\text{OTf})_2$) to afford Michael adducts.⁹¹ Chen and coworkers

describe the Friedel-Crafts type addition of **126** to cyclohexenone in high yield using $\text{VO}(\text{OTf})_2$ and postulate that this oxometallic catalyst behaves as an strong Lewis acid at its vanadium center, which is amplified by the electron withdrawing counter ions to activate enones for conjugate addition. Moreover, the polarizability of the oxovanadium double bond allows the oxygen to activate nucleophiles by behaving as a Lewis base, resulting in a push-pull mechanism to afford the desired 1,4-addition.



Scheme 10: Vanadyl Triflate Catalyzed Michael Addition of Phloroglucinol^a

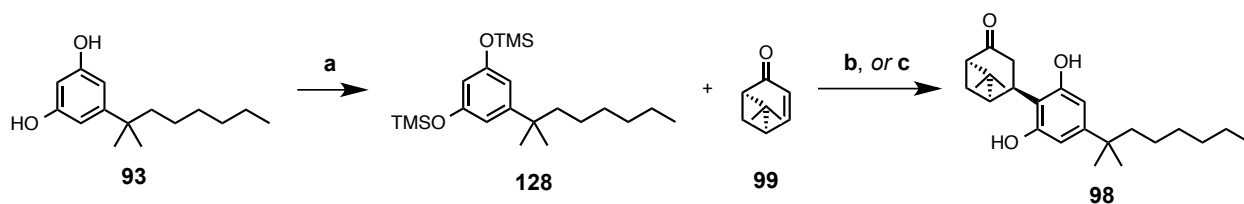
^aReagents and Conditions: (a) K_2CO_3 , DMF, MeI, rt, 4 h; 80%; (b) cat. $\text{VO}(\text{OTf})_2$, CH_2Cl_2 , rt; 50% from **99**; (c) Et_3N , TMSCl , 0 °C to rt, 3 h; (d) cat. $\text{VO}(\text{OTf})_2$, CH_2Cl_2 , rt, 40 h; (e) Ac_2O , Pyr, DMAP, CH_2Cl_2 , rt, 12 h; 63% from **99**

Although the use of the permethyl ether of phloroglucinol is less attractive than persilylated phloroglucinol **101**, due to the less practical cleavage of $-\text{OCH}_3$ compared to $-\text{OTMS}$, the exceptional 91% yield of its 1,4-addition to cyclohexenone urged its use. Preparation of $\text{VO}(\text{OTf})_2$ and suspending it with **126** and **99** in dichloromethane (DCM) resulted in the complete consumption of apoverbenone while producing **127** in 50% yield (b; **Scheme 10**).

Spurred by this encouraging result, the vanadyl triflate catalyzed Michael addition of persilylated phloroglucinol **101** to apoverbenone was carried out (**d**; **Scheme 10**). Michael addition was successful using the amphoteric Lewis acid. After exchanging the trimethylsilyl for acetyl groups, triacetate **104** was provided in 63% yield over two steps, a five percent decrease in yield from the analogous condensation and peracetylation depicted in **Scheme 4** (**e, f**). Comparing this result with Dixon's route to triacetate intermediate **104** from **95**, the four steps using either diacetates **97** and *p*-TsOH, or apoverbenone and VO(OTf)₂ followed by acetylation, provide **104** in 48% or 54% overall yield, respectively.

This new method which provides triacetate **104** via vanadyl triflate catalyzed Michael addition demonstrates that a high yielding synthesis of enantioenriched ketocannabinoids **107-109** can be performed without having to proceed through diacetates **97** and hence without the toxic lead tetraacetate. Moreover, in the presence of vanadyl triflate (**b, d**; **Scheme 10**), apoverbenone was shown to behave as a competent Michael acceptor.

Impressed by the reactivity of apoverbenone in the presence of catalytic vanadyl triflate, we attempted to perform a Michael addition using a less electron rich aromatic system, the C-5 substituted resorcinol **93** (**Scheme 11**). To ensure solubility in DCM, dimethylheptyl resorcinol was silylated and charged to a vessel containing Michael acceptor **99** and the vanadium catalyst. These conditions led to a heterogeneous reaction mixture that provided Michael adduct **98** in 49% yield after chromatography. (**b**; **Scheme 11**). Because resorcinols are less electron rich and therefore less nucleophilic than phloroglucinol this reaction did not go to completion after four days at ambient temperature. The rather low yield obtained after the addition of **128** to apoverbenone was discouraging. However, the yield could be improved by exploiting the regiospecificity exhibited by dimethylheptyl resorcinol during conjugate addition as well as the thermal stability of **99**, a combination of features not found during the addition of **93** to the diacetates (**97**) or the addition of phloroglucinol to apoverbenone (**99**).

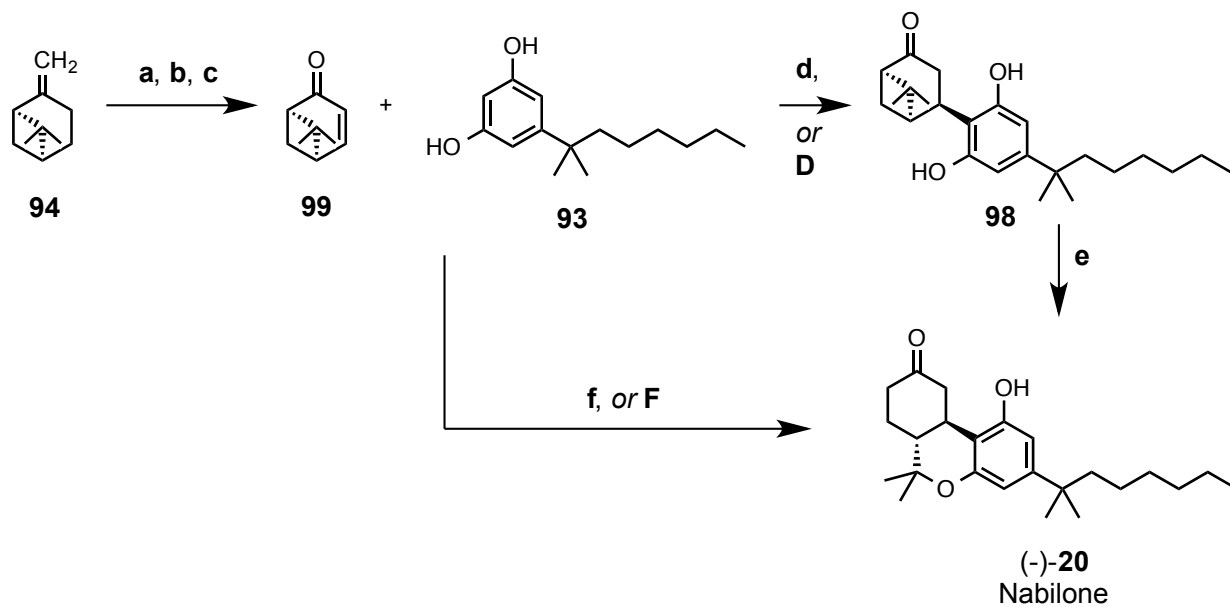


Scheme 11: Vanadyl Triflate Catalyzed Michael Addition of Dimethylheptyl Resorcinol^a

^aReagents and Conditions: (a) Et₃N, TMSCl, 0 °C, 0.5 h; (b) cat. VO(OTf)₂, CH₂Cl₂, rt, 48 h; 49% yield; (c) cat. VO(OTf)₂, ClCH₂CH₂Cl, 60 °C, 36 h; 73%

Apoverbenone, unlike the diacetates, **97**, can be heated above 60 °C for prolonged periods of time without decomposition. The thermal stability of apoverbenone allows any Michael addition to **99** to be driven to completion by heating the reaction mixture. Also, the tertiary benzylic alkyl group of dimethylheptyl resorcinol is able to block *ortho*-substitution — suppressing the formation of abnormal and double addition adducts even at elevated temperatures. Furthermore, because the addition of **93** or **128** takes place regioselectively, a slight excess of enone **99** was found to be advantageous to drive the reaction to completion instead of an excess of **128**. The use of excess **99** also simplified the purification of **98** because of the complete consumption of **93**, and the large difference in chromatographic mobility of the Michael adduct and **99**. Taking all this into account, DCM was replaced by the higher boiling 1,2-dichloroethane (DCE) and the vanadyl triflate catalyzed Michael addition of **128** to **99** was repeated (**c**; **Scheme 11**). These adjustments reduced the reaction time by 25% and bolstered the yield of **98** to 73%. While monitoring the reaction by thin layer chromatography (TLC) it was noted that at elevated temperature, rapid desilylation of **128** took place. Critically, however, this did not impede the production of **98**, suggesting the use of free dimethylheptyl resorcinol **93** in this reaction. Surprisingly, **93** was quite soluble in warm DCE and a day of heating with **99** and the vanadium catalyst rendered the reaction mixture a slurry, characteristic of the formation of **98** (**d**; **Scheme 12**). Circumventing the unstable *bis*-silyl ether **128** not only simplified the

experimental effort to produce **98**, but eliminated complications of the vanadyl catalyzed Michael addition that were encountered if crude **128** was contaminated with any reagents used for its production.



Scheme 12: Vanadyl Triflate Catalyzed Michael Addition
Applied to The Total Synthesis of (-)-Nabilone^a

^aReagents and Conditions: **(a)** O₃, CH₃OH/CH₂Cl₂, -78 °C, ii. Me₂S, -78 °C to rt; 89%; **(b)** LDA, TMSCl, -78 °C to 0 °C, 0.5 h; **(c)** cat. Pd(OAc)₂, DMSO, O₂; 85% over 2 steps; **(d)** cat. VO(OTf)₂, DCE, 60 °C, 24 h; 83%; **(e)** TMSOTf, CH₂Cl₂/CH₃NO₂, 0 °C to rt, 3 h; 73% **(f)** Conditions **d** followed by **e** without isolation of **98**; 60% over 2 steps **(D)** DCE, 60 °C, 10 h; **(F)** TMSOTf, CH₂Cl₂/CH₃NO₂, 0 °C to rt, 3 h

Note: Conditions **D** and **F** are controls, *see text*

Optimization of the Michael addition of free resorcinol **93** to apoverbenone showed that even 1 mol% of vanadyl triflate with heating in DCE for two days was sufficient to produce 83% yield of Michael adduct **98** following chromatography (**d**; **Scheme 12**). A decrease in the reaction time was achieved with an increase in catalyst loading (10 mol%, 24 hours); notably, when the reaction mixture was heated for a day without the addition of vanadyl triflate, **93** and

99 were recovered unchanged (**D**; **Scheme 12**). The mild anhydrous conditions of this reaction make it possible to introduce TMSOTf after the Michael addition has proceeded to completion so as to catalyze the formation of the tricyclic cannabinoid skeleton in a single operation. Charging a reaction vessel with vanadyl triflate, **99** and **93** followed by TMSOTf *after* the complete consumption of **93** provided (-)-**20** in 60% overall yield after chromatography (**f**; **Scheme 12**). The vanadyl triflate catalyzed one pot procedure to (-)-nabilone represents a great improvement over the one pot addition of **93** to **99** described by Archer, and increases the yield nearly four-fold (3.75x), bringing the overall yield of this synthesis to 49% from **94**.

To determine whether trimethylsilyl triflate could catalyze the Michael addition of **93** to apoverbenone *as well as* the cyclobutane ring opening to produced (-)-**20**, TMSOTf was used in place of vanadyl triflate (**F**; **Scheme 12**). These reaction conditions led to the complete decomposition of enone **99** within three hours while leaving dimethylheptyl resorcinol unchanged. By analysis of the crude reaction mixture by HRMS and by comparison of HPLC retention times with an authentic sample the presence of trace amounts of (-)-nabilone was confirmed.

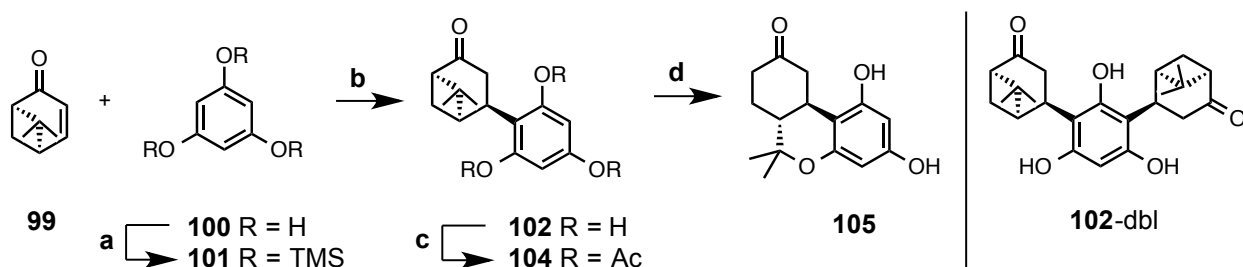
Although this improved synthesis of optically active nabilone avoids the use of the toxic heavy metal reagents employed during previous syntheses, it relies upon vanadyl triflate. Vanadium (V^0) is a genotoxin but is not mutagenic and is designated as a Class 2A element, having toxicity on par with nickel and cobalt, with an essential biological role in humans not yet established. The primary targets for vanadium toxicity are the GI tract, cardiovascular and hematological systems, however, oral administration of ammonium vanadyl tartrate or vanadyl sulfate (V^{IV}) to humans was conducted during a study and no significant alterations to these physiological systems was found.⁷⁹ Moreover its catalytic role during the synthesis of (-)-nabilone and simple chromatographic separation from **98** or (-)-**20** justify it's use.

The unexpectedly high reactivity of apoverbenone as a Michael acceptor that was revealed during the execution of the preceding work prompted a critical reexamination of the relevant literature. The following four points are worth reiteration: (1) "Successful condensation of diacetates with dimethylheptyl resorcinol is achieved at room temperature with *p*-toluenesulfonic acid in chloroform after three days",^{75,77} (2) "Apoverbenone does not react under [condensation] conditions",^{72a,74} (3) "[apoverbenone] formation is one of the reasons for the observed low yield of [the condensation] reaction",⁷⁴ (4) "In the absence of [resorcinol], the mixture of diacetates **97** are completely converted to apoverbenone **99** in about 1.5 hours in the presence of *p*-toluenesulfonic acid".⁷⁴

Claims **1**, **2**, and **3** are in agreement, however claim **4**, when read in conjunction with the others aroused skepticism. Why would the decomposition of **97** to **99** be somehow slowed or inhibited by the addition of resorcinol to the reaction mixture? And how do the diacetates survive three days of acid exposure in claim **1**, but decompose within hours according to claim **4**?

Suspecting that apoverbenone was the active electrophile during previously reported Brønsted acid catalyzed condensations with resorcinols and phloroglucinol, **99** was combined with stoichiometric *p*-TsOH and excess persilylated phloroglucinol **101** in a mixed solvent of chloroform and acetone (**Scheme 13**). The reaction mixture instantly became homogenous and golden in color, but quickly turned milky and heterogeneous, presumably due to the acid catalyzed desilylation of **101** that leads to insoluble phloroglucinol. The heterogeneous mixture was allowed to stir and remarkably after seven hours apoverbenone was completely consumed as judged by TLC! Examination of the crude reaction mixture by ¹H NMR revealed that **102** was the major product, which was isolated in 32% yield after column chromatography on silica gel (**Scheme 13**). Because the *p*-TsOH led to the rapid cleavage of the silyl groups of **101**, free phloroglucinol was subsequently used at the outset of this reaction. This drastically reduced the reaction time to two hours, however, the free phenolic groups increased the nucleophilicity of

the aromatic starting material, and produced large amounts of **102-dbl** (**Scheme 13**). The problematic *bis*-addition was suppressed by using an addition funnel with metering stopcock to slowly introduce a dilute solution of **99** to a mixture of phloroglucinol and *p*-TsOH in acetone. Additionally, dissolving **99** in dichloroethane instead of chloroform provided exclusively **102** in a completely homogeneous reaction mixture at a much higher concentration than the one previously used (0.1M vs. 0.03M). Moreover, with adequately slow addition of **99**, *bis*-addition can be avoided even when fewer than 2 equivalents of **100** are used for this reaction.



Scheme 13: Michael Addition of Phloroglucinol to Apoverbenone
Catalyzed by *p*-Toluenesulfonic Acid^a

^aReagents and Conditions: **(a)** Et₃N, TMSCl, 0 °C to rt, 3 h; **(b)** *p*-TsOH, 1:4 acetone:DCE (0.1M), rt; ~70% from **100** **(c)** Ac₂O, Pyr, DMAP, CH₂Cl₂, rt, 12 h; 57% from **100** **(d)** TMSOTf, CH₃NO₂, 0 °C, 2.5 h; 54% from **100** (2 steps).

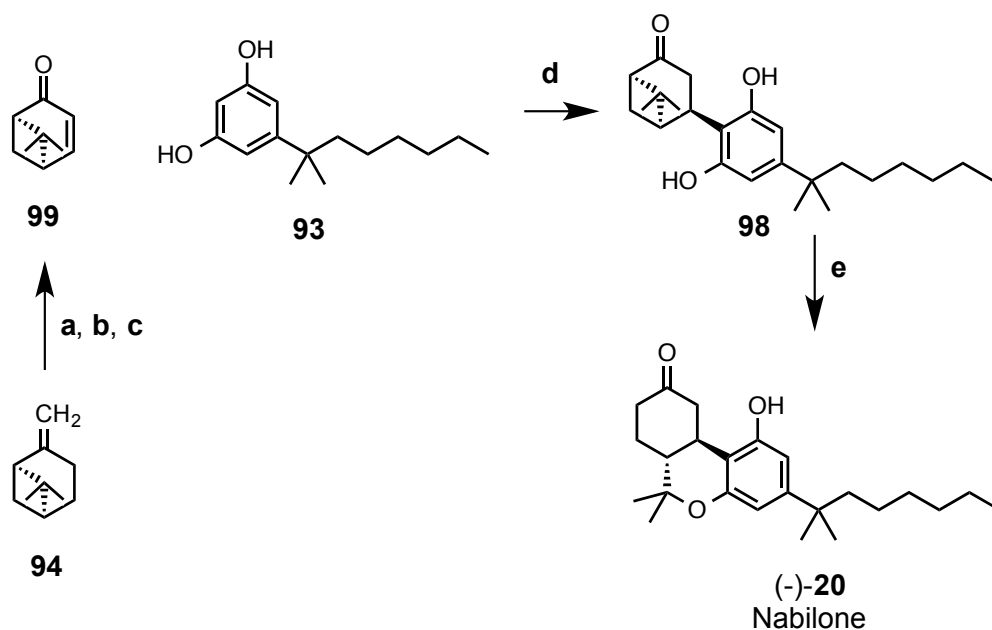
Further improvement to this route was achieved through a simplified isolation procedure for Michael adduct **102**. Consultation of Armarego and Chai's *Purification of Laboratory Chemicals* revealed that water is the preferred solvent for the recrystallization of phloroglucinol, prompting the use of hot water during extraction, or (for large reactions) a continuous extractor to separate crude **102** from free phloroglucinol (**Scheme 13**).⁹² This trivially simple exploitation of physical properties allowed **102** to be isolated essentially pure in ~70% yield following the

revised extraction procedure. Unfortunately, **102** rapidly oxidizes in air which led to variable yields of purified product, and it was found to be convenient to peracetylate **102** to **104** for storage. This triacetate could be consistently provided in 57% yield over two steps — a 10% increase to the overall yield from **95** while avoiding the persilylation of **100** (**b, c; Scheme 13**). Alternatively, **102** could be cyclized to the more stable **105** by the methods described by Dixon in 54% yield over two steps — a meager 8% improvement to the overall yield from nopinone but in *three fewer* operations than previously reported (**Scheme 4; 8; 13**).⁷⁸

That Brønsted acid catalyzed Michael addition of phloroglucinol to apoverbenone should occur is not surprising, however, we found no precedent for such a straightforward process for the synthesis of tricyclic ketocannabinoids. The optimized solvent system of 1:4 acetone:DCE dissolved unprotected phloroglucinol and obviated the cumbersome persilylation step. This, combined with the simple hot water extraction of **100** from Michael adduct **102**, vastly reduced the experimental effort needed to provide triacetate **104** or tricyclic **105**. Moreover, the improvements described above resolved a major experimental complication of this route which *required* peracetylation and two additional steps to obtain purified **102** and subsequently **105** while achieving an increase in the overall yield (**Schemes 4; 8; 13**).⁷⁸

Large scale preparation of **102** by the method described above is somewhat impractical due to the lengthy reaction times which are required to ensure the addition of apoverbenone is adequately slow so as to avoid formation of **102-dbl**. This reaction sequence which may be further optimized by using a milder Brønsted acid to discourage the formation of **102-dbl** while still polarizing **99** toward conjugate addition, however, the screening of alternative acids was not completed because the synthesis of **102** was ancillary to the desired conjugate addition of the less nucleophilic **93** to **99**, which would require a strongly polarizing Brønsted acid to provide **98** and subsequently (-)-nabilone.

Ventre à terre the Brønsted acid catalyzed addition of a less nucleophilic aromatic ring was examined. *p*-Toluenesulfonic acid was added to a solution of apoverbenone and dimethylheptyl resorcinol in dichloroethane. After two hours of heating, apoverbenone was completely consumed and examination of the crude reaction mixture by ^1H NMR showed decomposed enone as well as a 2.5:1 ratio of Michael adduct to nabilone. This direct, Brønsted acid catalyzed Michael addition of resorcinols to apoverbenone, which had been overlooked for close to four decades was optimized in short order, and can now be applied to expedited syntheses of bi- or tricyclic cannabinoids. The details of this effort are described in what follows.



Scheme 14: *p*-Toluenesulfonic Acid Catalyzed Michael Addition of Dimethylheptyl Resorcinol to Apoverbenone Applied to The Total Synthesis of Nabilone^a

^aReagents and Conditions: (a) O_3 , $\text{CH}_3\text{OH}/\text{CH}_2\text{Cl}_2$, $-78\text{ }^\circ\text{C}$, ii. Me_2S , $-78\text{ }^\circ\text{C}$ to rt; 89%; (b) LDA, TMSCl, $-78\text{ }^\circ\text{C}$ to $0\text{ }^\circ\text{C}$, 0.5 h; (c) cat. $\text{Pd}(\text{OAc})_2$, DMSO, O_2 ; 85% over 2 steps; (d) cat. *p*-TsOH, DCE, $60\text{ }^\circ\text{C}$, 18 h; 94%; (e) TMSOTf, $\text{CH}_2\text{Cl}_2/\text{CH}_3\text{NO}_2$, $0\text{ }^\circ\text{C}$ to rt, 3 h; 87%

During the optimization of this Michael reaction it was found that the undesired *p*-TsOH catalyzed intramolecular cyclobutane ring opening could be suppressed through the use of

catalytic acid, and/or performing the reaction at a lower concentration, both of which increase the reaction time of the bimolecular addition but selectively produce **98**. Reducing the load of acid also slowed the competitive decomposition of **99**. The use of ambient or inert atmosphere had a drastic effect on the time course of this reaction, but little to no effect on the yield of **98**. Under nitrogen or air, the Brønsted acid catalyzed Michael addition was complete in 20 hours or 108 hours, providing 82% or 83% of **98**, respectively. Reactions performed open to air did become red as time passed, indicative of quinone formation; however, this byproduct was in such low concentrations that its detection and isolation were challenging and the effort to do so was abandoned. Although a one pot procedure to (-)-nabilone by addition of TMSOTf to crude **98** was possible, it was found advantageous to isolate the Michael adduct. This phenolic intermediate has limited solubility in DCE, in contrast to its terpenic and aromatic starting materials. Rinsing **98** with cold DCE on a fine fritted glass filter attached to a rotary vane pump proved superior to purification by chromatography. The isolation of **98** by filtration increased the isolated yield of this Michael addition to 94% from the 83% obtained following column chromatography (**d**; **Scheme 14**). Unfortunately, this technique could not be applied to the vanadyl catalyzed Michael addition because unlike *p*-TsOH, VO(OTf)₂ is insoluble in DCE and would require chromatography to separate it from **98**. However, this filtration protocol may be applicable to the isolation of other phenolic cannabinoids in high enantiopurity, as the highly crystalline nature of resorcinol intermediates such as **98** has been previously noted.⁸²

The chemical purity of the filtered crystals was determined to be >99% by LCMS and HPLC with an evaporative light scattering detector (ELSD), and exhibited a sharp melting point (174.2–175.3 °C, [lit.^{54c} mp 174–176 °C]) immediately following filtration. For comparison, **98** obtained directly from column chromatography melted at 169.7–173.5 °C and was only 89% pure, as determined by LCMS (254 nm), requiring recrystallization to reach analytical purity. Additionally, the use of highly pure Michael adduct for the intramolecular cyclobutane ring

opening increases the yield of this step to 87%, compared with the typical 73% yield of (-)-**20** obtained by using chromatographically purified **98** (**e**, **Scheme 14**).

Surprisingly, the brilliant white crystalline Michael adduct obtained by filtration rotates the plane of polarization of polarized light to a greater degree than the samples prepared by Archer ($[\alpha]^{20}_D +83.6^\circ$ (c 1.0, CHCl_3) [lit.^{75a} $[\alpha]^{20}_D +55.8^\circ$ (c 1.0, CHCl_3)]. Subsequent cyclization resulted in (-)-nabilone with a specific rotation greater than *any yet reported* ($[\alpha]^{20}_D -62.5^\circ$ (c 1.0, CHCl_3) [lit.^{75a} $[\alpha]^{20}_D -55.7^\circ$ (c 1.0, CHCl_3)]. The discrepancy between these data and those reported in the literature required further investigation, the details of which are described in what follows.

Archer and coworkers' synthesis of (-)-nabilone starting from enantioenriched (-)-*trans*-verbenol exhibited the highest optical purity (-55.7° (c 1.0, CHCl_3)) of all the routes described in 1977,^{75e} however, this monoterpene was prepared according to Whitham's procedure from (-)- α -pinene and exhibited a specific rotation of -118° (c 0.96, MeOH).^{75a,c} Although the specific rotation reported by Archer was recorded under different conditions, Mori's synthesis of optically pure (-)-*trans*-verbenol from (-)- α -pinene suggests the enantiopurity of Archer's monoterpene to be 87.4% based on the value -135° (c 0.81, CHCl_3) for pure (-)-*trans*-verbenol,^{75d} a purity which is supported by the specific rotation of Archer's (-)- α -pinene (-44.6° (c 1.0, MeOH)). Without mention of chiral resolution, it follows that the (-)-**20** prepared by Archer using (-)-*trans*-verbenol should have enantiopurity of 87.5%. Since nabilone has no natural source, the only means to determine its absolute enantiopurity would be analyze (-)-**20** by chiral HPLC with comparison against its racemate, however, to the author's knowledge this has yet to be performed. If indeed (-)-**20** exhibiting a specific rotation of -55.7° correlates to 87.5% enantiopurity, then the (-)-nabilone provided following filtration and cyclization as described above corresponds to 98.2% enantiopurity. Unfortunately, an authentic sample of (\pm)-**20** is currently unavailable for comparison with (-)-**20** prepared by the author, as such the definitive determination of enantiopurity will be deferred for the time being. Nevertheless, this synthetic route is able to

produce (-)-nabilone in greater enantiopurity than previously reported presumably due to the filtration process developed to purify **98**.

The Michael adduct **98** was originally prepared by the condensation with diacetates **97** (**Scheme 3**; **Chpt. 1**) and the specific rotation of this material has varied only slightly between the last two preparations (+57.2° (*c* 1.0, CHCl₃)^{54c} and +55.8° (*c* 1.0, CHCl₃)^{75a}). However, when **98** is prepared and purified by the filtration described above, the specific rotation dramatically increases to +83.6° (*c* 1.0, CHCl₃). This corresponds to a ~32% increase in *ee*, which is difficult to rationalize considering that the diacetates are prepared from (-)-β-pinene (**94**) which is generally purchased at 92.5% optical purity, however, this critical data was not included in previous communications.^{54c,75a} During the author's measurement of the optical rotation of filtered **98**, the material was observed to be notably less soluble under the conditions described by Archer or Drake than samples of Michael adduct that had been purified using column chromatography. Suspecting the data to be skewed by the heterogeneity of the sample, the optical rotation measurement was repeated with a dilution factor of 10, resulting in a specific rotation of +63.7° (*c* 0.1, CHCl₃). Although a direct comparison of these specific rotations is not precise, the diluted sample is potentially enantiopure. Unfortunately, without the exact optical purity of Archer's or Drake's (-)-β-pinene or more specifically their diacetates, the optical purity of the final product cannot be determined. The optical purity of the (-)-apoverbenone (**99**) used to prepare **98** has been recorded and may offer insight as to the enantiopurity of the Michael adduct. However, this is complicated by the persistent contamination of **99** with (+)-nopinone (**95**) which rotates the plane of polarization of polarized light in the opposite direction and is present in variable amounts due to the shortcomings of the method described above. Attempts to determine the enantiopurity of **98** without an authentic sample of its racemate was challenging but eventually a logical method was developed.

Curiously, samples of **98** purified by column chromatography exhibited a specific rotation in agreement with Archer and Drake when diluted to the same concentration ($+54.5^\circ$ (c 1.0, CHCl_3)). This prompted a further investigation of the filtration process. Michael adduct that had been purified by column chromatography was rinsed as previously described and the filtrate, which contained small amounts of **98** as judged by TLC, was concentrated and the specific rotation of the resulting residue was measured at $+35.7^\circ$ (c , 1.0, CHCl_3). The increase in the specific rotation of the filtered **98** coupled with the decrease in the specific rotation of the Michael adduct in the filtrate suggested that the process designed to quickly purify **98** from the Brønsted acid reaction mixture was also removing the racemate of **98** with greater ease than the major enantiomer. Additional rinsing of **98** with DCE then presumably dissolves amounts of the major enantiomer, giving rise to the nonracemic dextrorotary filtrate. Excited by this result, chiral HPLC was performed on the three samples of **98** at the author's disposal; material that was purified by column chromatography, or by filtration, and the filtrate (**Experimental** p.116). According to the data, the Brønsted acid catalyzed Michael addition of **93** to **99** affords a 95.5:4.5 enantiomeric ratio or 91% enantiomeric excess of **98** following flash chromatography. When the scalemic mixture was filtered as previously described and the white crystalline Michael adduct was examined under the same conditions the *ee* improved to $>99\%$ — the minor enantiomer being undetectable. The postulate that the filtration process successfully removed the racemate of **98** more rapidly than the desired antipode was further confirmed when the filtrate was analyzed concurrently, resulting in a *er* of 72:28. It then follows that the (-)-nabilone prepared from the filtered Michael adduct is enantiopure, as the intramolecular cyclobutane ring opening occurs without scrambling of the stereochemistry at C-6a. This solves the problem of the cumbersome and unreliable determination of optical purity without the need for chiral HPLC comparison of (-)-**20** with its racemate.

In conclusion, efficient routes to the versatile and optically active ketocannabinoids **105** and **98** have been developed. During these syntheses, a new facile, catalytic route to apoverbenone was developed, which proceeds by the Saegusa-Ito oxidation of nopinone and showcases the robust nature of this named reaction. The key step in the synthesis of **105** and **98** is a Michael addition to apoverbenone which is catalyzed by *either* Lewis or Brønsted acid and precludes the use of lead tetraacetate — a reagent deemed necessary prior to this work (**Scheme 11, 12, 13, 14**). The efficiency of the Michael addition is exemplified during the abbreviated total synthesis of (-)-nabilone, which can be performed in four (**Scheme 12**) or five steps (**Scheme 14**), and was accomplished in 49% or 65% overall yield, respectively. This represents a great improvement to the state-of-the-art synthesis of optically active nabilone, which led to product in 28% yield over 5 steps. Although the Lewis acid catalyzed Michael addition can provide (-)-nabilone in fewer steps, the route that makes use of a Brønsted acid is higher yielding. Moreover, this method utilizes *p*-toluenesulfonic acid and is the preferred route, due to the convenience of the filtration process developed to isolate **98**, which easily separates the racemate of **98** from its major enantiomer in a practical and scalable manner. The synthesis of (-)-nabilone which utilizes the Brønsted acid catalyzed Michael addition is complemented by the simple reaction conditions, commercially available reagents, and experimental ease. Furthermore, the improved syntheses to **105** or **98** require no exotic or toxic reagents, and, importantly, can be applied to the synthesis of classical, non-classical, and hybrid cannabinoids.

Chapter 3

The Total Synthesis of C-9 and C-11 Functionalized Classical Cannabinoids

Because of the work outlined in **Chapter 2** of this thesis, enantiopure (-)-nabilone was at the author's disposal as the common starting material for the synthesis of targeted cannabinoids **83 - 90 (Figure 26)**. These ligands were prepared to complement the work of Mr. Ogawa, and to introduce reactive functionality at C-9 and C-11 so as to probe the cannabinoid receptors through LBAs, SARs, and LAPS experiments. These experiments will be performed by our collaborators at Northeastern University. Ligands that exhibit high receptor affinity and irreversible agonism could potentially be utilized for co-crystallization experiments with CB₁ or CB₂. Successful results from LAPS and co-crystallization would then provide a very highly detailed description of the receptor binding pocket, its steric and chemical demands for activation, and a framework for logical ligand design. All of this will aid in the ultimate goal of modulating the selective activation of the individual regulatory functions controlled by the endocannabinoid system.

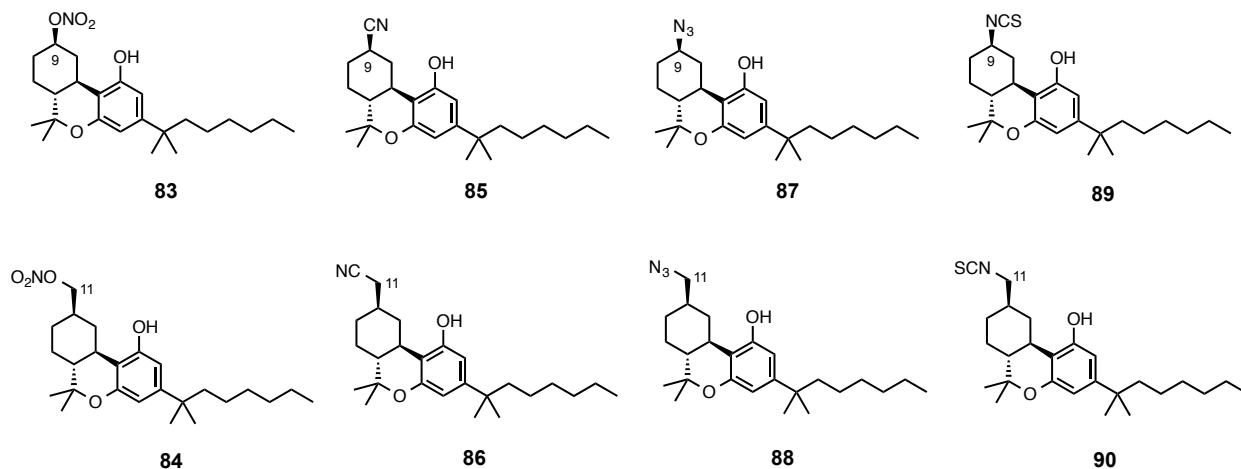


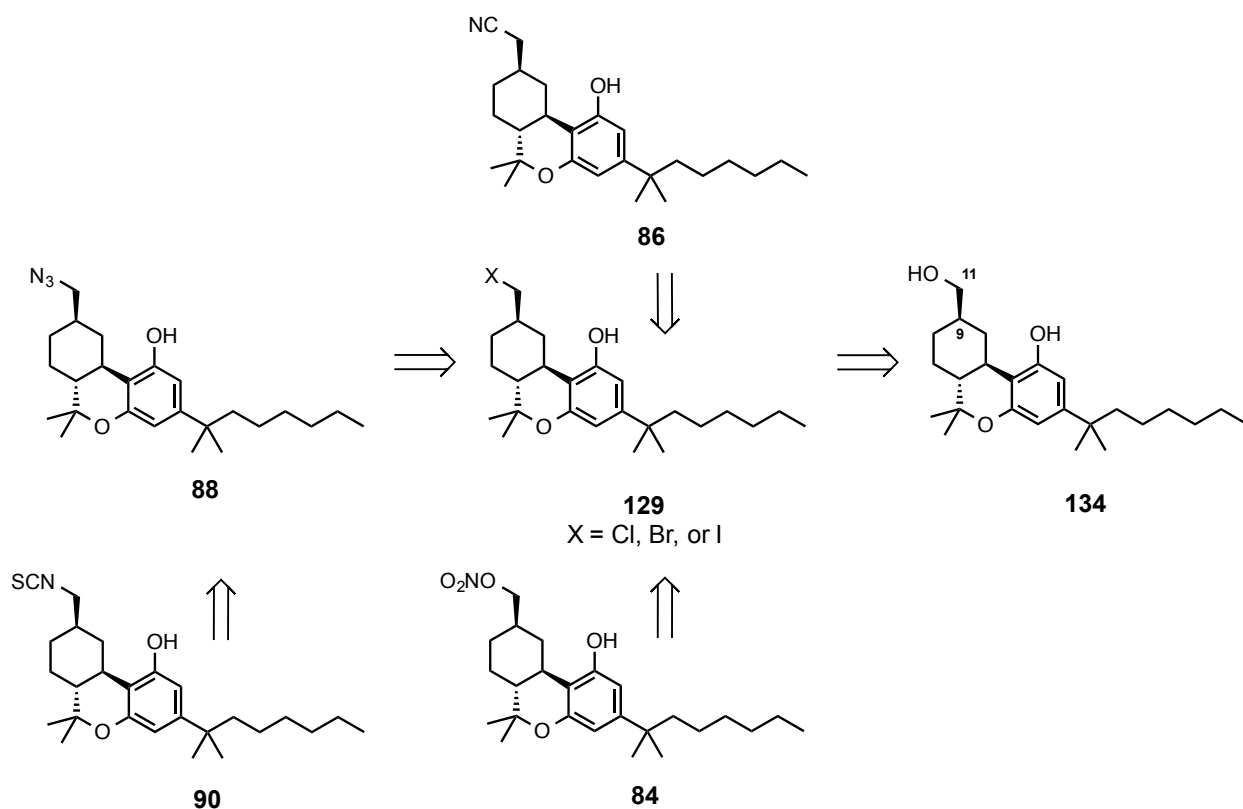
Figure 26: Targeted C-9 and C-11 Functionalized Ligands

The same functional groups, nitrate ester, nitrile, azide, and isothiocyanate were chosen for both the C-9 and C-11 series. This simplified the retrosynthetic analysis and guided the

synthetic plans of both series to an alkyl halide intermediate which could be used for a facile displacement by the appropriate nucleophile to furnish the desired functionality. Nitrate esters have been prepared by exposure of alcohols to a variety of reagents, however, depending on the substrate a number of side reactions or stereochemical scrambling may occur.⁹³ Moreover, the reagents necessary for the conversion of alcohols to nitrate esters are often noxious or difficult to handle. In contrast, the formation of nitrate esters from alkyl halides by treatment with silver nitrate is selective and tolerates a range of substrate functionality — providing nitrate esters in good yields with predictable stereochemistry following filtration of the silver halide salt. The alkyl halide which could provide a nitrate ester in one step could also furnish nitrile, or azide functionality following its treatment with NaCN or NaN₃. Although organic azides and nitriles may be also be installed by a Mitsunobu reaction of the corresponding alcohol, this is not an option for the preparation of a nitrate ester, further increasing the attractiveness of proceeding through an alkyl halide — especially for the C-9 series where an axial substitution results in an extreme loss of receptor affinity. The resulting azides could then, in a single operation, provide the desired isothiocyanate ligands using a Staudinger/aza-Wittig reaction by treatment with triphenylphosphine followed by carbon disulfide.⁹⁴

Examining first the C-11 series, the first goal was to prepare the primary halide (**129**; **Scheme 15**). This could be made in a number of ways. Based on earlier work from our group,⁶² ketone (-)-**20** can be homologated and hydrolyzed to provide an aldehyde at C-11, which upon reduction would give primary alcohol **134** (**Scheme 15**). Following the introduction of C-11 *via* a Wittig reaction, the hydrolysis which affords the C-11 aldehyde is complicated by an additional stereocenter at C-9, and provides a mixture of β -equatorial and α -axial isomers. The β -equatorial orientation at C-9 is critical to receptor affinity and can fortunately be controlled by base catalyzed epimerization of the diastereomeric C-11 aldehyde mixture. This epimerization provides the more stable and potent β -series aldehyde prior to the reduction which furnishes

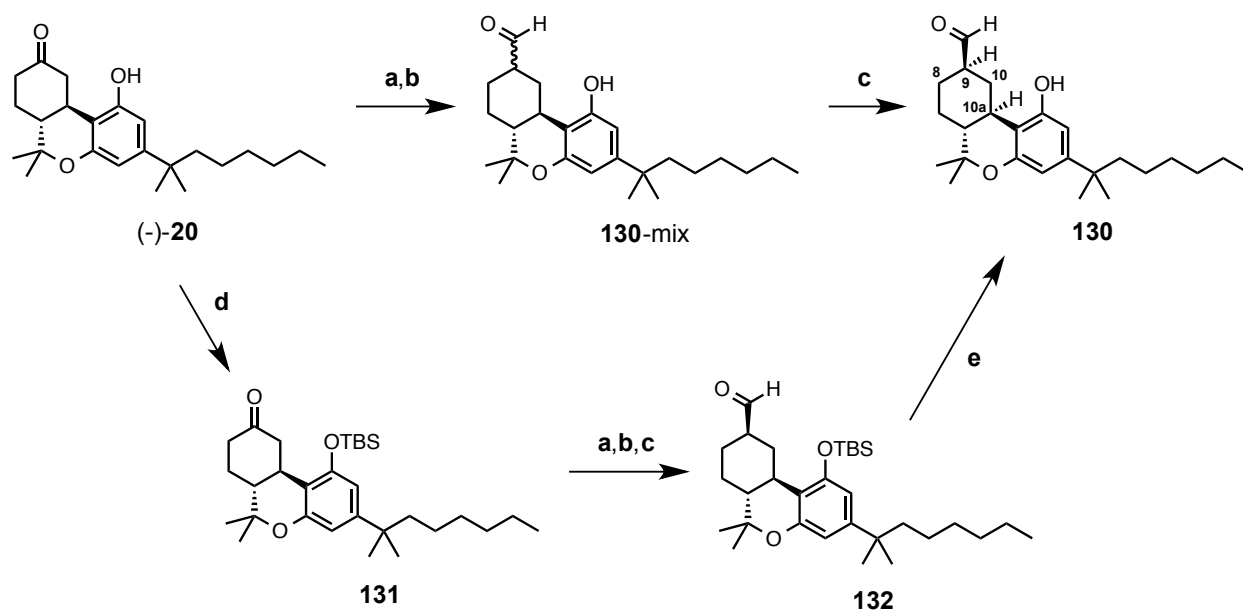
134. Makriyannis and coworkers have recently shown that C-11 hydroxy tricyclic cannabinoids, like **134** are well suited for iodination by treatment with triphenylphosphine, imidazole, and iodide — providing a straightforward route to halide **129** (X = I; **Scheme 15**).⁹⁵



Scheme 15: Retrosynthetic Analysis of C-11 Ligands Using Intermediate **129**

Following the strategy outlined by the retrosynthetic analysis, a Wittig reaction was performed on (-)-**20** using (methoxymethyl)triphenylphosphonium chloride and *n*-BuLi (**Scheme 16**). The resulting enol ether was hydrolyzed to a mixture of α and β aldehydes (**130-mix**) using wet trichloroacetic acid in DCM, and epimerized with potassium carbonate in absolute ethanol to the β -aldehyde (**130**; **Scheme 16**). Although the proton-proton coupling constants of H-9 were difficult to discern at 500 MHz, extrapolating the *J*-values from the four α -protons at H-8 and

H-10 supported the axial orientation of H-9 — with coupling constants of 3.8, 3.8, 12.5, and 12.5 Hz.⁶² The stereochemistry of β -equatorial aldehyde **130** was further confirmed by the positive nuclear Overhauser effect (nOe) of H-9 with axial and benzylic H-10a (**Scheme 16**).



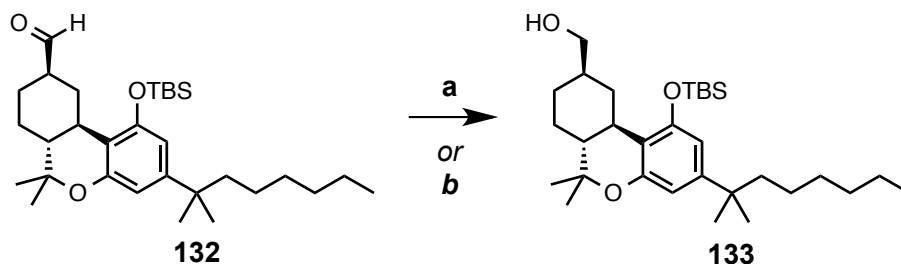
Scheme 16: Preparation of β -Aldehyde **130** or **132** from (-)-Nabilone^a

^aReagents and Conditions: (a) $\text{Ph}_3\text{PCH}_2\text{OMe}^+\text{Cl}^-$, $n\text{BuLi}$, THF, $-30\text{ }^\circ\text{C}$ to $0\text{ }^\circ\text{C}$, 0.5 h; (b) CCl_3COOH , H_2O , CH_2Cl_2 , rt, 1 h; 62% from (-)-**20** (2 steps) (c) K_2CO_3 , EtOH, rt, 4 h; 57% from **130-mix**; 85% from **131** (3 steps) (d) TBSCl, Imidazole, $80\text{ }^\circ\text{C}$, 10 min; 98%; (e) TBAF, Et_2O , rt, 0.5 h; 83%

The synthesis of **130** was accomplished in 35% yield over three steps. Although serviceable, this rather low yield was unpleasant and the loss of material was determined to be occurring during the crucial epimerization step. This was confirmed by the isolation of **130-mix** which was obtained in 62% overall yield as a 2:1 mixture of β : α aldehydes (a, b; **Scheme 16**). The subsequent epimerization of **130-mix** then provided 57% yield of enantioenriched **130**. Attempts to track the material loss during the epimerization with potassium carbonate afforded

no definitive answers, however, performing the homologation, hydrolysis, and epimerization reactions on the phenolic silyl ether **131** provided β -aldehyde **132** in 85% over three steps with small amounts of a coeluting impurity (**Scheme 16**). Aldehyde **132** could be deprotected to **130** in acceptable yield but was instead used for the subsequent transformations to avoid any competitive side reactions of the free phenol en route to halide **129**.

Aldehyde **132** was reduced with sodium borohydride in methanol to afford the primary alcohol phenolic silyl ether, **133**, in 71% yield (**a**; **Scheme 17**). The yield could be improved to 82% by the use of ethanol as the reaction medium (**b**; **Scheme 17**). Although the yield of this reduction remained relatively low for a reduction of an aldehyde with NaBH_4 ,⁹⁶ primary alcohol **133** was isolated without the inseparable impurity that contaminated aldehyde **132**, and the loss of this adulterant may account for the lower yield.



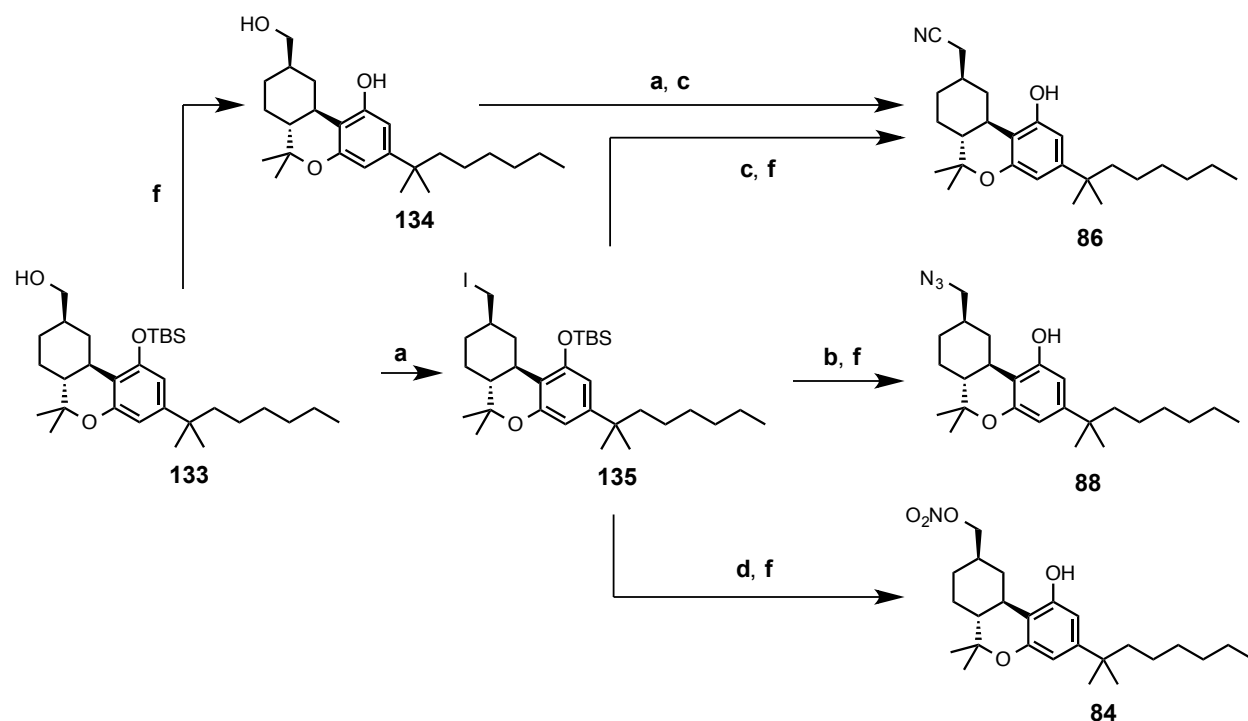
Scheme 17: Reduction of C-9 β -Aldehyde^a

^aReagents and Conditions; (**a**) NaBH_4 , MeOH, rt, 71%; (**b**) NaBH_4 , EtOH, 0 °C to rt, 82%.

Due to the intended uses of intermediate **129**, we initially aspired to install a bromine atom at C-11. This bromide would be less reactive than its iodo counterpart, yet would be amenable to long term storage, free from the light catalyzed decomposition common to organic

iodides.⁹⁷ Although this reaction had been performed by our collaborators on an analogous alcohol,⁹⁵ treatment of **133** with triphenylphosphine and tetrabromomethane only returned starting materials. In an attempt to drive the reaction to form the oxophosphonium intermediate, NBS was used in place of tetrabromomethane as described by Still and Mitra.⁹⁸ Under these conditions bromination of the electron rich aromatic ring took place before substitution at C-11. Similar results were obtained when **133** was added to a premixed solution of Ph_3P and Br_2 while attempting the bromination at C-11.^{98b} The lack of reactivity of **133** toward CBr_4 , and the undesired electrophilic bromination of the aromatic ring by other reagents discouraged any consideration of preparing the C-11 chloride. The problem of electrophilic ring chlorination was predicted to be more severe with the more highly reactive chlorinating agents.

Conversion of hydroxyl groups of similar cannabinoids to alkyl iodides has been reported a number of times,^{54c,62,95} without the complicating aromatic substitution that derailed the bromination. Thus, heating **133** with triphenylphosphine (Ph_3P) in benzene in the presence of imidazole and iodine led smoothly to primary monoiodide **135** through a Mitsunobu reaction (**Scheme 18**). Isolation of this halide by column chromatography was accomplished in *ca.* 85% yield, but as **135** was exposed to silica or light, the formation of an exocyclic alkene could be detected. This alkene is the result of elimination and was troublesome to separate from **135**. This led us to use the crude iodide for the subsequent substitution reactions. A major concern with using crude **135** was the potential of left over Ph_3P from the Mitsunobu reaction which could perform a Staudinger reaction on the azide product following displacement. The Staudinger reaction could be avoided, however, by carefully controlling the stoichiometry during iodination by adding 2.05 equivalents of Ph_3P as a standard solution in benzene. Application of these modifications followed by nucleophilic displacement with either sodium azide (NaN_3), sodium cyanide (NaCN), or silver nitrate (AgNO_3), and deprotection afforded **88**, **86**, and **84** in 76%, 77%, or 82% yield, respectively, over three steps (**Scheme 18**).



Scheme 18: Formation of and Substitutions on Advanced Intermediate **135^a**

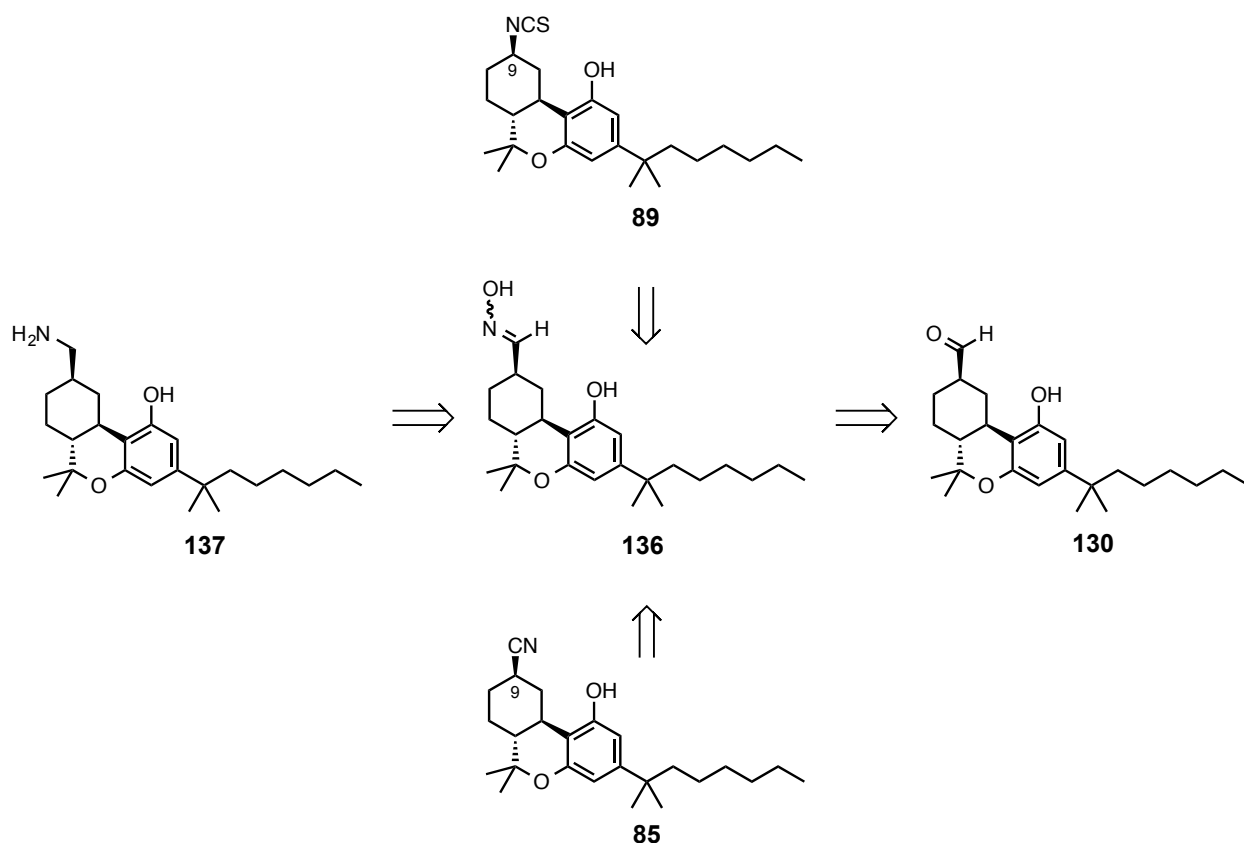
^aReagents and Conditions: **(a)** Ph_3P , imidazole, I_2 , PhH, 80 °C, 1 h; **(b)** NaN_3 , DMF, rt, 12 h; 76% after **f** (three steps); **(c)** NaCN , DMSO, rt, 24 h; 77% from **135** after **f** (three steps); 60% from **134** (2 steps); **(d)** AgNO_3 , CH_3CN , rt, 12 h; 82% after **f** (three steps); **(f)** $n\text{-Bu}_4\text{NF}$, Et_2O , rt, 1 h; 83% from **133**.

Although protecting the phenolic hydroxyl group in ketone **131** greatly improved the yield of the C-11 aldehyde, iodination of aliphatic hydroxy cannabinoids has been performed in the presence of free phenolic hydroxy functionality without deleterious effect to the yield.⁹⁵ To examine if the phenolic silyl ether was necessary during the Mitsunobu reaction and perhaps to avoid carrying a protecting group through a number of steps **133** was deprotected to **134** in 83% yield prior to its exposure to Ph_3P , imidazole, and I_2 (**f**; **Scheme 18**). Following iodination and nucleophilic displacement by sodium cyanide, **86** was formed in 60% yield over two steps (**Scheme 18**). The low yield was unexpected because the reaction appeared to be clean by TLC, suggesting that this process may merit closer scrutiny to determine where the material

loss is occurring. Regardless, deprotection of the phenolic silyl ether after the substitution of **135** leads to **86** in higher yield and with no greater difficulty.

With three of the four targeted C-11 ligands in hand, work to convert **88** to isothiocyanate **90** was initiated. Although the conversion of azide to isothiocyanate has been described many times before, a number of the published reaction conditions when applied to **88** failed to produce material that exhibited the broad 2200 and 2100 cm^{-1} stretching in the infrared spectrum characteristic of an -NCS group.¹⁰³ Initial attempts at the Staudinger/aza-Wittig were performed on a model system in which cyclohexylmethyl azide was cleanly converted to cyclohexylmethyl isothiocyanate by treatment with triphenylphosphine in chloroform followed by carbon disulfide. However, the same conditions applied to **88** produced a complex reaction mixture with none of the desired product detected by IR or LCMS. Changing the solvent to dioxane, toluene, or benzene, at either room temperature or reflux, and using purified reagents provided similarly complex mixtures.

While it is still unclear why this transformation was so troublesome on the real system, the transformation of azide to isothiocyanate was attempted by Mr. Ogawa using carbon disulfide and triphenylphosphine during the synthesis of **81** and **82** from their corresponding azides with no success (**Figure 21**).^{70b} The Staudinger reaction has been shown through DFT calculations to prefer a *cis* trajectory with regard to the azide nitrogen bound to carbon ($-\text{CH}_2\text{N}=\text{N}=\text{N}$),⁹⁹ and this approach may be challenged by the preferred orientation of azide **88**. Moreover, during the attempts to transform C-11 azide to isothiocyanate, starting material could be observed by TLC, suggesting that the initial Staudinger reaction, which provides the iminophosphorane ($-\text{CH}_2\text{N}=\text{PPh}_3$) required for the aza-Wittig reaction with carbon disulfide, was disfavored resulting in side reactions. The failure of the Staudinger/aza-Wittig led to the examination of another route to **90** which could be exploited provide C-9 functionalized ligands as well.



Scheme 19: Retrosynthetic Analysis using C-11 Oxime

Aldehyde **130** could provide, *via* reductive amination, primary amine **137** that could be converted to isothiocyanate **90** in one additional step. A major complication of the reductive amination of aldehydes to primary amines is the potential to form symmetric secondary amines. To avoid this, numerous methods have been developed, but the most versatile of these is one which proceeds through an oxime intermediate (**136**; **Scheme 19**). This oxime could not only provide access to a C-11 amine (**137**), but access to two other targets belonging to the C-9 series as well, nitrile **85** and isothiocyanate **89** (**Scheme 19**).

The rearrangement of oxime to isothiocyanate has been described by Kim,¹⁰⁰ and was subsequently validated by Rawal¹⁰¹ during the total synthesis of *N*-methylwelwitindolinone

derivatives. This reaction proceeds through the hydroximoyl chloride (**VI**) of an aldoxime that is formed by exposure to *N*-chlorosuccinimide, which is treated with triethylamine to provide a nitrile oxide (**VII**; **Figure 27**). This nitrile oxide then undergoes a [3+2] cycloaddition with thiourea in a second step to form an oxathiazoline (**VIII**) *in situ* which rapidly rearranges to the desired isothiocyanate **89** expelling urea in the process (**Figure 27**).

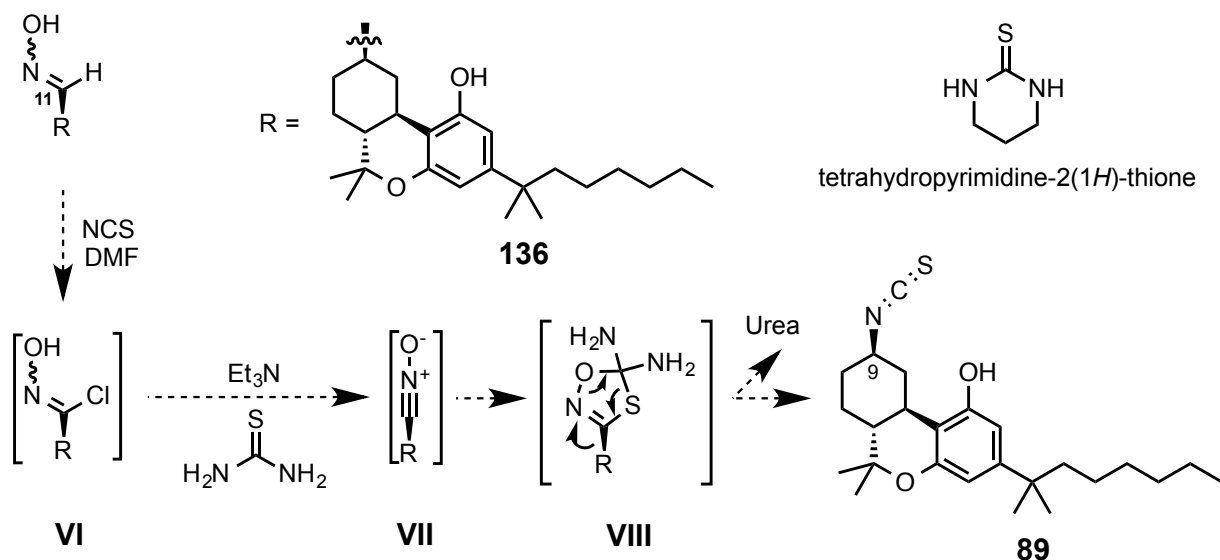


Figure 27: C -9 Isothiocyanate Formation from C-11 Aldoxime *via* Hydroximoyl Chloride **VI**

This transformation would provide the C-9 isothiocyanate and avoid entirely the conversion of azide to isothiocyanate that was found to be challenging in the C-11 series. Moreover, the aldoxime to isothiocyanate rearrangement has been shown to proceed with retention of stereochemistry at the α carbon atom, further simplifying the synthesis of **89** which would retain the β -equatorial orientation of **136**.

Oxime **136** was rapidly formed upon heating **130** with hydroxylamine hydrochloride ($\text{NH}_2\text{OH}\cdot\text{HCl}$) and Et_3N in dimethylsulfoxide (**a**; **Scheme 20**).¹⁰² After chromatography, a ~3:1

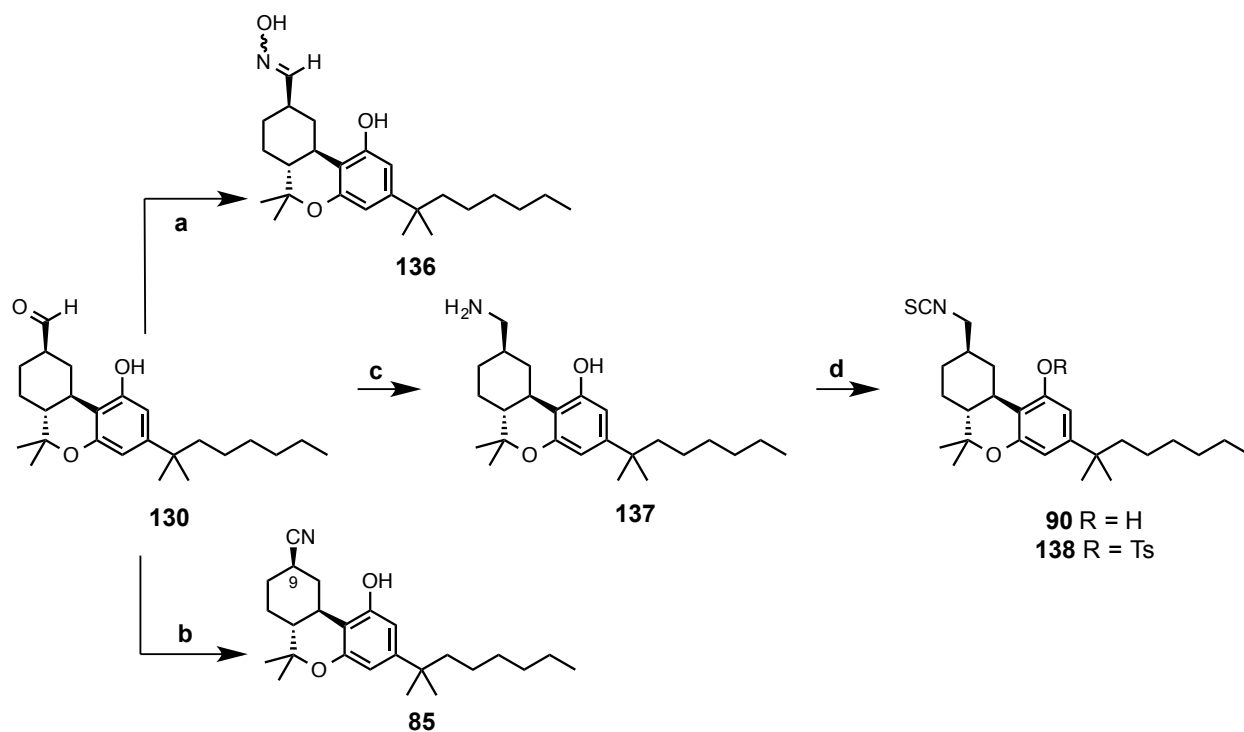
trans:cis mixture of aldoximes was isolated in 82% yield. Following Kim's procedure, the purified oximes were suspended in DMF with one equivalent of *N*-chlorosuccinimide. Using the modifications of Rawal and coworkers, tetrahydropyrimidine-2(1H)-thione and triethylamine were added to this solution. These conditions did provide a C-9 isothiocyanate, however, the reaction mixture also contained unreacted C-11 aldoxime. Moreover, the electron rich aromatic ring of **136** and **89** underwent mono- and dichlorination at C-2 and C-4 rendering a six component reaction mixture. The unwanted chlorination was a result of the electrophilic source of chlorine and is not surprising, although we had hoped that the formation of the hydroximoyl chloride would be faster than aromatic chlorination.

Examining other methods for the formation of hydroximoyl chlorides from aldoximes revealed an interesting reagent, *N*-*tert*-butyl-*n*-chlorocyanamide (NTBNCC).¹⁰³ This reagent, although a powerful electrophilic source of chlorine, had been shown to provide hydroximoyl chlorides of substrates incorporating electron-rich aromatic rings or even free phenols *without* chlorination of the ring.^{103a} Thus, 4-hydroxybenzaloxime was treated with NTBNCC in dichloromethane in the presence of tetrahydropyrimidine-2(1H)-thione followed by Et₃N. Although this model system has functionality that both activates and deactivates the aromatic ring, these conditions provided the desired isothiocyanate *without* chlorination of the aromatic system. Unfortunately, when this reaction was repeated with oxime **136**, the dually activated electron rich aromatic system was chlorinated. Although discouraging, the formation of a hydroximoyl chloride need not be the only method to prepare the C-9 isothiocyanate from the C-11 oxime.

The mechanism of the transformation described by Kim depends upon the formation of a nitrile oxide, and numerous methods have been developed for this task.¹⁰⁴ Searching for a procedure that would produce nitrile oxides while employing reagents which do not lead to substitution on electron rich aromatic systems suggested a number of iodine reagents.¹⁰⁵ The

most attractive of these reagents was diacetoxyiodobenzene (DIB), which was described by Singhal and coworkers^{105e} and was used to oxidize aromatic oximes to nitrile oxides *in situ*. Although applied to the formation of di- and trisubstituted isoxazoles *via* [3+2] cycloaddition with electron poor olefins, this method should lead to the same unstable intermediate **VIII** in the presence of thiourea, which upon rearrangement would provide isothiocyanate **89**. Unfortunately, treating the model hydrocinnamaldoxime with DIB in acetonitrile and water in the presence of tetrahydropyrimidine-2(1H)-thione did not produce the corresponding isothiocyanate, but instead returned the oxime unchanged. Altering the reaction conditions with additional sodium acetate to encourage the formation of the crucial nitrile oxide, and/or by using CS₂ to act as a less electron rich carbon-sulfur olefin were both unsuccessful at forming an isothiocyanate from hydrocinnamaldoxime. The failure to generate a nitrile oxide from the model system was discouraging given the simplification this reaction would grant to the synthesis of **89**.

Turning attention to the other C-9 functionalized ligand which is derived from the C-11 aldoxime, **130** was treated with NH₂OH•HCl in DMSO and heated for one hour.¹⁰² This allowed for a simple one step formation of C-9 nitrile in 86% yield after chromatography (**b**; **Scheme 20**). Although the stepwise formation of **85** was also possible by the subsequent treatment of purified **136** with hydrochloric acid in DMSO, this two step process led to a lower yield than the one step procedure and also required more effort, so this approach was abandoned.



Scheme 20: Functional Group Conversions of C-11 Aldehyde^a

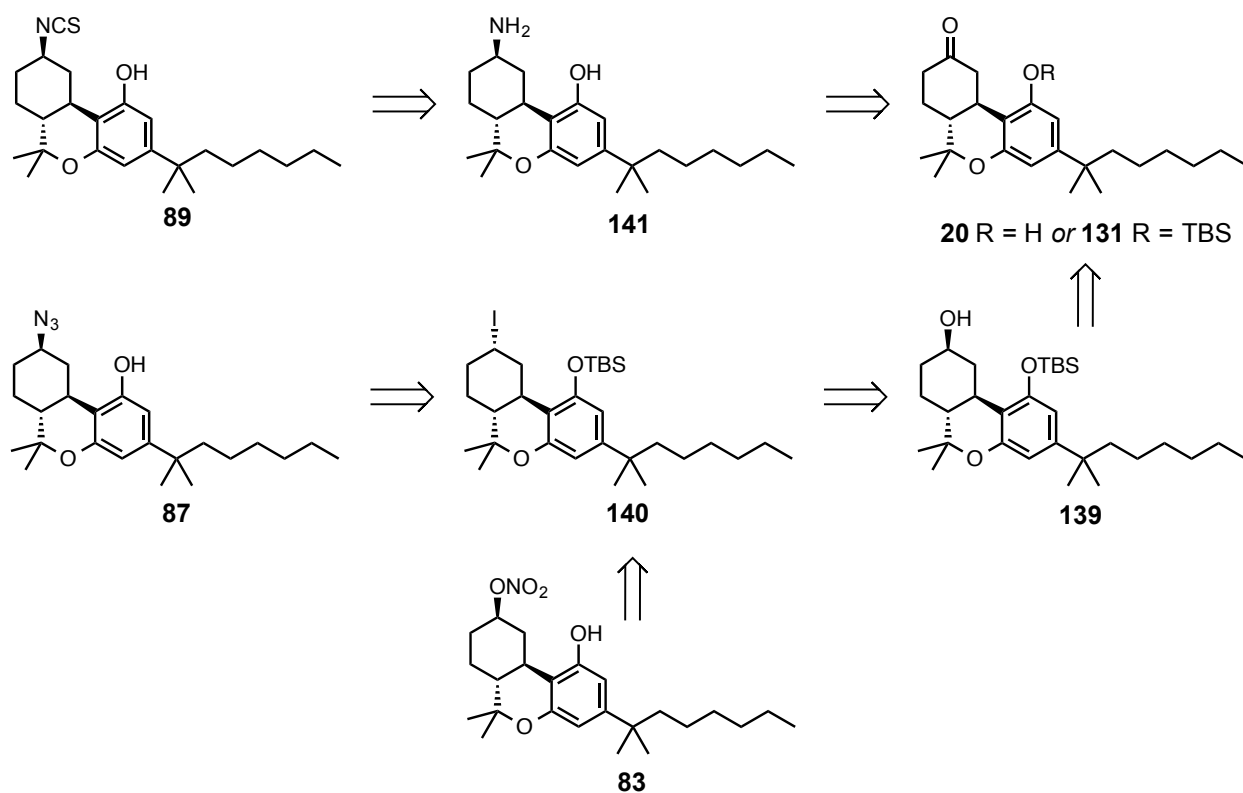
^aReagents and Conditions: (a) $\text{NH}_2\text{OH}\cdot\text{HCl}$, Et_3N , DMSO, 90°C , 1 h; 82%; (b) $\text{NH}_2\text{OH}\cdot\text{HCl}$, DMSO, 90°C , 1 h; 86%; (c) $\text{NH}_2\text{OH}\cdot\text{HCl}$, EtOH, rt, 6 h, then Zn^0 , HCl (conc.) (d) CS_2 , Et_3N , THF, 0°C , 2 h, then *p*-TsCl, 0°C to rt, 2 h; 61% from **130**

Primary amine **137** could be obtained by the reduction of either **136** or nitrile **85** using lithium aluminum hydride, but these routes were poor yielding, mostly due to difficulties encountered during the isolation of the product from the reaction mixture. The most convenient and simple stepwise reductive amination which provided primary amine **137** was performed by treating aldehyde **130** with hydroxylamine hydrochloride in ethanol, followed by the addition of zinc dust and concentrated HCl (c; **Scheme 20**).^{106a} This reaction was further simplified by a clever work-up which eased the isolation of the **137**. Primary amines have been shown to form complexes with Zn^{2+} which is produced during the course of this reduction,^{106b} however, treatment of the resulting crude reaction mixture with ammonia in the presence of sodium

hydroxide can dissociate this complex, allowing the desired primary amine to be isolated by a simple extraction with DCM. This crude amine was then used to provide the final C-11 ligand, isothiocyanate **90**. Treating the primary amine with triethylamine and carbon disulfide followed by *p*-toluenesulfonyl chloride (*p*-TsCl) as described by Ho¹⁰⁷ provided a 3:1 mixture of isothiocyanates; the desired **90**, and phenolic tosylate **138** (**Scheme 20**). The formation of **138** could be suppressed by using equimolar amounts of *p*-TsCl and **137**. Using optimized conditions **90** was produced in 61% overall yield from aldehyde **130** (**d**; **Scheme 20**).

This concluded the total synthesis of the four C-11 targets, all of which could be obtained in seven synthetic steps in overall yields between 41-54% from optically active nabilone. This route also conveniently provided C-9 nitrile **85** after 6 steps in 58% overall yield from (-)-nabilone.

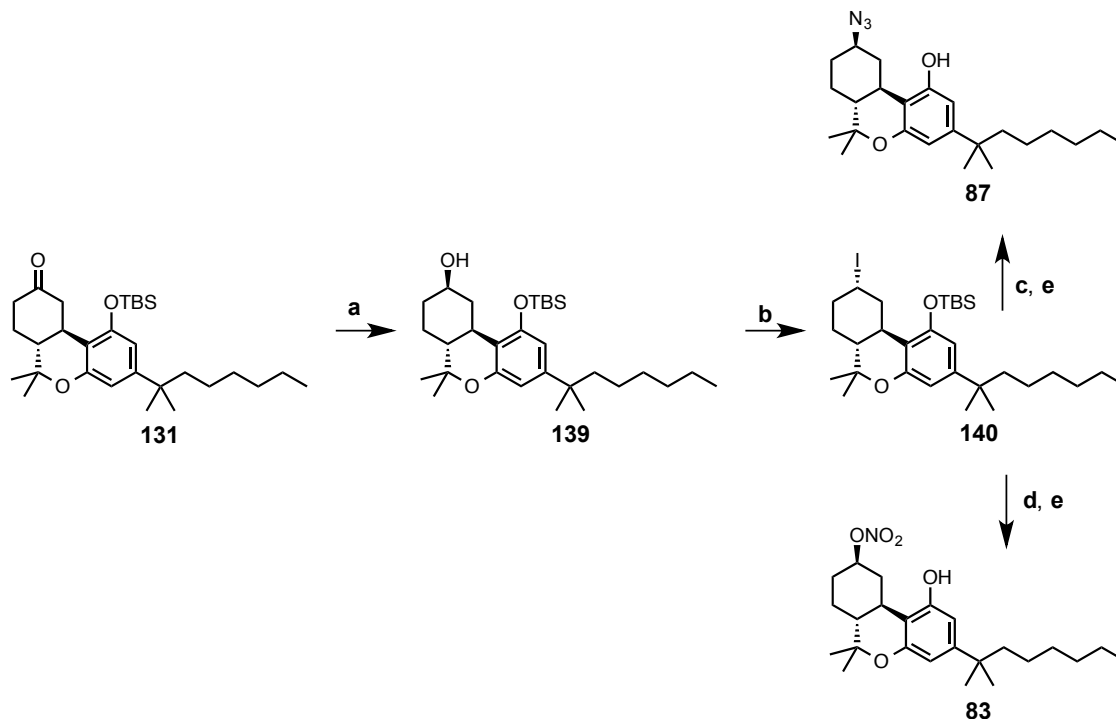
The remaining three targets consisted of C-9 nitrate ester, azide, and isothiocyanate. The relative ease by which the C-11 nitrate ester and azide were produced *via* iodide **135** led the author to a similar synthetic plan for the C-9 targets, using axial iodide **140** (**Scheme 21**). Given the challenge presented by the direct conversion of C-11 azide to the corresponding isothiocyanate, a stereospecific reductive amination of **20** to produce **141** was considered for the expeditious synthesis of **89** (**Scheme 22**). Whether this reductive amination would proceed through an oxime intermediate, as with the C-11 series, was unclear at the time and both methods were eventually explored.



Scheme 21: Retrosynthetic Plan for Remaining C-9 Targets

Starting with the more straightforward synthesis of the secondary iodide **140**, phenolic silyl ether **131** was reduced with sodium borohydride to afford secondary equatorial alcohol **139** in 85% yield (**a**; **Scheme 22**). Treatment of **139** under the Mitsunobu conditions previously described for the preparation of the C-11 primary iodide led to a large amount of Δ^8 and Δ^9 elimination products. This was unfortunate but not surprising given the elevated temperature used for this transformation, and that the axial iodide is locked into the ideal configuration for elimination with two different antiperiplanar α -hydrogens. The unwanted elimination could be ameliorated by reducing the temperature at which this reaction was performed. Similar to the C-11 series, crude iodide **140** was used directly for the substitution with either sodium azide or

silver nitrate providing **87** or **83** after deprotection in 65% or 72% yield over three steps, respectively (**b**, **c** or **d**, then **e**; **Scheme 22**).



Scheme 22: Formation of and Substitutions on Advanced Intermediate **140^a**

^aReagents and Conditions: **(a)** NaBH₄, EtOH, 0 °C to rt, 85%; **(b)** Ph₃P, imidazole, I₂, PhH, 50 °C, 1 h; **(c)** NaN₃, DMF, rt, 12 h; 65% after **e** (three steps); **(d)** AgNO₃, CH₃CN, rt, 12 h; 72% after **e** (three steps) **(e)** *n*-Bu₄NF, Et₂O, rt, 1 h

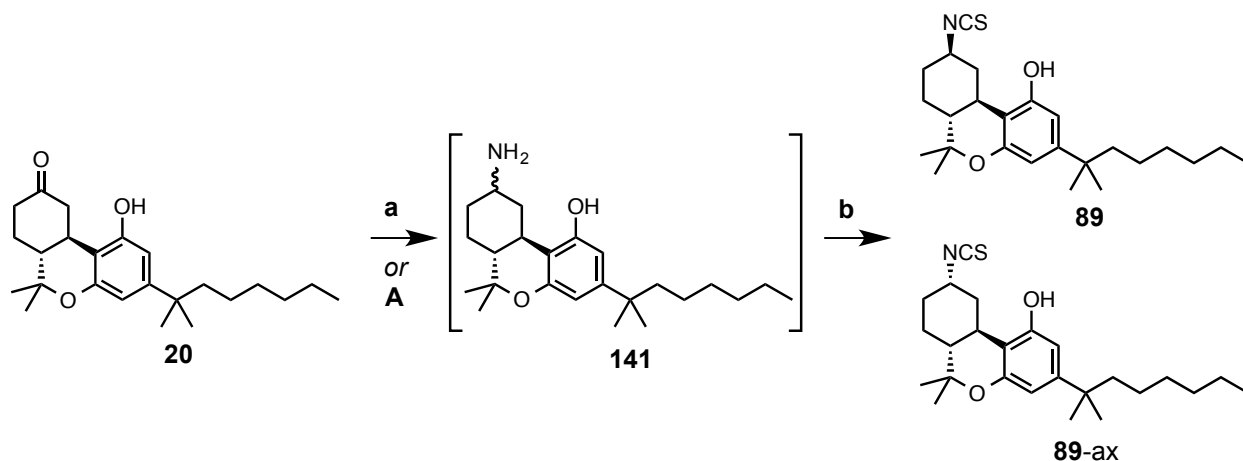
The reductive amination needed to furnish primary amine **141** posed a greater challenge than that of the C-11 amine because stereochemistry at C-9 had to be controlled. While there is a large volume of research dedicated to reductive aminations of cyclic ketones,¹⁰⁸ we desired a simple method that could control stereochemistry without the need for expensive or exotic ligands or catalyst. Moreover, to provide the desired β-equatorial primary amine at C-9, a small

reducing agent would need to be employed to favor axial approach to the rigid tricyclic scaffold. With this in mind, the stepwise reductive amination of the C-9 ketoxime was initially attempted.

Although the method employed for the preparation of C-11 amine was not described for ketoximes, its experimental ease and success urged its employment for the stepwise reductive amination of (-)-**20**. (-)-Nabilone was treated with hydroxylamine hydrochloride in ethanol followed by zinc dust and hydrochloric acid. Unfortunately, this provided only a mixture of *cis* and *trans* oximes which were not reduced by the treatment with Zn⁰ and HCl. Turning our attention to other stepwise methods of reductive amination which could provide **141**, the ketoxime derivatives of (-)-nabilone were heated in methanol with ammonium formate and Zn⁰ following the work described by Abiraj or Johnson.¹⁰⁹ Unfortunately neither of these methods was successful in producing the primary amine **141**, and left the mixture of ketoximes unchanged.

Contemporaneously with the ketoxime reductions discussed above, one-step reductive aminations of (-)-**20** were attempted. The comprehensive review of the reductive amination of carbonyls using sodium triacetoxyborohydride which has been written by Abdel-Magid and coworkers described the stereoselective synthesis of primary amines from ketones.^{108a} When these methods were applied in combination with experimental efforts described by Cabral and coworkers¹¹⁰ an attractive procedure for the production of **141** was developed. Thus, (-)-nabilone was dissolved in methanol in the presence of sodium cyanoborohydride (NaBH₃CN) and ammonium acetate (NH₄OAc, **a**; **Scheme 23**). Within a day this produced a crude primary amine that was subjected to standard isothiocyanation conditions (**b**; **Scheme 23**). After purification of the final product, this two step process provided isothiocyanates **89** in 37% yield as a 3.2:1 β:α ratio. Due to the success, simple reagents, and experimental ease of this reductive amination method, the reductions of ketoximes were not examined any further. The synthesis of **89** was improved by conducting the reductive amination at a lower temperature.

Additionally, acetic acid was added to the reaction mixture to encourage imine formation. Keeping the temperature of the reduction at 4 °C for 48 hours provided a 4.3:1 *dr* after isothiocyanation to **89** while increasing the yield to 71% over two steps (**b**; **Scheme 23**). Noting the increased diastereoselectivity at lower temperature encouraged further investigation, and the reductive amination of (-)-**20** was repeated at -15 °C. The decreased temperature did further improve the *dr* to 5.1:1 of β : α amines as judged by the integration of the resulting C-9 methine proton by ¹H NMR. However, the amination did not proceed to completion at this temperature after 5 days, and following the isothiocyanation of **141**, the mixture of **89-ax** and **89** was isolated in 49% yield. This decrease in yield is presumably caused by the low solubility of NaBH₃CN in methanol at low temperature, an issue which has been previously noted with NaBH₄ and shown to cause similar deleterious effects on reductive aminations.¹¹⁰ While the lack of stereospecificity is an issue for the synthesis of **89**, or more specifically **141**, this method is simple to perform, requires no exotic reagents, and the only byproduct is **89-ax**, which can be separated from the desired **89** by chromatography.



Scheme 23: Reductive Amination of Nabilone^a

^aReagents and Conditions: **(a)** NaCNBH₃, MeOH, NH₄OAc, 4 °C, 24 h; **(b)** CS₂, Et₃N, THF, 0 °C, 2 h, then *p*-TsCl, 0 °C to rt, 2 h; 71% from (-)-**20**

This concludes the total synthesis of the functionalized C-9 and C-11 classical cannabinoid series. Ligands **83 - 90** have been transferred to our collaborators at Northeastern University, who are charged with the completion of ligand binding assays, structure activity relationships, and ligand assisted protein structure experiments.

In Chapter 2, the synthesis of enantioenriched ketocannabinoids was described. The improvements to the synthetic route to ketocannabinoids have been exemplified by the abbreviated total synthesis of enantiopure nabilone — whose racemate is the only synthetic cannabinoid to currently hold FDA approval. The state of the art total synthesis of (-)-nabilone prior to the work of Chapter 2 was accomplished in 5 steps to afford 28% overall yield. Revisions herein allow (-)-nabilone to be prepared in 5 steps, but increase the overall yield to 65% by utilizing a Brønsted acid catalyzed Michael addition to apoverbenone which had been overlooked for decades. The high yield is complemented by a filtration process developed for the Michael adduct, which is provided in exceptional *ee* as is the resulting (-)-nabilone following cyclization. Additionally, the abbreviated synthesis exhibits greater experimental ease than the previously described routes and avoids the use of highly toxic lead tetraacetate which has served as a constant reminder of the era in which the total syntheses of (-)-nabilone and ketocannabinoids were initially reported.

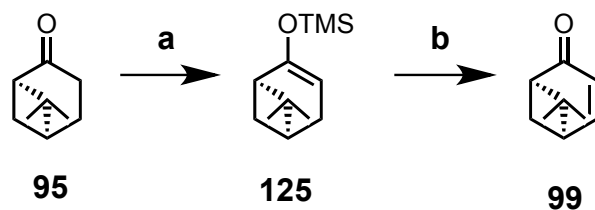
Chapter 3 utilized the work of the previous chapter by describing the derivitization of nabilone to eight target ligands — the syntheses of which is described. These eight ligands were prepared to examine the pharmacological properties of the azide, cyano, isothiocyanate, and nitrate ester functionality at C-9 and C-11 of the classical cannabinoid scaffold. The challenges that have been encountered during the preparation of these ligands have been largely overcome with the exception of the reductive amination of (-)-nabilone which is not highly stereoselective but is simple to perform and adequate for the preparation of C-9 β -isothiocyanate **89**.

With a more efficient route to highly enantiopure (-)-nabilone and related synthetic cannabinoids at the disposal of chemists, many more unique ligands can be prepared and examined for their pharmacological properties. The availability of functionalized bi- and tricyclic cannabinoids will enable the mapping of the CB₁ and CB₂ receptors. A better knowledge of the receptor binding site may make it possible to design cannabinoids with modulated selectivity and affinity for CB₁, CB₂, or both cannabinoid receptors to potentially aid in the selective manipulation of the endocannabinoid system. Attached is a description of the key experiments performed.

Experimental

General

^1H NMR and ^{13}C NMR spectra were recorded at 500 MHz (^1H) and 126 MHz (^{13}C). Chemical shifts are reported in parts per million (δ) and are referenced to the solvent, i.e. 7.26/77.0 for CDCl_3 . Multiplicities are indicated as; app (apparent), br (broadened), s (singlet), d (doublet), t (triplet), q (quartet), p (pentet), or m (multiplet). Coupling constants (J) are reported in Hertz (Hz). Thin layer chromatography (TLC) was performed on glass plates 250 μm , particle size 5-17 μm , pore size 60 Å. Flash column chromatography was performed on silica gel, 200-400 mesh, or premium silica gel, 60 Å, 40-75 μm . All moisture sensitive reactions were performed under a static atmosphere of nitrogen or argon in oven-dried or flame-dried glassware. Purity and homogeneity of all materials was determined to be at least 95% from TLC, ^1H NMR, ^{13}C NMR, and LC–MS. Target ligands prepared for biological examination were purified to 99% as evaluated at 254 nm as well as 230 nm by normal phase HPLC using a Shimadzu system consisting of LC-20AT solvent delivery modules, an SPD-20A VP diode photodiode array detector, and an SCL-20A VP system controller. High-resolution mass spectrometric data were obtained on an Agilent LC-MSTOF with ESI ionization in the positive or negative mode. All infrared spectroscopy were measured using a Shimadzu IRAffinity-1 FT-IR using NaCl plates. All optical rotations were measured on a Jasco-DIP-370 polarimeter at the sodium line (589 nm) in a 0.1 dL cell and concentration, c , is expressed in g/100mL. Melting points were measured using a DigiMelt MPA 160.



Synthesis of 99 — (Scheme 8; Chpt. 2). Under N₂, diisopropylamine (2.33 g, 23.03 mmol, 1 eq) was dissolved in THF (23 mL, 1 M) and cooled to -78° C. A solution of *n*-BuLi (10 mL of 1.4 M solution in hexanes, 21.87 mmol, 0.95 eq) was added dropwise to the diisopropylamine solution and the resulting mixture was stirred for 10 minutes at -78 °C. The resulting LDA solution was warmed to 0 °C and let stir for 10 minutes before cooling again to -78 °C.

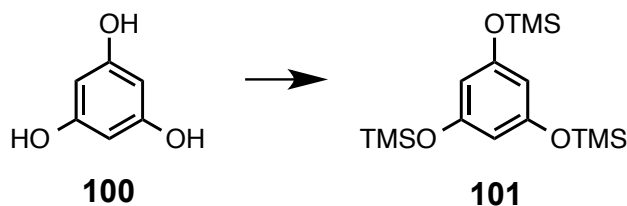
In a separate flame dried flask under N₂, **95** (2 g, 14.47 mmol) was dissolved in THF (4 mL) and slowly added to the LDA solution. The reaction was allowed to stir at -78 °C for one hour to ensure adequate enolate formation. TMSCl* (2.52 g, 23.15 mmol, 1.6 eq) was then added to the solution and stirring was continued at -78 °C for 10 minutes. At this time, the reaction mixture was warmed to 0 °C and stirred for an additional 10 minutes before the addition of aqueous NH₄Cl. The aqueous phase was extracted with EtOAc (3x), and the combined organic layers were washed with water and brine before drying over MgSO₄ and concentrating under reduced pressure. The crude silyl enol ether was azeotroped in benzene to afford intermediate **125** (3.03 g, 99% yield).

A flame dried, 2-neck flask equipped with a 3-way gas inlet and O₂ balloon was charged with Pd(OAc)₂ (0.161 g, 0.72 mmol, 0.05 eq). Anhydrous DMSO (150 mL, 0.096 M) was added to the flask and the resulting suspension was vigorously stirred. Crude **125** (3.03 g, 14.46 mmol) was added to the resulting suspension and the reaction mixture was purged with oxygen twice before stirring at room temperature for 36 h under an O₂ atmosphere. After 36 hours water was added to the reaction mixture and the aqueous layer was extracted with Et₂O (3x). The organic

layers were combined and washed with water and brine before drying over MgSO_4 and concentrating under reduced pressure. The resulting oil was purified *via* flash chromatography (5:95 EtOAc:Hexanes as eluent) to afford **99**** (1.67g, 85% yield) as a clear oil. Alternatively **99** may be distilled under reduced pressure following the method described by Grimshaw in *J. Chem. Soc. Perkin Trans. I*, **1972**, 50–52. Spectral data matched previous report by Grimshaw. $R_f = 0.60$ (1:4 EtOAc:*n*-hexanes); $[\alpha]^{20}_D +311.0^\circ$ (*c* 2.4, CHCl_3) [lit.^{84a} $[\alpha]^{25}_D +319^\circ$ (*c* 2.4% in CHCl_3)]; ^1H NMR (500 MHz, CDCl_3) δ 7.50 (dd, $J = 8.7, 7.0$, Hz, 1H), 5.92 (dddd, $J = 8.9, 1.7, 1.0, 1.0$ Hz, 1H), 2.82 (dddd, $J = 9.7, 5.5, 5.5, 1.0$ Hz, 1H), 2.68 (ddd, $J = 6.1, 6.1, 1.9$ Hz, 1H), 2.57 (app q, $J = 5.8$ Hz, 1H), 2.11 (app d, $J = 9.2$ Hz, 1H), 1.48 (s, 3H), 1.00 (s, 3H); ^{13}C NMR (125 MHz, CDCl_3) δ 204.2, 157.1, 125.7, 58.7, 55.1, 43.9, 42.0, 26.6, 22.3; IR (neat); 2980, 2955, 2872, 1683, 1468, 1387, 1369, 1302, 1279, 1245, 1233, 1202, 1130, 1064, 1043, 978, 859, 840, 789, 764, 731, 668 cm^{-1} ; HRMS (ESI) m/z : 137.0961 $[\text{M}+\text{H}]^+$. Exact mass calculated for $\text{C}_9\text{H}_{12}\text{O}$ 136.0888; found 136.0882.

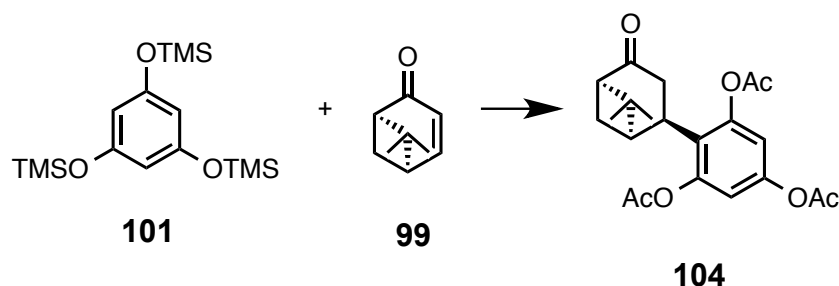
*Note: TMSCl was either distilled prior to use *or* pre-mixed with Et_3N and centrifuged prior to use avoid introducing residual HCl.

Note: Using 5% $\text{Pd}(\text{OAc})_2$ to catalyze the Saegusa-Ito oxidation of **125 provides a 96:4 mixture of **99** and **95** as determined by ^1H NMR. See **Appendix I**, pages 179-181.



In general: Silylation was performed according to the procedure outlined by M. A. Tius et al. in *J. Med. Chem.*, **2010**, 53, 5656-5666. Due to the instability of **101**, it is freshly prepared before use.

Synthesis of 101 — (c; **Scheme 10**; **Chpt. 2**). A flask equipped with a strong stir bar and under a N₂ atmosphere was charged with phloroglucinol, **100** (5.50 g, 43.7 mmol) suspended in CH₂Cl₂ (300 mL, 0.15 M) and cooled to 0° C. Triethylamine (24.3 mL, 174.6 mmol, 4 eq) was added to the suspension followed by slow addition of TMSCl (22.3 mL, 174.6 mmol, 4 eq). The reaction mixture was allowed to warm to room temperature and was monitored by TLC. [eluting with EtOAc:Hexanes 1:4, **100** R_f = 0.01, **101** R_f = 0.92]. When the reaction was complete (~3 h) the reaction was quenched with saturated aqueous NH₄Cl. The organic layer was separated, washed with brine and water, and dried briefly over Na₂SO₄ and concentrated under reduced pressure. The resulting residue was azeotroped with benzene to provide crude **101** (12.57 g, 84% yield), as a ruby colored oil which was used without further purification.

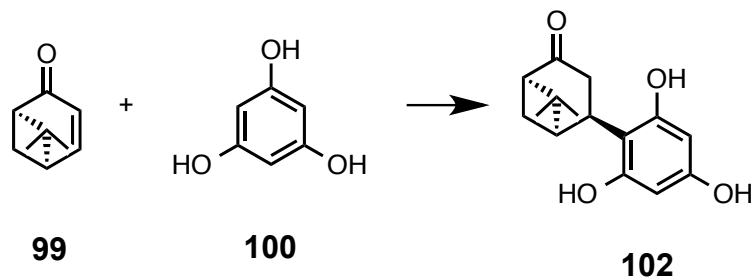


Synthesis of 104 — (d, e; Scheme 10; Chpt. 2). A dry 2-neck round bottom flask equipped with a stir bar, septum and 3-way gas inlet was purged with nitrogen. Under a stream of nitrogen vanadyl triflate* (36 mg, 0.1 mmol, 0.1 eq) and freshly generated **101** (685.3 mg, 2.0 mmol, 2.0 eq) were added to the reaction vessel. The mixture of catalyst and **101** was allowed to stir under inert atmosphere briefly before the addition of CH₂Cl₂ (9 mL) to the flask. In a separate dry flask **99** (136.2 mg, 1.0 mmol) was dissolved in CH₂Cl₂ (1 mL) and added to the 2-neck flask *via* cannula. The reaction mixture was stirred at ambient temperature until judged to be complete by TLC (~48 h), at which point the reaction mixture was transferred to a separatory funnel using EtOAc. Warm water (~50 °C) was added to the reaction mixture and the organic layer was separated. The aqueous phase was extracted with EtOAc, and the combined organic layers were dried over Na₂SO₄, and concentrated *in vacuo*.

To the resulting residue was added DMAP (6.1 mg, 0.05 mmol, 0.05 eq) followed sequentially by DCM (10 mL), pyridine (0.644 mL, 8.0 mmol, 8 eq), and acetic anhydride (754 mL, 8.0 mmol, 8 eq). This mixture was allowed to stir for 12 hours at room temperature before cold water was added to the reaction mixture. The organic layer was washed with 1M HCl, brine, dried over MgSO₄, and concentrated under reduced pressure. Purification by flash chromatography (1:4 EtOAc:*n*-hexanes eluent) provided **104** (166 mg, 63% yield over two steps) as a white solid. Spectral data matched previous reports by Dixon in *J. Med. Chem.* **2010**, 53, 5656–5666.

Note:* Vanadyl triflate was prepared as described by Chien-Tien Chen *et al.* in *Org. Lett.* **2007, 9, 5195-5198, as follows:

To a 50-mL, two-necked, round-bottomed flask was added vanadyl sulfate, vanadyl sulfate (342 mg, 2.1 mmol) followed by addition of MeOH (2 mL). To the methanolic solution of vanadyl sulfate was slowly added a solution of Ba(OTf)₂ (872 mg, 2.0 mmol) in MeOH (2 mL) at ambient temperature. After stirring for 30 min, the reaction mixture was filtered through a short pad of dry Celite® to remove the precipitate, barium sulfate. The filtrate was concentrated to give faint blue solid which was further dried at 120 °C for 4 hours under vacuum to furnish vanadyl triflate (622 mg, 85% yield) as a blue powder, which was stored in a dessicator.



Synthesis of 102 — (b; Scheme 13; Chpt. 2). A dry 2-neck round bottom flask equipped with a stir bar, septum and an addition funnel with a metering stopcock and 3-way gas inlet was purged with nitrogen. Under a stream of nitrogen **100** (116.0 mg, 0.92 mmol, 2 eq) followed by *p*-TsOH (114.0 mg, 0.60 mmol, 1.3 eq) were added to the reaction vessel and dissolved in acetone (1 mL). The mixture of acid and **100** were allowed to stir for until homogeneous (~3 min). In a separate dry flask **99** (63.0 mg, 0.46 mmol) was dissolved in DCE (4 mL) and added to the addition funnel *via* cannula. The entire system was purged with nitrogen for 5 min before the stopcock was opened at a flow rate of 1 drop/20 sec. *Note: A flow rate faster than this will result in the formation of large amounts of bis-addition denoted by heterogeneity of the reaction mixture.* When the addition of **99** to **100** was complete the reaction was quenched with phosphate buffer and extracted with EtOAc (3x). *Depending on the size of reaction, either of two extraction methods can be employed. A description of both follows;*

1. The organic layers were combined and washed with warm water (~70 °C; 5x)* before being dried over MgSO₄ and concentrated *in vacuo* to afford **102** (84.2 mg, 69% yield) as a white foam which was used without purification. Spectral data matched previous reports by Dixon in *J. Med. Chem.* **2010**, 53, 5656–5666.

2. Using an Aldrich® modified convertible liquid-liquid continuous extractor (**Figure 28**): A round bottom flask (**C**) equipped with a boiling chip, continuous extractor, and reflux condenser (**B**) is filled halfway with water and purged with nitrogen (**Figure 28**). The extractor (**G**) is also

filled halfway with water, and the stopcock (**D**) is opened to allow the water in **G** to flow through **E** to the round bottom flask. Under a stream of nitrogen the combined organic layers are carefully added to **G**. Heat is applied to the round bottom flask to achieve rapid reflux, which is continued until **100** is completely removed from the organic portion of **G** as judged by TLC (~24 h). The contents of **G** are transferred to a separator funnel where the aqueous layer is removed and the organic layer is washed with brine then dried over MgSO_4 and concentrated *in vacuo* to afford **102** (79.4 mg, 65% yield) as a white foam. Spectral data matched previous reports by Dixon in *J. Med. Chem.* **2010**, *53*, 5656–5666.

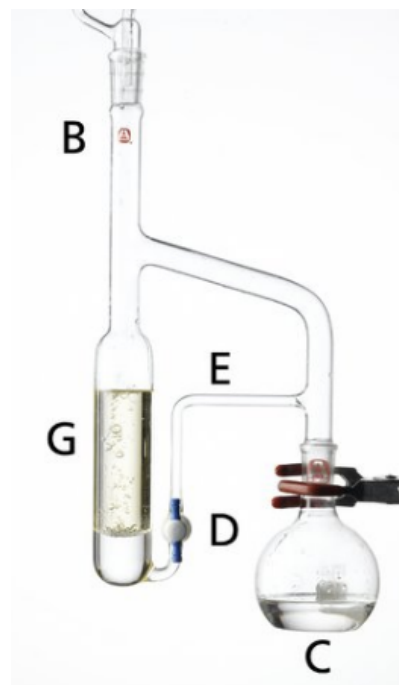
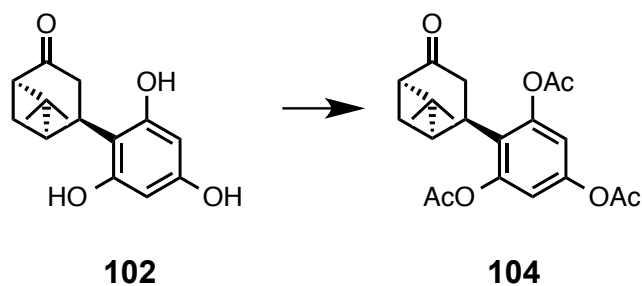
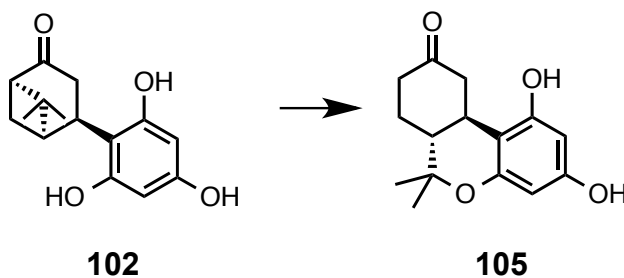


Figure 28: Continuous Extraction Apparatus, Courtesy of Sigma-Aldrich®, *ref.*^{92b}

**Note: Care should be taken when handling warm water. Also, EtOAc boils at 77.1° C — as such the warm water wash should be performed quickly in a separatory funnel to avoid the build up of excess pressure.*

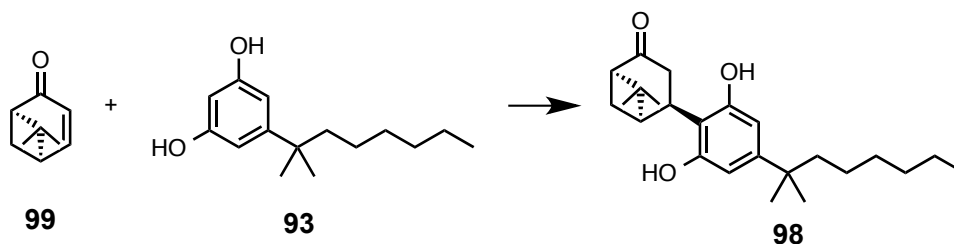


Synthesis of 104 — (c; **Scheme 13**; **Chpt. 2**) To the foam **102** (96.4 mg, 0.36 mmol) was added DMAP (2.0 mg, 0.02 mmol, 0.05 eq) followed sequentially by DCM (5 mL), pyridine (0.12 mL, 1.47 mmol, 4 eq), and acetic anhydride (0.140 mL, 1.47 mmol, 4 eq). This mixture was allowed to stir for 12 hours at room temperature before cold water was added to the reaction mixture. The organic layer was washed with 1M HCl, brine, dried over MgSO₄, and concentrated under reduced pressure. Purification by flash chromatography (1:4 EtOAc:*n*-hexanes eluent) provided **104** (117.5 mg, 82% yield) as a white solid. Spectral data matched previous reports by Dixon in *J. Med. Chem.* **2010**, 53, 5656–5666.



Synthesis of 105 — (d; **Scheme 13**; **Chpt. 2**) The foam of **102** (85.0 mg, 0.32 mmol) was dissolved in CH_3NO_2 (5 mL) and cooled to 0°C under a nitrogen atmosphere before the dropwise addition of TMSOTf (0.17 mL, 0.97 mmol, 3.0 eq). The reaction was stirred at 0°C for 2.5 hours before quenching with solid K_2CO_3 . The suspension was stirred for an additional 45 min before the solids were filtered off and the solution was concentrated under reduced pressure. The residue was purified by flash chromatography (50% EtOAc in hexanes eluent) to afford **105** (66.4 mg, 78% yield) as a white foam that typically contains 10-15% EtOAc. Spectral data matched previous reports by Dixon in *J. Med. Chem.* **2010**, 53, 5656–5666..

$J = 15.0, 3.5, 2.5$ Hz, 1H), 2.89 (ddd, $J = 15.0, 11.5, 3.5$ Hz, 1H), 2.63 (dddd, $J = 15.0, 4.0, 3.5, 2.0$ Hz, 1H), 2.47 (ddd, $J = 15.0, 13.5, 7.0$ Hz, 1H), 2.21-2.11 (m, 2H), 1.97 (ddd, $J = 12.0, 11.5, 2.5$ Hz, 1H), 1.56-1.46 (m, 3H), 1.48 (s, 3H) 1.28-1.15 (m, 6H), 1.21 (s, 6H) 1.13 (s, 3H), 1.10-1.02 (m, 2H), 0.84 (t, $J = 7.0$ Hz, 3H); ^{13}C NMR (125 MHz, CDCl_3) δ 213.7, 154.7, 154.2, 150.8, 107.7, 107.2, 105.5, 76.6, 47.3, 45.0, 44.3, 40.8, 37.3, 31.7, 29.9, 28.7, 28.6, 27.8, 26.8, 24.5, 22.6, 18.8, 14.0; IR (neat) 3300, 2920, 1680, 1580, 1420, 1370, 1330, 1265 cm^{-1} ; HRMS ESI m/z : 373.2743 $[\text{M}+\text{H}]^+$. Exact mass calculated for $\text{C}_{24}\text{H}_{36}\text{O}_3$, 372.2655; found, 372.2648.



Synthesis of 98 — (d; **Scheme 15**; **Chpt. 2**). To a dry 2-neck round bottom flask equipped with a 3-way gas inlet, stir bar, and septum was added *p*-toluenesulfonic acid (95.7 mg, 0.5 mmol, 0.1 eq) followed by white crystalline **93** (1.19 g, 5.03 mmol). The reaction vessel was then purged with N₂. In a separate dry flask **99** (760.2 mg, 5.58 mmol, 1.11 eq) was dissolved in dichloroethane (10 mL, 0.5M with respect to **93**) under N₂ and transferred to the 2-neck flask *via* cannula. The resulting reaction mixture was warmed to 60 °C at which point the reaction solution became homogenous. Stirring was continued at 60 °C for 24 h. The resulting heterogenous reaction mixture was concentrated under reduced pressure to provide a light brown amorphous solid. The solid was washed with cold DCE (3 x 1mL) to provide **98** (1.75 g, 94% yield - as determined from **93**) as a white solid. Purity of the solid was 99% as determined by LCMS and ELSD. Physical and spectral data with the exception of specific rotation and melting point were identical to those reported earlier in *ACS Med. Chem. Lett.* **2014**, 5, 400–404. **98**; R_f = 0.26 (1:4 EtOAc:*n*-hexanes eluent); mp 174.2–175.3 °C, [lit.⁷⁵ mp 171–174 °C]; [α]²⁰_D +83.6° (*c* 1.0, CHCl₃) and [α]²⁰_D +63.8° (*c* 0.1, CHCl₃), [lit.⁷⁵ [α]²⁰_D +55.8° (*c* 1.0, CHCl₃)]; ¹H NMR (500 MHz, CDCl₃) δ 6.28 (s, 2H), 5.14 (s, 2H), 3.94 (app t, *J* = 8.2 Hz, 1H), 3.51 (dd, *J* = 18.8, 7.8 Hz, 1H), 2.67–2.57 (m, 2H), 2.55–2.44 (m, 2H), 2.31 (app t, *J* = 5.5 Hz, 1H), 1.52–1.45 (m, 2H), 1.36 (s, 3H), 1.28–1.14 (m, 6H), 1.19 (s, 6H), 1.05 (m, 2H), 0.99 (s, 3H), 0.85 (t, *J* = 6.7 Hz, 3H); ¹³C NMR (125 MHz, CDCl₃) δ 216.9, 154.7 (2 C), 150.0, 113.5, 106.6 (2 C), 57.9, 46.8, 44.4, 42.2, 37.9, 37.2, 31.8, 30.0, 29.5, 28.7, 26.2, 24.6, 24.4, 22.7, 22.2, 14.1; IR (neat) 3300, 2920, 1680, 1580, 1420, 1370, 1330, 1265 cm⁻¹; HRMS ESI *m/z*: 373.2743 [M +H]⁺. Exact mass calculated for C₂₄H₃₆O₃, 372.2655; found, 372.2648.

Resolution of 98. Following flash chromatography, small amounts of **98** were resolved using a Shimadzu system consisting of LC-20AT solvent delivery modules, an SPD-20A VP diode photodiode array detector, and an SCL-20A VP system controller equipped with a Chiralpak OD column using 7% isopropanol in hexanes as the mobile phase at a flow rate of 2 mL/min. Additionally, **98** was filtered as described above and the freshly filtered crystals as well as the filtrate were resolved under the same conditions. Fractions were detected by UV ($\lambda = 254$ nm). Retention times for (+)-**98** and (-)-**98**, under these conditions were 4.2 min and 8.8 min, respectively, and the enantiomeric ratio, and consequently the enantiomeric excess, of **98** was determined by the integration of these peaks and are as followed: **Column:** 95.5:4.5; **Filtrate:** 71.8:28.2. No minor isomer was detected in **98** purified by **filtration**. The existence of (-)-**98** was confirmed by HRMS and ^1H NMR and the spectral data was identical to that obtained for **98**.

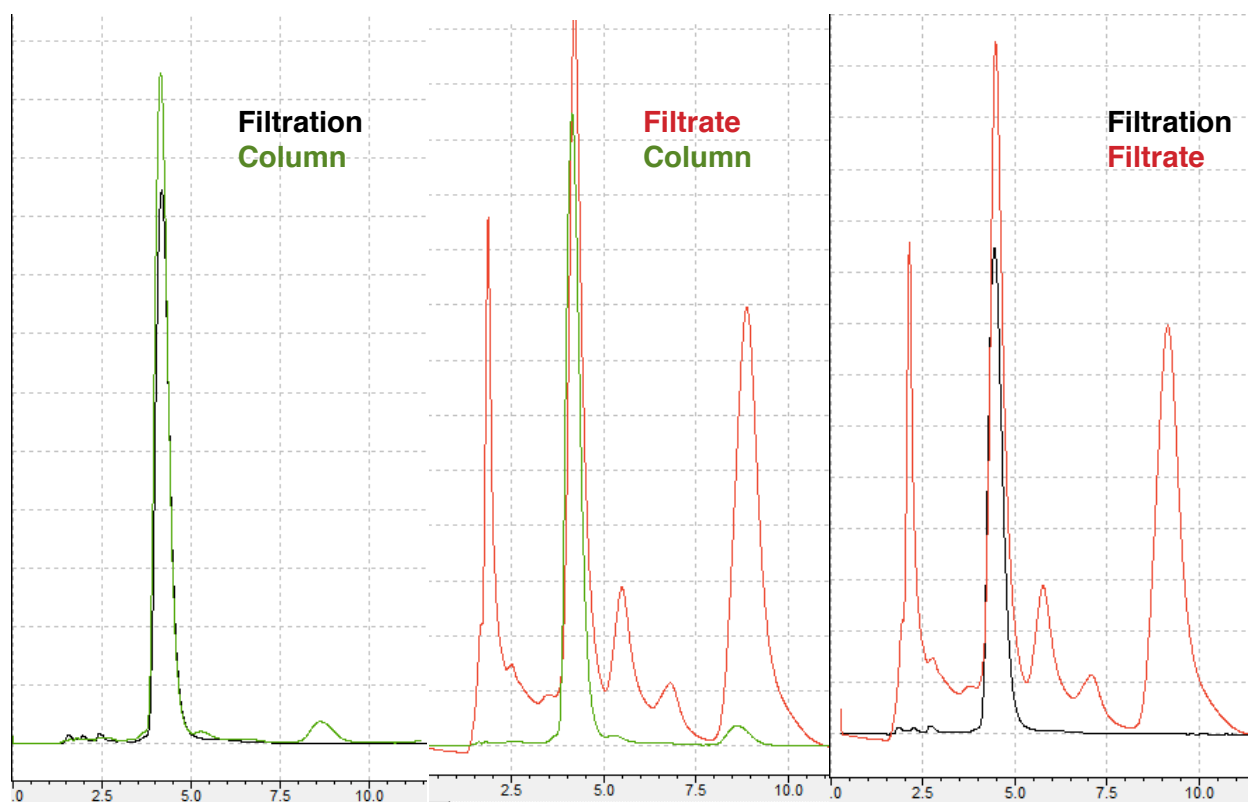


Figure 29: Overlaid Chromatograms Obtained from Chiral HPLC. **98** Purified by Flash Chromatography (**Green**), **98** Purified by Filtration (**Black**), Filtrate Obtained after Filtration of **98** (**Red**)

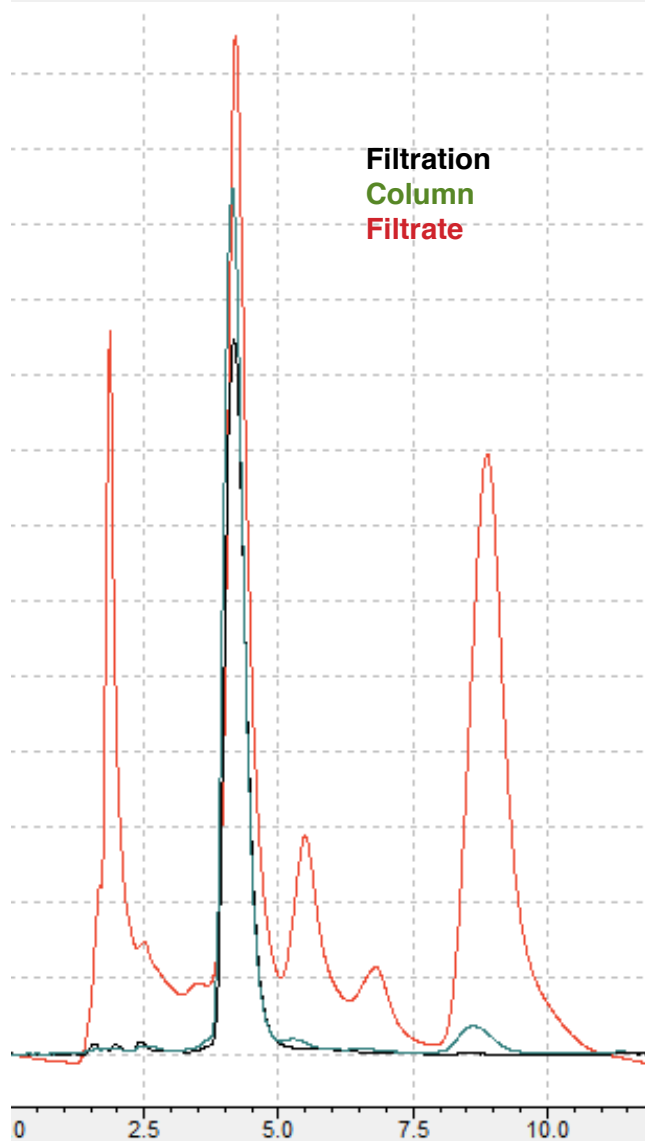
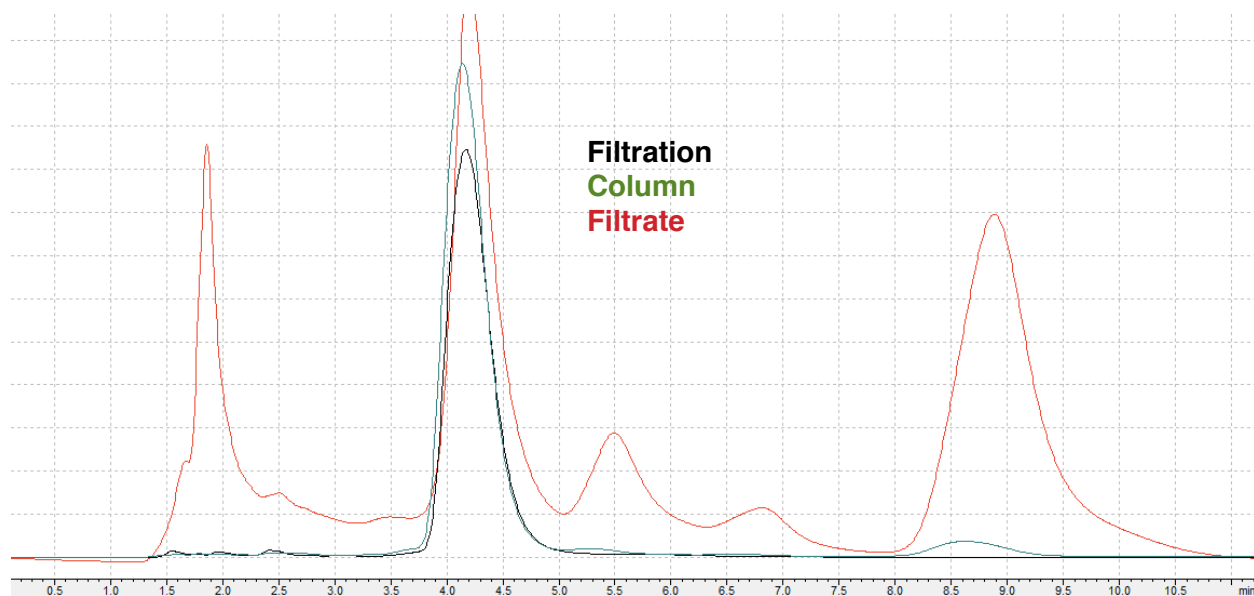
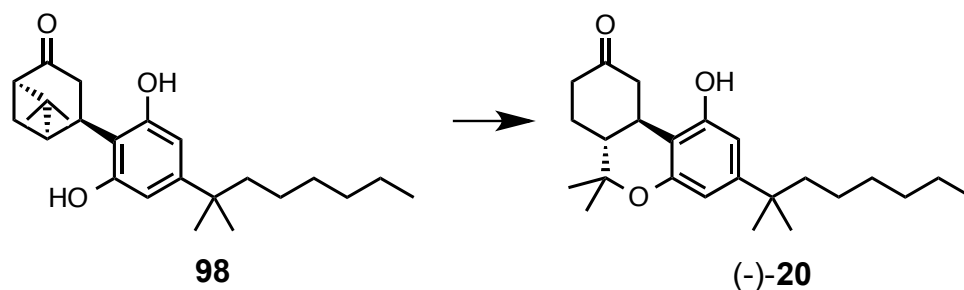


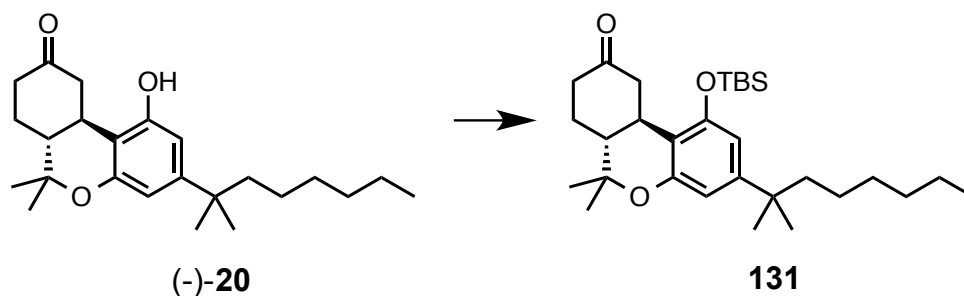
Figure 30: Overlaid Chromatograms
Obtained from Chiral HPLC.
98 Purified by **Chromatography**,
98 Purified by **Filtration**,
Filtrate Obtained after Filtration of **98**



In general: Cyclobutane ring opening was performed according to the general procedure outlined by S. P. Nikas et al. in *Tetrahedron* **2007**, 63, 8112–8123.

Synthesis of (-)-20 — (e; **Scheme 15**; **Chpt. 2**) A dry round bottom flask under nitrogen equipped with a stir bar and septum was charged with **98** (373.3 mg, 1.0 mmol). To the flask was added a 3:1 mixture of CH_2Cl_2 : CH_3NO_2 (7 mL) and the resulting suspension was cooled to 0 °C before the addition of trimethylsilyl trifluoromethanesulfonate solution (1.0 mL of a 0.3M solution in CH_3NO_2 , 0.34 mmol, 0.3 eq). The reaction mixture was allowed to warm to room temperature while stirring and progress was monitored by TLC using an eluent of 15% acetone in *n*-hexanes [**98** R_f = 0.09, (-)-**20** R_f = 0.19]. When full conversion to (-)-**20** was observed by TLC, the reaction was quenched by the addition of a 1:1 mixture of saturated aqueous NaHCO_3 and brine, and diluted with Et_2O . The organic layer was separated and the aqueous phase was extracted with Et_2O . The combined organic phase was washed with brine and water before drying over MgSO_4 . After filtration, solvent evaporation, and purification by flash chromatography on silica gel (15% acetone in *n*-hexanes) the white foam (-)-**20** was isolated (327 mg, 87%). Physical and spectral data with the exception of specific rotation were identical to those reported earlier in *ACS Med. Chem. Lett.* **2014**, 5, 400–404. (-)-**20** R_f = 0.16 (15% acetone in *n*-hexanes); $[\alpha]_D^{20}$ -62.5° (*c* 1.0, CHCl_3) [lit.⁷⁵ $[\alpha]_D^{20}$ -55.7° (*c* 1.0, CHCl_3)]; ^1H NMR (500 MHz, CDCl_3) δ 6.81 (br s, 1H), 6.37 (d, J = 2.0 Hz, 1H), 6.33 (d, J = 2.0 Hz, 1H), 4.09 (ddd,

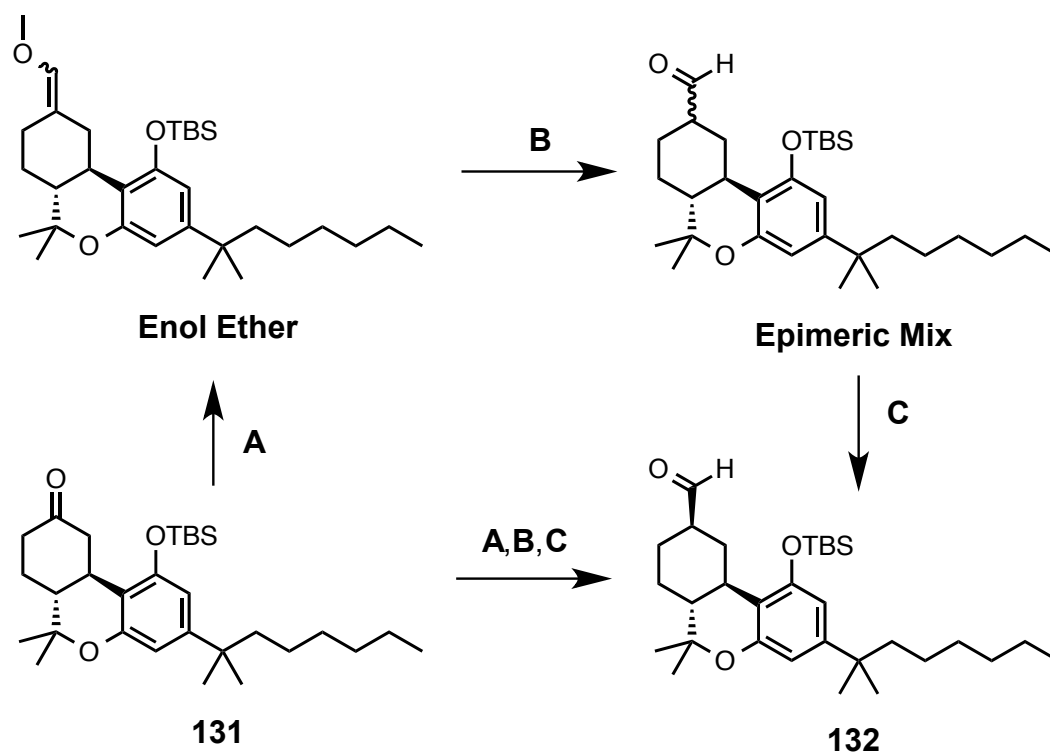
$J = 15.0, 3.5, 2.5$ Hz, 1H), 2.89 (ddd, $J = 15.0, 11.5, 3.5$ Hz, 1H), 2.63 (dddd, $J = 15.0, 4.0, 3.5, 2.0$ Hz, 1H), 2.47 (ddd, $J = 15.0, 13.5, 7.0$ Hz, 1H), 2.21-2.11 (m, 2H), 1.97 (ddd, $J = 12.0, 11.5, 2.5$ Hz, 1H), 1.56-1.46 (m, 3H), 1.48 (s, 3H) 1.28-1.15 (m, 6H), 1.21 (s, 6H) 1.13 (s, 3H), 1.10-1.02 (m, 2H), 0.84 (t, $J = 7.0$ Hz, 3H); ^{13}C NMR (125 MHz, CDCl_3) δ 213.7, 154.7, 154.2, 150.8, 107.7, 107.2, 105.5, 76.6, 47.3, 45.0, 44.3, 40.8, 37.3, 31.7, 29.9, 28.7, 28.6, 27.8, 26.8, 24.5, 22.6, 18.8, 14.0; IR (neat) 3300, 2920, 1680, 1580, 1420, 1370, 1330, 1265 cm^{-1} ; HRMS ESI m/z : 373.2743 $[\text{M}+\text{H}]^+$. Exact mass calculated for $\text{C}_{24}\text{H}_{36}\text{O}_3$, 372.2655; found, 372.2648.



In general: Protection was performed according to the general procedure outlined by Bunpei Hatano et al. in *Green Chemistry*, **2001**, 3, 140–142.

Synthesis of 131 — (d; **Scheme 17**; **Chpt. 3**). A dry pear shaped flask equipped with a stir bar was charged with (-)-**20** (219.0 mg, 0.587 mmol), imidazole (140.6 mg, 2.06 mmol, 3.5 eq), and *t*-butyldimethylsilyl chloride (177.3 mg, 1.18 mmol, 2 eq), and the flask was capped. The neat mixture of solids was heated to 80 °C at which point the mixture became a pale yellow oil. Heating was continued for 1 hour and then the reaction mixture was cooled, diluted with hexanes and filtered through Celite®. The Celite® was washed with ether. The combined filtrate and wash were concentrated under reduced pressure and the resulting residue was suspended in hexanes and added to the top of a silica column. The column was eluted with hexanes followed by 8% EtOAc in hexanes to afford **131** (280.3 mg, 98% yield) as a colorless oil. (R_f = 0.46 in 1:8 EtOAc:hexanes). $[\alpha]_D^{20}$ -12.0° (c 0.2, CHCl_3); ^1H NMR (500 MHz, CDCl_3) δ 6.42 (d, J = 1.9 Hz, 1H), 6.34 (d, J = 1.9 Hz, 1H), 3.78 (ddd, J = 2.1, 3.4, 14.8 Hz, 1H), 2.72 (ddd, J = 3.4, 11.1, 11.1 Hz, 1H), 2.56 (d, J = 15.0 Hz, 1H), 2.41 (m, 1H), 2.14 (m, 1H), 2.09 (dd, J = 13.5, 14.0 Hz, 1H), 1.95 (ddd, J = 2.9, 12.4, 13.8 Hz, 1H), 1.52-1.46 (m, 3H), 1.47 (s, 3H), 1.23-1.15 (m, 6H), 1.21, (s, 3H), 1.19 (s, 3H), 1.04 (m, 2H), 1.10 (s, 3H), 1.00 (s, 9H), 0.84 (t, J = 6.8 Hz, 3H), 0.24 (s, 3H), 0.16 (s, 3H); ^{13}C NMR (125 MHz, CDCl_3) δ 210.3, 154.2, 154.0, 150.1, 111.8, 109.8, 108.4, 76.5, 47.8, 45.6, 44.5, 40.8, 37.4, 35.1, 31.8, 30.0, 28.9, 28.6, 27.8, 26.9, 26.0,

24.7, 22.6, 18.6, 18.3, 14.1, -3.7, -4.1; IR (neat) 3019, 2959, 2931, 2859, 1707, 1612, 1560, 1472, 1413, 1332, 1256, 1185, 1111, 1097, 1057, 978, 841 cm^{-1} ; HRMS (ESI) m/z : 487.3601 $[\text{M} + \text{H}]^+$. Exact mass calculated for $\text{C}_{30}\text{H}_{50}\text{O}_3\text{Si}$ 486.3529; found 486.3529.



In general: Homologation was performed according to the procedure outlined by Busch-Peterson et al. in *J. Med. Chem.* **1996**, *39*, 3790-3796.

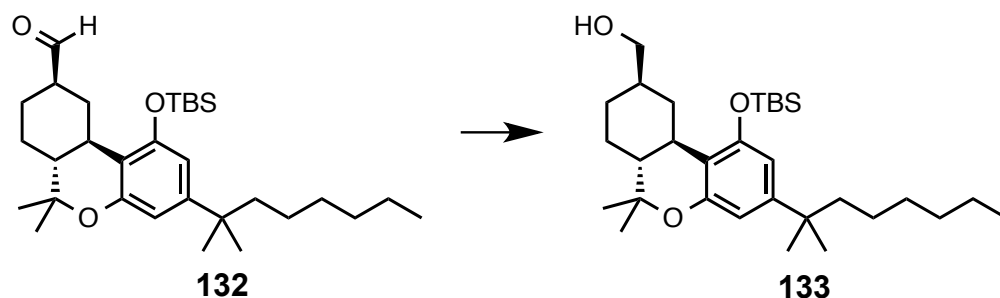
Synthesis of 132 — (A, B, C; Scheme 17; Chpt. 3). A dry 2-neck round bottom flask equipped with a 3-way gas inlet, stir bar, and septum under nitrogen was charged with (methoxymethyl)-triphenylphosphonium chloride (1.02 g, 2.97 mmol, 8.4 eq) followed by anhydrous THF (10 mL). The reaction vessel was cooled to $-30\text{ }^{\circ}\text{C}$ before the slow addition of *n*-BuLi (1.20 mL of a 2.09M in hexanes, 2.51 mmol, 7.1 eq). The resulting orange suspension, was allowed to warm to $0\text{ }^{\circ}\text{C}$ over 30 minutes, at which point the color changed to blood red. In a separate dry flask **131** (172.2 mg, 0.353 mmol) was suspended in anhydrous THF (5 mL) under N_2 , cooled to $-30\text{ }^{\circ}\text{C}$ and then added to the 2-neck flask *via* cannula, keeping the temperature at $0\text{ }^{\circ}\text{C}$ or below. Stirring was continued at $0\text{ }^{\circ}\text{C}$ until the reaction was complete, as determined by TLC (30 min).

To the resulting red reaction mixture was added water and the mixture was stirred at room temperature until it became colorless (~30 min). The mixture was poured into water and extracted with ether (2x). The combined organic extract was washed with brine, dried over MgSO_4 and concentrated under reduced pressure to provide crude enol ether. [Using a 1:4 EtOAc:*n*-hexanes eluent. enol ether $R_f = 0.85$; **131** $R_f = 0.57$]

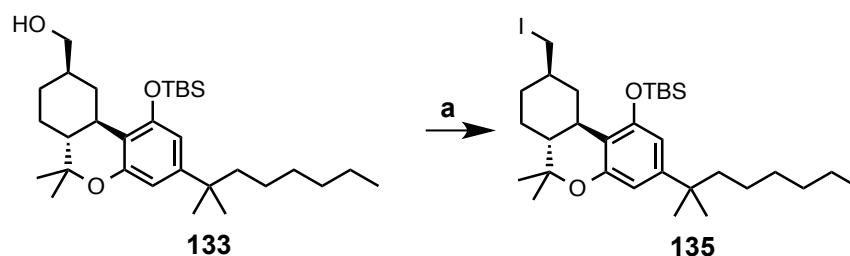
The resulting crude enol ether residue (~800 mg) was dissolved in CH_2Cl_2 (20 mL) and wet trichloroacetic acid (404.4 mg, 2.47 mmol, 7 eq) was added in one portion. The mixture was stirred at room temperature until hydrolysis of the enol ether was complete, as determined by TLC (~1 h). The reaction was quenched with aqueous NaHCO_3 , and the mixture was extracted with CH_2Cl_2 (2x). The combined organic layers were washed with water and brine, dried over MgSO_4 , and concentrated to afford the aldehyde as a 2:1 mixture of epimers. [Using a 1:4 EtOAc:*n*-hexanes eluent the inseparable mixture of epimers has a $R_f = 0.68$]

To a dry flask was added freshly powdered, anhydrous K_2CO_3 (380.4 mg, 2.75 mmol, 6 eq) and the flask was purged with N_2 . In a separate flask, the epimeric mixture of aldehydes was dissolved in absolute ethanol (10 mL) under nitrogen and then transferred to the flask containing K_2CO_3 powder *via* cannula. The reaction mixture was stirred for 4 h at ambient temperature. The reaction was monitored by ^1H NMR, using the disappearance of the α -aldehyde to confirm full conversion to the β -aldehyde. [^1H NMR (300 MHz, CDCl_3): α -aldehyde proton at 9.88, β - at 9.62]. The reaction was then quenched with aqueous NaH_2PO_4 and diluted with DCM. The aqueous phase was separated and extracted with DCM. The combined organic layers were washed with water then brine, dried over MgSO_4 , concentrated under reduced pressure and the resulting residue was purified by flash chromatography (0% to 10% EtOAc:*n*-hexanes gradient) to give **132** (150.7 mg, 85% overall yield). $R_f = 0.55$ (1:8 EtOAc:*n*-hexanes eluent); $[\alpha]^{20}_{\text{D}} -59.6^\circ$ (c 0.2, CHCl_3); ^1H NMR (500 MHz, CDCl_3): δ 9.63 (s, 1H), 6.39 (d, $J = 1.9$ Hz, 1H), 6.32 (d, $J = 1.9$ Hz, 1H), 3.49 (d, $J = 12.9$ Hz, 1H), 2.48-2.27 (m, 1H), 2.41 (ddd, $J =$

2.9, 11.4, 11.4 Hz, 1H), 2.15-1.92 (m, 1H), 2.10 (d, $J = 13.5$ Hz, 1H), 1.99 (d, $J = 11.3$ Hz, 1H), 1.53-1.43 (m, 4H), 1.39 (s, 3H), 1.33-1.11 (m, 4H), 1.20 (s, 3H), 1.19 (s, 3H), 1.11-0.94 (m, 2H), 1.07 (s, 3H), 1.01 (s, 9H), 0.91-0.79 (m, 2H), 0.84 (t, $J = 6.9$ Hz, 3H), 0.25 (s, 3H), 0.14 (s, 3H); ^{13}C NMR (75 MHz, CDCl_3) δ 203.3, 154.4, 154.2, 149.2, 113.4, 109.7, 108.4, 76.6, 49.6, 44.5, 40.5, 37.2, 35.4, 33.2, 31.8, 30.0, 29.8, 28.9, 28.6, 27.6, 27.5, 25.9, 24.6, 22.6, 18.8, 18.2, 14.0, -3.6, -4.3 ; IR (neat) 3020, 2959, 2931, 2859, 1722, 1612, 1564, 1468, 1412, 1263, 1216, 1141, 1063, 908, 841, 756, 668 cm^{-1} ; HRMS (ESI) m/z : 501.3768 $[\text{M}+\text{H}]^+$. Exact mass calculated for $\text{C}_{31}\text{H}_{52}\text{O}_3\text{Si}$ 500.3686; found 500.3690.

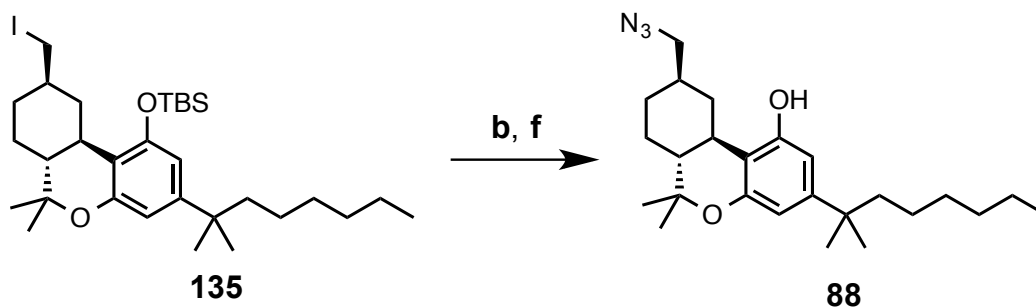


Synthesis of 133 — (**b**; **Scheme 18**; **Chpt. 3**). A dry round bottom flask equipped with a stir bar and septum was charged **132** (62.5 mg, 0.124 mmol) under N₂. The flask was cooled to 0 °C and EtOH (3.5 mL) was added, followed by the portion-wise addition of NaBH₄ (19.8 mg total, 0.52 mmol, 4.2 eq). Stirring was continued at 0 °C until complete conversion to alcohol was confirmed by TLC (~30 min). The reaction was quenched by the addition of 10% aqueous acetic acid, and diluted with EtOAc. The aqueous layer was separated and extracted with EtOAc. The combined organic layers were washed with brine, dried over MgSO₄, and concentrated in vacuo. The crude material was purified by flash chromatography (5% and then 10% EtOAc in hexanes eluent) to provide **133** (51.3 mg, 82% yield) as a pale yellow oil. *R*_f = 0.19 (1:8 EtOAc:*n*-hexanes eluent); $[\alpha]_D^{20}$ -63.4° (*c* 0.2, CHCl₃); ¹H NMR (500MHz, CDCl₃) δ 6.38 (d, *J* = 1.9 Hz, 1H), 6.31 (d, *J* = 1.9 Hz, 1H), 3.54 (dd, *J* = 5.6, 10.6 Hz, 1H), 3.44 (dd, *J* = 6.9, 10.6 Hz, 1H), 3.16 (d, *J* = 12.8 Hz, 1H), 2.36 (ddd, *J* = 2.6, 11.0, 11.0 Hz, 1H), 2.00 (m, 1H), 1.91 (m, 1H), 1.71 (m, 1H), 1.51-1.44 (m, 3H), 1.38 (s, 3H), 1.27- 1.10 (m, 9H), 1.20 (s, 3H), 1.18 (s, 3H), 1.06 (s, 3H), 1.03 (m, 2H), 1.00 (s, 9H), 0.83 (t, *J* = 7.0 Hz, 3H), 0.76 (dddd, *J* = 11.8, 11.9, 11.9, 12.0, 1H), 0.23 (s, 3H), 0.16 (s, 3H); ¹³C NMR (125 MHz, CDCl₃) δ 154.4, 154.2, 149.2, 113.4, 109.7, 108.4, 76.6, 68.5, 49.6, 40.5, 37.2, 35.5, 33.2, 31.8, 30.0, 29.8, 28.9, 28.6, 27.6, 27.5, 26.2, 25.9, 24.7, 22.6, 18.8, 18.2, 14.1, -3.6, -4.4; IR (neat) 3320, 3020, 2959, 2931, 1612, 1564, 1468, 1412, 1263, 1216, 1141, 1063, 908, 841, 756, 668 cm⁻¹; HRMS (ESI) *m/z*: 503.3905 [M+H]⁺. Exact mass calculated for C₃₁H₅₄O₃Si 502.3842; found 502.3842.



Synthesis of 135 — (a; Scheme 19; Chpt. 3). **a.** A dry 2-neck round bottom flask equipped with a reflux condenser, stir bar and septum was charged **133** (15.1 mg, 0.03 mmol) followed by imidazole (12.2 mg, 0.18 mmol, 6 eq), and iodine (15.2 mg, 0.06 mmol, 2 eq) at room temperature under argon. Benzene (0.5 mL) was added and a solution of triphenylphosphine (0.06 mL of a 1.0 M solution in benzene, 0.06 mmol, 2 eq) was added to the reaction vessel. The reaction mixture was heated at 90 °C for 1 h and then cooled to room temperature. The reaction mixture was diluted with Et₂O. The ethereal layer was washed sequentially with water, aqueous sodium thiosulfate, and brine, then dried over MgSO₄. After filtration and evaporation of solvent, the iodide **135** was used for the next step without further purification. [Using a 1:8 EtOAc:*n*-hexanes eluent; **133** R_f = 0.19, **135** R_f = 0.63].

154.6, 154.2, 150.3, 108.9, 108.0, 105.4, 77.9, 48.9, 44.4, 37.3, 35.9, 34.8, 32.9, 31.8, 30.0, 29.8, 28.7, 28.6, 27.7, 27.1, 24.6, 22.7, 19.0, 14.1, 1.0; IR (neat) 3463, 3054, 2986, 1652, 1648, 1635, 1421, 1265, 895, 744, 705 cm^{-1} ; HRMS (ESI) m/z : 434.2898 $[\text{M}+\text{H}]^+$. Exact mass calculated for $\text{C}_{25}\text{H}_{39}\text{NO}_5$ 433.2828; found 433.2824.

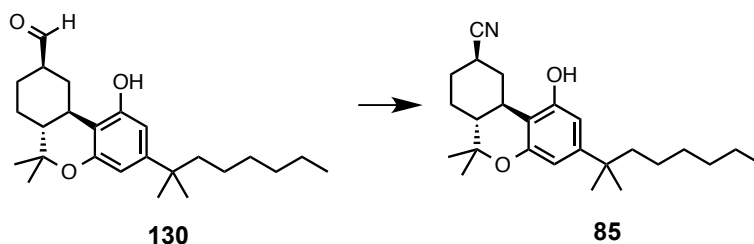


Synthesis of 88 — (b, f; Scheme 19; Chpt. 3). A dry round bottom flask equipped with a stir bar and septum was charged with NaN₃ (10.1 mg, 0.155 mmol, 5 eq) under N₂. In a separate flask, crude iodide **135** was dissolved in anhydrous DMF (5 mL) under N₂, and transferred *via* cannula to the flask containing NaN₃. The resulting reaction mixture was stirred at ambient temperature until the consumption of **135** was complete as determined by TLC (~12 h). EtOAc and water were added to the reaction mixture, and the material was transferred to a separatory funnel where the layers were separated and the aqueous layer was further extracted with EtOAc. The combined organic layers were washed with water, dried over MgSO₄, and concentrated under reduced pressure. [Using 1:10 EtOAc:*n*-hexanes eluent: **135** R_f = 0.78]

The resulting residue was suspended in anhydrous Et₂O (3 mL) and to this suspension was added tetrabutylammonium fluoride (0.04 mL of a 1M in THF, 0.41 mmol, 1.4 eq). The reaction mixture was stirred at room temperature for 1 hour before addition of water and extraction with Et₂O (2x). The combined ethereal layers were washed with brine, dried over MgSO₄, and concentrated under reduced pressure. Purification by flash chromatography (15% EtOAc in hexanes eluent) provided **84** (9.5 mg, 76% overall yield, from 15.3 mg of hydroxy **133**). R_f = 0.22 (1:10 EtOAc:*n*-hexanes eluent); [α]_D²⁰ -67.3° (c 0.2, CHCl₃); ¹H NMR (500 MHz, CDCl₃) δ 6.36 (d, *J* = 1.8 Hz, 1H), 6.18 (d, *J* = 1.8 Hz, 1H), 4.65 (s, 1H), 3.26 (dd, *J* = 6.1, 12.0 Hz, 1H), 3.20 (br d, *J* = 12.7 Hz, 1H), 3.15 (dd, *J* = 7.0, 12.0 Hz, 1H), 2.47 (ddd, *J* = 2.8, 11.1, 11.1 Hz, 1H), 1.98 (m, 1H), 1.92 (m, 1H), 1.83 (m, 1H), 1.52-1.44 (m, 3H), 1.39 (s, 3H), 1.28-1.11 (m,

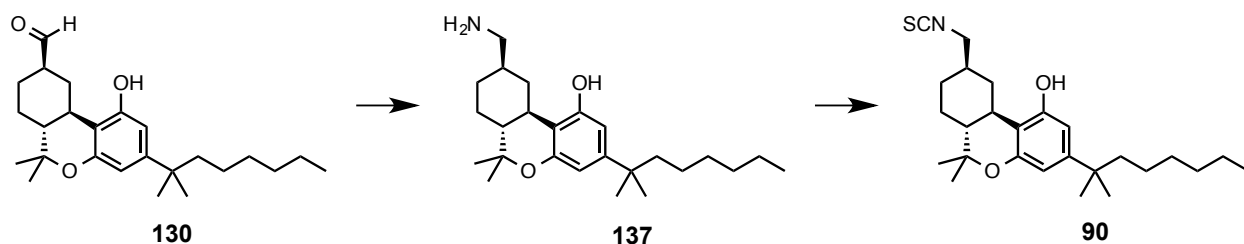
8H), 1.20 (s, 6H), 1.09 (s, 3H), 1.05 (m, 2H), 0.90-0.81 (m, 1H), 0.84 (t, $J = 7.0$ Hz, 3H); ^{13}C NMR (125 MHz, CDCl_3) δ 154.6, 154.2, 150.1, 109.2, 108.0, 105.4, 76.8, 57.8, 49.0, 44.4, 38.1, 37.3, 34.9, 34.1, 31.8, 30.8, 30.0, 28.7, 28.6, 27.7, 27.4, 24.6, 22.7, 19.0, 14.1; IR (neat); 3386, 3019, 2930, 2871, 2400, 2100, 1623, 1572, 1414, 1331, 1215, 1138, 1038, 670 cm^{-1} ; HRMS (ESI) m/z : 412.2972 $[\text{M}-\text{H}]^+$. Exact mass calculated for $\text{C}_{25}\text{H}_{39}\text{N}_3\text{O}_2$ 413.3042; found 413.3046.

2.36 (dd, $J = 6.1, 16.7$ Hz, 1H), 2.29 (dd, $J = 6.9, 16.7$ Hz 1H), 2.06 (d, $J = 12.0$ Hz, 1H), 2.00-1.89 (m, 2H), 1.53-1.45 (m, 3H), 1.39 (s, 3H), 1.32-1.11 (m, 8H), 1.19 (s, 6H), 1.09 (s, 3H), 1.05 (m, 2H), 0.97 (ddd, $J = 11.9, 12.0, 12.0$ Hz, 1H), 0.84 (t, $J = 7.1$ Hz, 3H); ^{13}C NMR (125 MHz, CDCl_3) δ 154.6, 154.2, 150.3, 118.7, 108.8, 108.0 105.3, 77.2, 48.6, 44.4, 37.3, 36.0, 35.0, 34.7, 32.5, 31.8, 30.0, 28.7, 28.6, 27.7, 27.3, 24.6 (2C), 22.7, 19.0, 14.1; IR (neat); 3396, 3054, 2986, 2253, 1623, 1575, 1415, 1265, 909 cm^{-1} ; HRMS (ESI) m/z : 396.2909 $[\text{M-H}]^+$. Exact mass calculated for $\text{C}_{26}\text{H}_{39}\text{NO}_2$ 397.2981; found 397.2982.



In general. This reaction was performed following the work of Augustine, J. K. *et al.* in *Synlett*, **2011**, 2223-2227.

Synthesis of 85 — (c; Scheme 21; Chpt. 3). To a vial equipped with a stir bar was added **130** (14.1 mg, 0.036 mmol) followed by hydroxylamine hydrochloride (3.1 mg, 0.043 mmol, 1.2 eq) and DMSO (0.3 mL). The vial was capped and heated at 90 °C for 1 h. The reaction mixture was cooled to room temperature and water and Et₂O were added to the vial. The aqueous layer was removed and extracted with Et₂O. The combined ethereal layers were washed with water then brine, dried over MgSO₄, and concentrated under reduced pressure. The resulting residue was purified by flash chromatography (0% to 8% EtOAc in hexanes gradient) to provide **85** (12.0 mg, 86% yield) as a white amorphous solid. R_f = 0.49 (1:4 EtOAc:*n*-hexanes); $[\alpha]_D^{20}$ -32.0° (*c* 0.2, CHCl₃); ¹H NMR (500 MHz, CDCl₃) δ 6.36 (d, *J* = 1.8 Hz, 1H), 6.19 (d, *J* = 1.8 Hz, 1H), 4.80 (s, 1H), 3.61 (d, *J* = 13.5 Hz, 1H), 2.68 (dddd, *J* = 3.8, 3.8, 12.5, 12.5 Hz, 1H), 2.43 (ddd, *J* = 2.8, 11.2, 11.2 Hz, 1H), 2.27 (d, *J* = 13.6 Hz, 1H), 1.95 (dddd, *J* = 2.8, 2.8, 2.9, 13.0 Hz, 1H), 1.72 (dddd, *J* = 4.1, 12.9, 13.0, 13.0 Hz, 1H), 1.54 (ddd, *J* = 2.6, 11.8, 11.9 Hz, 1H), 1.51-1.46 (m, 2H), 1.43-1.33 (m, 1H), 1.38 (s, 3H), 1.28-1.08 (m, 7H), 1.19 (s, 6H), 1.08-1.00 (m, 2H), 1.07 (s, 3H), 0.84 (t, *J* = 7.0 Hz, 3H); ¹³C NMR (125 MHz, CDCl₃) δ 154.5, 154.1, 150.7, 122.5, 108.1, 107.6, 105.4, 76.4, 47.9, 44.4, 37.3, 34.7, 33.3, 31.8, 30.1, 30.0, 28.7, 28.6, 28.3, 27.5, 26.9, 24.6, 22.6, 19.0, 14.1; IR (neat); 3396, 3054, 2986, 2253, 1623, 1575, 1415, 1265, 909 cm⁻¹; HRMS (ESI) *m/z*: 384.2895 [M+H]⁺. Exact mass calculated for C₂₅H₃₇NO₂ 383.2824; found 383.2822.

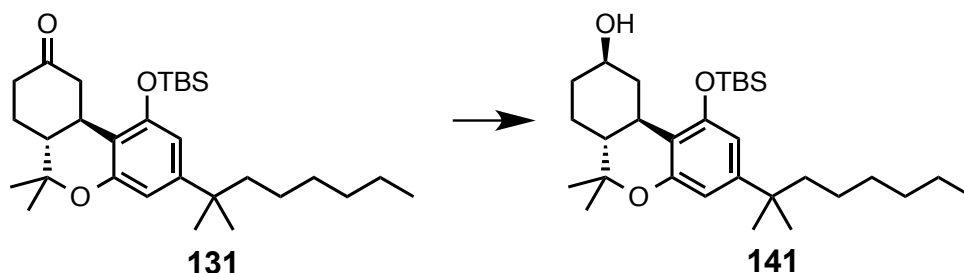


In general. The reductive amination was carried out according to Ayedi, M. A., *et al.* in *Synth. Commun.*, **2013**, 43, 2127–2133. Formation of isothiocyanate followed the work of Ogawa, G. *et al.* in *J. Med. Chem.*, **2015**, 58, 3104–3116.

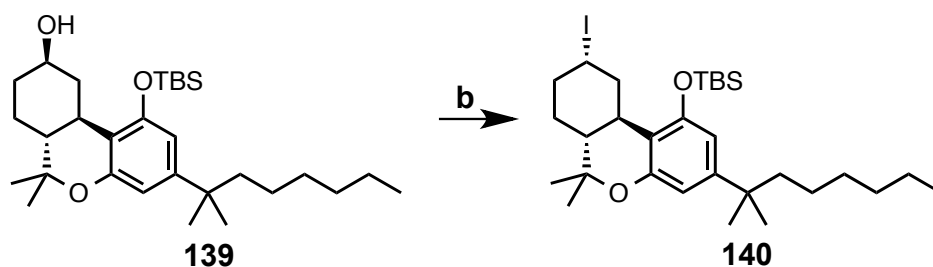
Synthesis of 90 — (a, b; **Scheme 22; Chpt. 3**). A dry 2-neck round bottom flask equipped with a 3-way gas inlet, stir bar, and septum was charged with **130** (15.0 mg, 0.038 mmol) at room temperature, under N₂. Absolute EtOH (0.5 mL) followed by hydroxylamine hydrochloride (6.7 mg, 0.097 mmol, 2.5 eq) was added to the flask under a stream of nitrogen. The reaction mixture was allowed to stir at room temperature until the starting materials were consumed completely as determined by TLC (~16 h). To the flask was added zinc dust (12.4 mg, 0.189 mmol, 4.9 eq) followed by *conc.* hydrochloric acid (three drops, *ca.* 41.3 mg, 0.419 mmol, 11.8 eq). Stirring was continued for 30 minutes and reaction mixture became a slurry. A solution of aqueous ammonia (30%, 7 mL) and sodium hydroxide (6M, 15 mL) was added dropwise to the slurry, and the mixture was stirred at room temperature for 15 minutes. The reaction mixture was transferred to a separatory funnel and extracted with dichloromethane twice. The combined organic layers were dried over Na₂SO₄, and concentrated under reduced pressure to afford **137**, which was used without further purification.

Crude **137** (*ca.* 14 mg) was dissolved in anhydrous THF (2 mL) under a nitrogen atmosphere, and cooled to 0 °C. Triethylamine (0.05 mL, 0.389 mmol, 10 eq) was added to the

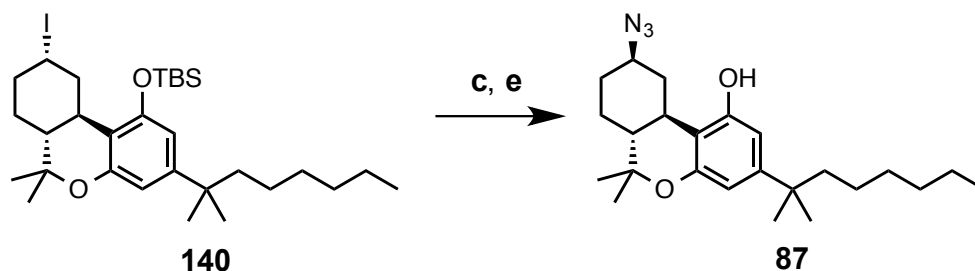
reaction flask slowly, followed by the dropwise addition of carbon disulfide (0.09 mL, 1.48 mmol, 41 eq). Stirring was continued at 0 °C for 30 minutes at which point more carbon disulfide (0.09 mL, 1.48 mmol, 41 eq) was added dropwise. The temperature was maintained at 0° C and stirring continued for 90 minutes. Solid *p*-toluenesulfonyl chloride (6.89 mg, 0.036 mmol, 1.0 eq) was then added in one portion. The reaction mixture was allowed to warm to room temperature and was stirred for an additional 90 minutes before quenching with pH 7 phosphate buffer. The mixture was diluted with Et₂O and transferred to a separatory funnel where the aqueous phase was separated and extracted with Et₂O. The ethereal layers were combined, washed with brine, dried over Na₂SO₄, and concentrated under reduced pressure. Purification by flash chromatography (0% — 5% EtOAc in hexanes eluent) provided **90** (10.1 mg, 61% overall yield) as a white amorphous solid. *R*_f = 0.73 (1:4 EtOAc:*n*-hexanes); [*α*]²⁰_D -65.0° (*c* 0.2, CHCl₃); ¹H NMR (500 MHz, CDCl₃) δ 6.36 (d, *J* = 1.8 Hz, 1H), 6.18 (d, *J* = 1.8 Hz, 1H), 4.66 (br s, 1H), 3.47 (dd, *J* = 5.6, 14.1 Hz, 1H), 3.40 (dd, *J* = 6.4, 14.2 Hz, 1H), 3.24 (d, *J* = 12.1 Hz, 1H), 2.49 (ddd, *J* = 2.7, 11.1, 11.1 Hz, 1H), 2.03-1.89 (m, 3H), 1.53-1.45 (m, 3H), 1.39 (s, 3H), 1.28-1.11 (m, 8H), 1.19 (s, 6H), 1.09 (s, 3H), 1.05 (m, 2H), 0.92 (m, 1H), 0.84 (t, *J* = 6.9 Hz, 3H); ¹³C NMR (125 MHz, CDCl₃) δ 154.6, 154.2, 150.2, 129.7, 108.9, 108.0, 105.4, 77.0, 51.0, 48.8, 44.4, 38.5, 37.3, 34.8, 33.8, 31.8, 30.5, 30.0, 28.7, 28.6, 27.7, 27.2, 24.6, 22.7, 19.0, 14.1; IR (neat) 3408, 3960, 2930, 2860, 2192, 2108, 1623, 1574, 1466, 1413, 1389, 1333, 1265, 1139, 1038 cm⁻¹; HRMS (ESI) *m/z*: 428.2619 [M-H]⁺. Exact mass calculated for C₂₆H₃₉NO₂S 429.2692, found 429.2702.



Synthesis of 141 — (a; **Scheme 24**; **Chpt. 3**). A dry round bottom flask equipped with a stir bar and septum was charged with **131** (137.1 mg, 0.281 mmol) under N₂. The flask was cooled to 0 °C and EtOH (5 mL) was added to it, followed by the portion-wise addition of NaBH₄ (42.6 mg total, 1.13 mmol, 4.0 eq). Stirring was continued at 0 °C until the reaction was complete, as judged by TLC (~1 h). The reaction was quenched by the addition of 10% aqueous acetic acid, and diluted with EtOAc. The aqueous layer was separated and extracted with EtOAc. The combined organic layers were washed with brine, dried over MgSO₄, and concentrated under reduced pressure. The crude residue was purified by flash chromatography (5% - 10% EtOAc in hexanes gradient) to provide **141** (114.3 mg, 83% yield) as a white amorphous solid. *R*_f = 0.48 (1:4 EtOAc:*n*-hexanes); [α]_D²⁰ -75.4° (*c* 0.2, CHCl₃); ¹H NMR (500 MHz, CDCl₃) δ 6.39 (d, *J* = 1.9 Hz, 1H), 6.32 (d, *J* = 1.9 Hz, 1H), 3.77 (dddd, *J* = 4.5, 4.9, 10.5, 11.0 Hz, 1H), 3.38 (d, *J* = 12.0 Hz, 1H), 2.34 (ddd, *J* = 2.5, 11.2, 11.2 Hz, 1H), 2.17 (d, *J* = 12.4 Hz, 1H), 1.88 (dddd, *J* = 3.2, 3.4, 3.5, 12.8 Hz, 1H), 1.53-1.45 (m, 3H), 1.41-1.34 (m, 2H), 1.38 (s, 3H), 1.26-1.12 (m, 7H), 1.20 (s, 3H), 1.19 (s, 3H), 1.10-1.00 (m, 3H), 1.05 (s, 3H), 1.02 (s, 9H), 0.84 (t, *J* = 7.0 Hz, 3H), 0.24 (s, 3H), 0.14 (s, 3H); ¹³C NMR (125 MHz, CDCl₃) δ 154.3, 154.3, 149.4, 112.7, 109.7, 108.4, 76.6, 70.8, 48.7, 44.5, 39.5, 37.3, 35.8, 33.9, 31.8, 30.0, 28.9, 28.6, 27.8, 26.2, 25.9, 24.7, 22.6, 18.8, 18.2, 14.1, -3.7, -4.3; IR (neat) 3320, 2920, 1634, 1565, 1470, 1410, 775, 665 cm⁻¹; HRMS (ESI) *m/z*: 489.3759 [M+H]⁺. Exact mass calculated for C₃₀H₅₂O₃Si 488.3686, found 488.3687.



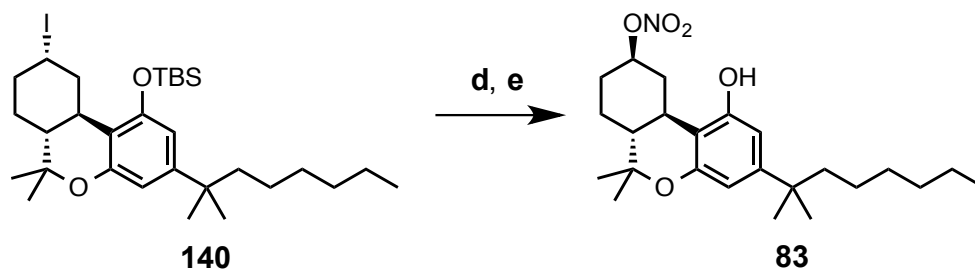
Synthesis of 140 — (b; Scheme 24; Chpt. 3). **b.** A dry 2-neck round bottom flask equipped with a 3-way gas inlet, stir bar, and septum was charged with imidazole (14.2 mg, 0.208 mmol, 6 eq), and iodine (17.6 mg, 0.07 mmol, 2 eq) followed by addition of a solution of **139** (0.58 mL as 0.06M solution in benzene, 17.1 mg, 0.034 mmol) at room temperature under argon. To the mixture was then added a solution of triphenylphosphine (0.06 mL of a 1M solution in benzene, 0.06 mmol) and reaction mixture was heated for 1 hour at 45 °C and then cooled to room temperature. The complete consumption of **139** was confirmed by TLC and the reaction mixture was diluted with Et₂O. The ethereal layer was separated, washed with water then aqueous sodium thiosulfate, brine, and dried over MgSO₄. Concentration *in vacuo* provided iodide **140** which was used for the next step without further purification. [1:10 EtOAc:*n*-hexanes eluent: **139** R_f = 0.15, **140** R_f = 0.77].



Synthesis of 87 — (c, e; Scheme 24; Chpt. 3) A dry round bottom flask equipped with a stir bar and septum was charged with sodium azide (13.5 mg, 0.208 mmol, 6 eq) under N₂. In a separate flask, crude iodide **140** was dissolved in anhydrous DMF (5 mL) under N₂, and transferred via cannula to the flask containing sodium azide. This reaction mixture was stirred at ambient temperature for 12 hours. When the **140** was completely consumed as determined by TLC, EtOAc and water were added to the reaction mixture. The reaction mixture was transferred to a separatory funnel where aqueous layer was removed and was further extracted with EtOAc. The combined organic layers were washed with water, brine, dried over MgSO₄, and concentrated under reduced pressure. [1:12 EtOAc:*n*-hexanes eluent: **140** R_f = 0.75]

The resulting residue was suspended in anhydrous Et₂O (3 mL) and to this suspension was added tetrabutylammonium fluoride (0.04 mL of a 1M in THF, 0.41 mmol, 1.4 eq). The reaction mixture was stirred at room temperature for one hour before addition of water and extraction with Et₂O (2x). The combined ethereal layers were washed with brine, dried over MgSO₄, and concentrated under reduced pressure. Purification by flash chromatography (0% - 1% acetone in hexanes gradient) provided **87** (9.4 mg, 76% overall yield). R_f = 0.13 (1:10 EtOAc:*n*-hexanes eluent); [α]_D²⁰ -54.5° (*c* 0.2, CHCl₃); ¹H NMR (500 MHz, CDCl₃) δ 6.37 (d, *J* = 1.8 Hz, 1H), 6.19 (d, *J* = 1.8 Hz, 1H), 4.74 (s, 1H), 3.53-3.46 (m, 2H), 2.50 (ddd, *J* = 2.2, 11.2, 11.2 Hz, 1H), 2.17 (d, *J* = 12.3 Hz, 1H), 1.95 (dddd, *J* = 2.8, 3.1, 3.1, 13 Hz, 1H), 1.55-1.42 (m, 4H), 1.39 (s, 3H), 1.27-1.11 (m, 8H), 1.20 (s, 6H), 1.08 (s, 3H), 1.05 (m, 2H), 0.84 (t, *J* = 6.9 Hz,

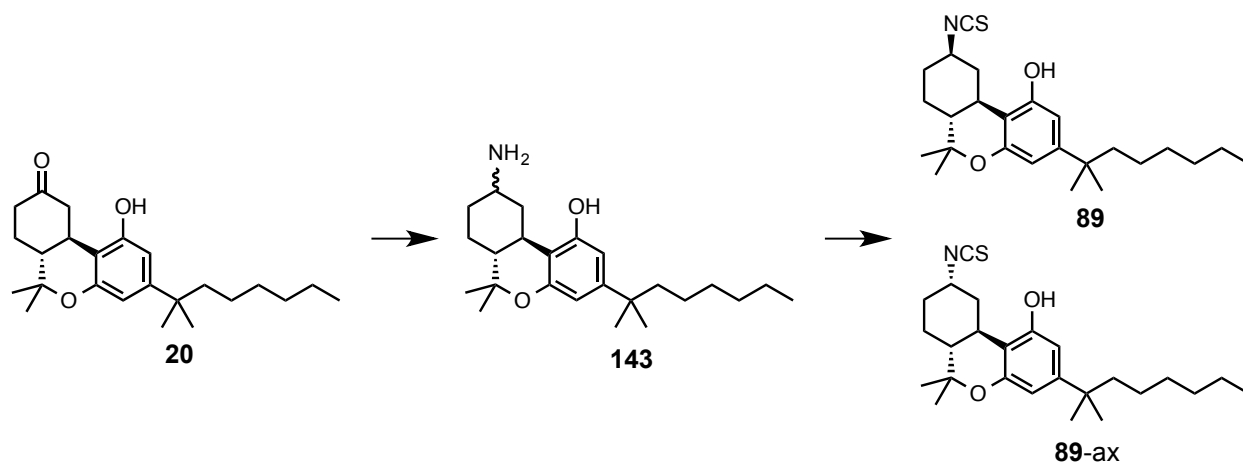
3H); ^{13}C NMR (125 MHz, CDCl_3) δ 154.6, 154.1, 150.4, 108.3, 108.0, 105.4, 76.7 (under CDCl_3), 59.9, 48.1, 44.4, 37.3, 35.1, 33.9, 32.0, 31.8, 30.0, 28.7, 28.6, 27.8, 26.4, 24.6, 22.7, 19.0, 14.1; IR (neat) 3431, 3019, 2931, 2872, 2098, 1643, 1518, 1415, 758, 670 cm^{-1} ; HRMS (ESI) m/z : 400.2994 $[\text{M}+\text{H}]^+$. Exact mass calculated for $\text{C}_{24}\text{H}_{37}\text{N}_3\text{O}_2$ 399.2886, found 399.2890.



Synthesis of 83 — (d, e; Scheme 24; Chpt. 3). Crude iodide **140** (ca. 18 mg) was dissolved at room temperature in anhydrous CH₃CN (1 mL) under N₂ in a dry, 2-neck round bottom flask equipped with a 3-way gas inlet, stir bar, and septum. The septum was opened under a small stream of nitrogen and AgNO₃ (24.9 mg, 0.146 mmol, 5 eq) was introduced. Immediately a yellow color was observed, and the reaction mixture was allowed to stir at room temperature until consumption of **140** was complete as determined by TLC (~12 h). The reaction mixture was filtered through Celite® and the Celite® was washed with Et₂O. The ethereal filtrate and washes were combined and washed with brine, dried over MgSO₄, and concentrated under reduced pressure.

The resulting residue was suspended in anhydrous Et₂O (3 mL) and to this suspension was added tetrabutylammonium fluoride (0.04 mL of a 1M in THF, 0.41 mmol, 1.4 eq). The reaction mixture was stirred at room temperature for one hour before addition of water and extraction with Et₂O (2x). The combined ethereal layers were washed with brine, dried over MgSO₄, and concentrated under reduced pressure. Purification by flash chromatography (15% EtOAc in hexanes eluent) provided **83** (10.5 mg, 82% overall yield). [α]_D²⁰ -40.5° (c 0.2, CHCl₃); ¹H NMR (500 MHz, CDCl₃) δ 6.37 (d, *J* = 1.8 Hz, 1H), 6.19 (d, *J* = 1.8 Hz, 1H), 5.13 (dddd, *J* = 4.4, 4.5, 11.4, 11.5 Hz, 1H), 4.69 (s, 1H), 3.60 (dddd, *J* = 2.4, 2.4, 4.4, 12.0 Hz, 1H), 2.58 (ddd, *J* = 2.7, 11.4, 11.5 Hz, 1H), 2.31 (d, *J* = 12.3 Hz, 1H), 2.00 (dddd, *J* = 3.0, 3.1, 3.8, 10.1 Hz, 1H), 1.61-1.45 (m, 4H), 1.41 (s, 3H), 1.31-1.15 (m, 8H), 1.20 (s, 6H), 1.09 (s, 3H), 1.05 (m, 2H), 0.84

(t, $J = 7.0$ Hz, 3H); ^{13}C NMR (125 MHz, CDCl_3) δ 154.6, 154.0, 150.6, 108.1, 107.7, 105.4, 82.4, 76.6, 48.0, 44.4, 37.3, 33.4, 33.2, 31.7, 30.1, 30.0, 28.7, 28.6, 27.8, 25.7, 24.6, 22.6, 19.0, 14.1; IR (neat) 3388, 2958, 2930, 2872, 1625, 1574, 1414, 1278, 760, 693 cm^{-1} ; HRMS (ESI) m/z : 418.2603 $[\text{M}-\text{H}]^+$. Exact mass calculated for $\text{C}_{24}\text{H}_{37}\text{NO}_5$ 419.2672, found 419.2676.



In general. Reductive amination procedure is adapted from the work of H.-W. Cui *et al.* in *Eur J. Med. Chem.*, **2015**, *95*, 240-248

Synthesis of 89 — (a, b; Scheme 25; Chpt. 3). A dry screw cap vial equipped with a stir bar was charged with (-)-**20** (14.4 mg, 0.038 mmol), ammonium acetate (44.6 mg, 0.579 mmol, 15 eq) and sodium cyanoborohydride (3.6 mg, 0.057 mmol, 1.5 eq). The vial was purged with N₂, sealed temporarily with a septum, and placed in an ice bath. MeOH (0.5 mL) was added to the vial followed by acetic acid (0.01 mL, 0.193 mmol, 5 eq) and the reaction mixture was stirred until homogeneous. At this point the septum was replaced by a screw cap under a stream of nitrogen and the vial was placed in a 4 °C refrigerator for 24 hours. The reaction mixture was concentrated under reduced pressure and basified to pH 9 using aqueous NaHCO₃. This aqueous mixture was extracted with DCM. The organic layer was washed with brine, dried over Na₂SO₄, and concentrated under reduced pressure to provide amine **143** which was used without purification.

Crude **143** (ca. 14 mg) was dissolved in anhydrous THF (2 mL) under a nitrogen atmosphere, and cooled to 0 °C. Triethylamine (0.05 mL, 0.389 mmol, 10 eq) was added to the reaction flask slowly, followed by the dropwise addition of carbon disulfide (0.09 mL, 1.48 mmol,

41 eq). Stirring continued at 0 °C for 30 minutes at which point more carbon disulfide (0.09 mL, 1.48 mmol, 41 eq) was added dropwise. The temperature was maintained at 0° C and stirring continued for 90 minutes. Solid *p*-toluenesulfonyl chloride (7.0 mg, 0.036 mmol, 1.0 eq) was added in one portion. The reaction mixture was allowed to warm to room temperature and was stirred for an additional 90 minutes before quenching with pH 7 phosphate buffer. The mixture was diluted with Et₂O and transferred to a separatory funnel where the aqueous phase was separated and extracted with Et₂O. The ethereal layers were combined, washed with brine, dried over Na₂SO₄, filtered, and concentrated under reduced pressure. Purification by flash chromatography (0% and then 4% EtOAc in hexanes gradient) provided a 4.3:1 mixture of **89** and **89**-ax (12.2 mg, 76% overall yield) as a white amorphous solid. This mixture was further purified by normal phase HPLC over 30 min (15% - 30% EtOAc in hexanes gradient) to provide pure **89** (9.2 mg). [α]_D²⁰ -85.0° (*c* 0.2, CHCl₃); ¹H NMR (500 MHz, CDCl₃) δ 6.37 (d, *J* = 1.8 Hz, 1H), 6.19 (d, *J* = 1.8 Hz, 1H), 4.69 (s, 1H), 3.76 (dddd, *J* = 4.2, 4.2, 11.7, 11.7 Hz, 1H), 3.62 (dddd, *J* = 2.3, 2.5, 3.5, 12.5 Hz, 1H), 2.44 (ddd, *J* = 2.8, 11.4, 11.4 Hz, 1H), 2.30 (d, *J* = 11.7 Hz, 1H), 1.92 (dddd, *J* = 2.7, 3.0, 3.6, 12.8, 1H), 1.66 (dddd, *J* = 4.2, 12.6, 12.7, 12.8 Hz, 1H), 1.54-1.45 (m, 2H), 1.41-1.34 (m, 1H), 1.38 (s, 3H), 1.27-1.10 (m, 8H), 1.19 (s, 6H), 1.09-1.00 (m, 2H), 1.06 (s, 3H), 0.84 (t, *J* = 7.0 Hz, 3H); ¹³C NMR (125 MHz, CDCl₃) δ 154.6, 154.0, 150.6, 130.0, 108.1, 107.7, 105.4, 76.5, 55.8, 47.8, 44.4, 37.3, 37.2, 34.0, 33.8, 31.8, 30.0, 28.7, 28.6, 27.7, 26.2, 24.6, 22.7, 19.0, 14.1; IR (neat) 3406, 2958, 2930, 2171, 2117, 1624, 1574, 1414, 1375, 1265, 738 cm⁻¹; HRMS (ESI) *m/z*: 414.2475 [M-H]⁺. Exact mass calculated for C₂₅H₃₇NO₂S 415.2545, found 415.2548.

Appendix I

Spectra for Selected Compounds in Chapter 2 and 3

Table of Contents for Appendix I

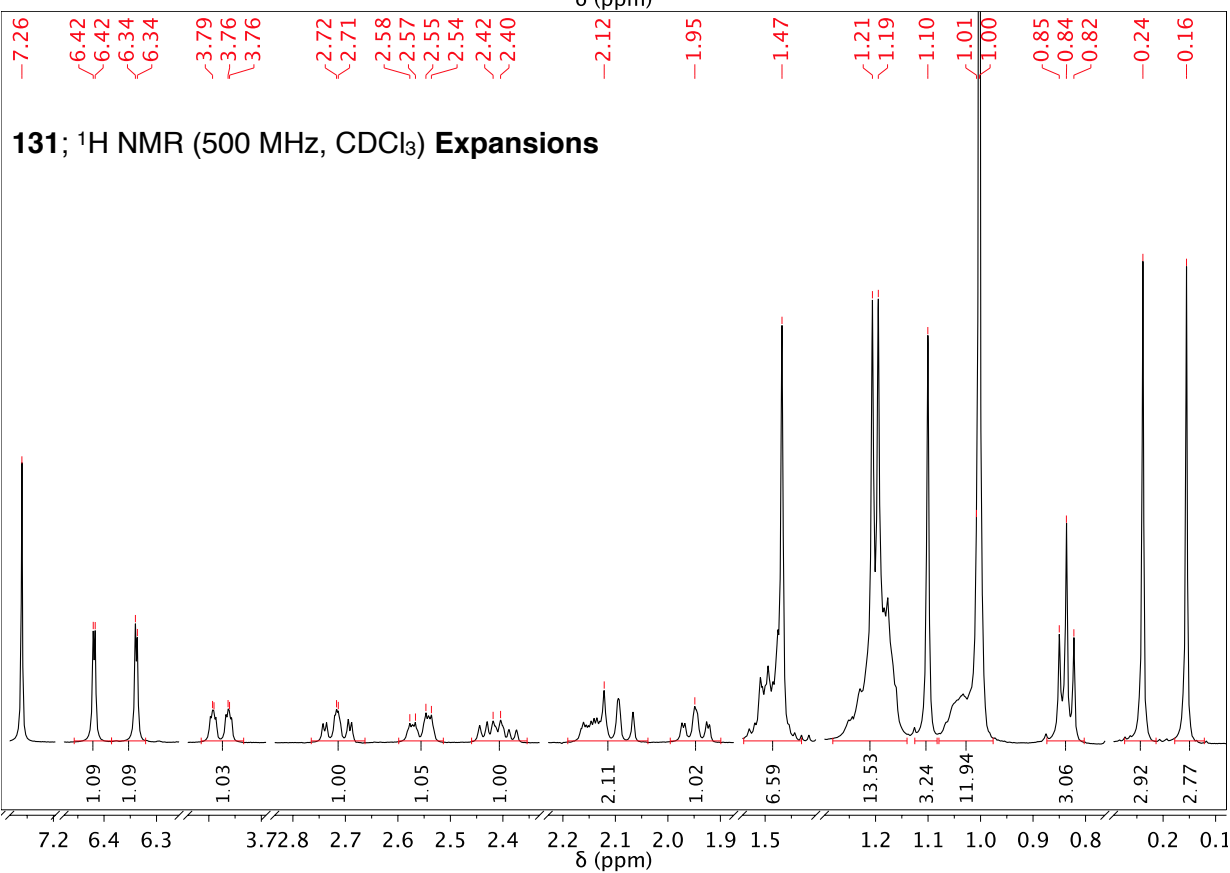
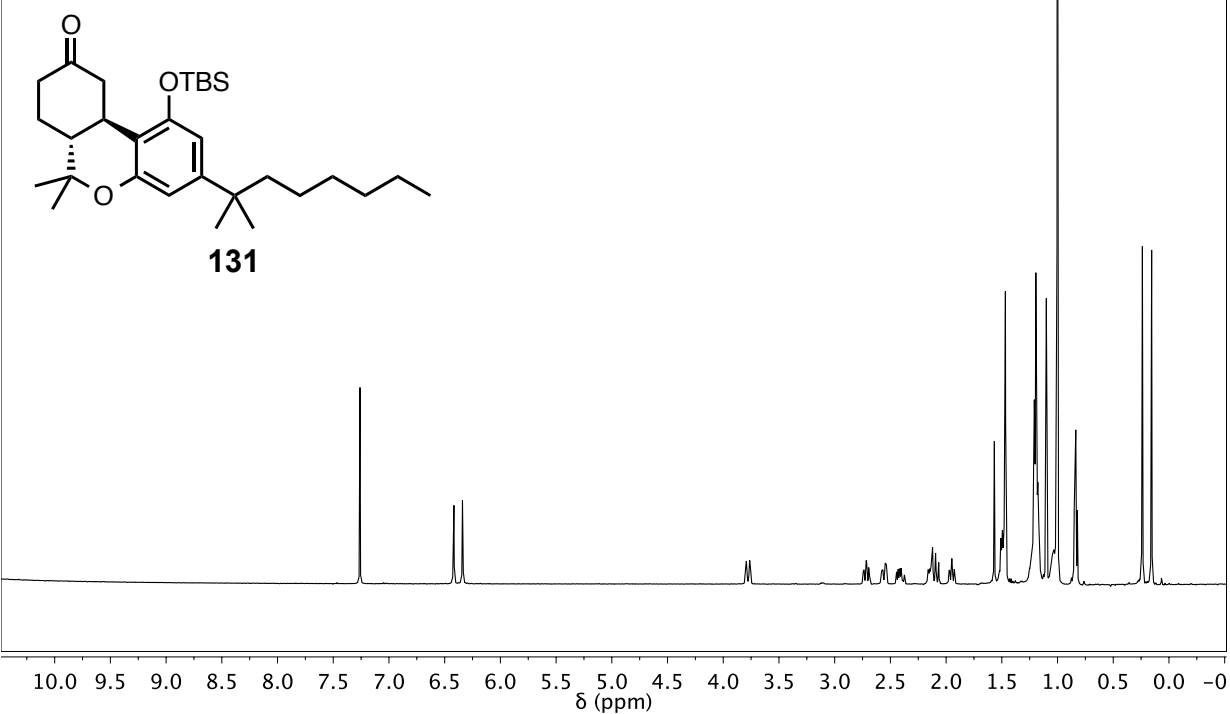
Select Compounds From Chapter 3

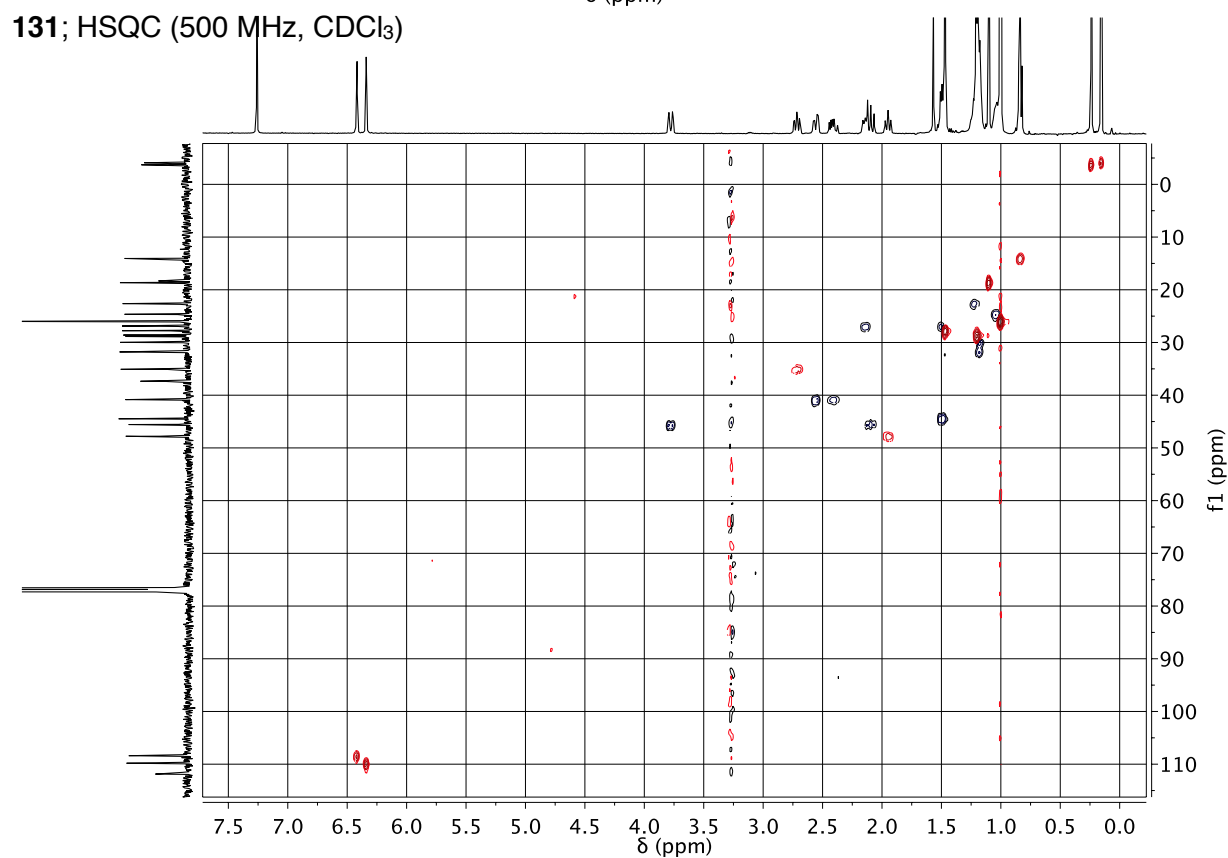
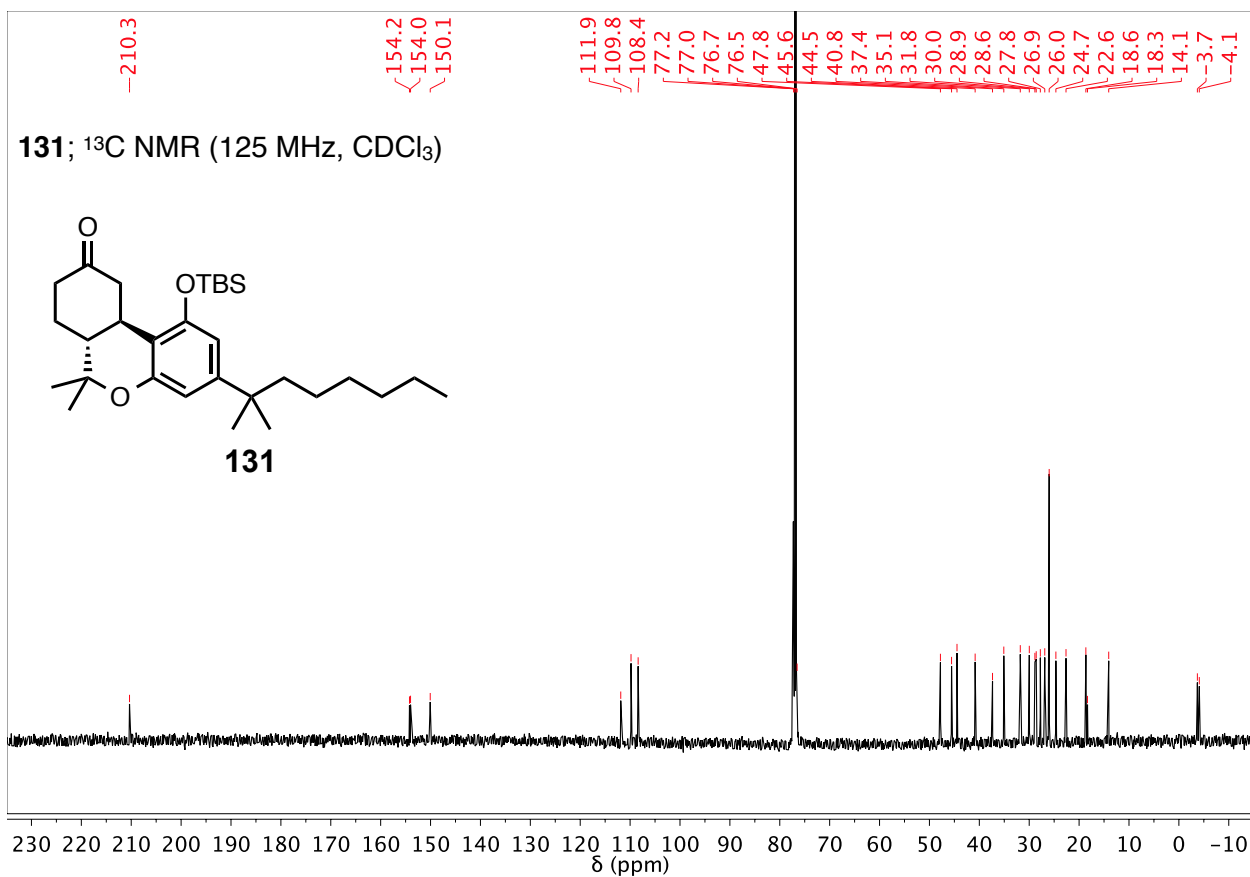
131 (¹ H, ¹³ C, HSQC, COSY, HMBC).....	146
132 (¹ H, ¹³ C, HSQC, nOe).....	149
133 (¹ H, ¹³ C, HSQC, COSY, HMBC)	152
84 (¹ H, ¹³ C).....	155
88 (¹ H, ¹³ C, nOe)	157
86 (¹ H, ¹³ C).....	160
90 (¹ H, ¹³ C).....	162
139 (¹ H, ¹³ C, HSQC, COSY, HMBC, nOe).....	164
83 (¹ H, ¹³ C, nOe)	169
87 (¹ H, ¹³ C, nOe)	172
85 (¹ H, ¹³ C).....	175
89 (¹ H, ¹³ C).....	177

Select Compounds From Chapter 2

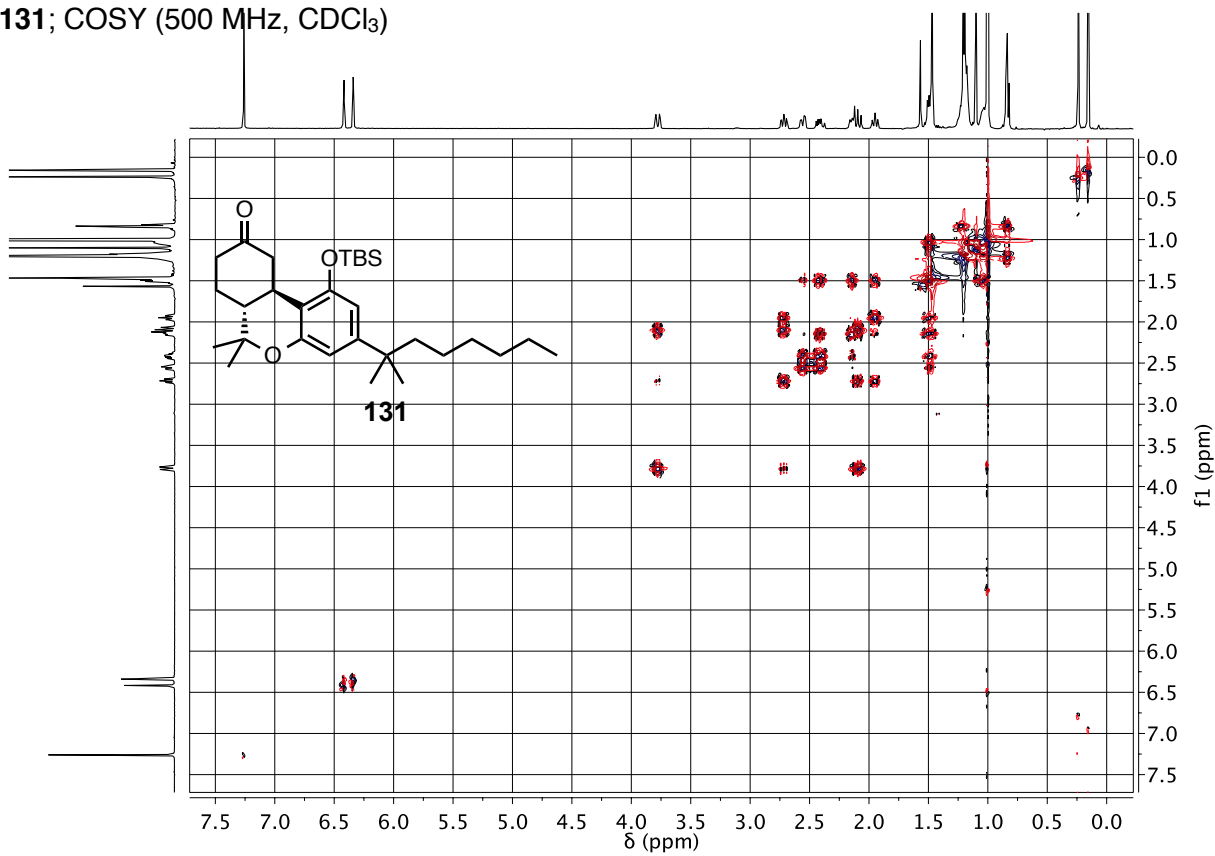
99 (¹ H, ¹³ C).....	179
125 (¹ H)	181
98 (¹ H, ¹³ C, HSQC, COSY, HMBC).....	182
(-)-20 (¹ H, ¹³ C, HSQC, COSY, HMBC)	185

131; ^1H NMR (500 MHz, CDCl_3)

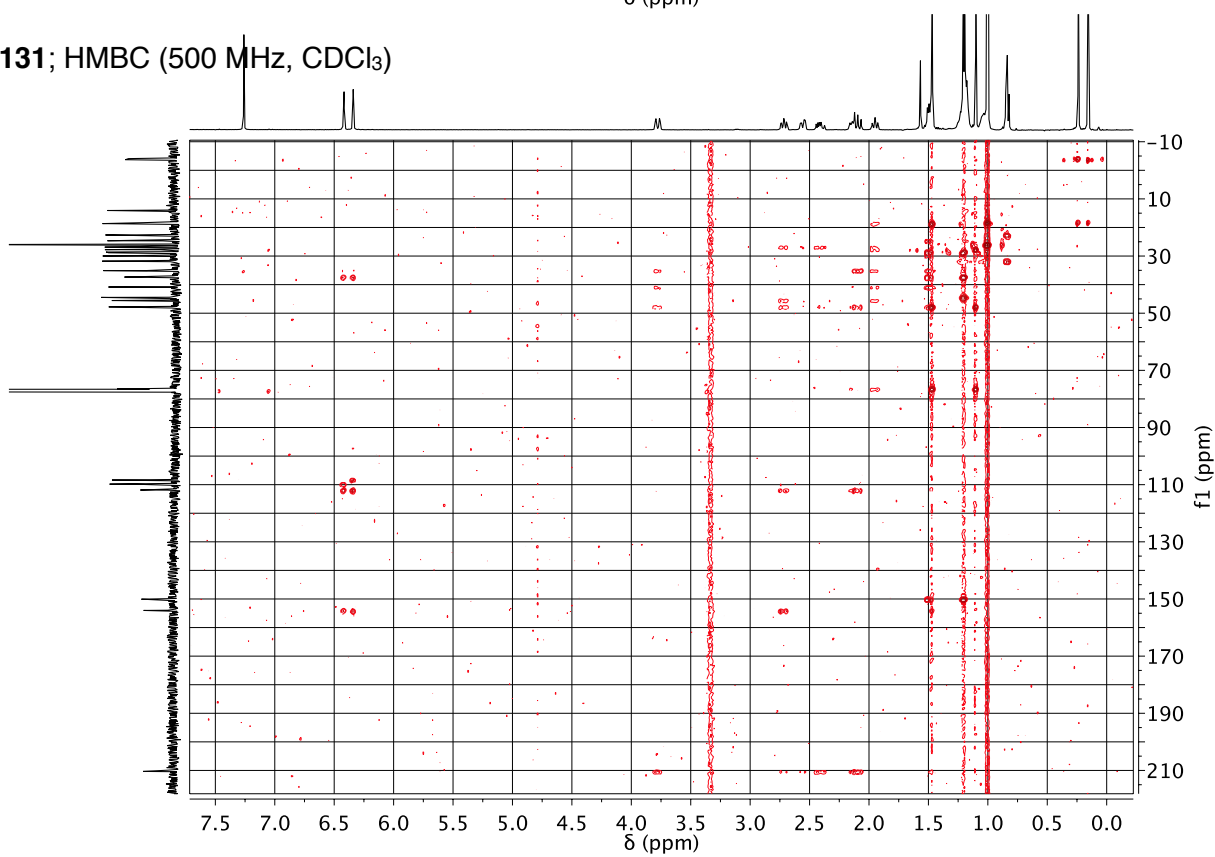




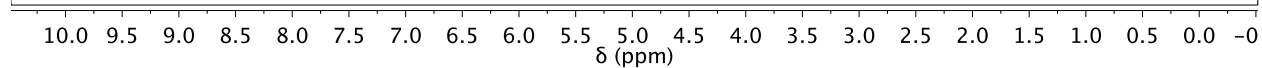
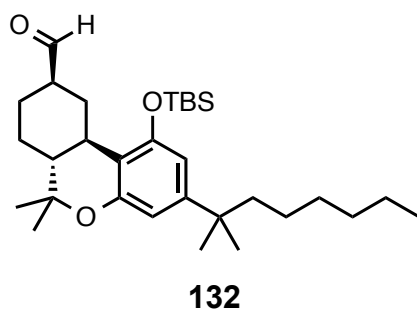
131; COSY (500 MHz, CDCl₃)



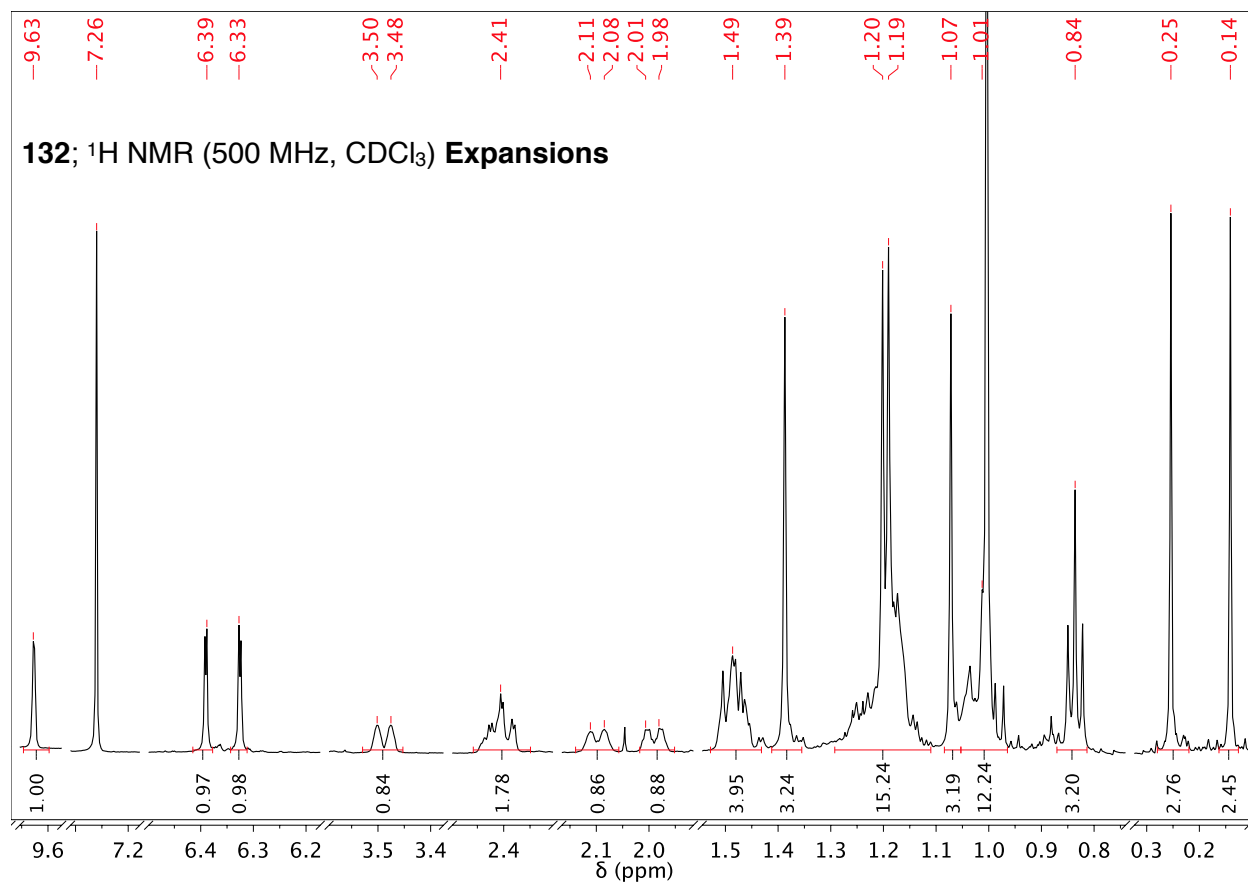
131; HMBC (500 MHz, CDCl₃)

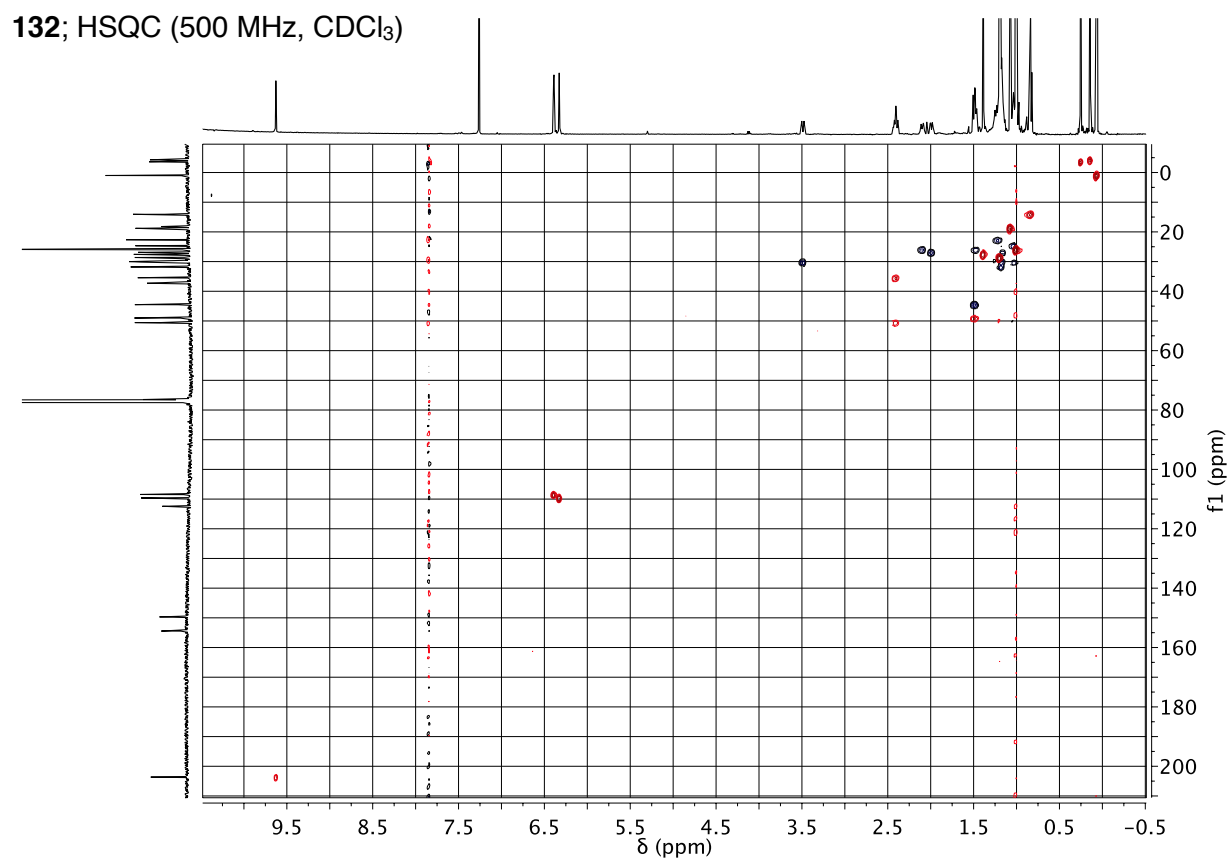
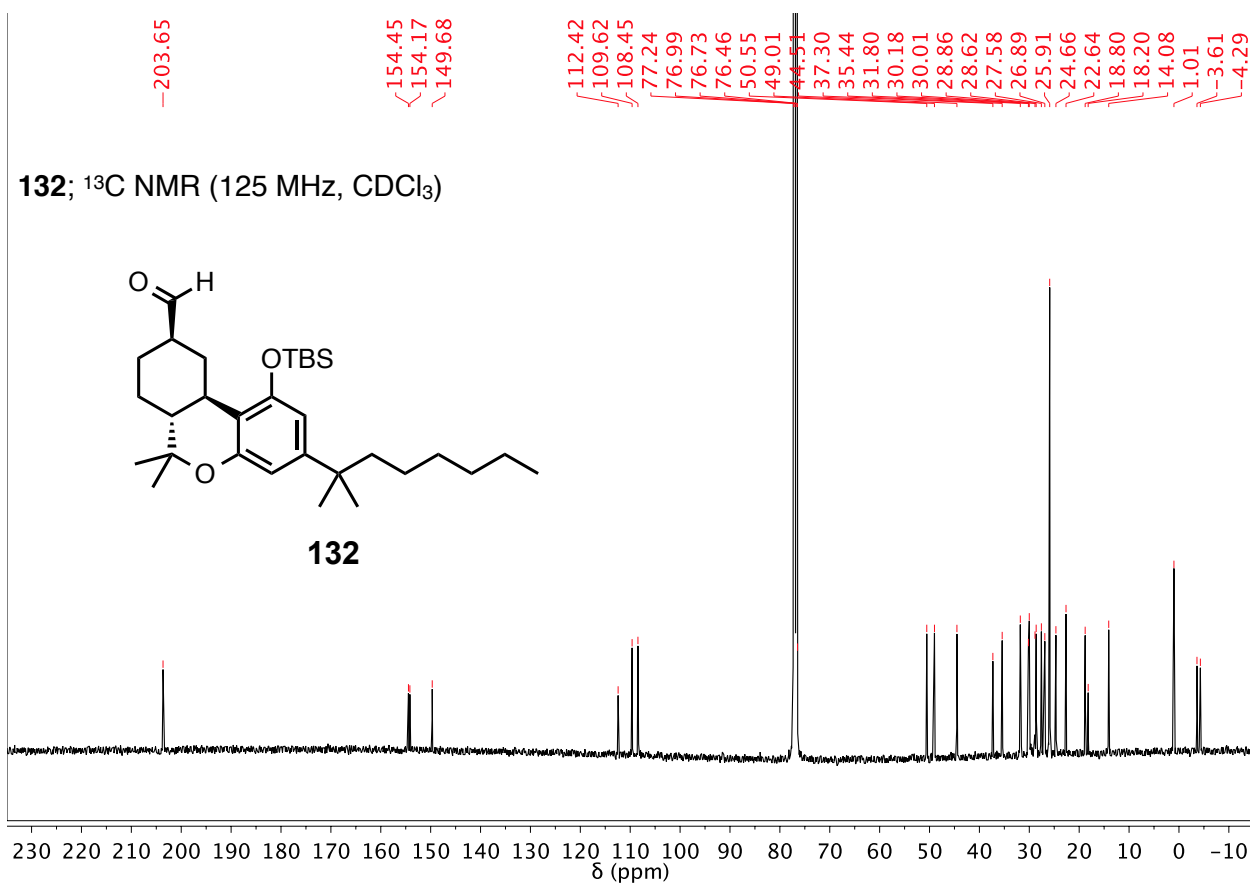


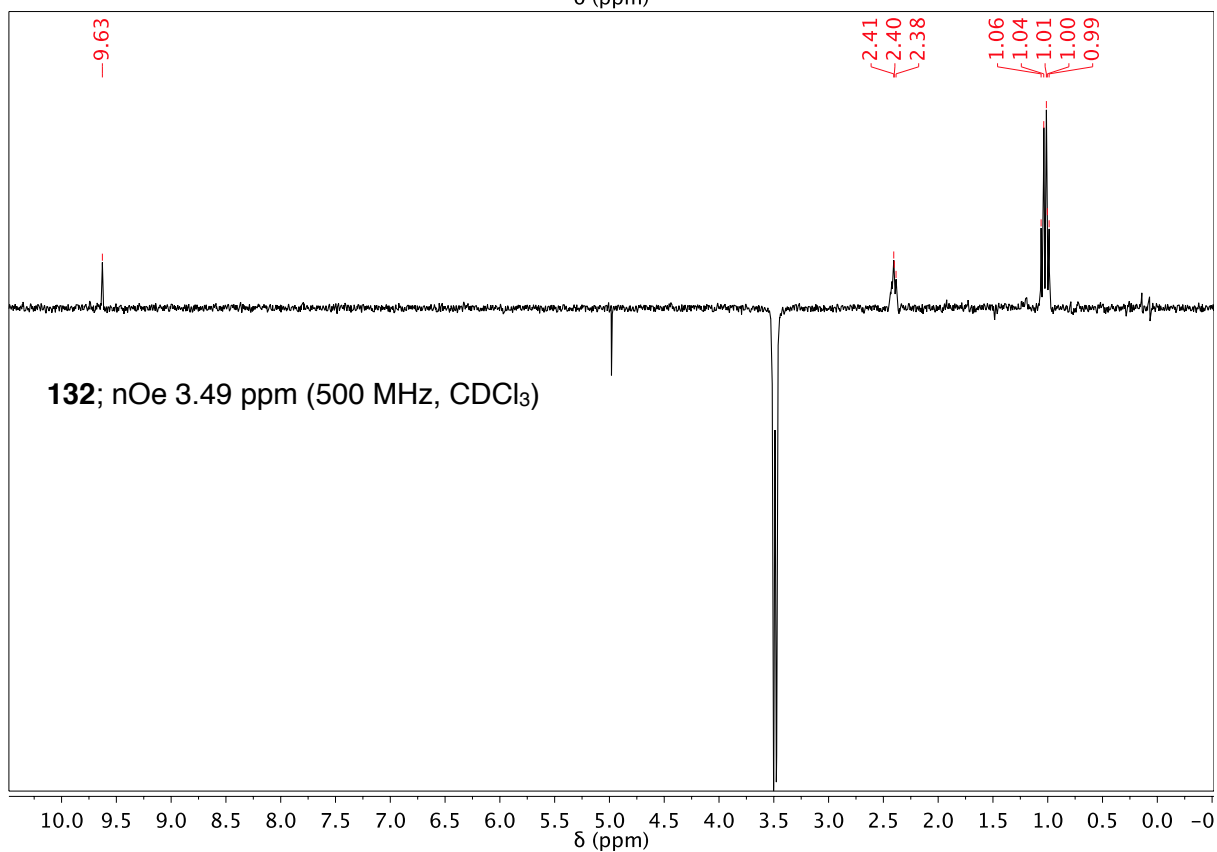
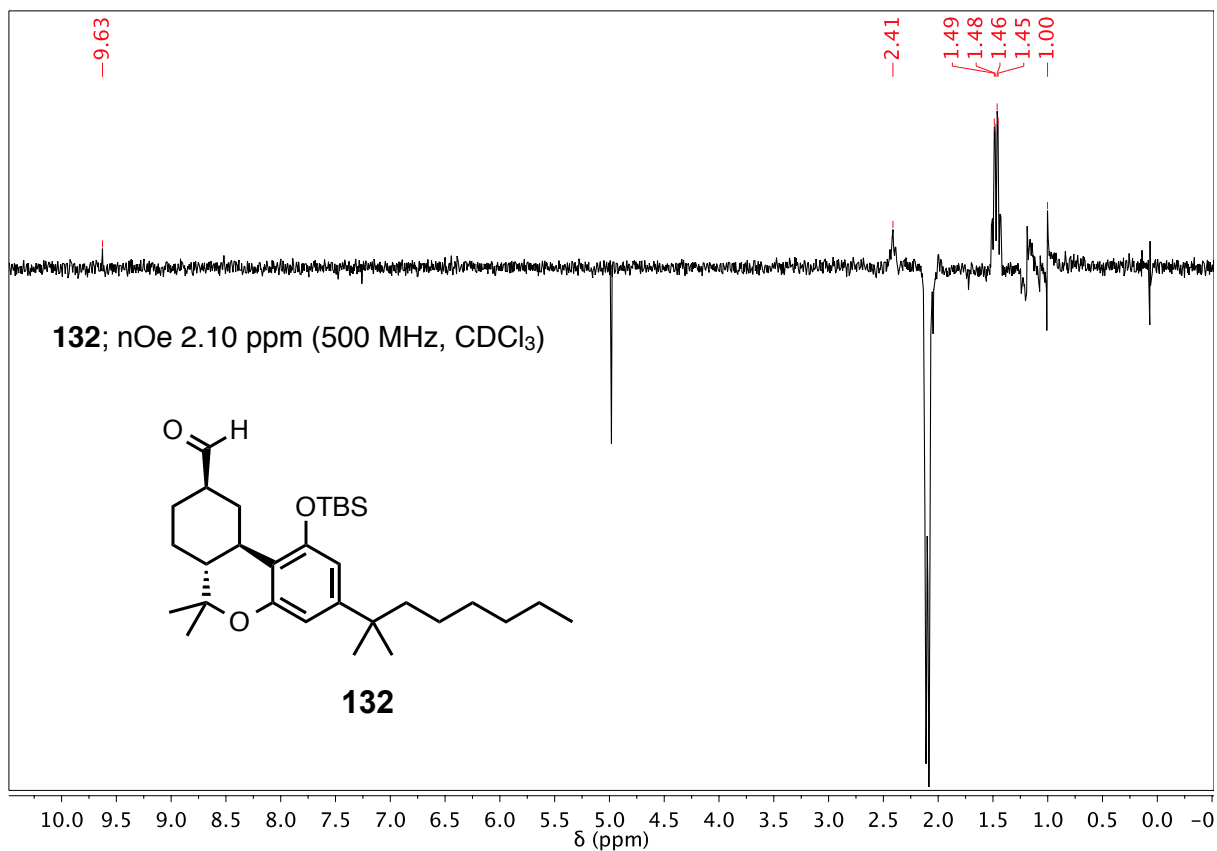
132; ^1H NMR (500 MHz, CDCl_3)



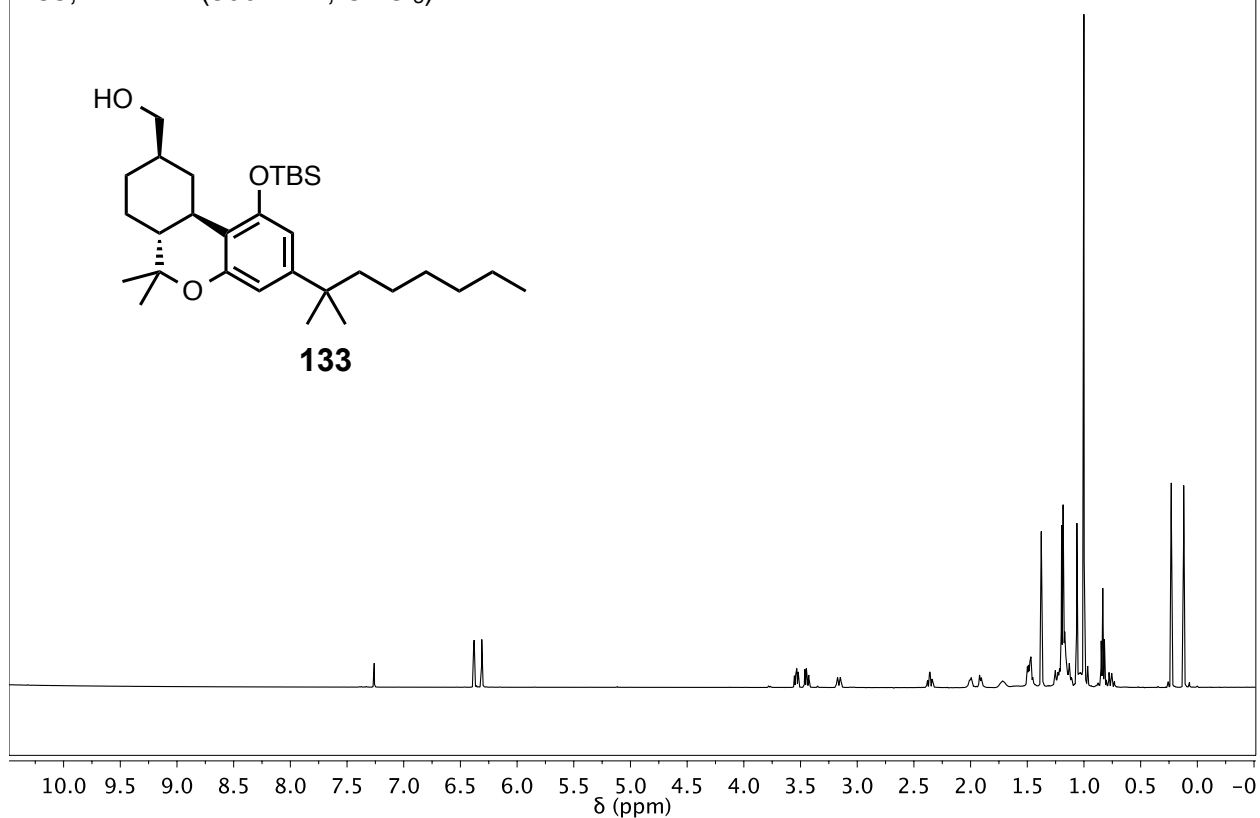
132; ^1H NMR (500 MHz, CDCl_3) Expansions



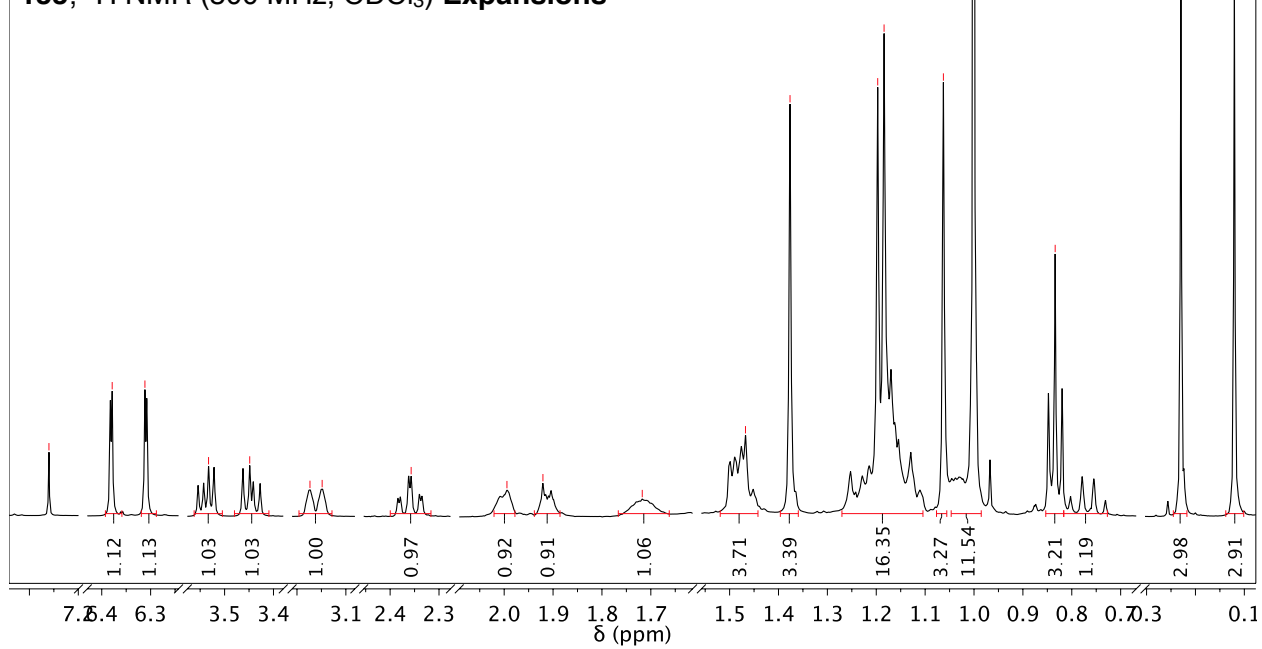


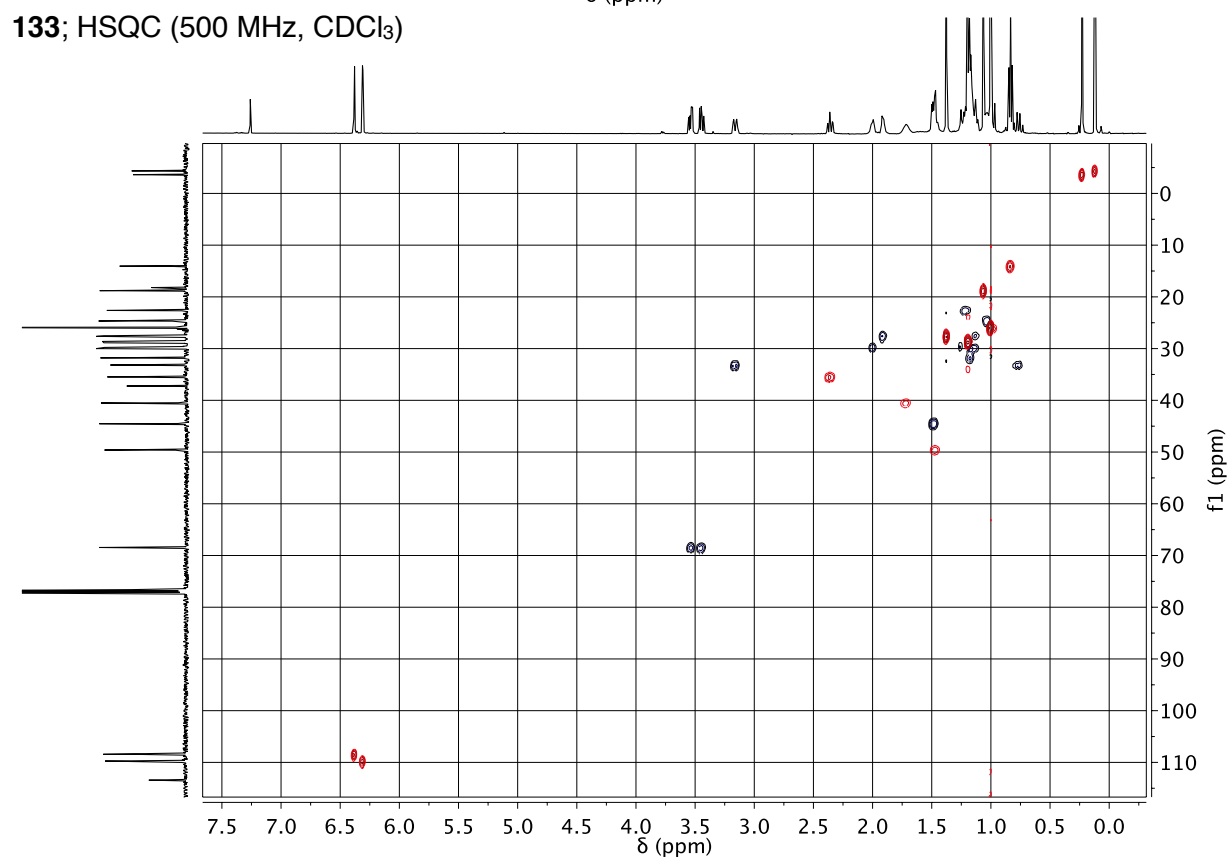
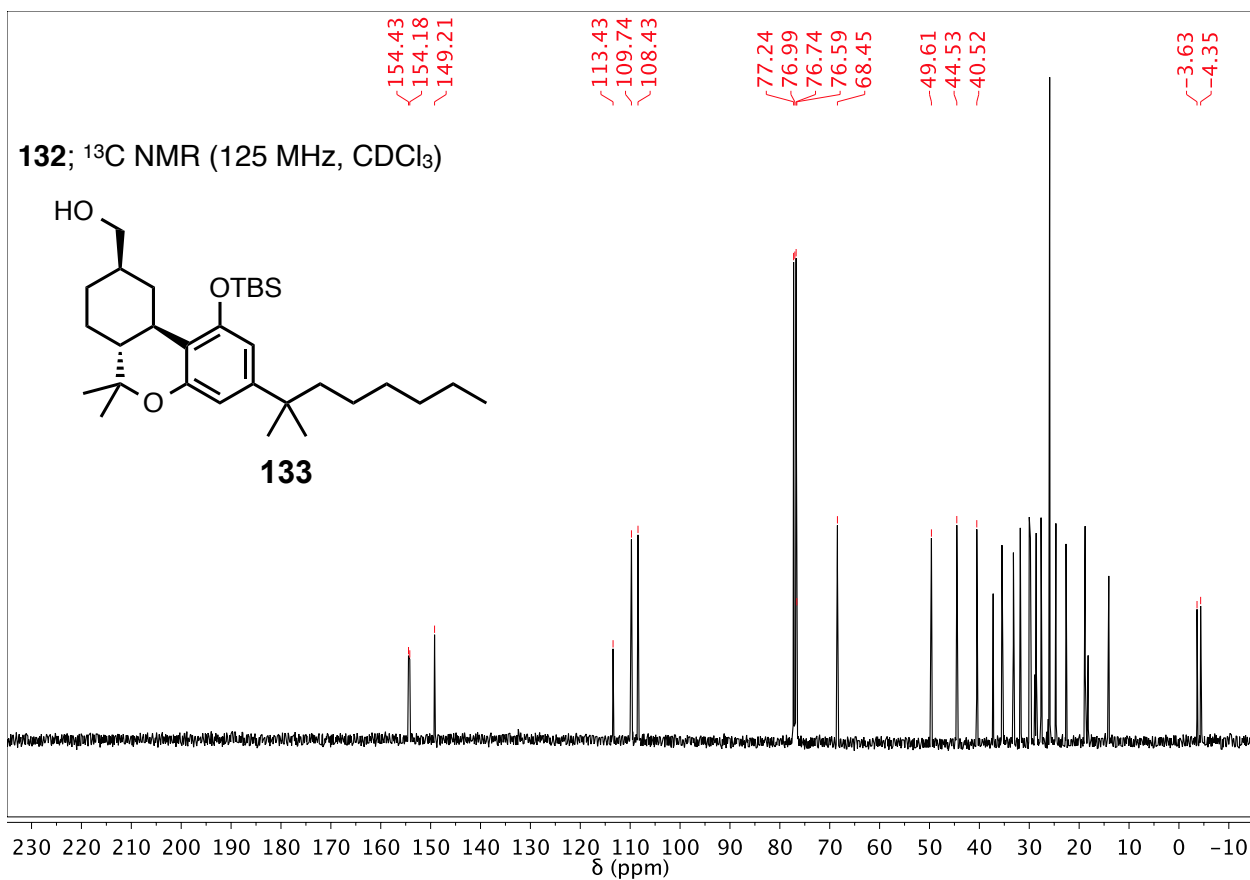


133; ^1H NMR (500 MHz, CDCl_3)

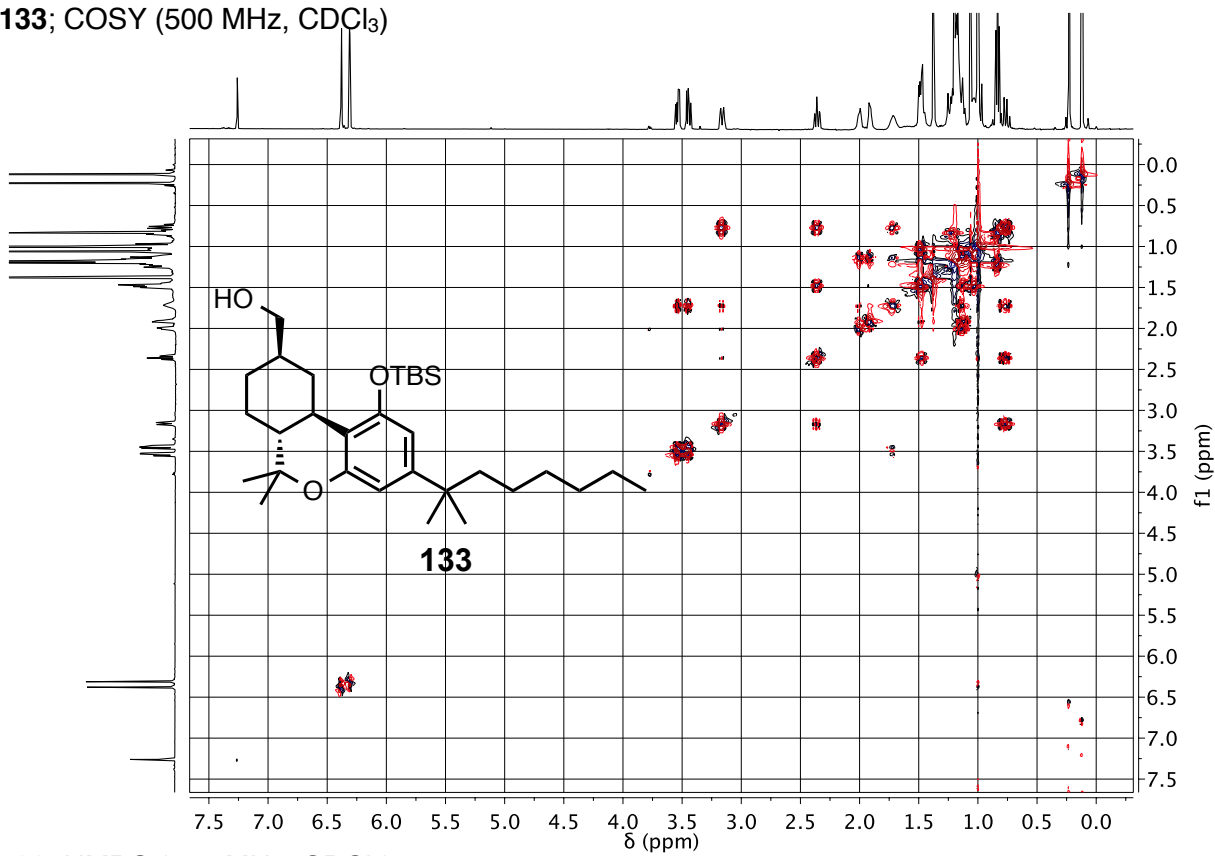


133; ^1H NMR (500 MHz, CDCl_3) Expansions

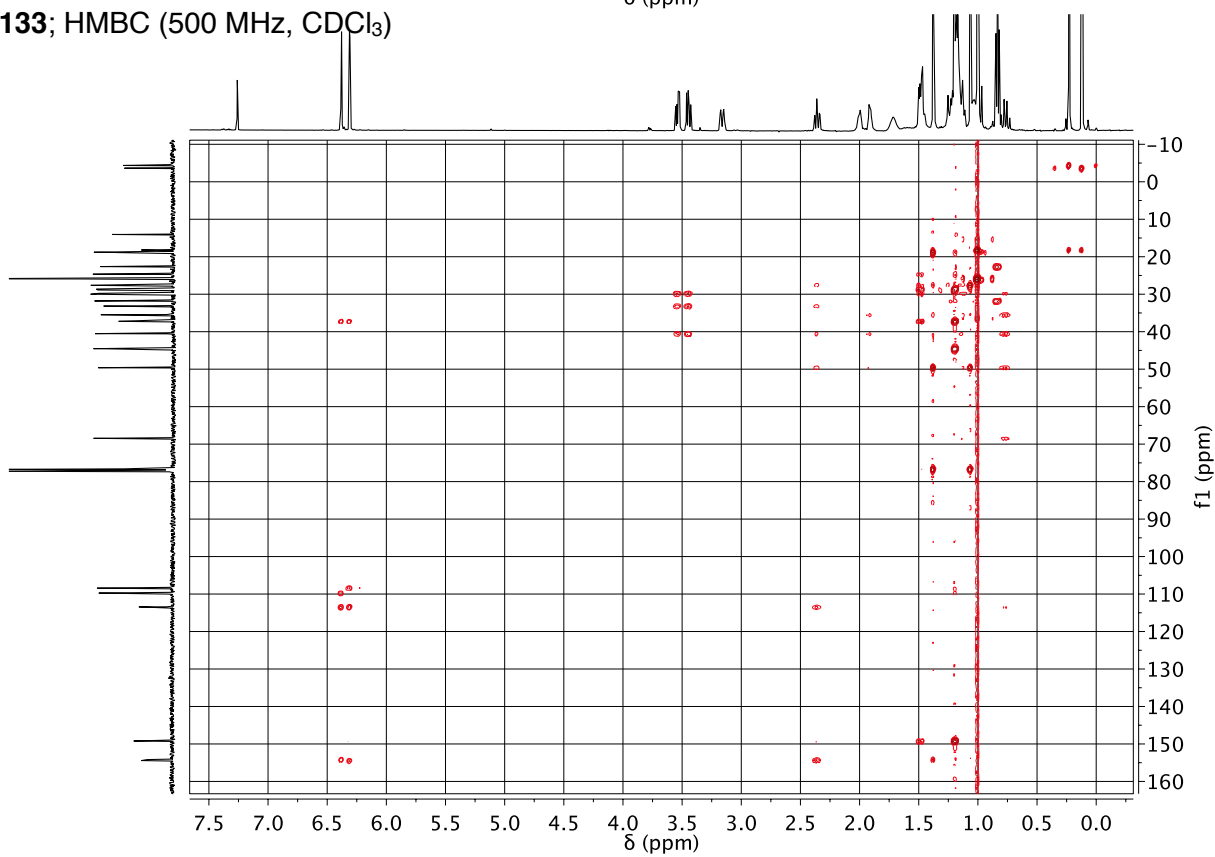


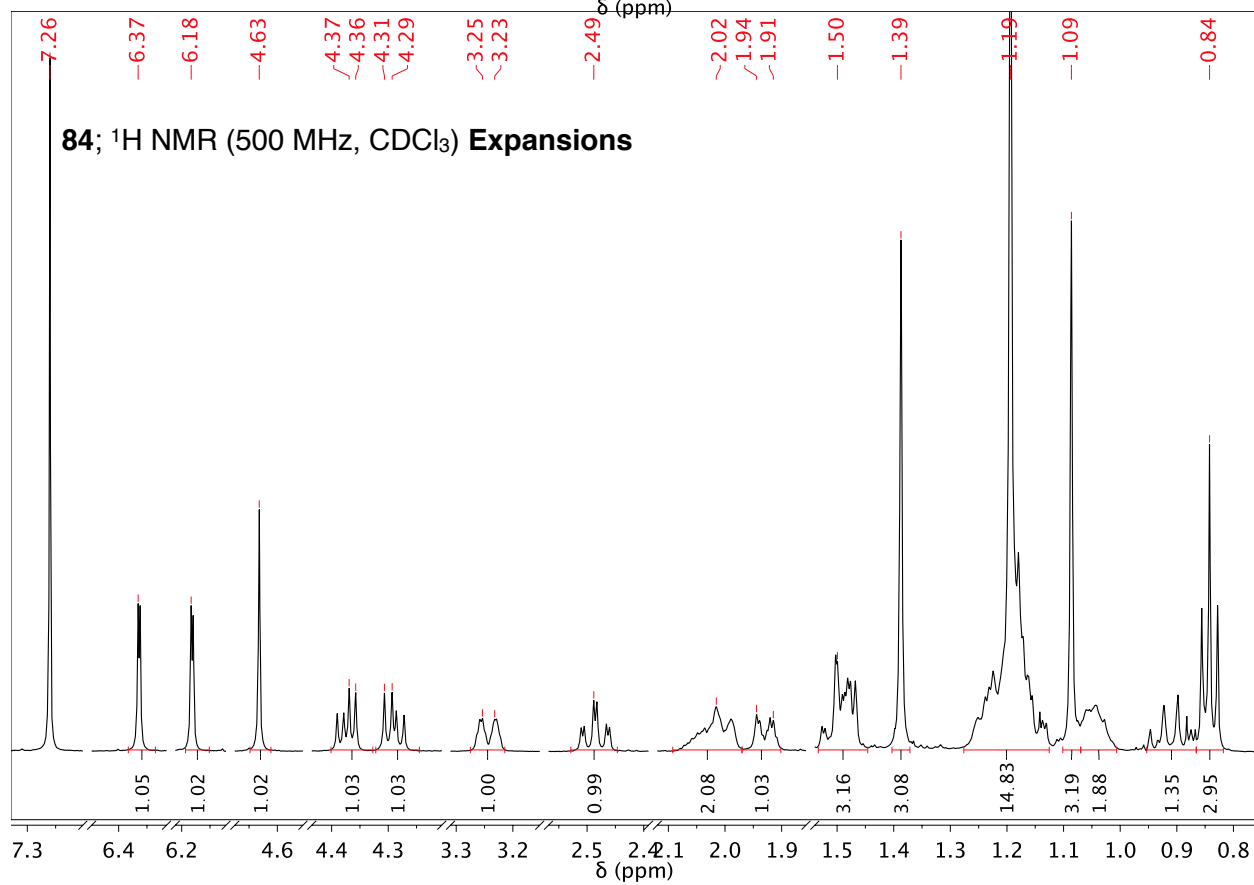
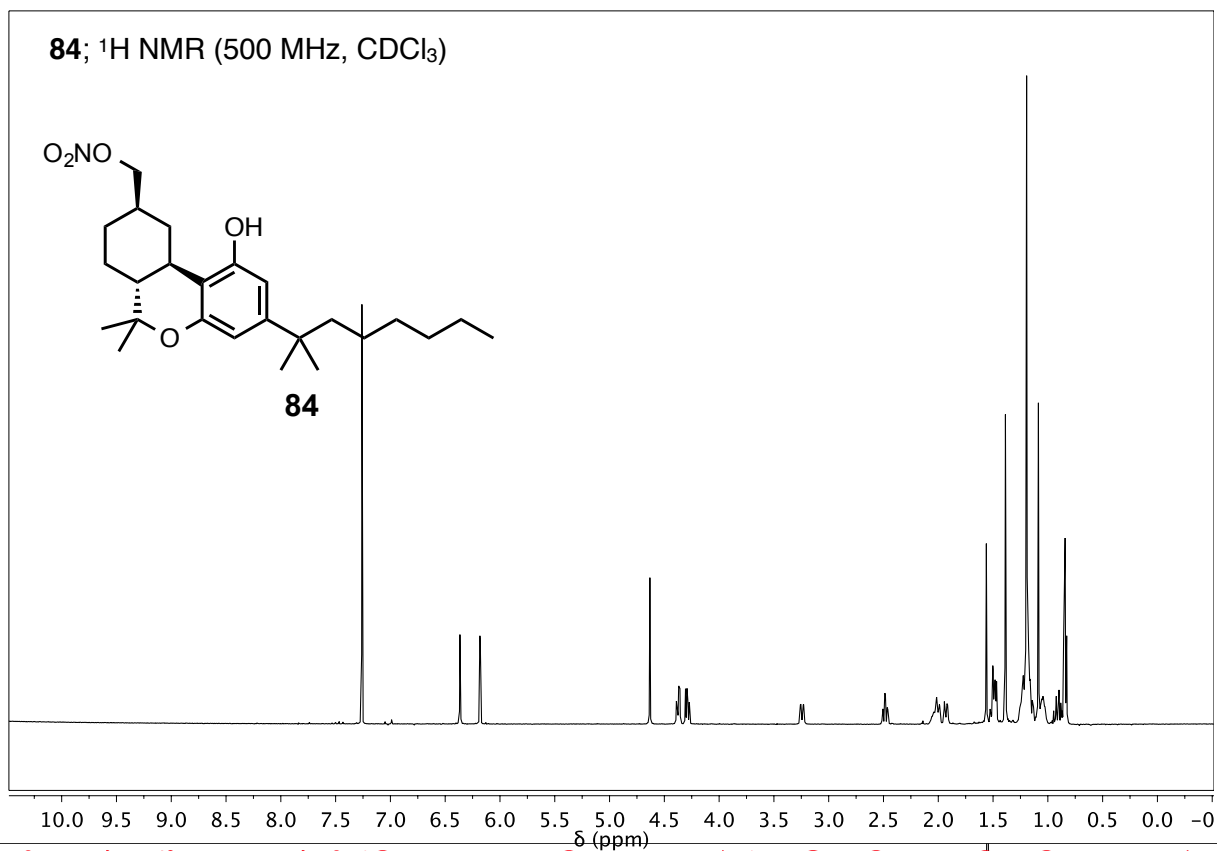


133; COSY (500 MHz, CDCl₃)

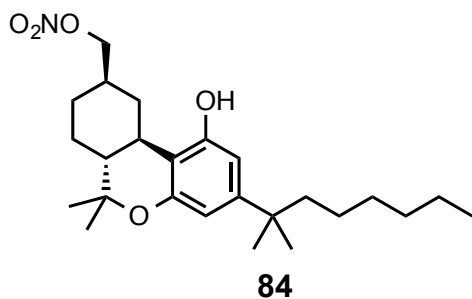


133; HMBC (500 MHz, CDCl₃)

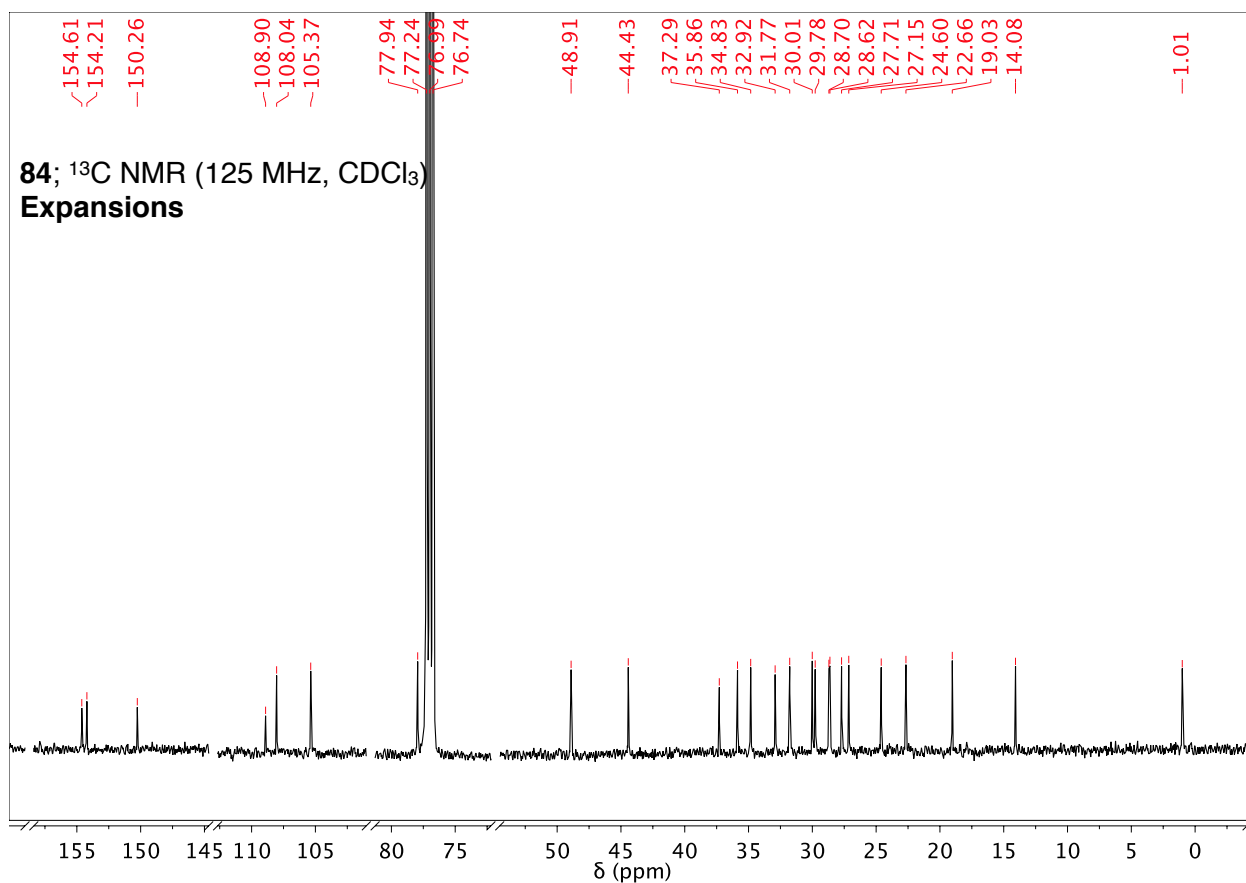




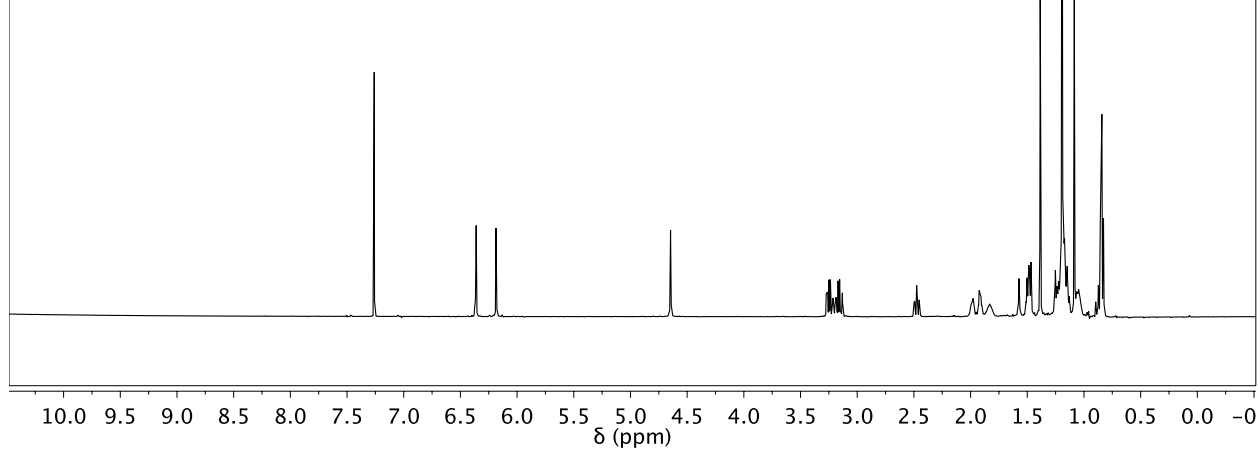
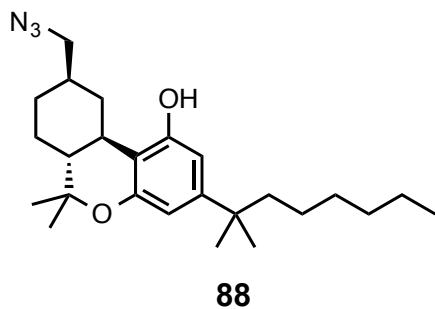
84; ^{13}C NMR (125 MHz, CDCl_3)



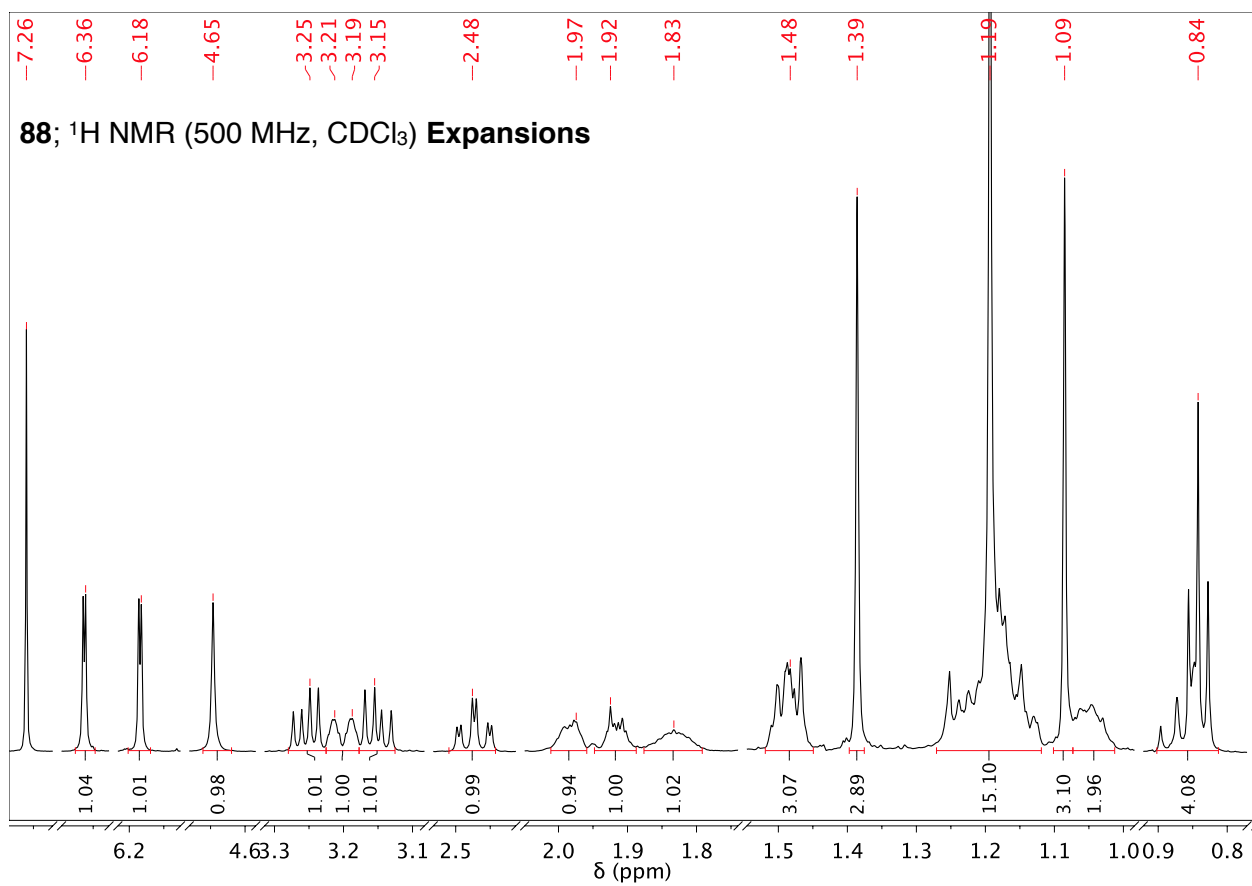
δ (ppm)



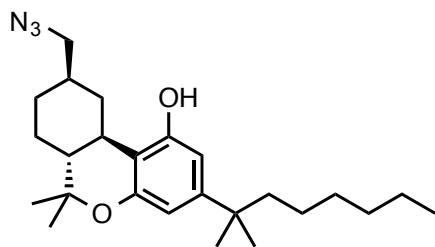
88; ^1H NMR (500 MHz, CDCl_3)



88; ^1H NMR (500 MHz, CDCl_3) **Expansions**

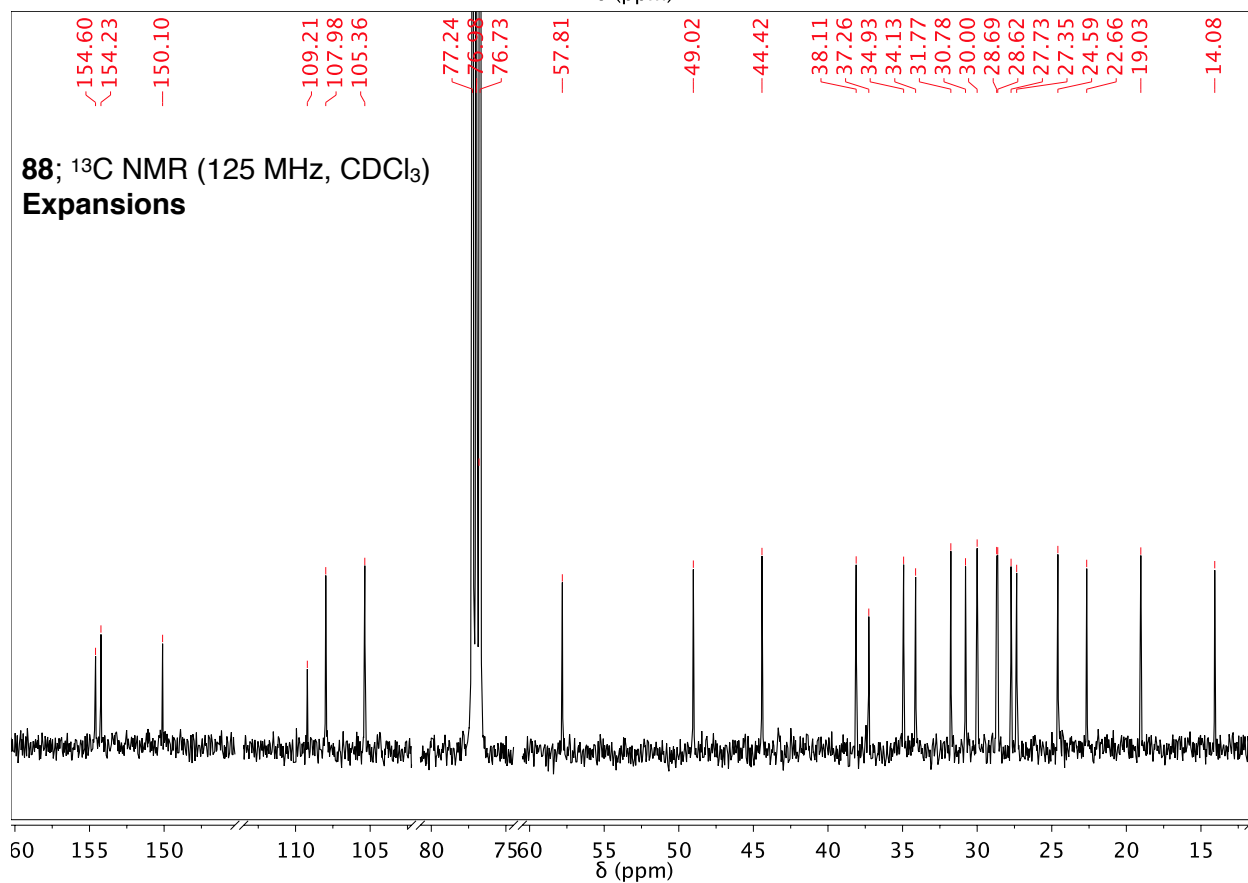


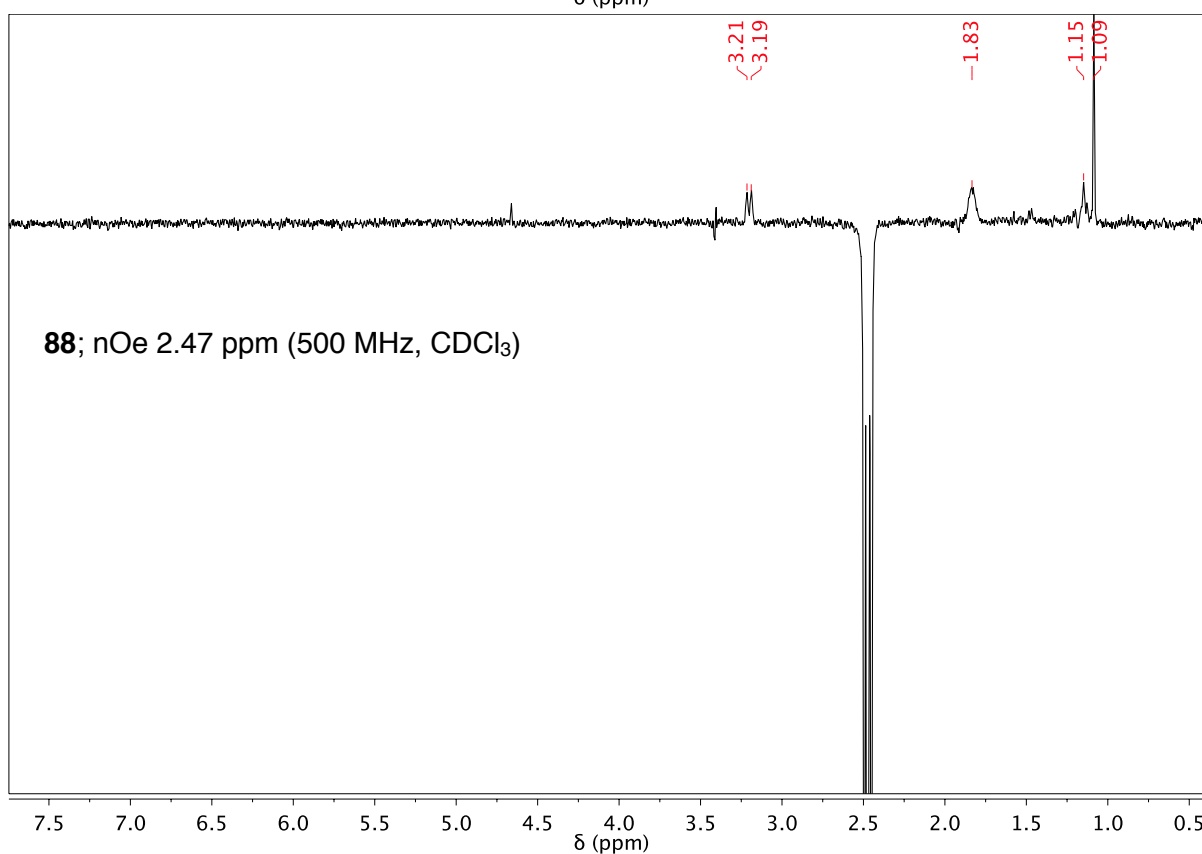
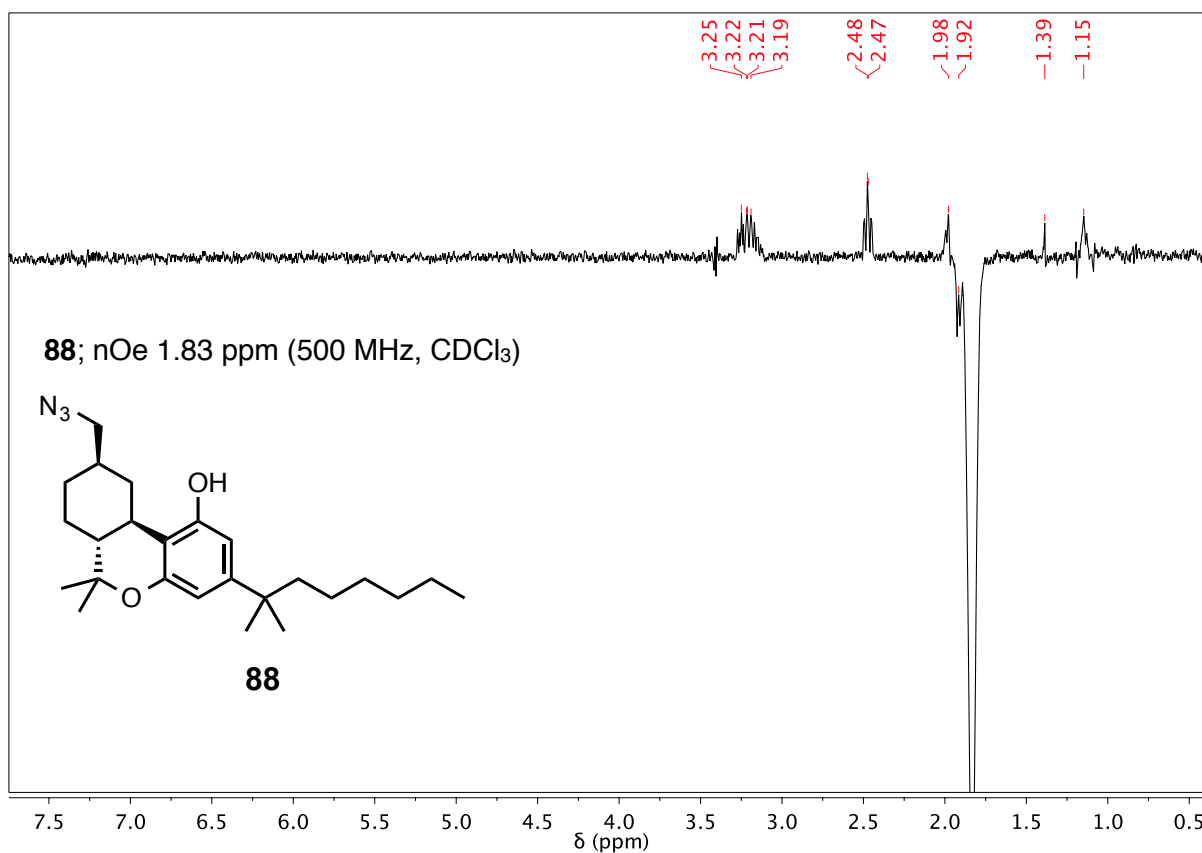
88; ^{13}C NMR (125 MHz, CDCl_3)



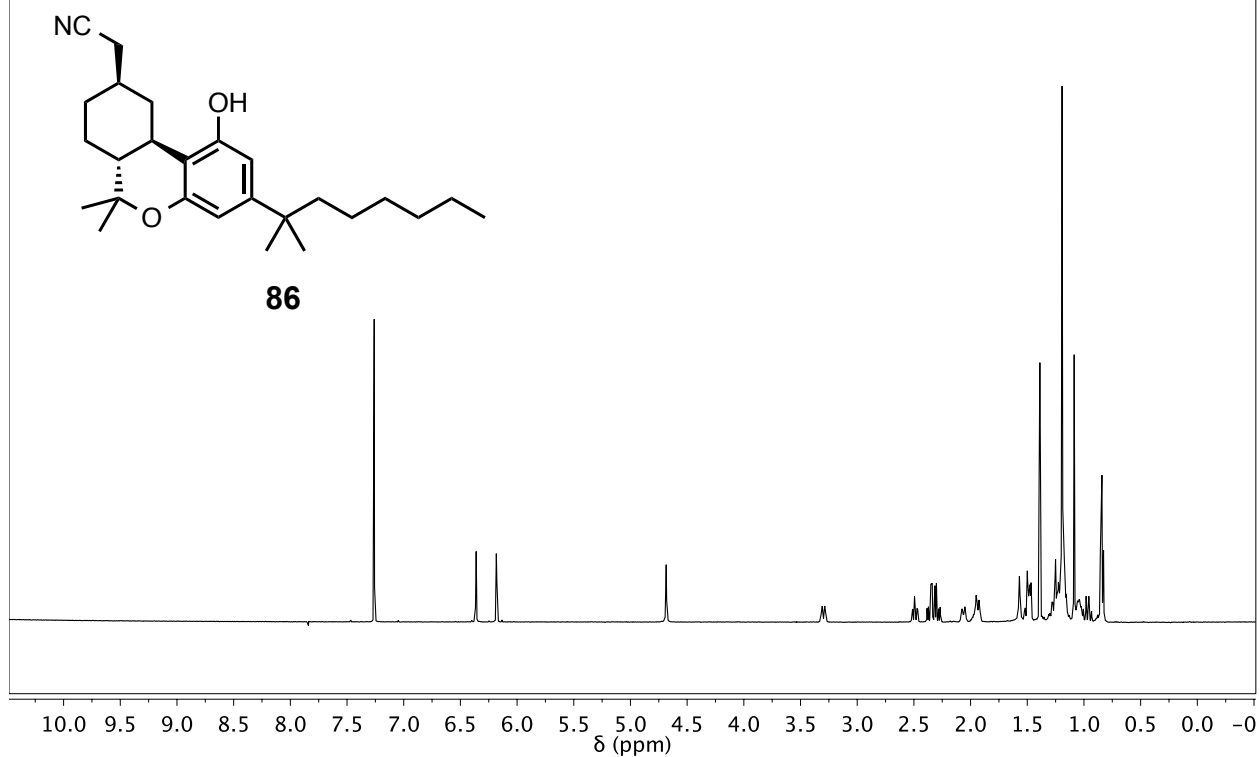
88

230 220 210 200 190 180 170 160 150 140 130 120 110 100 90 80 70 60 50 40 30 20 10 0 -10
 δ (ppm)

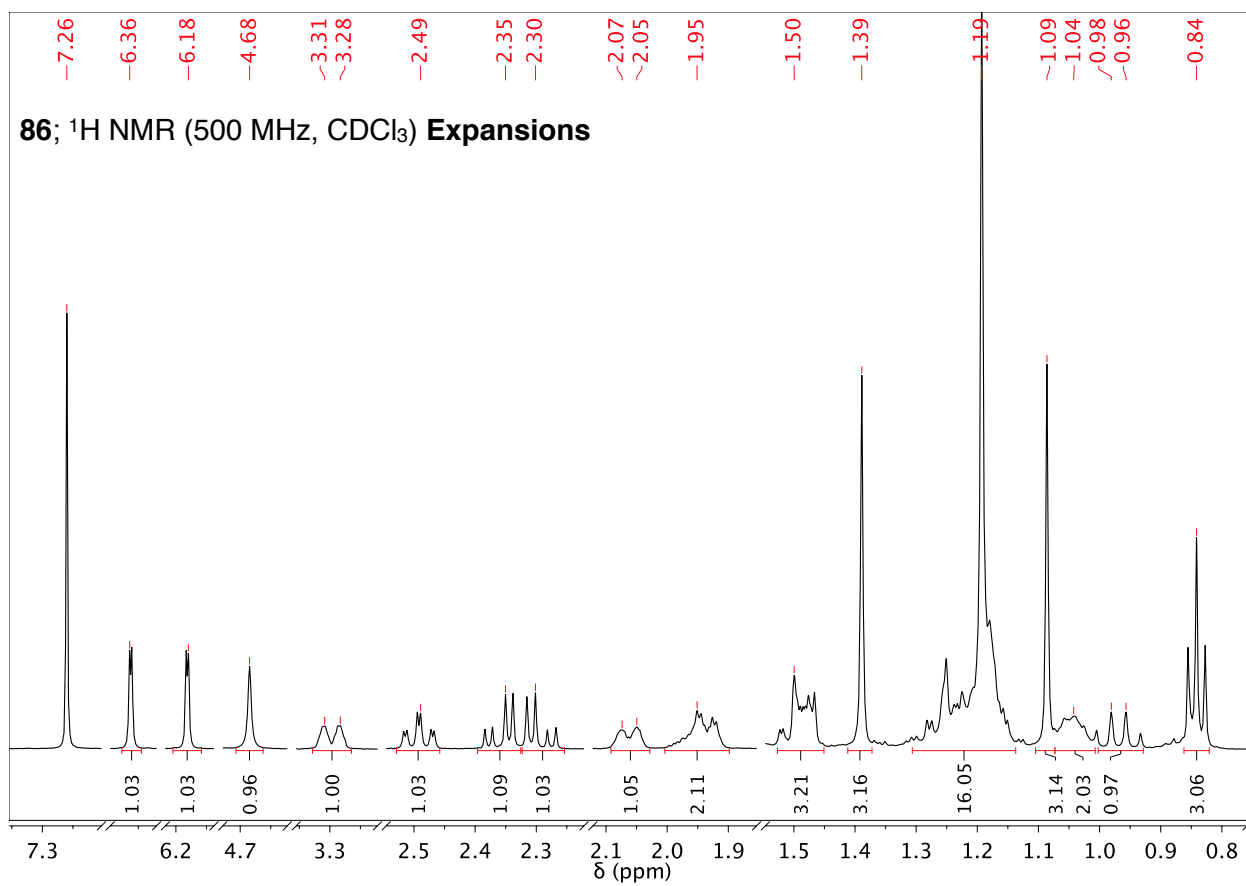




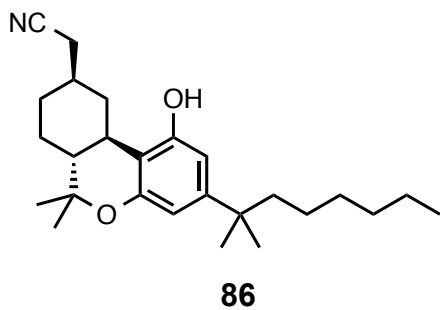
86; ^1H NMR (500 MHz, CDCl_3)



86; ^1H NMR (500 MHz, CDCl_3) **Expansions**

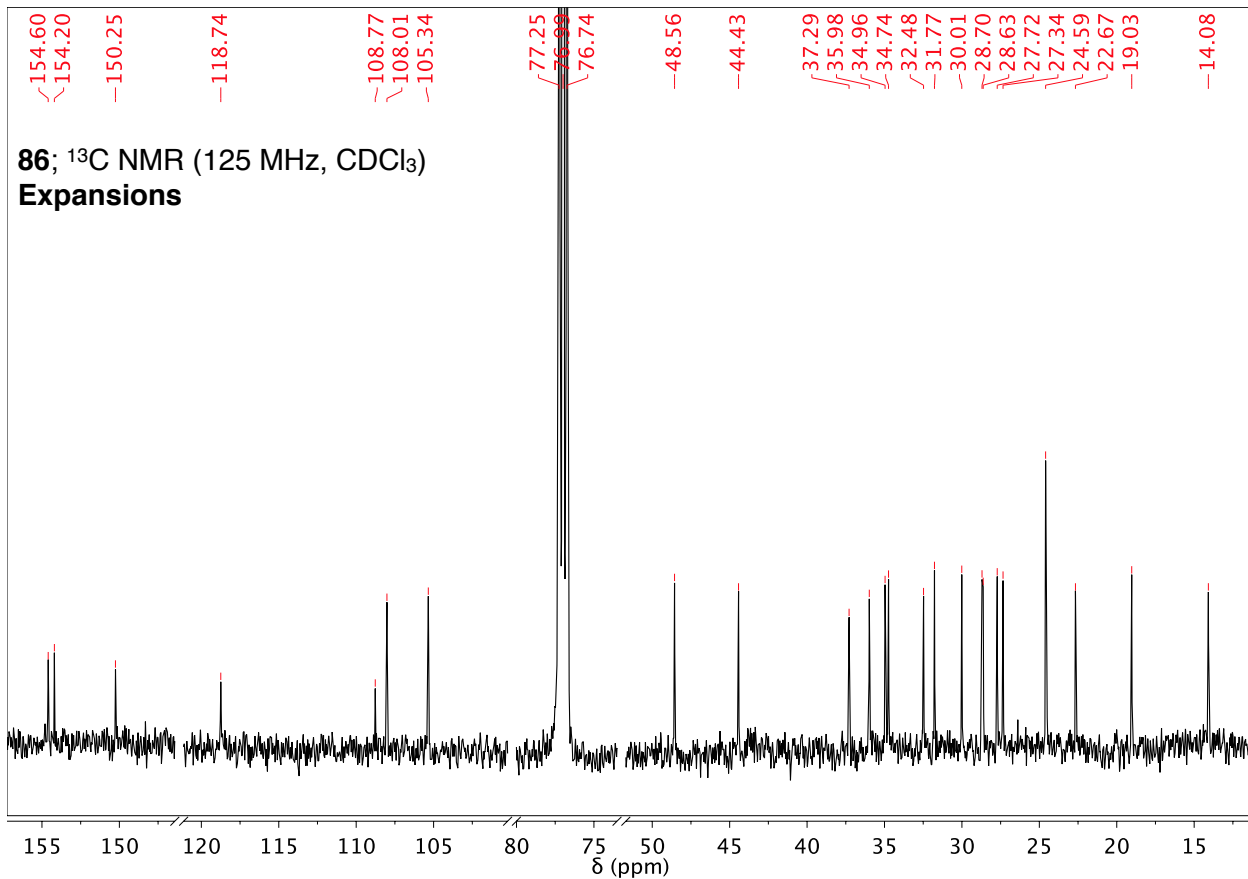


86; ^{13}C NMR (125 MHz, CDCl_3)

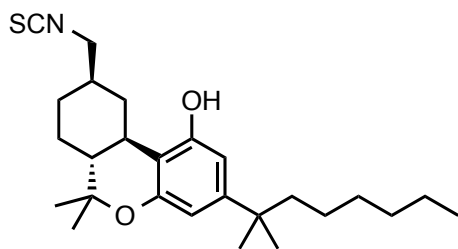


230 220 210 200 190 180 170 160 150 140 130 120 110 100 90 80 70 60 50 40 30 20 10 0 -10
 δ (ppm)

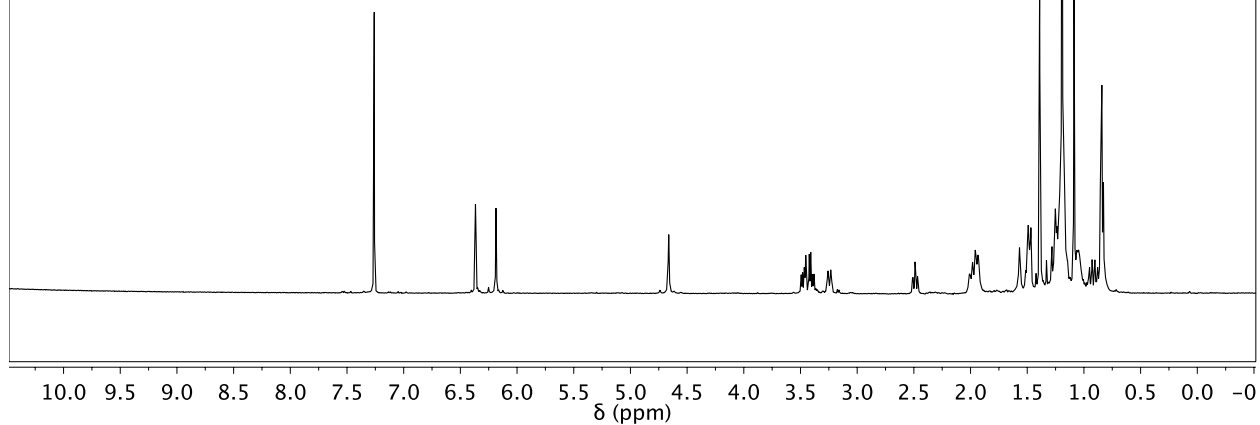
86; ^{13}C NMR (125 MHz, CDCl_3)
Expansions



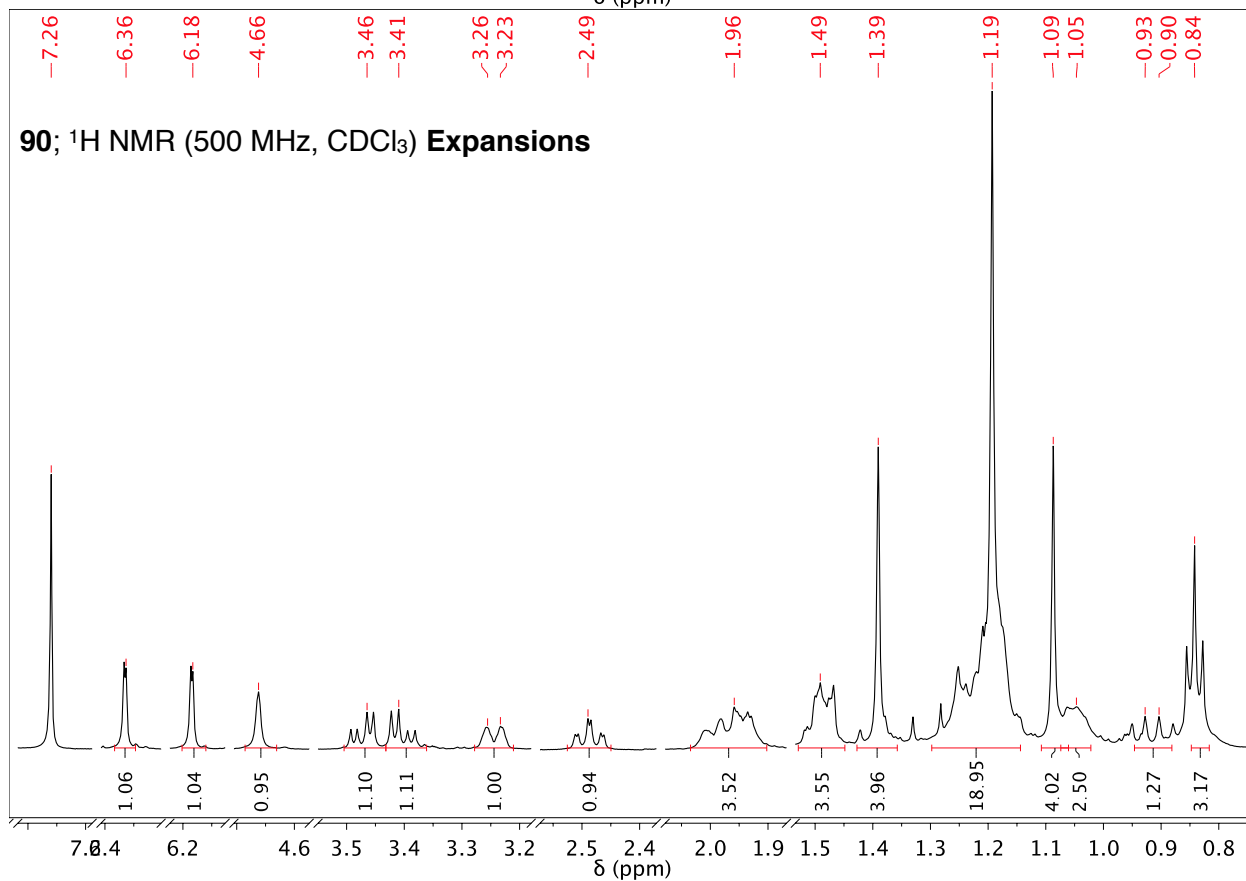
90; ^1H NMR (500 MHz, CDCl_3)



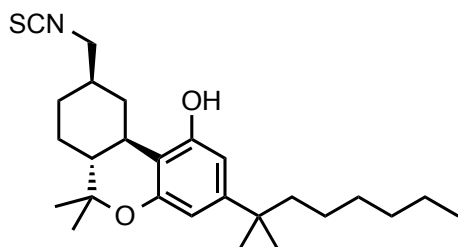
90



90; ^1H NMR (500 MHz, CDCl_3) **Expansions**

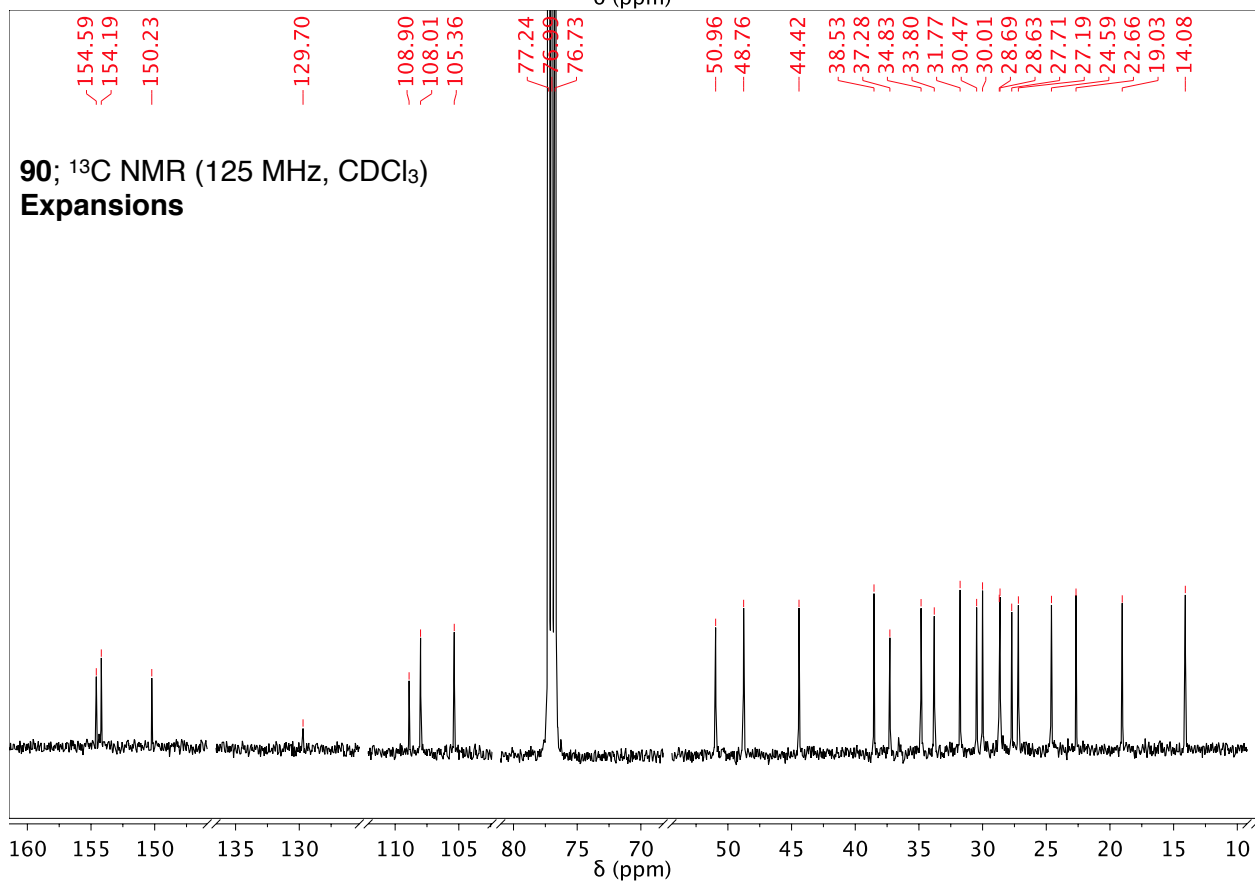


90; ^{13}C NMR (125 MHz, CDCl_3)

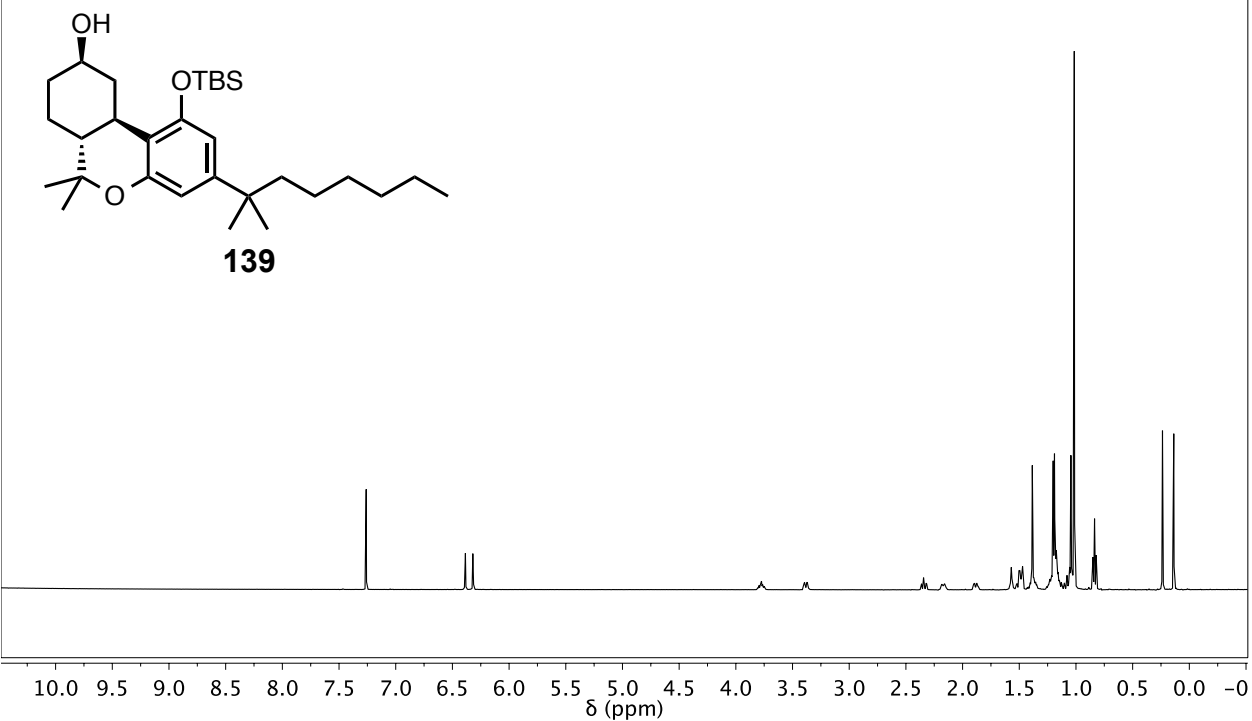


90

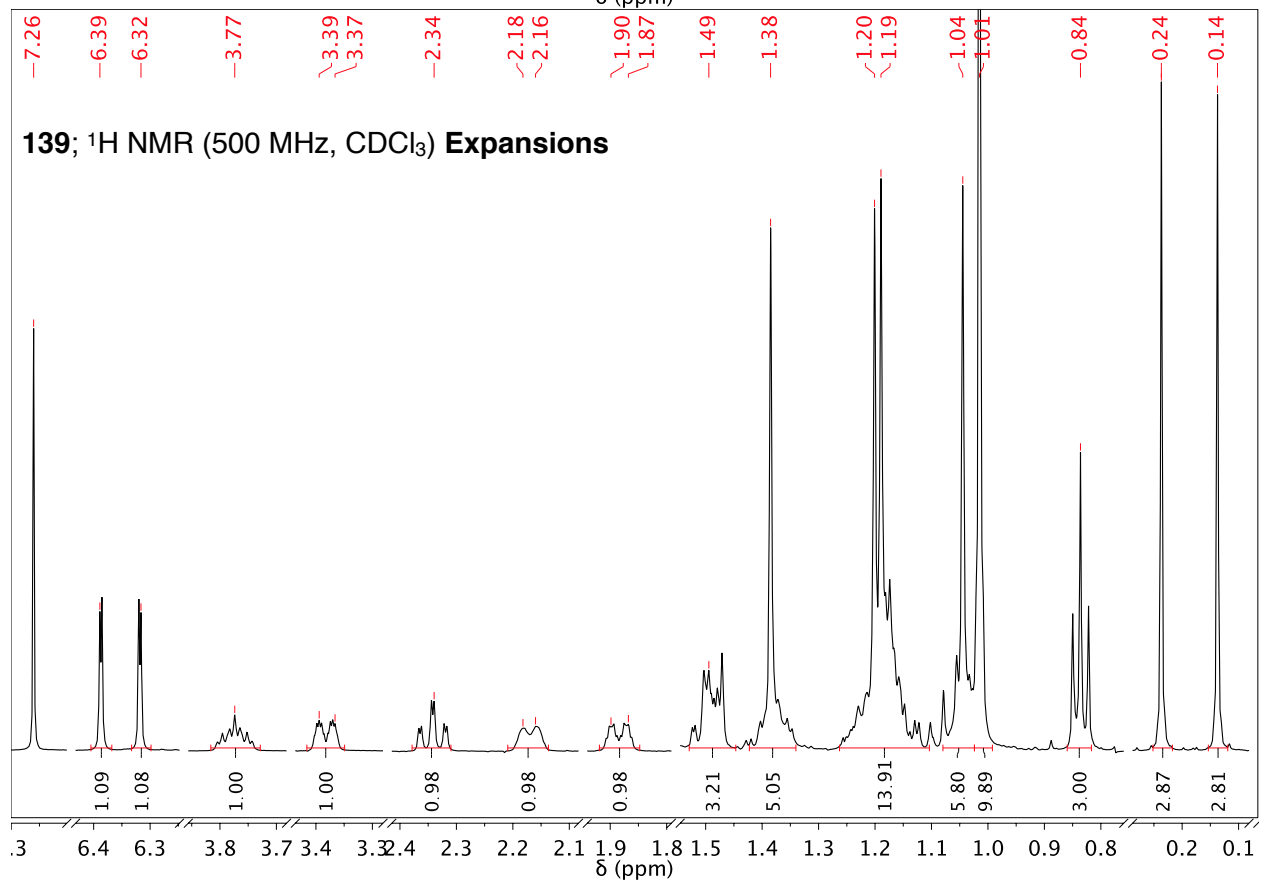
δ (ppm)



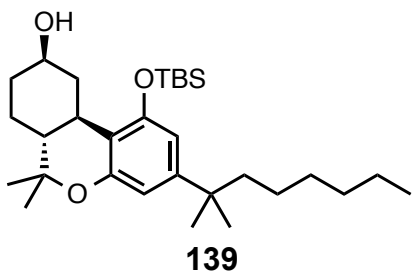
139; ^1H NMR (500 MHz, CDCl_3)



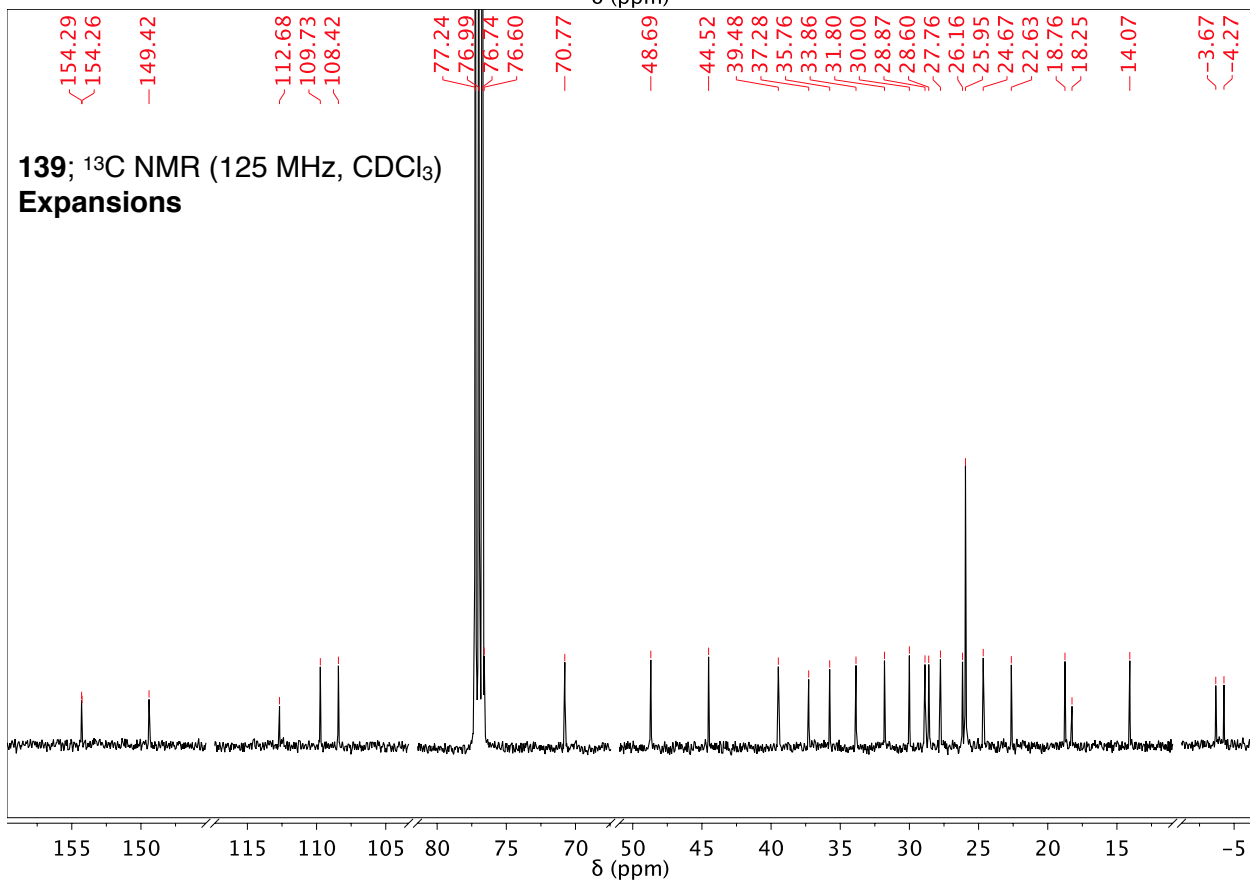
139; ^1H NMR (500 MHz, CDCl_3) Expansions



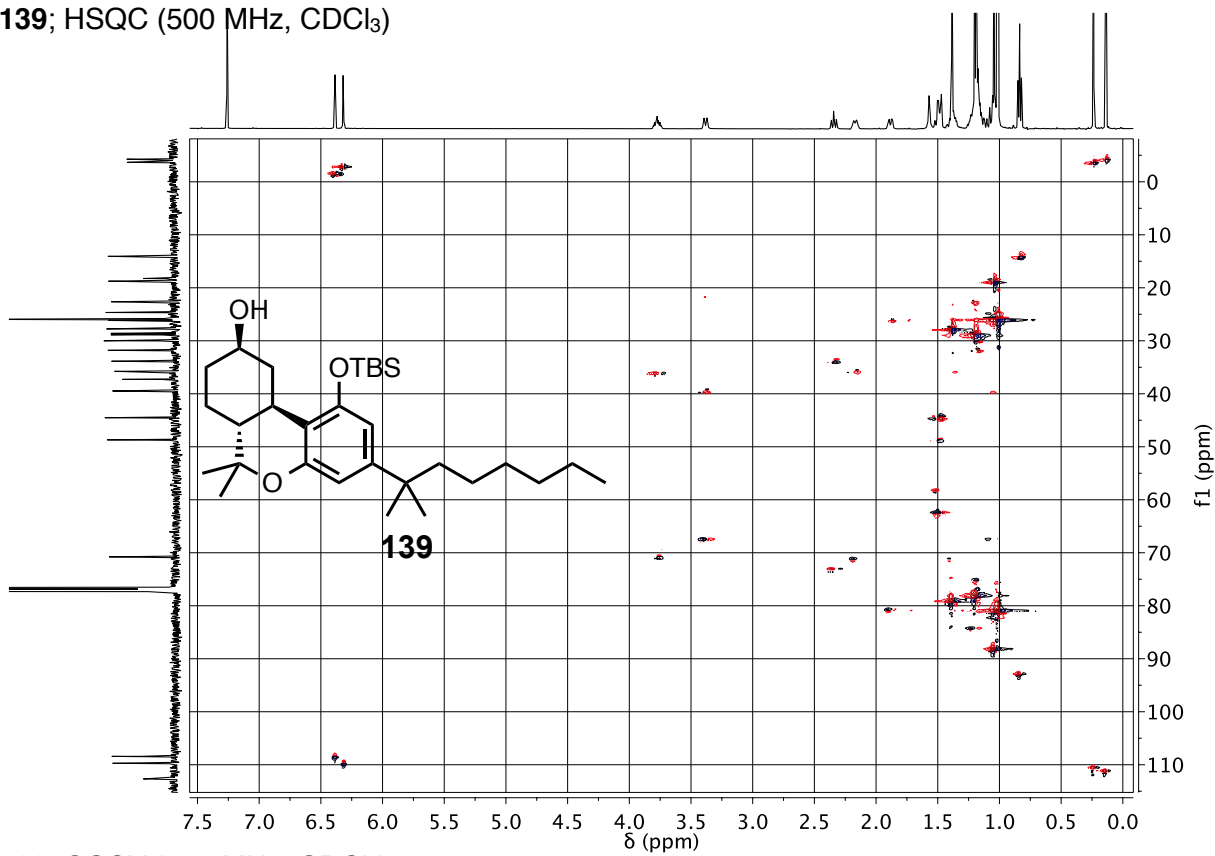
139; ^{13}C NMR (125 MHz, CDCl_3)



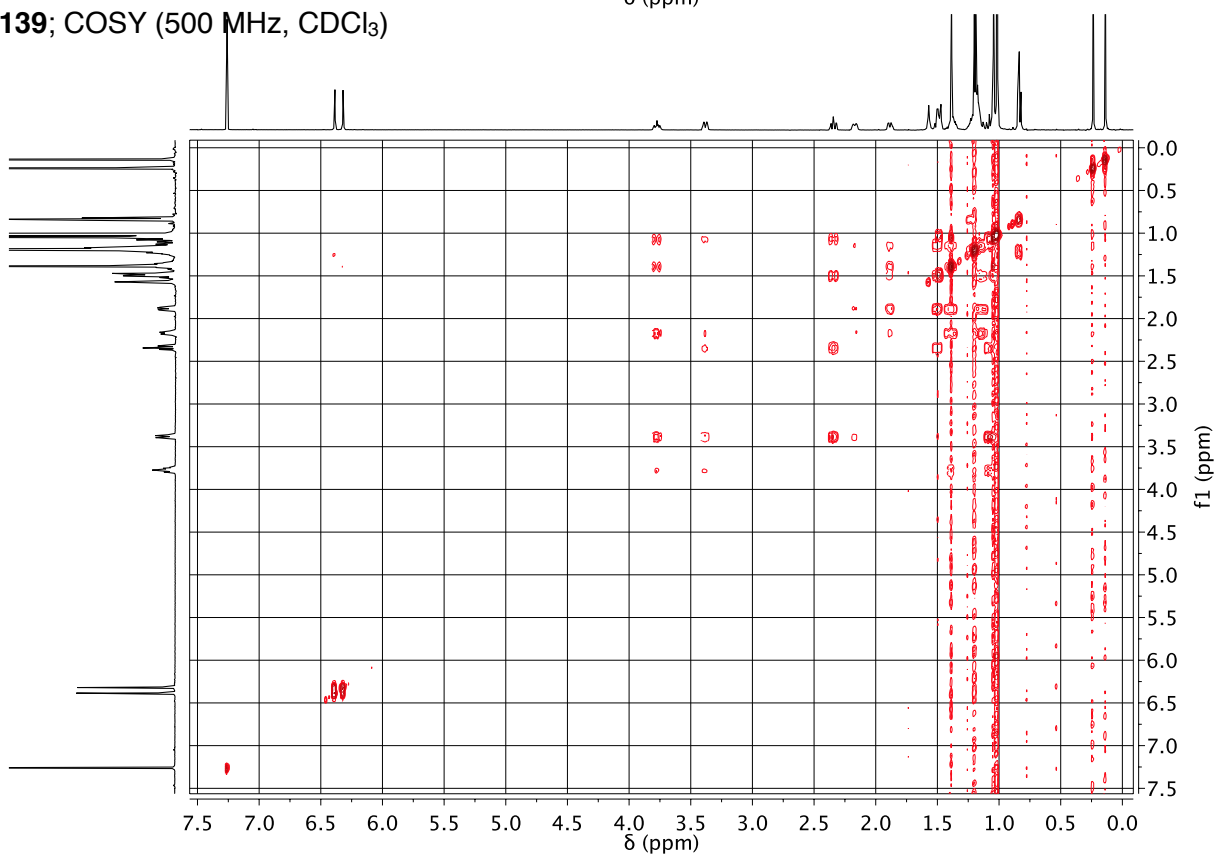
230 220 210 200 190 180 170 160 150 140 130 120 110 100 90 80 70 60 50 40 30 20 10 0 -10
 δ (ppm)



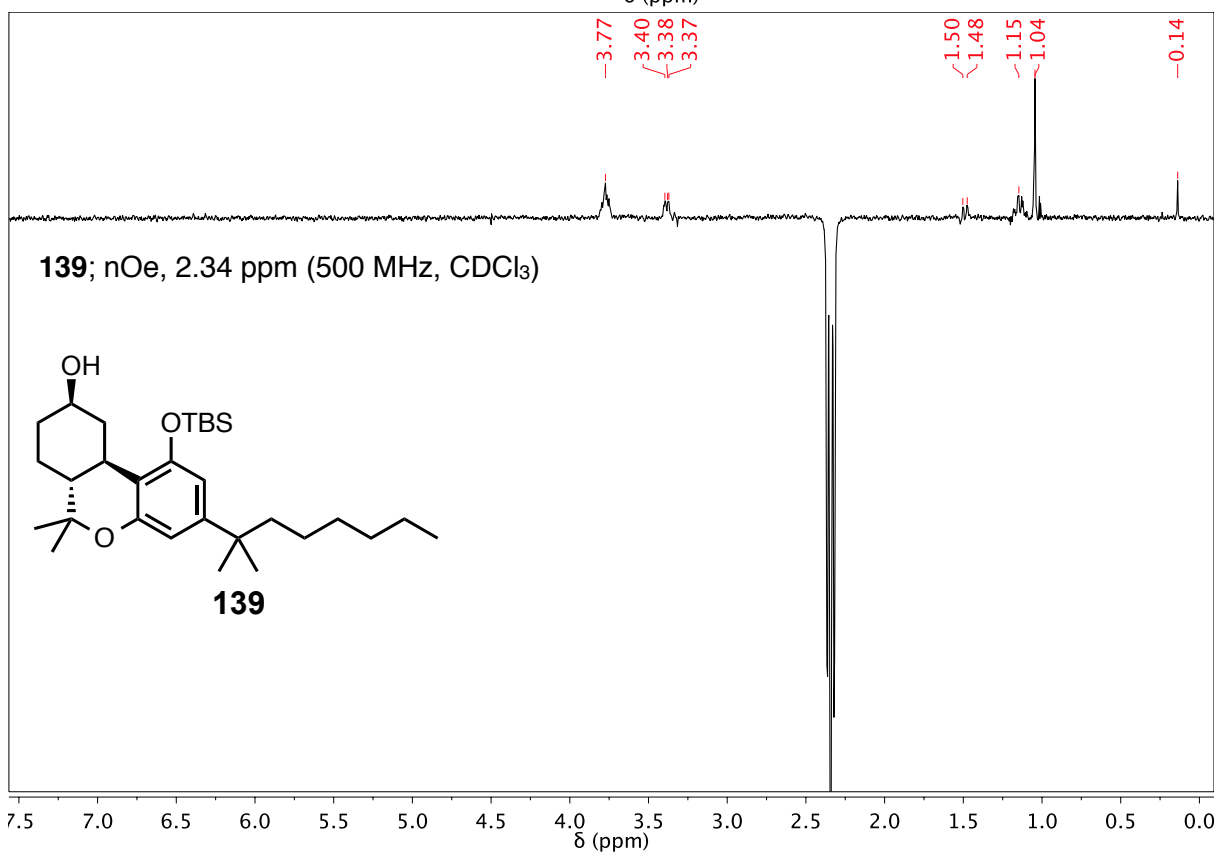
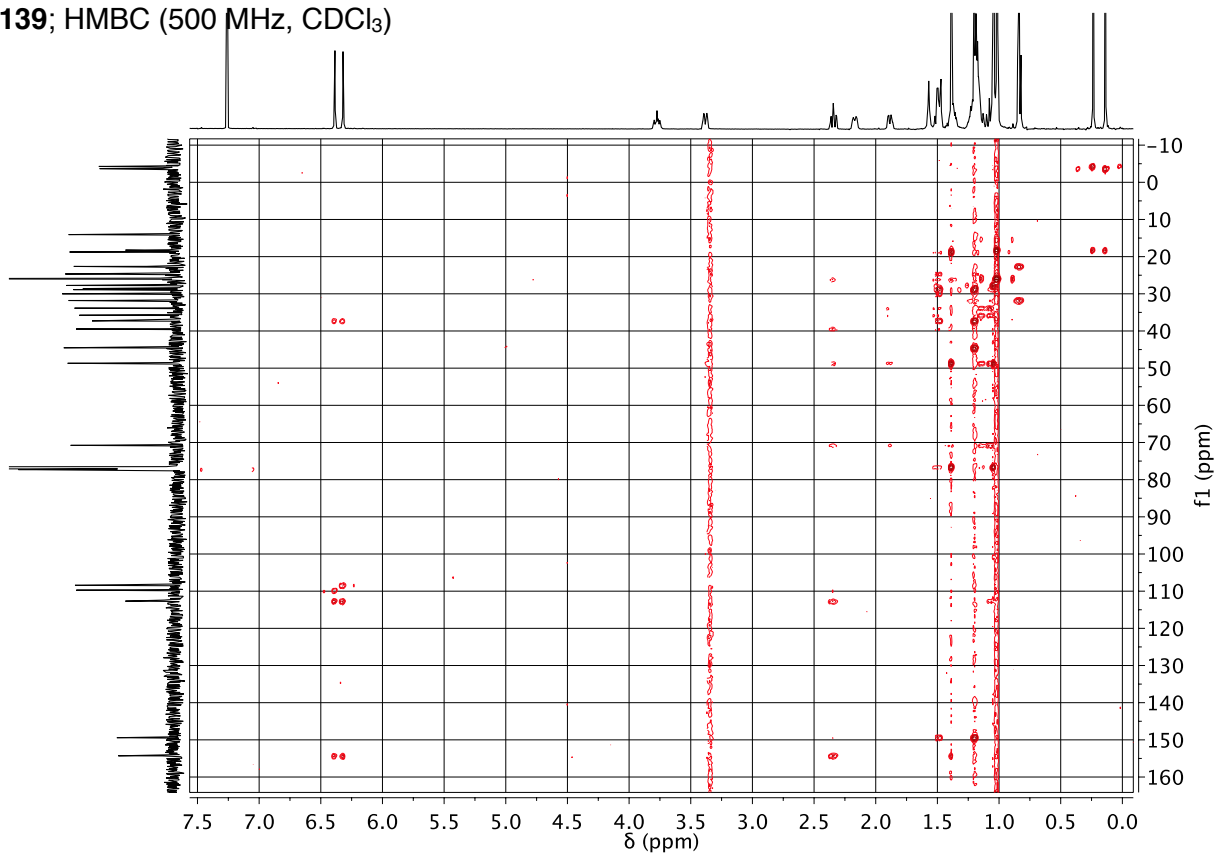
139; HSQC (500 MHz, CDCl₃)

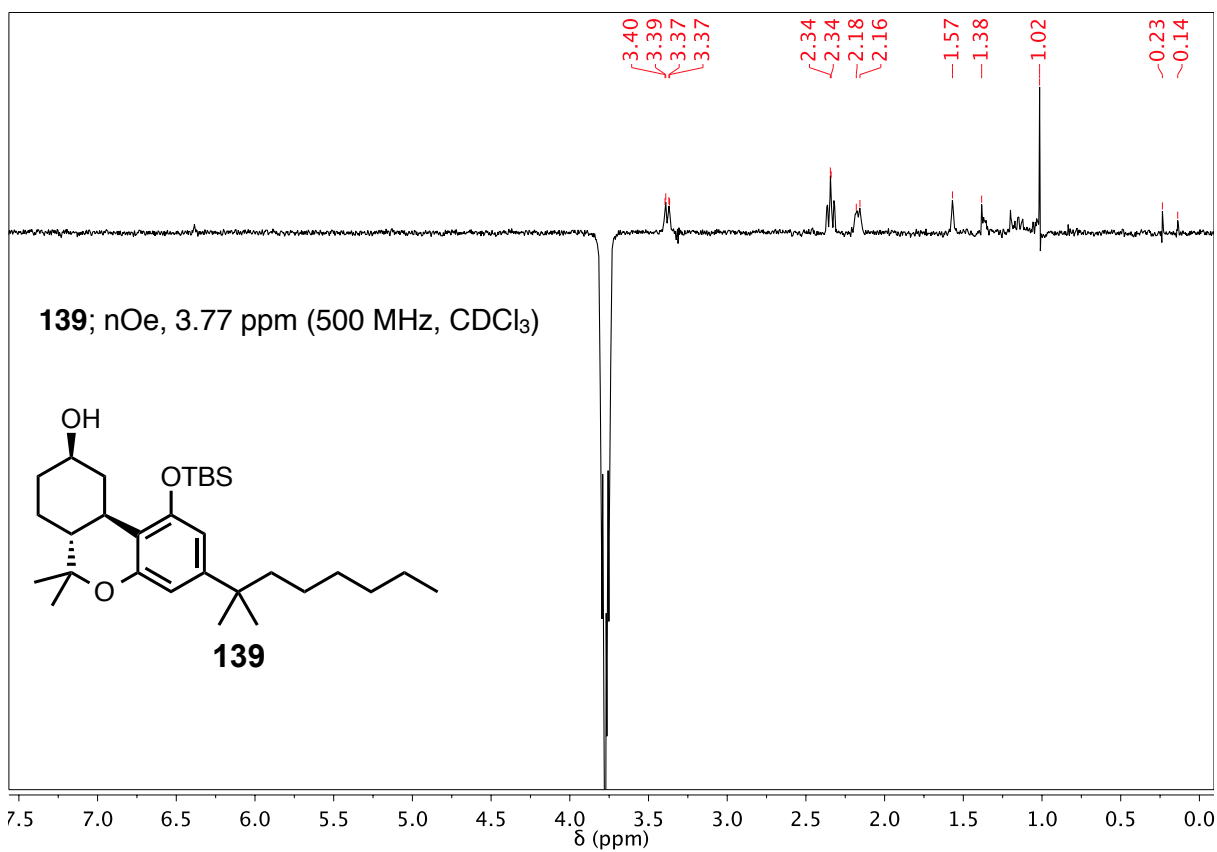


139; COSY (500 MHz, CDCl₃)

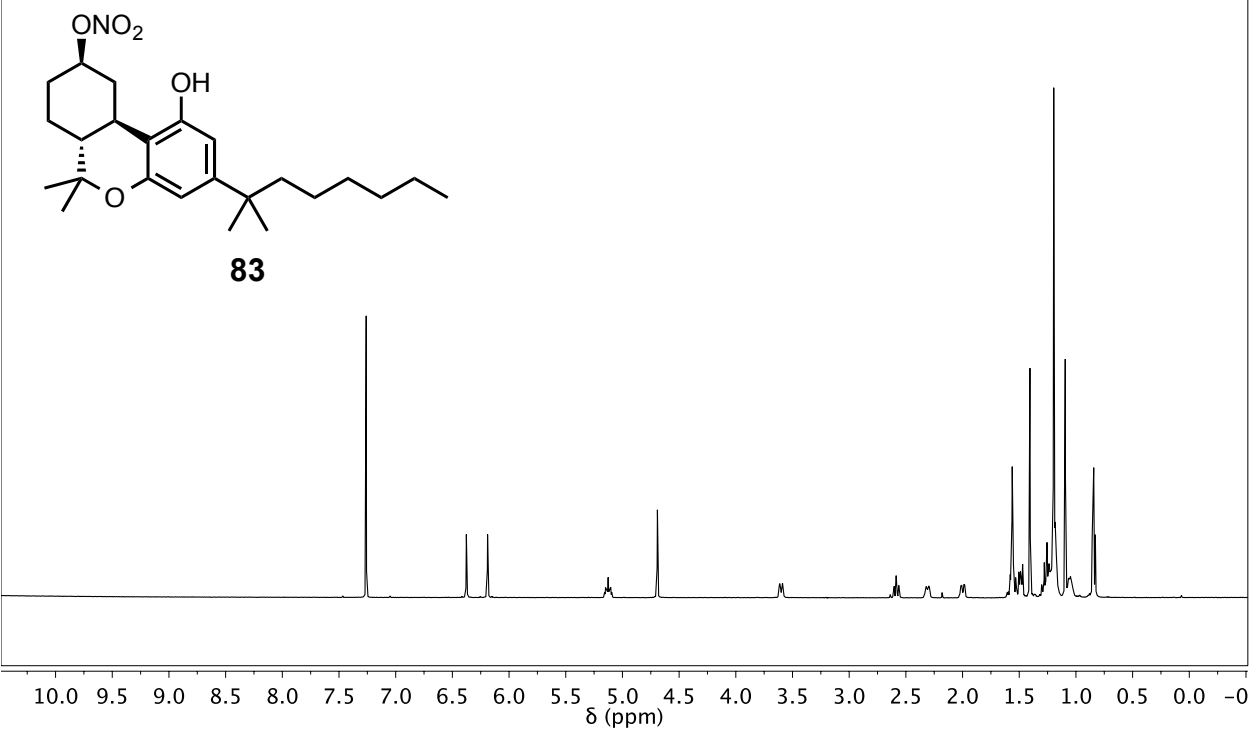


139; HMBC (500 MHz, CDCl₃)

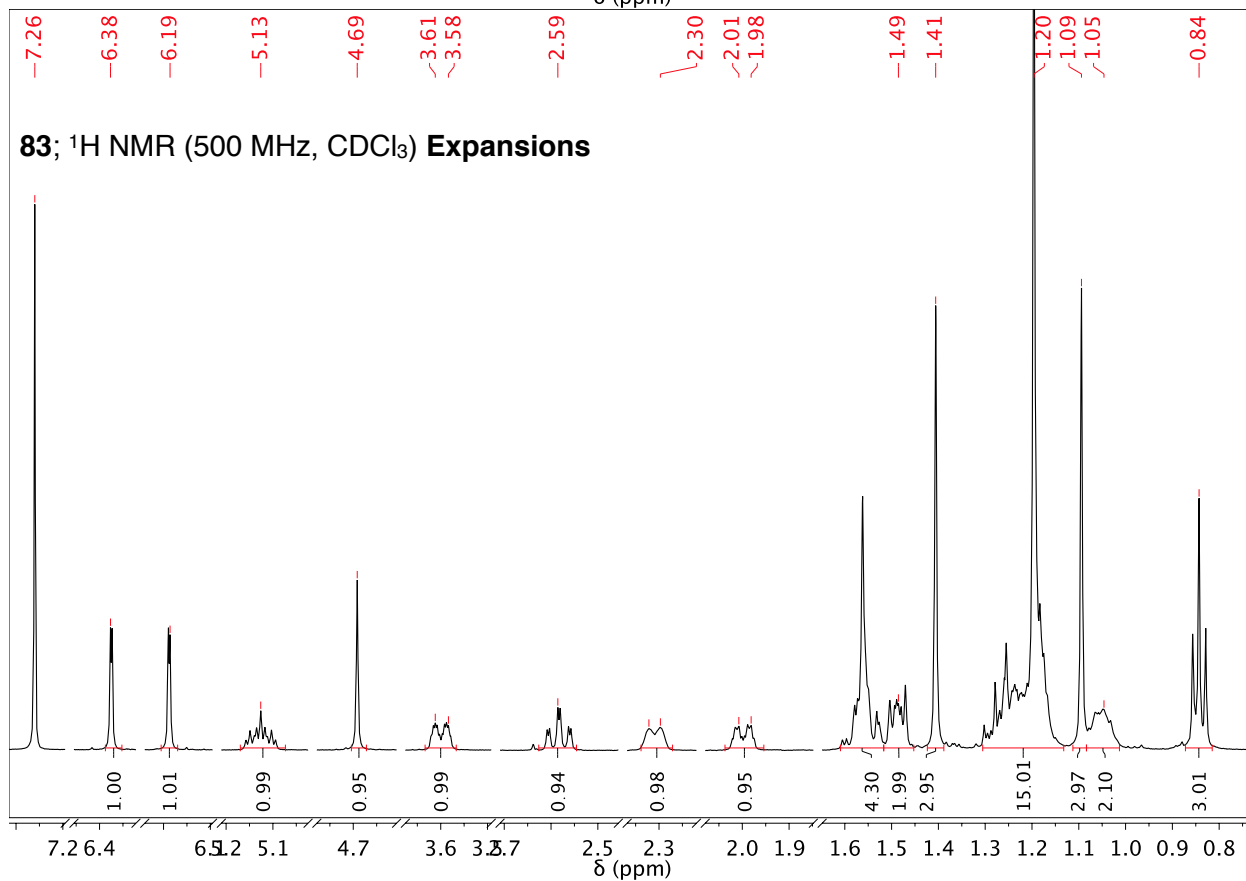




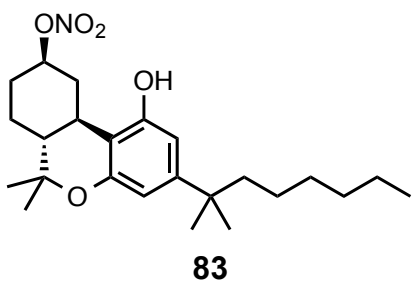
83; ^1H NMR (500 MHz, CDCl_3)



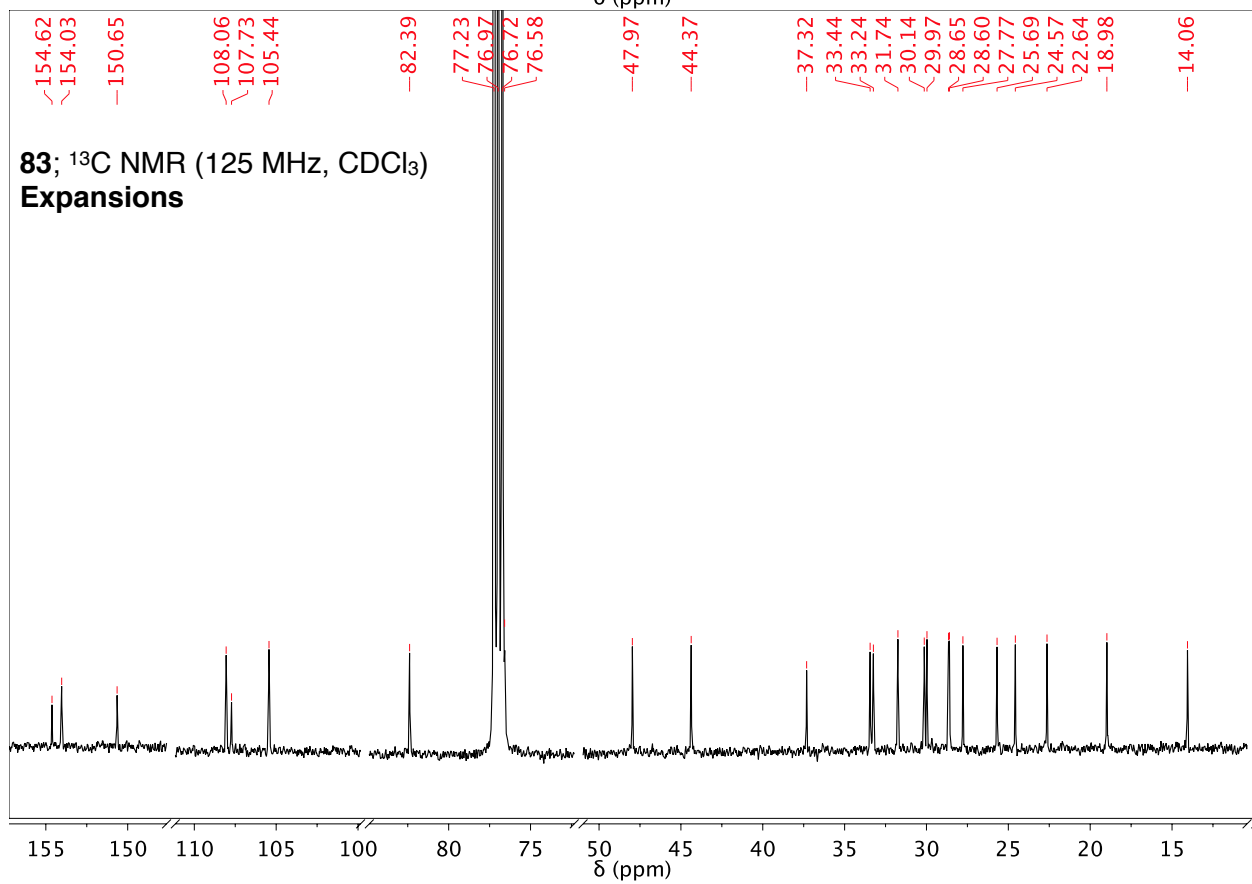
83; ^1H NMR (500 MHz, CDCl_3) **Expansions**

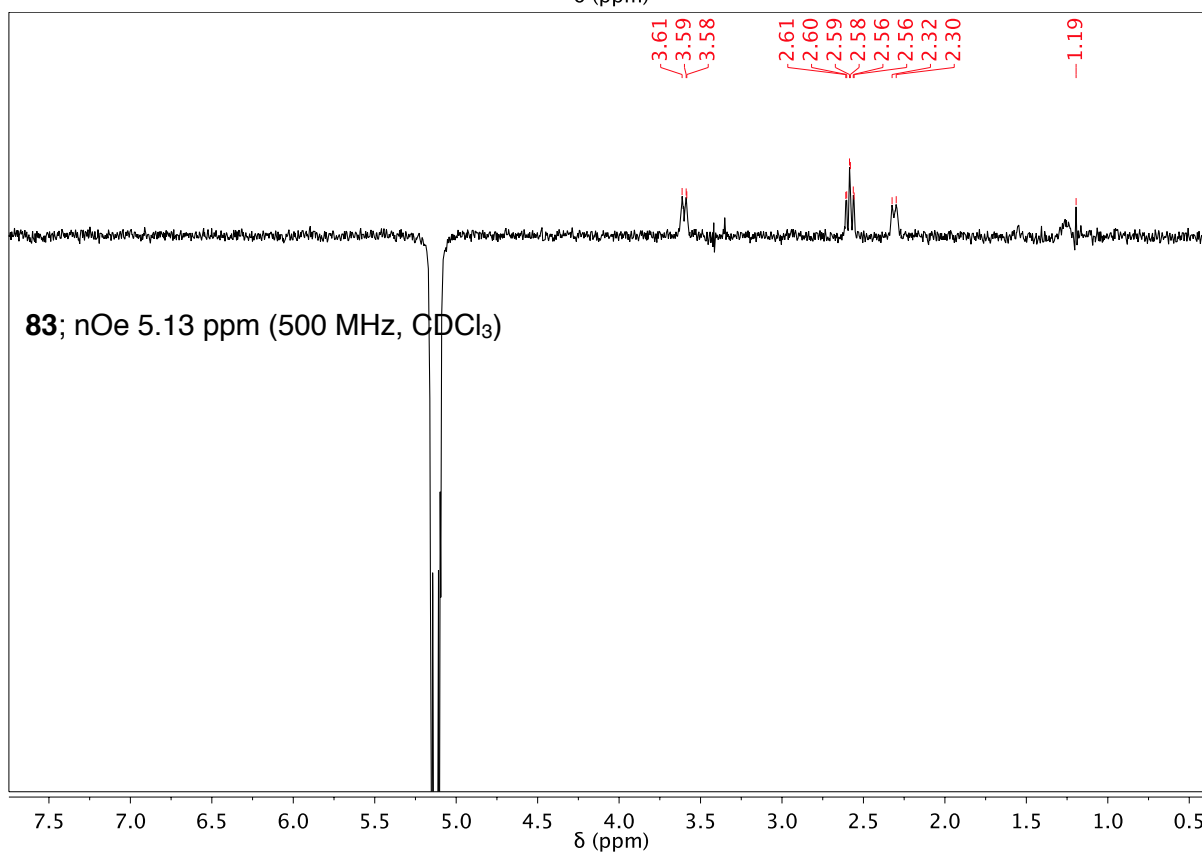
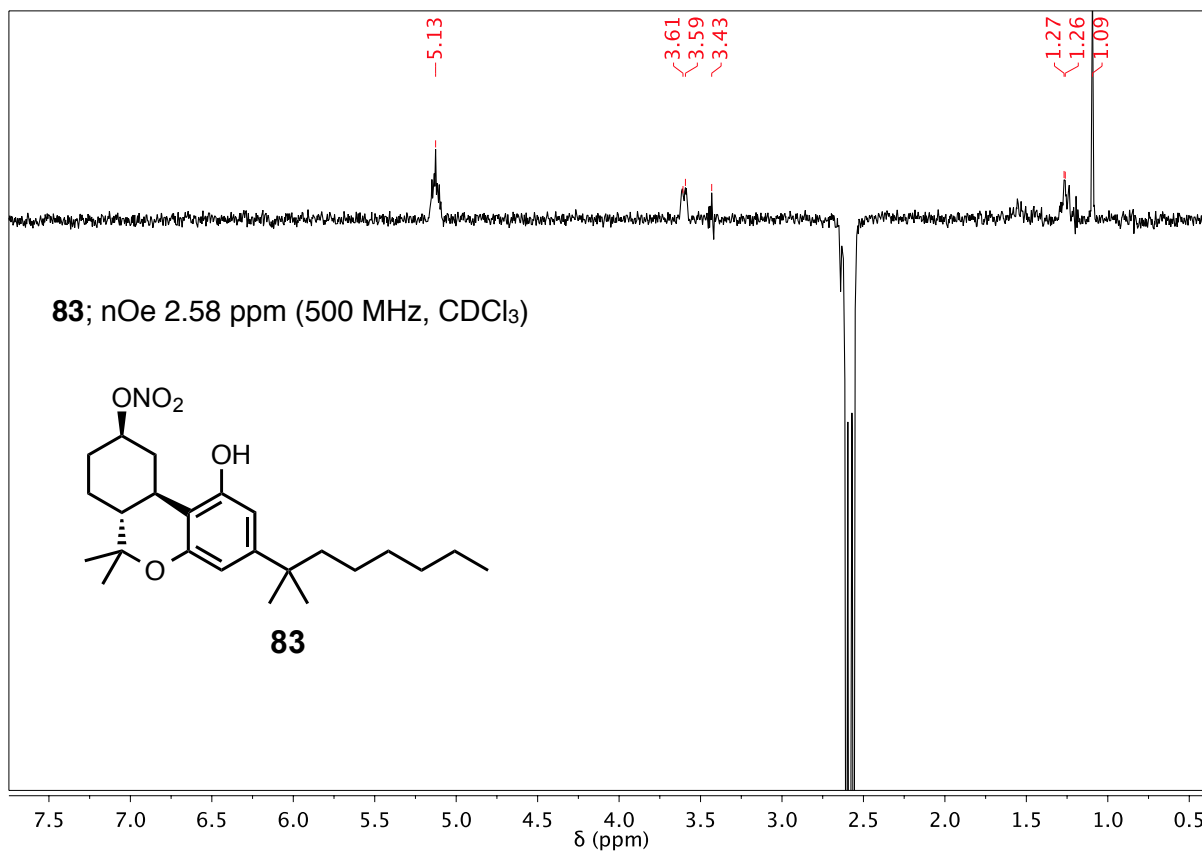


83; ^{13}C NMR (125 MHz, CDCl_3)

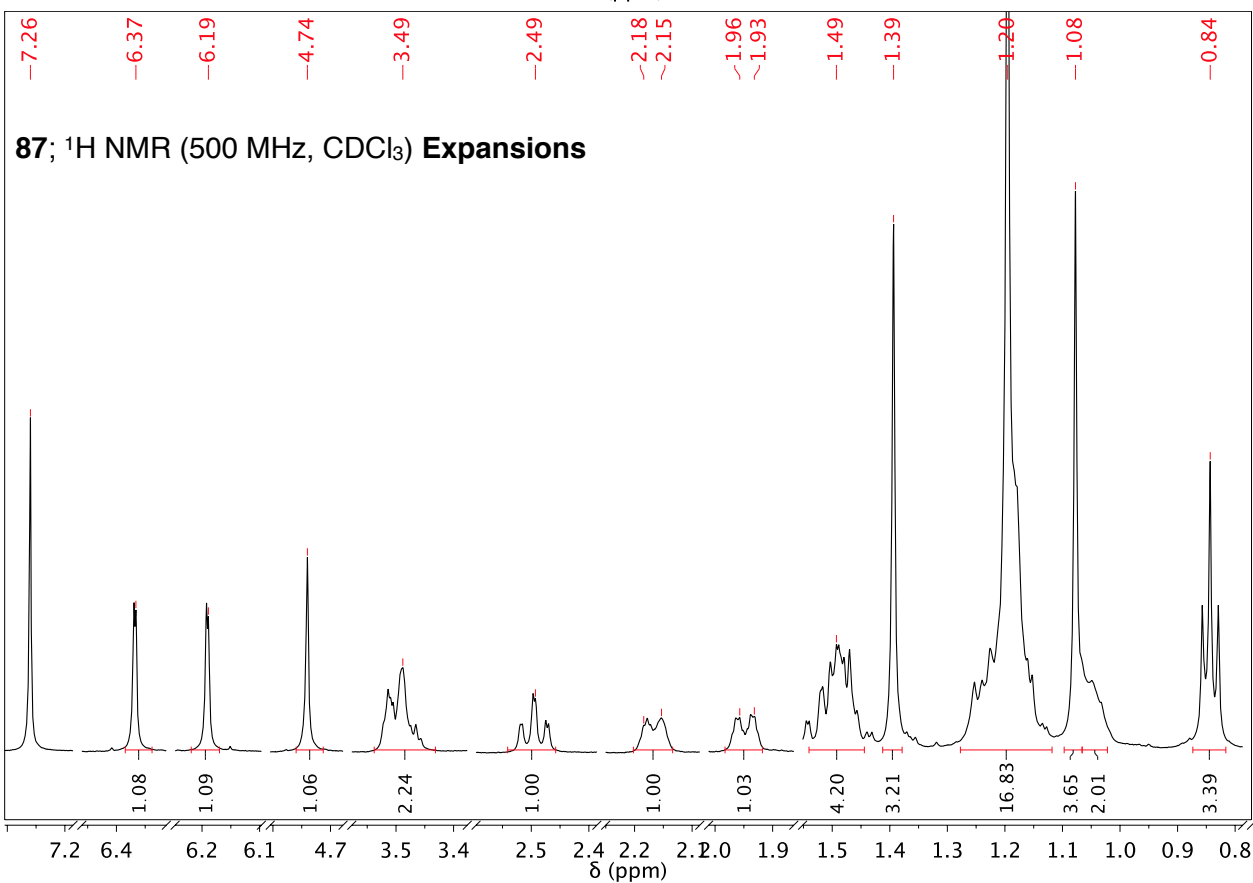
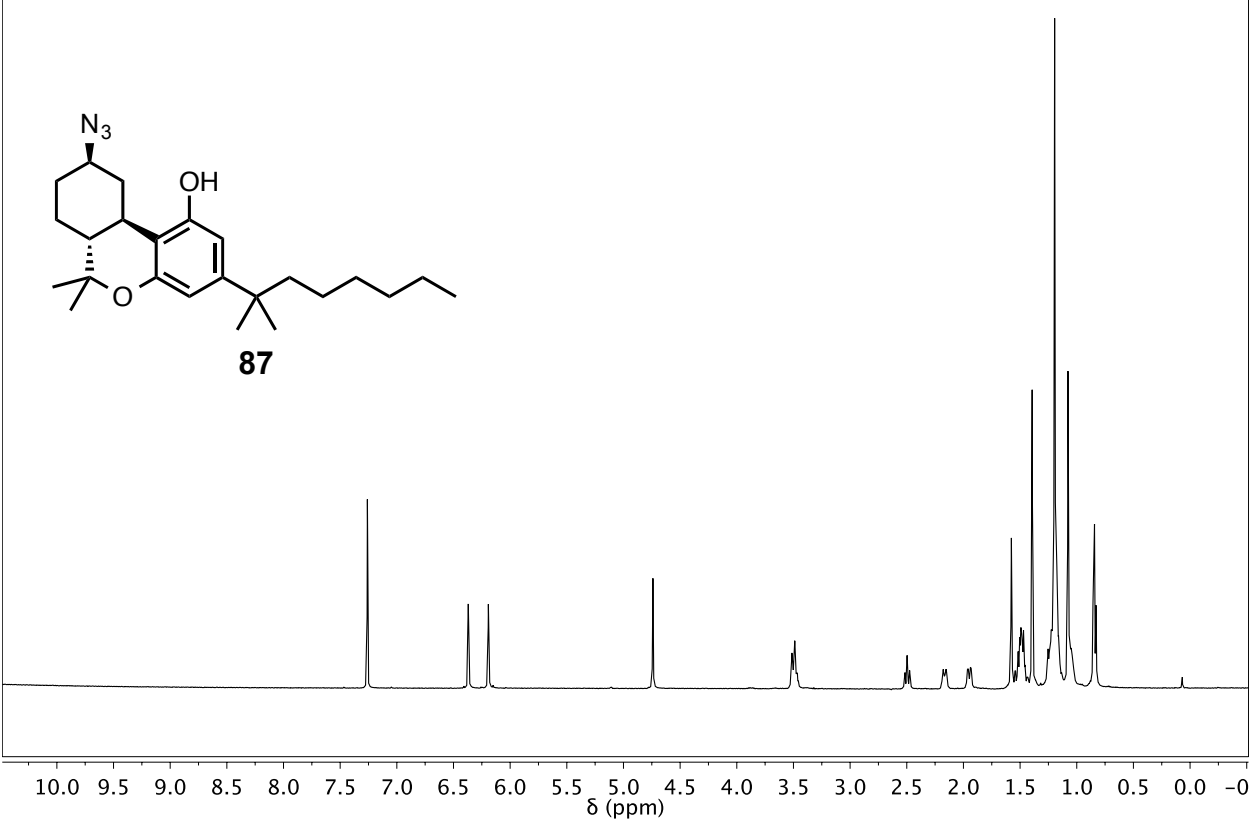


δ (ppm)

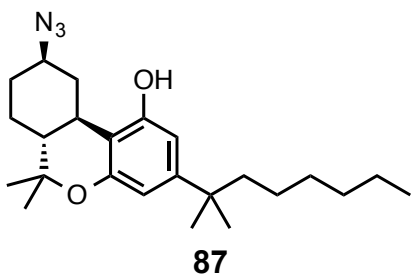




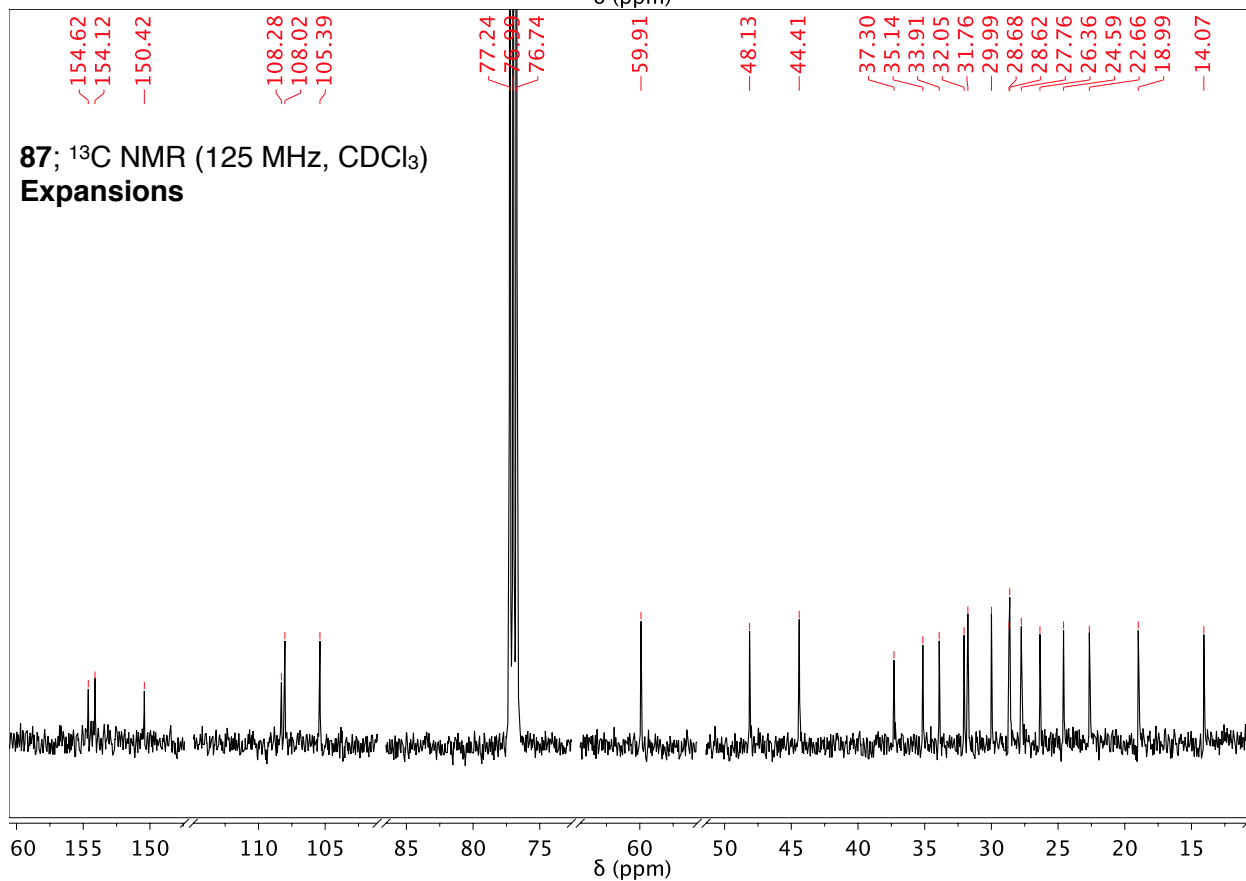
87; ^1H NMR (500 MHz, CDCl_3)

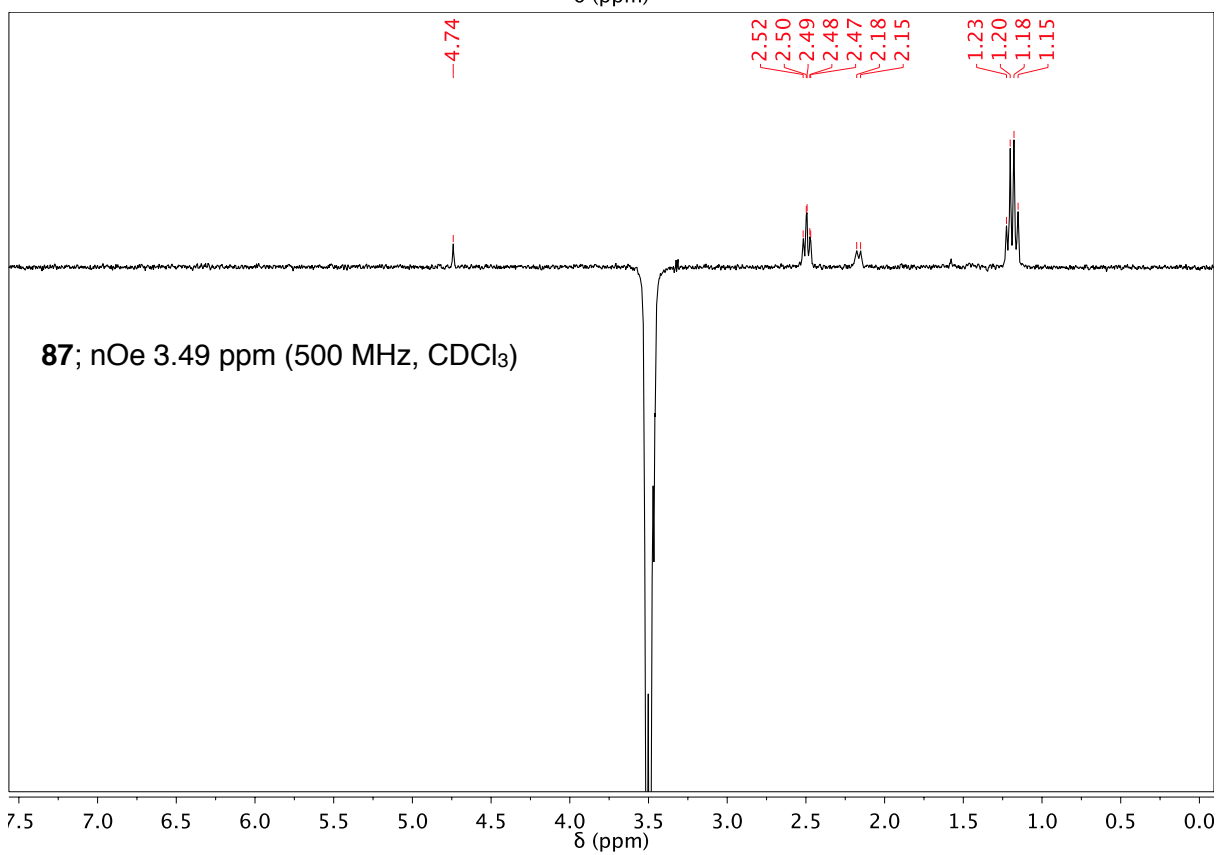
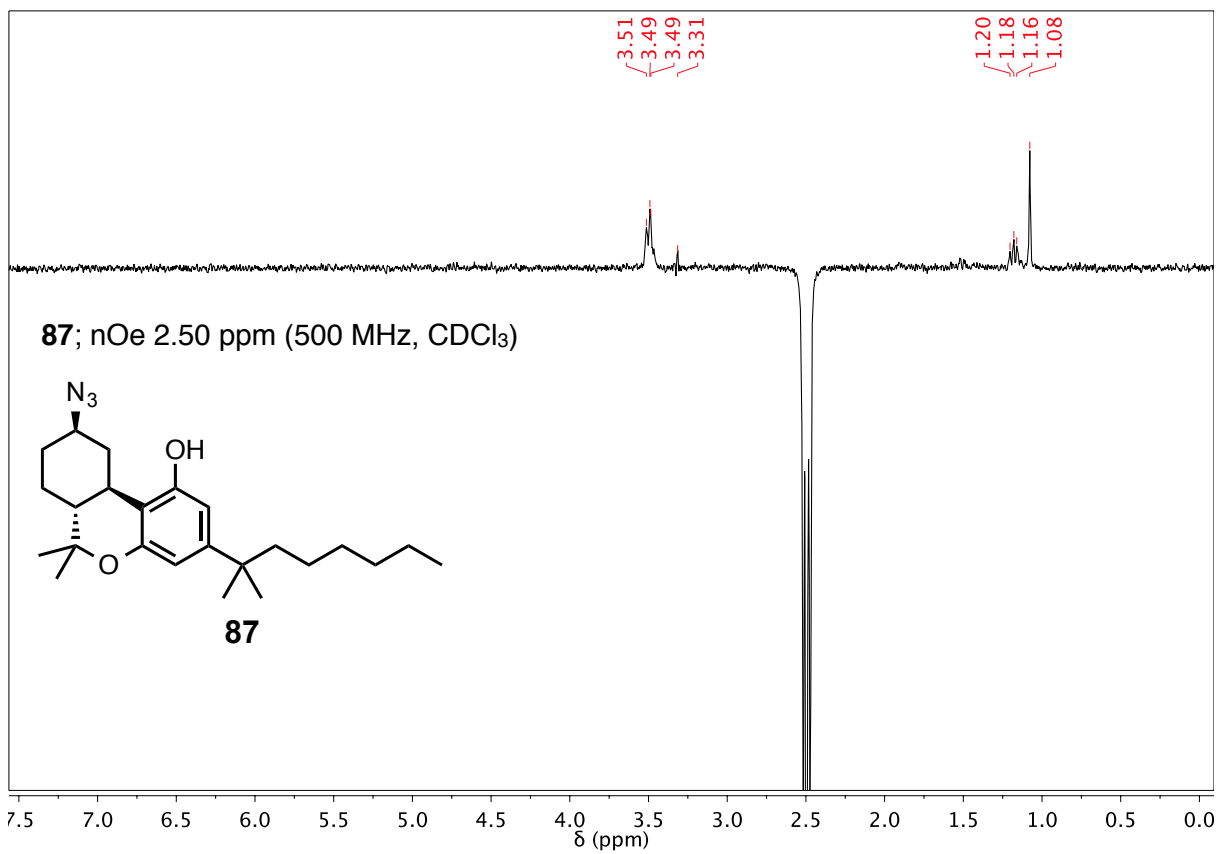


87; ^{13}C NMR (125 MHz, CDCl_3)

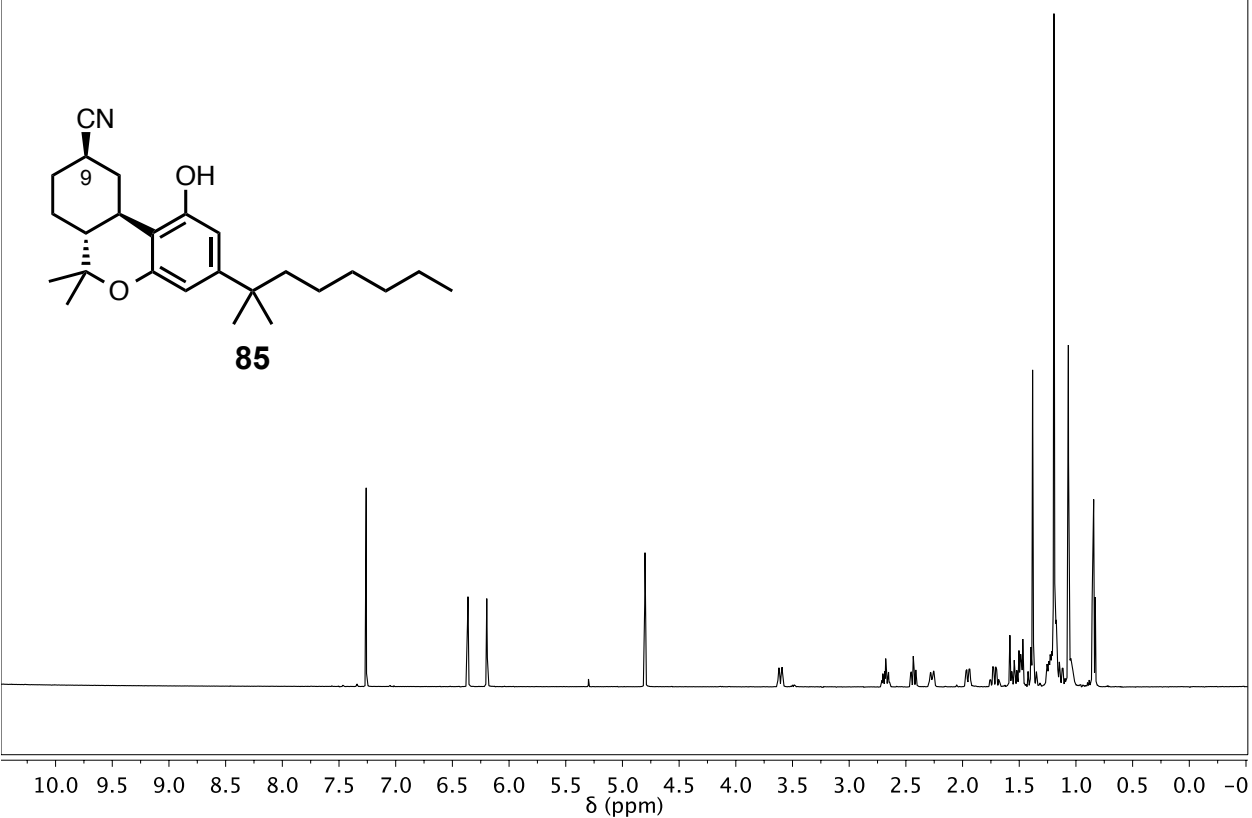


δ (ppm)

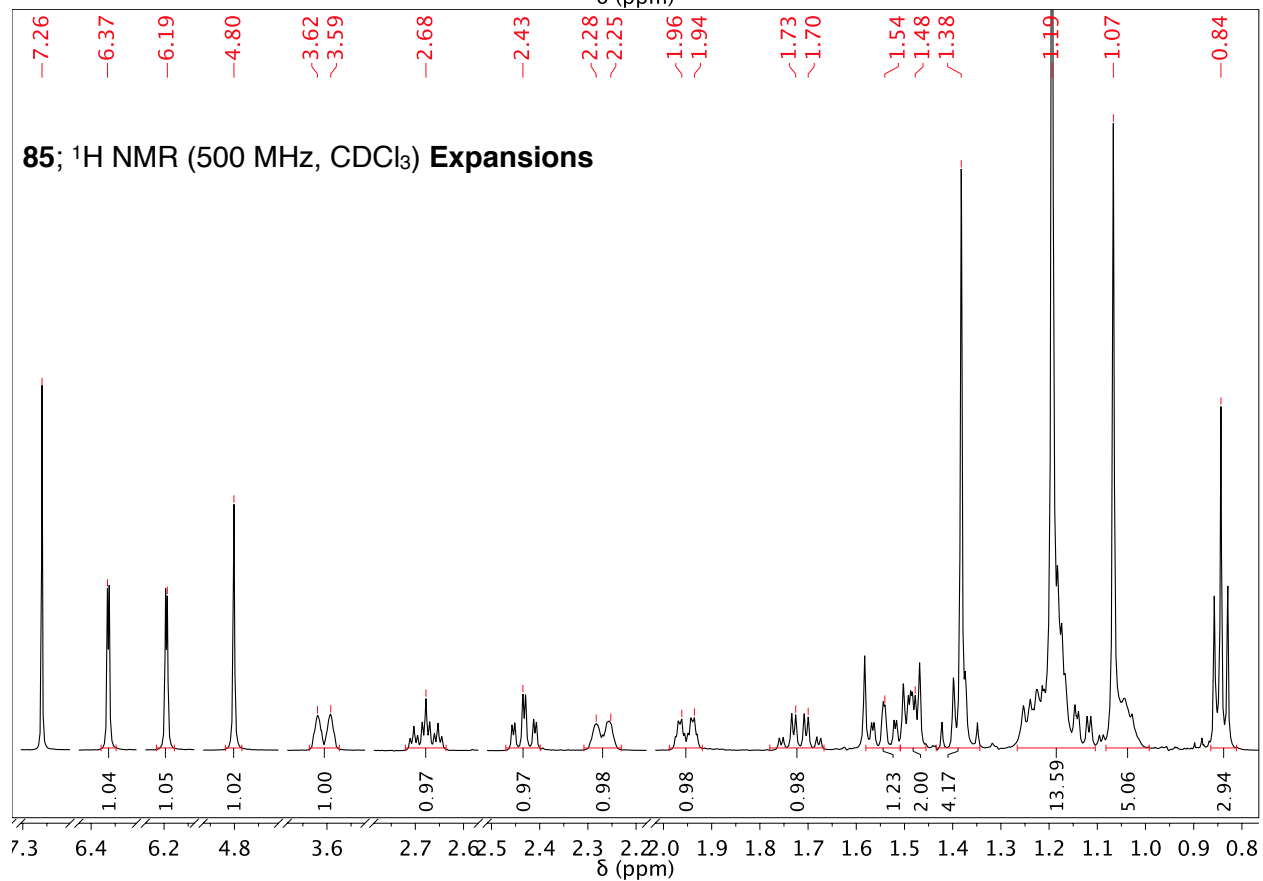




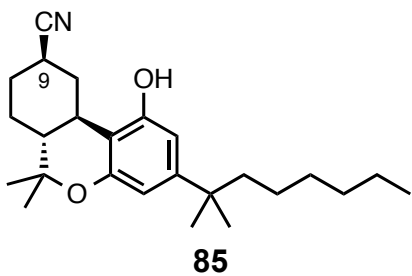
85; ^1H NMR (500 MHz, CDCl_3)



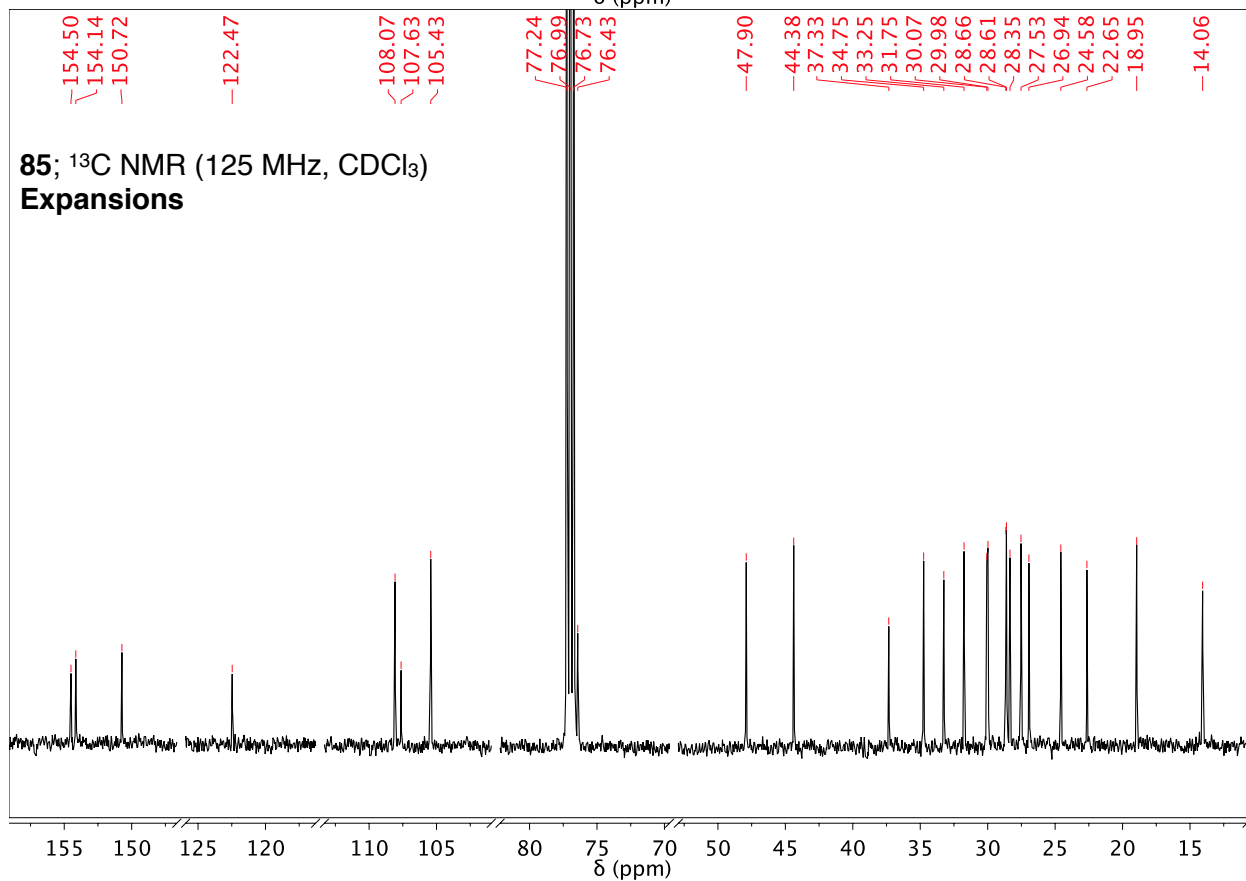
85; ^1H NMR (500 MHz, CDCl_3) **Expansions**



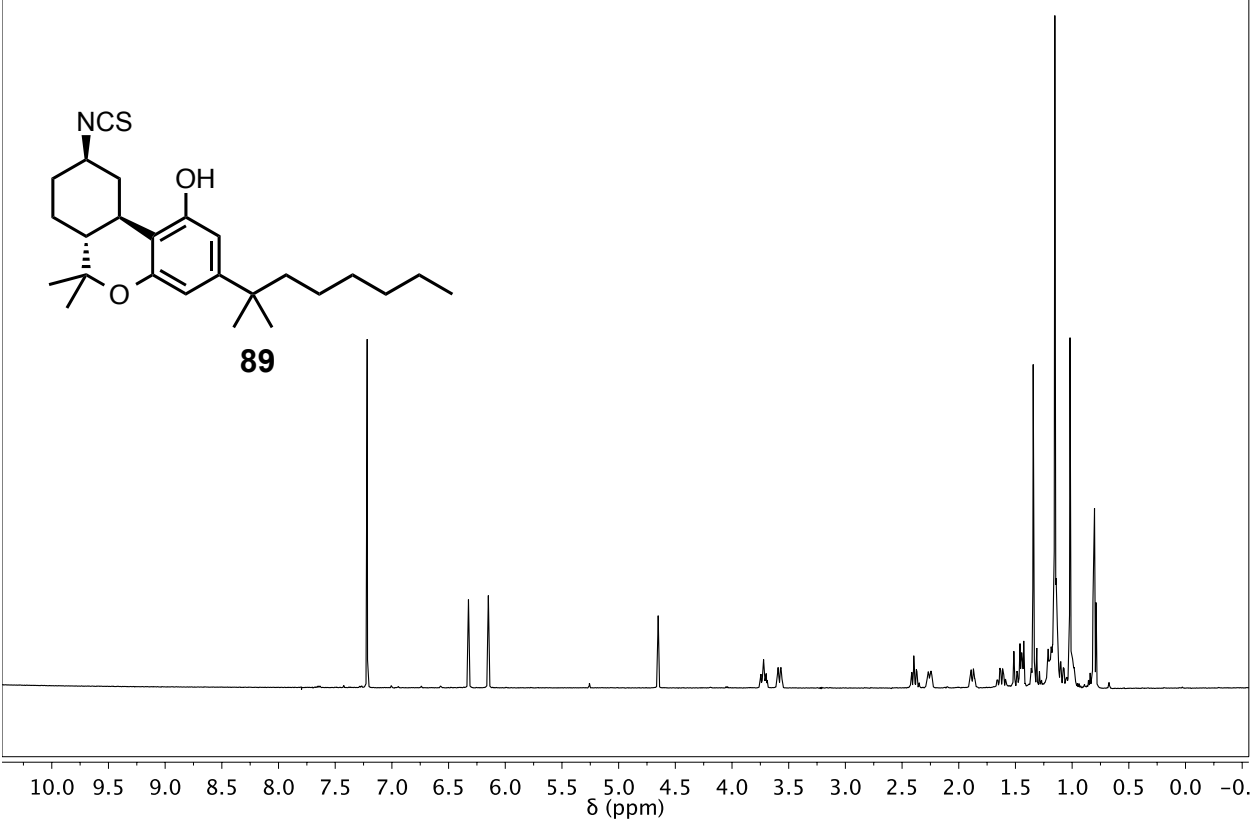
85; ^{13}C NMR (125 MHz, CDCl_3)



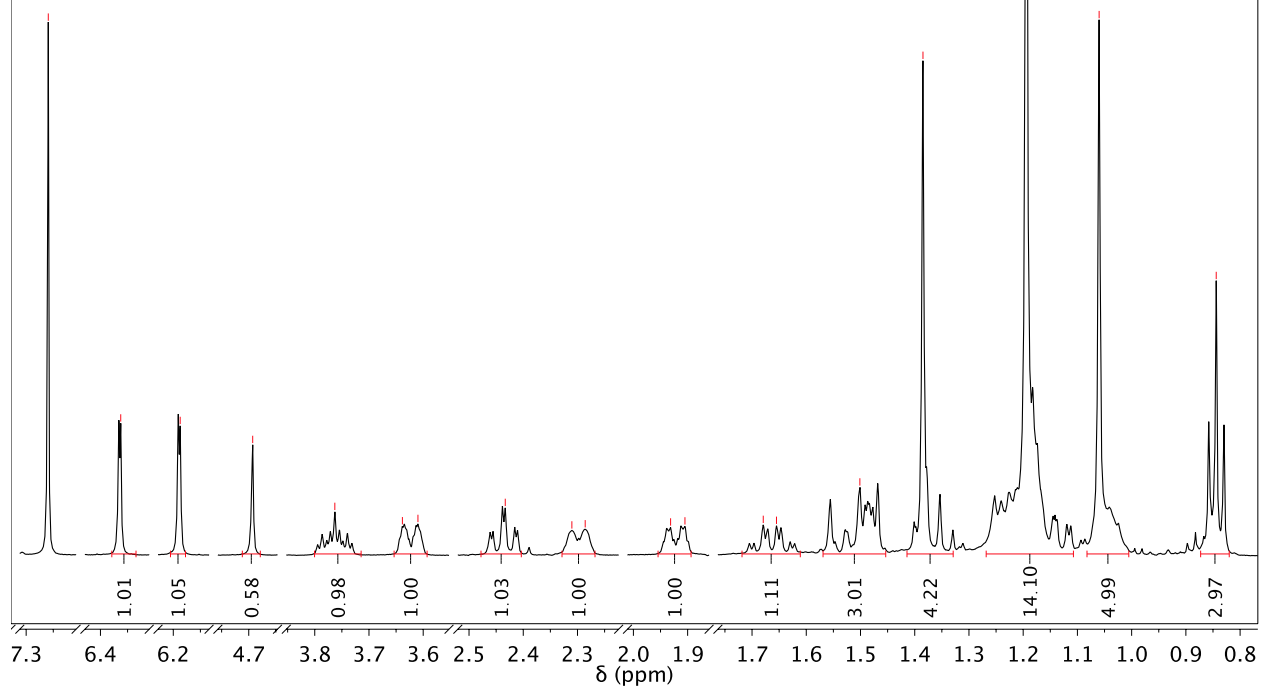
δ (ppm)



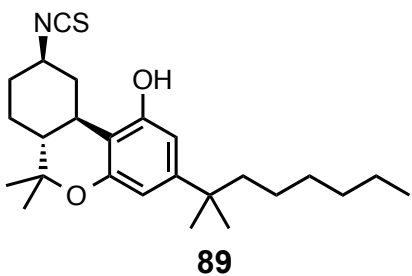
89; ^1H NMR (500 MHz, CDCl_3)



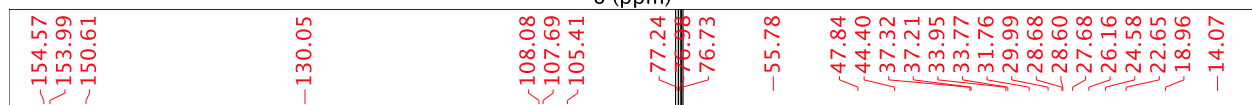
89; ^1H NMR (500 MHz, CDCl_3) **Expansions**



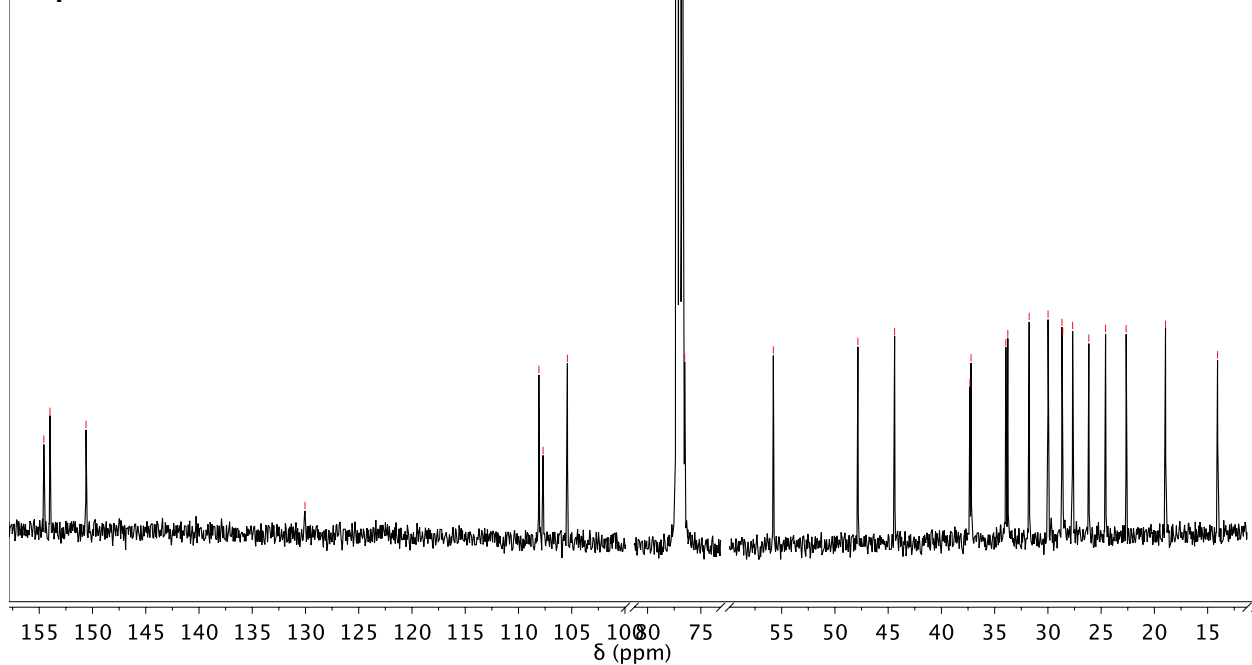
89; ^{13}C NMR (125 MHz, CDCl_3)



δ (ppm)



89; ^{13}C NMR (125 MHz, CDCl_3)
Expansions

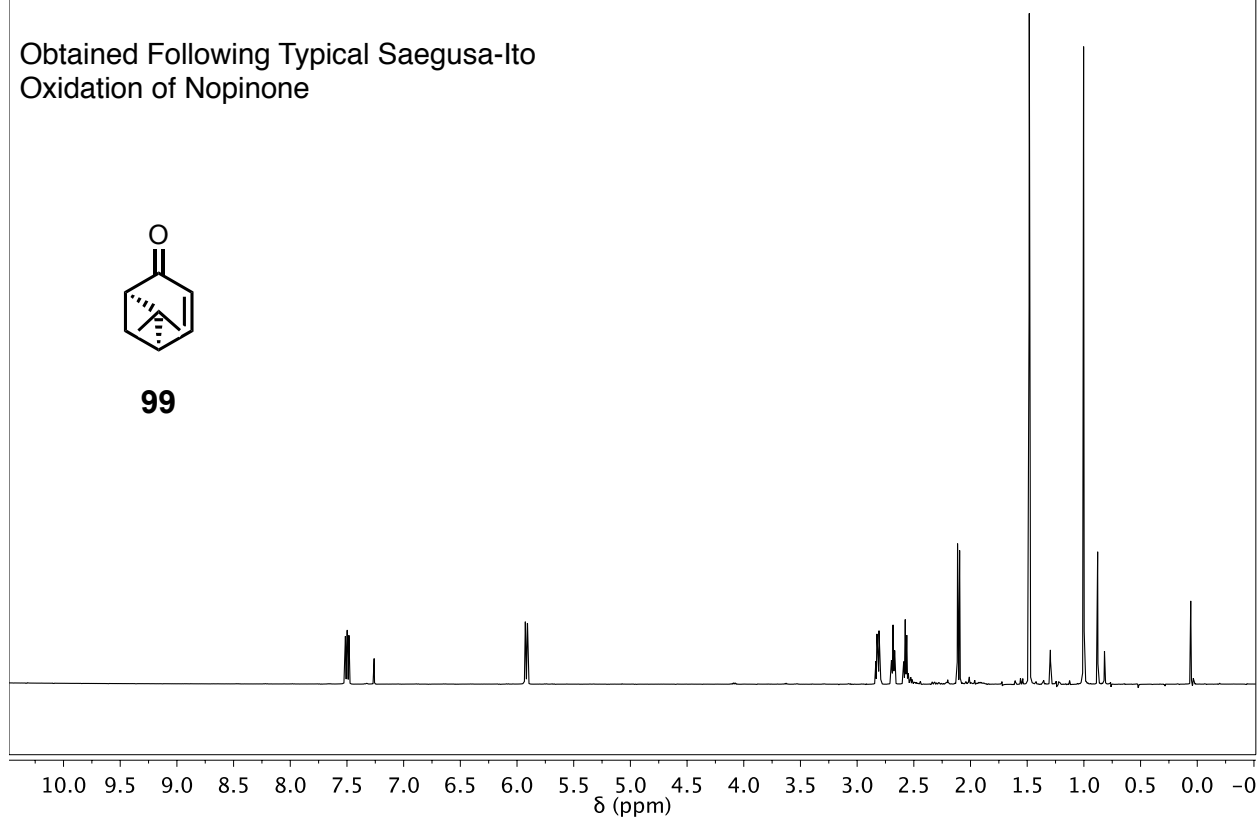


99; ^1H NMR (500 MHz, CDCl_3)

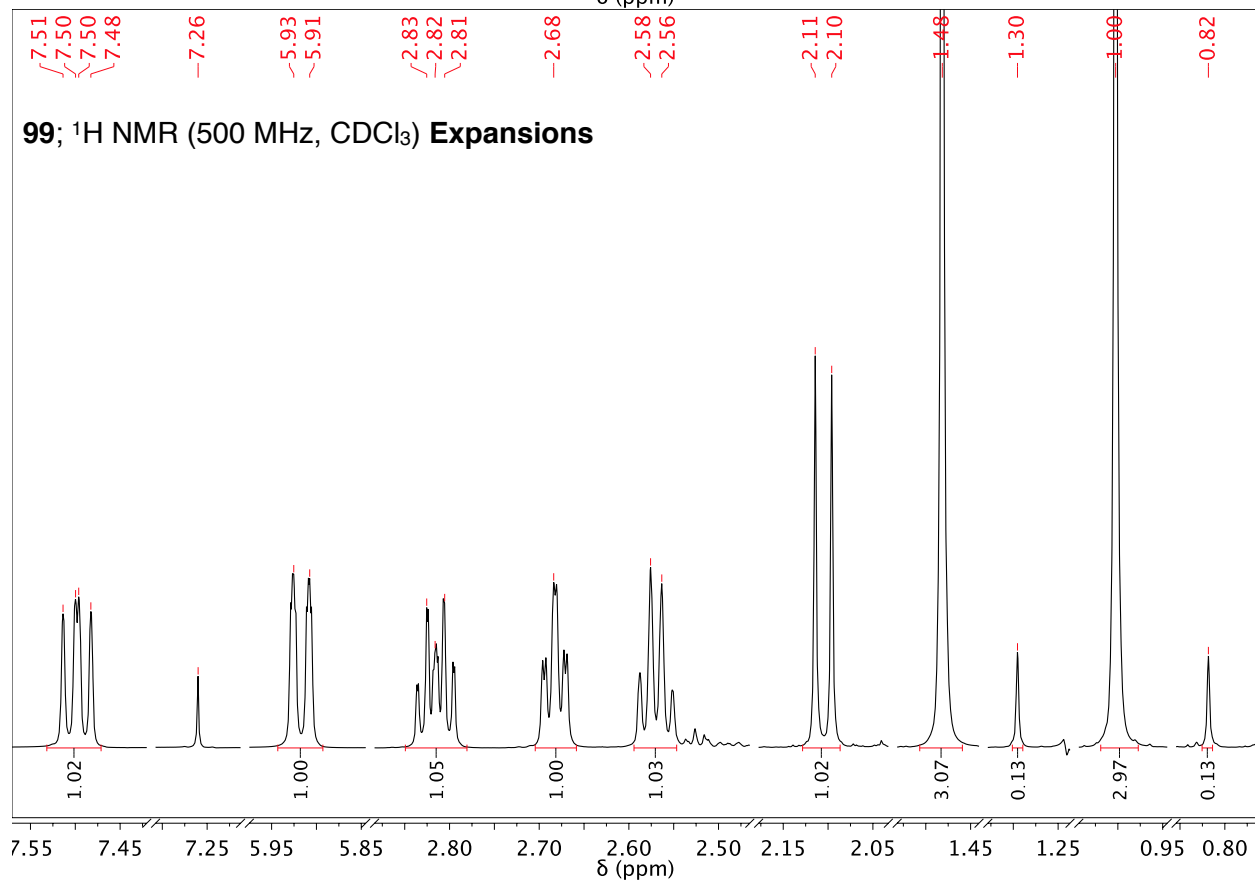
Obtained Following Typical Saegusa-Ito
Oxidation of Nopinone

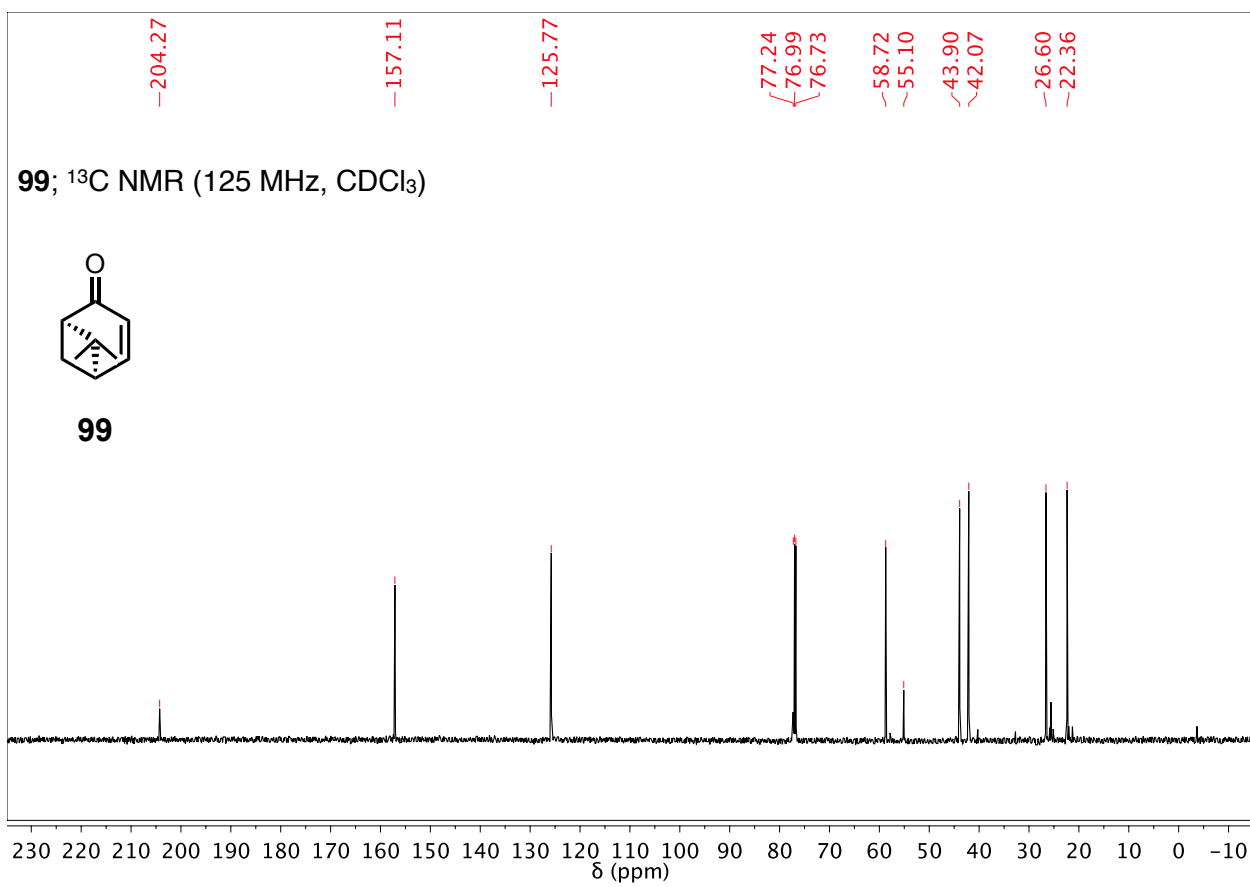


99

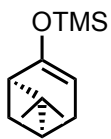


99; ^1H NMR (500 MHz, CDCl_3) **Expansions**

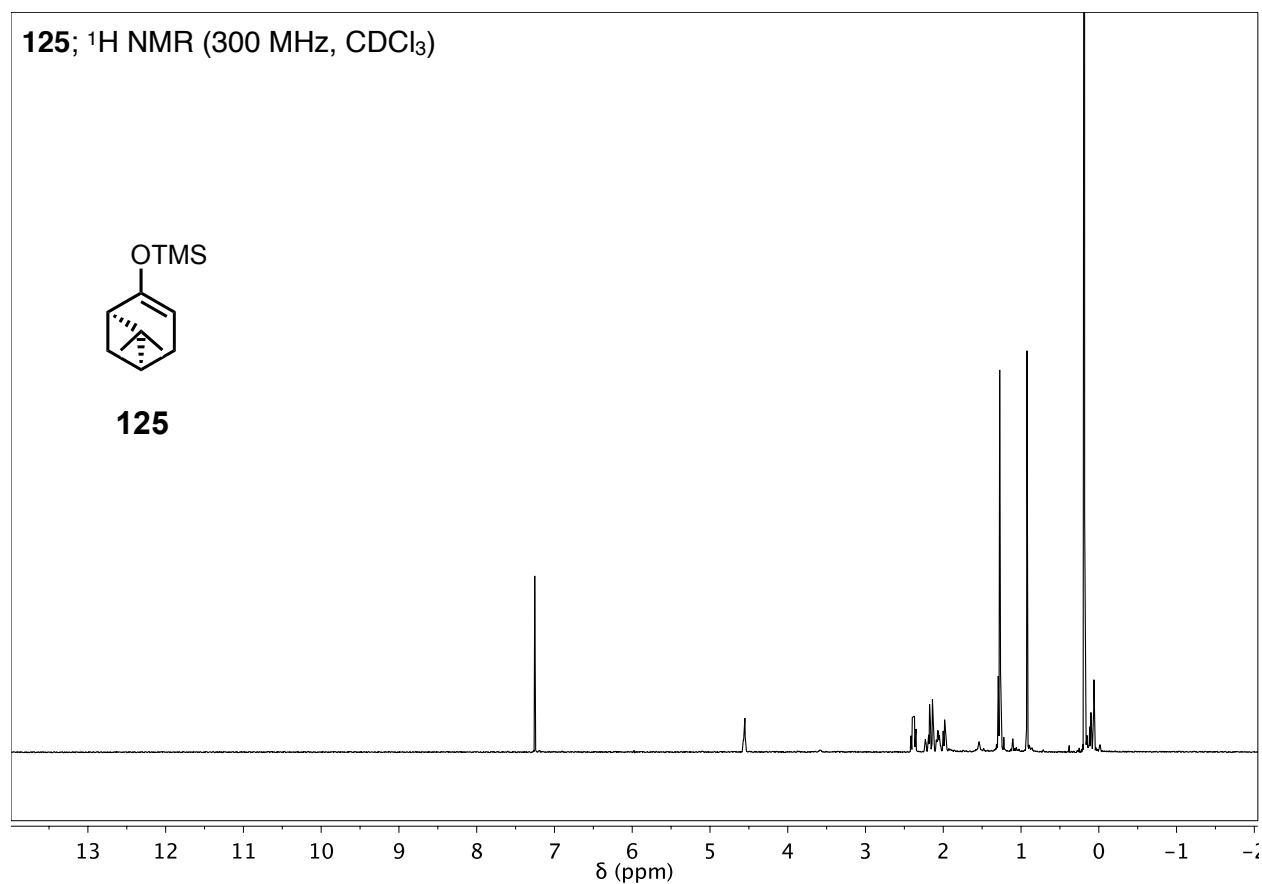




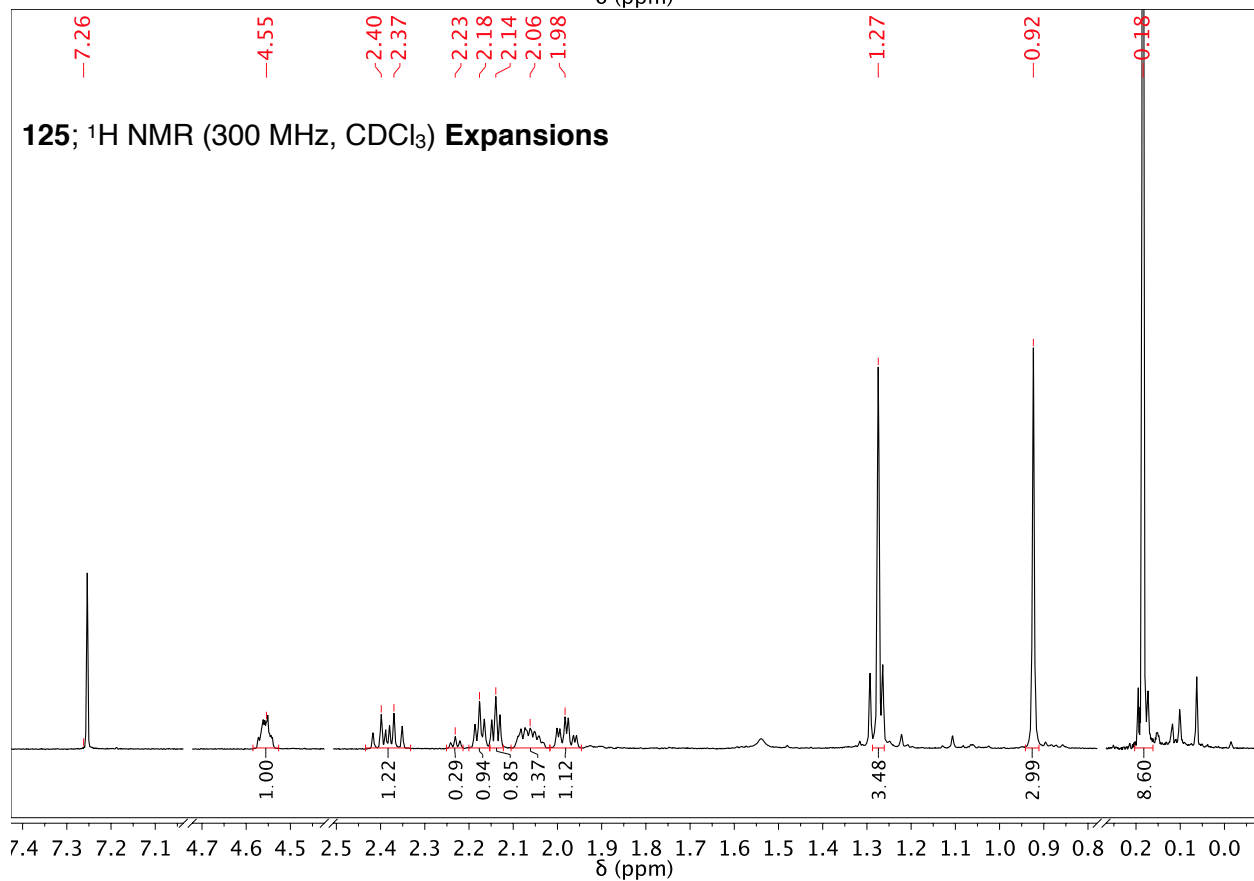
125; ^1H NMR (300 MHz, CDCl_3)



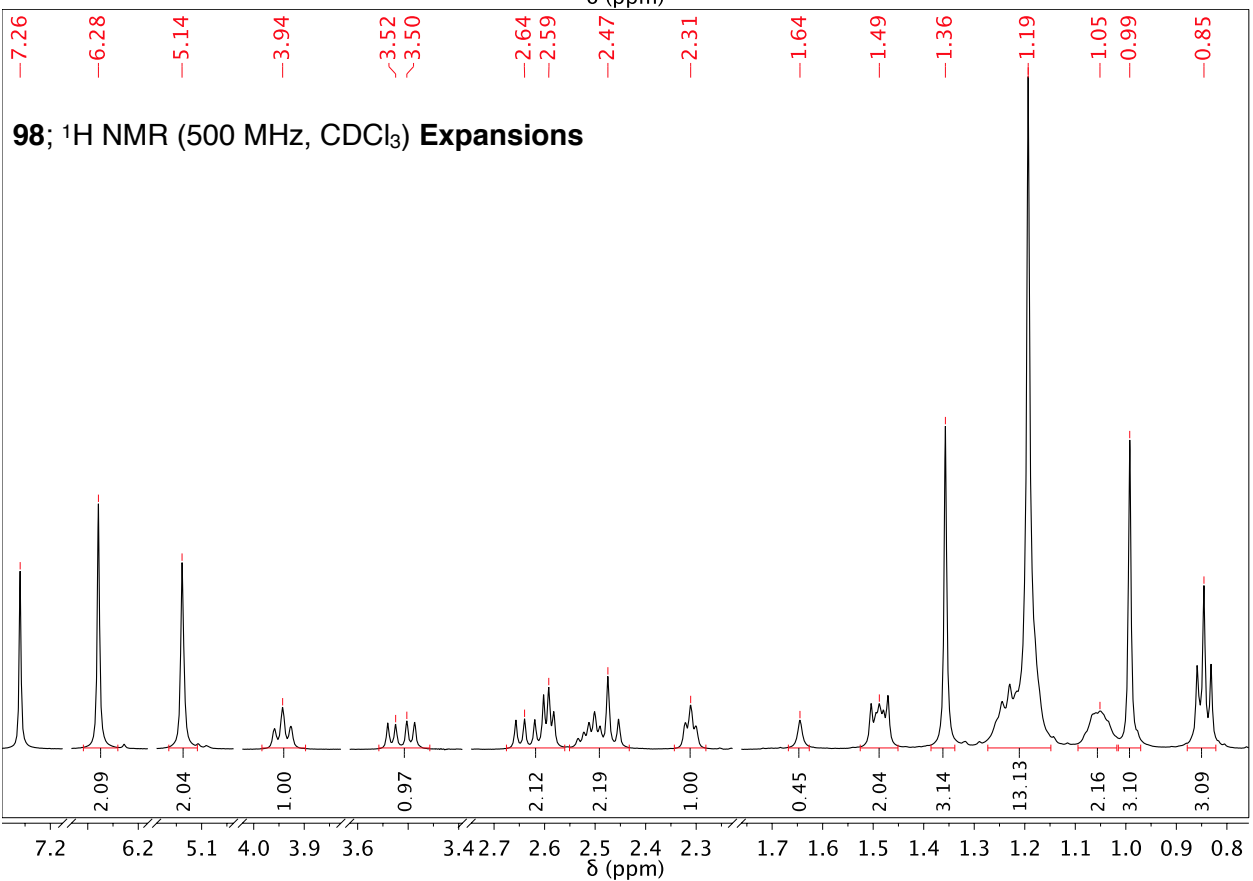
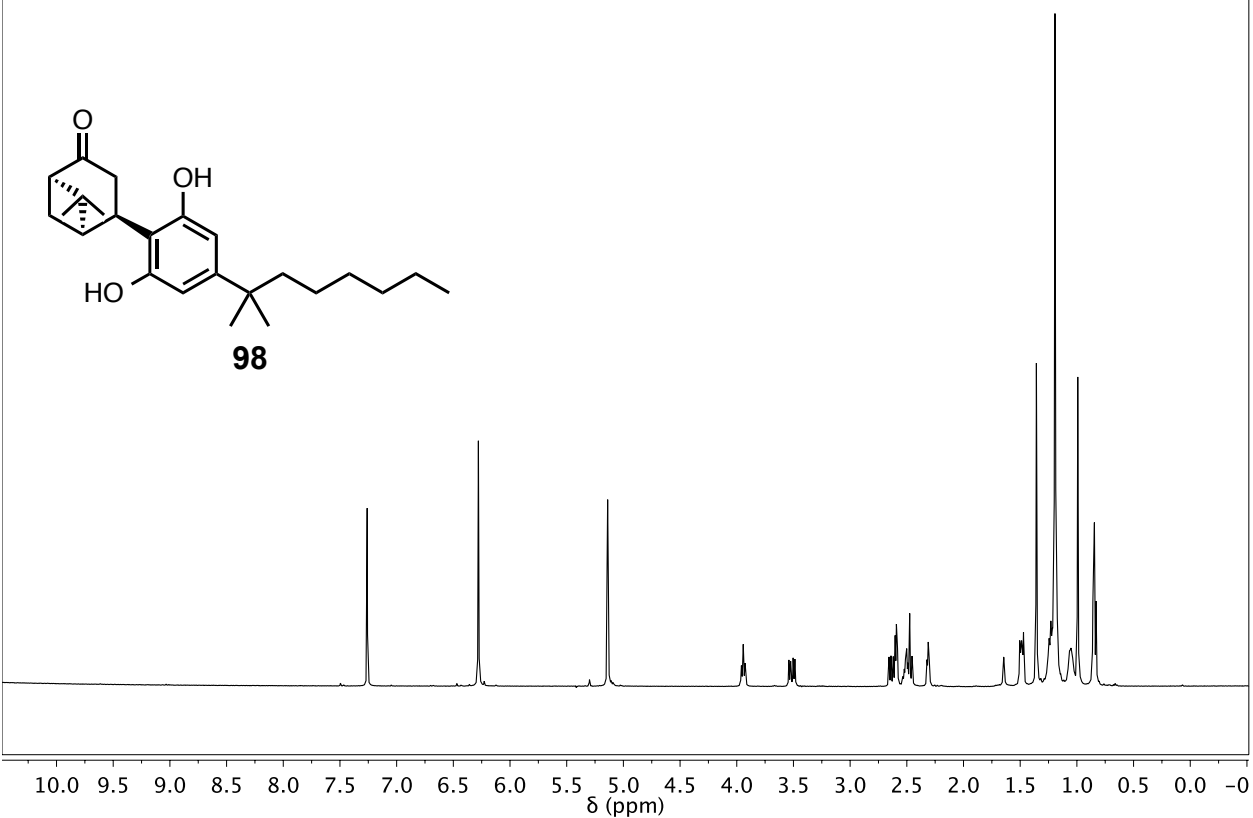
125

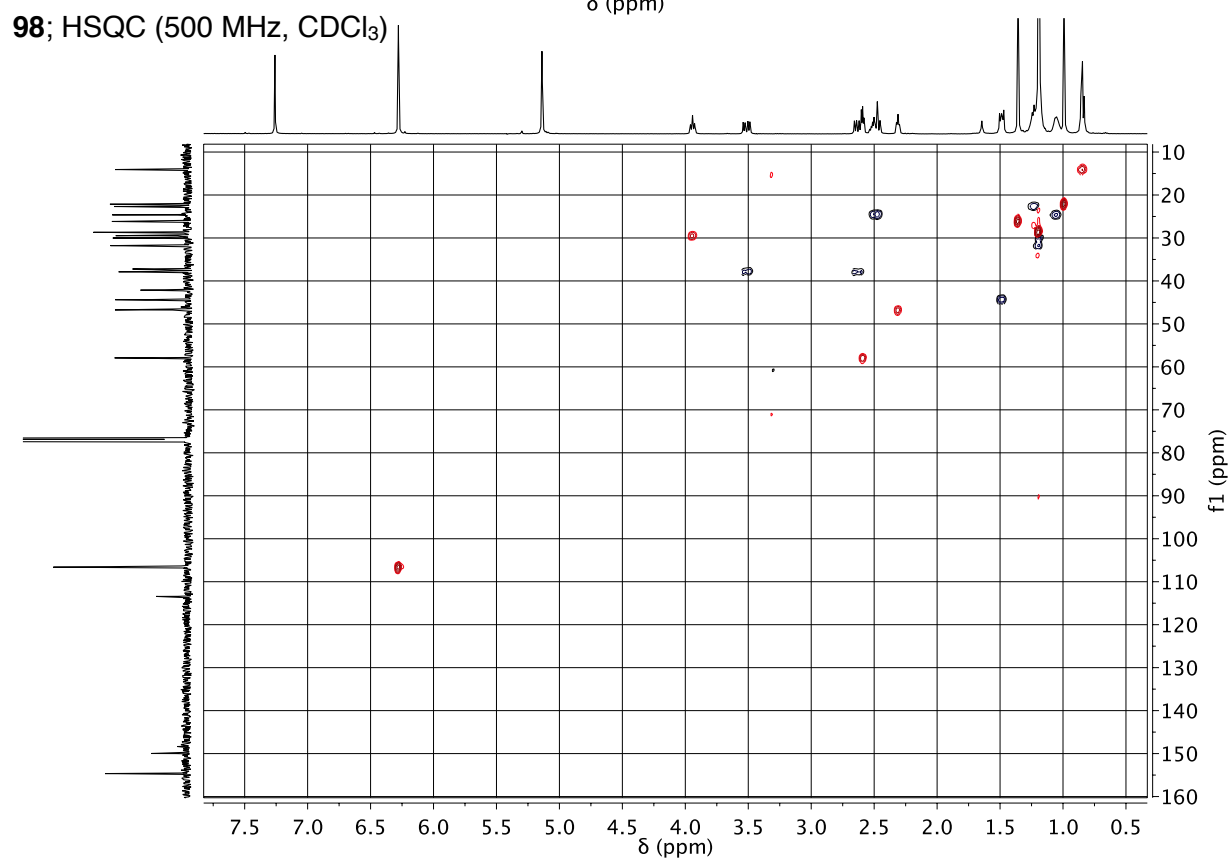
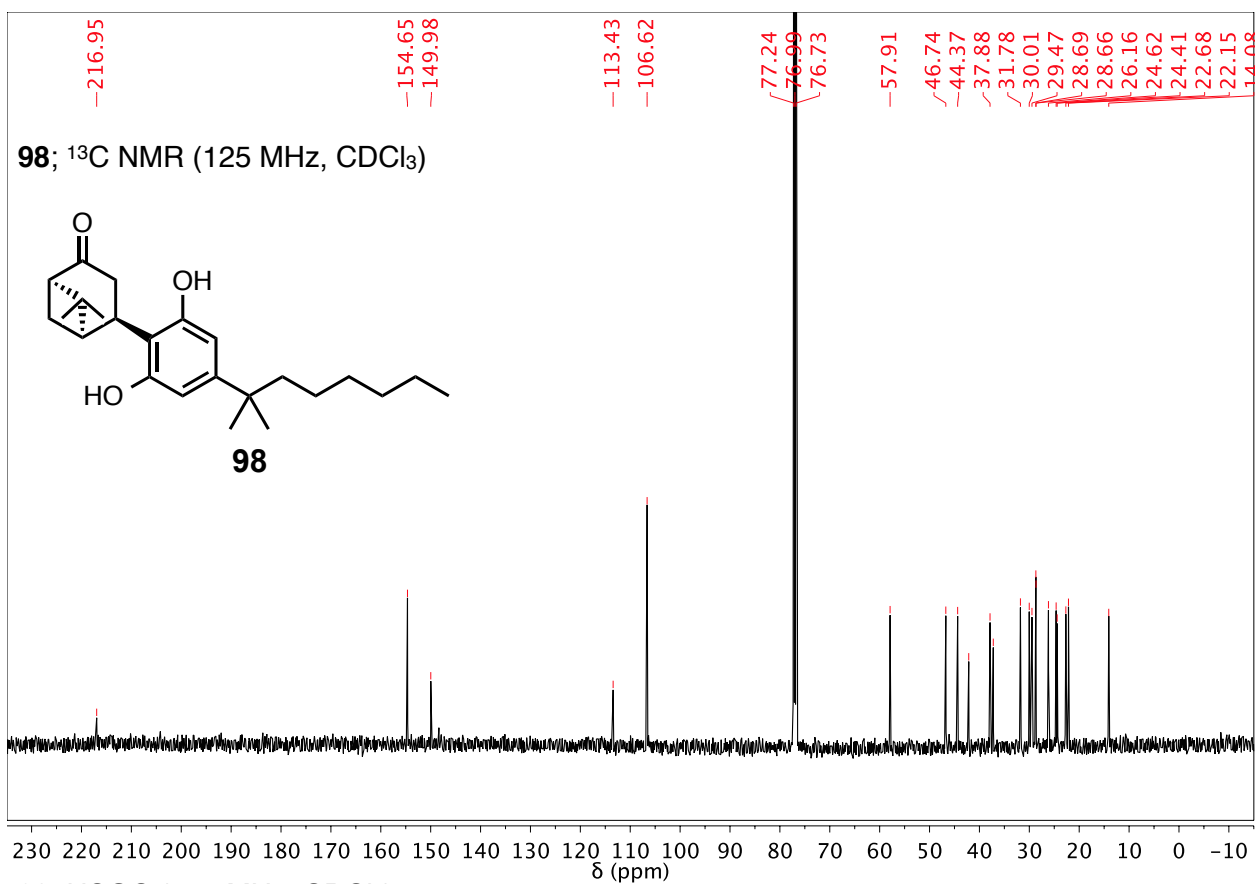


125; ^1H NMR (300 MHz, CDCl_3) **Expansions**

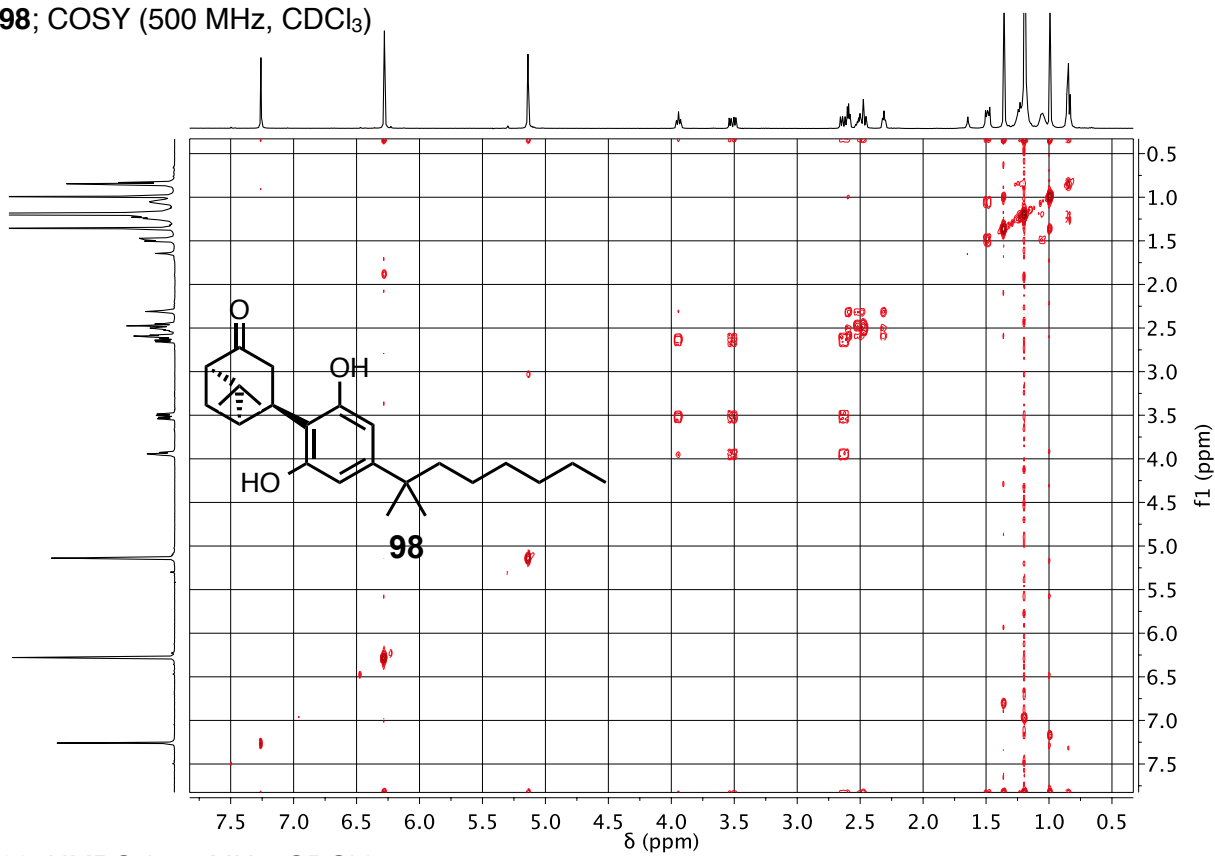


98; ^1H NMR (500 MHz, CDCl_3)

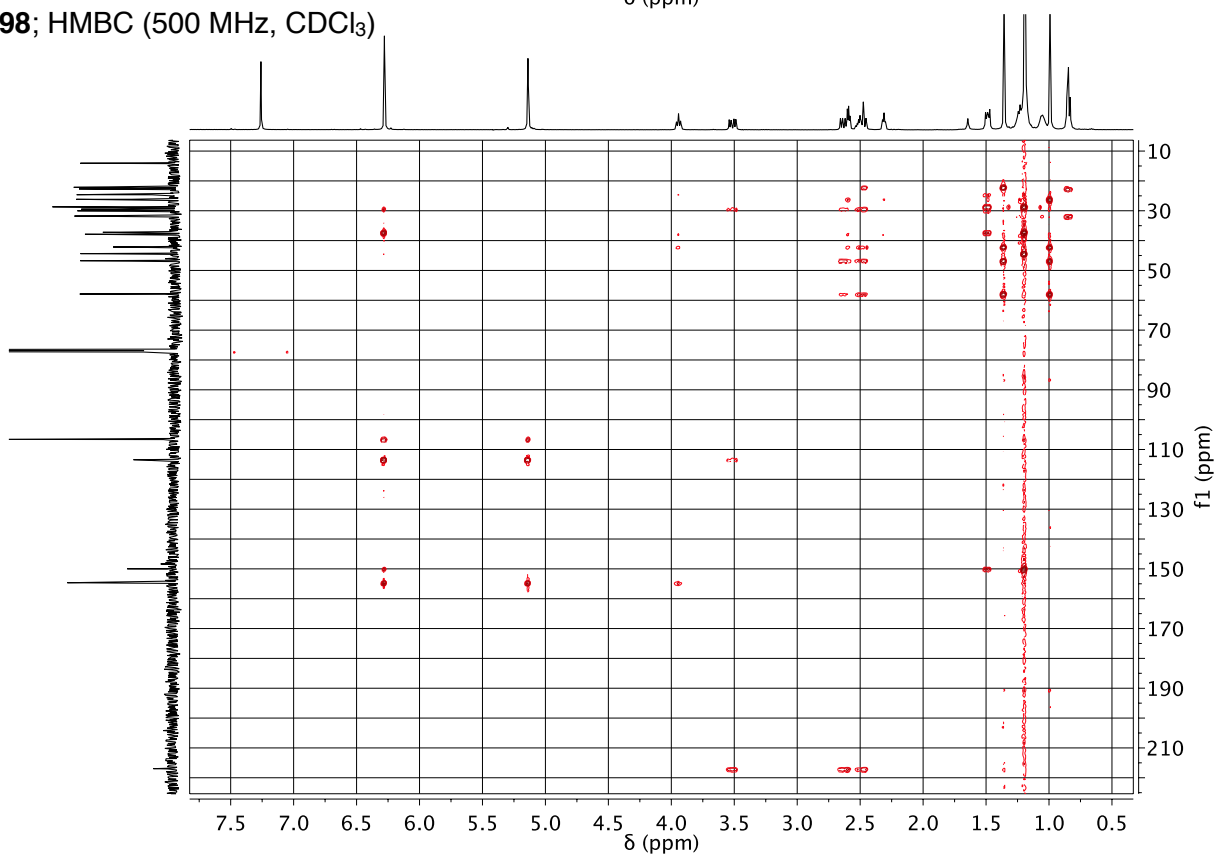




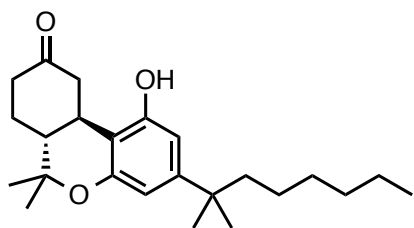
98; COSY (500 MHz, CDCl₃)



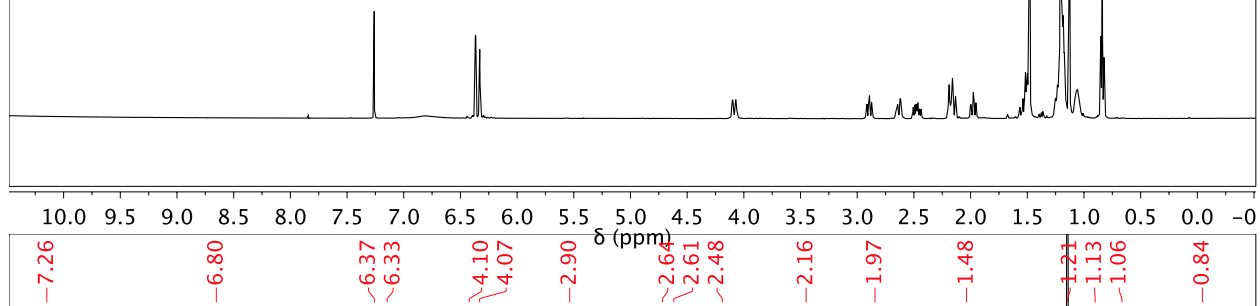
98; HMBC (500 MHz, CDCl₃)



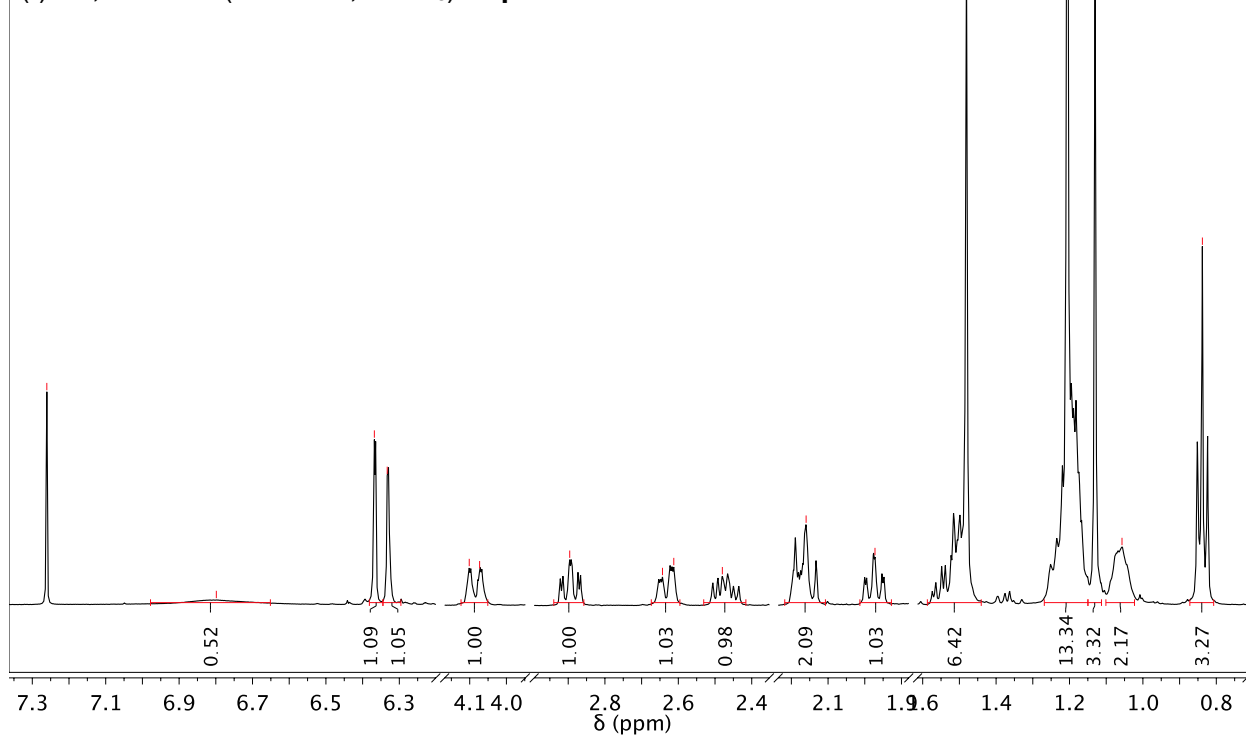
(-)-**20**; ^1H NMR (500 MHz, CDCl_3)

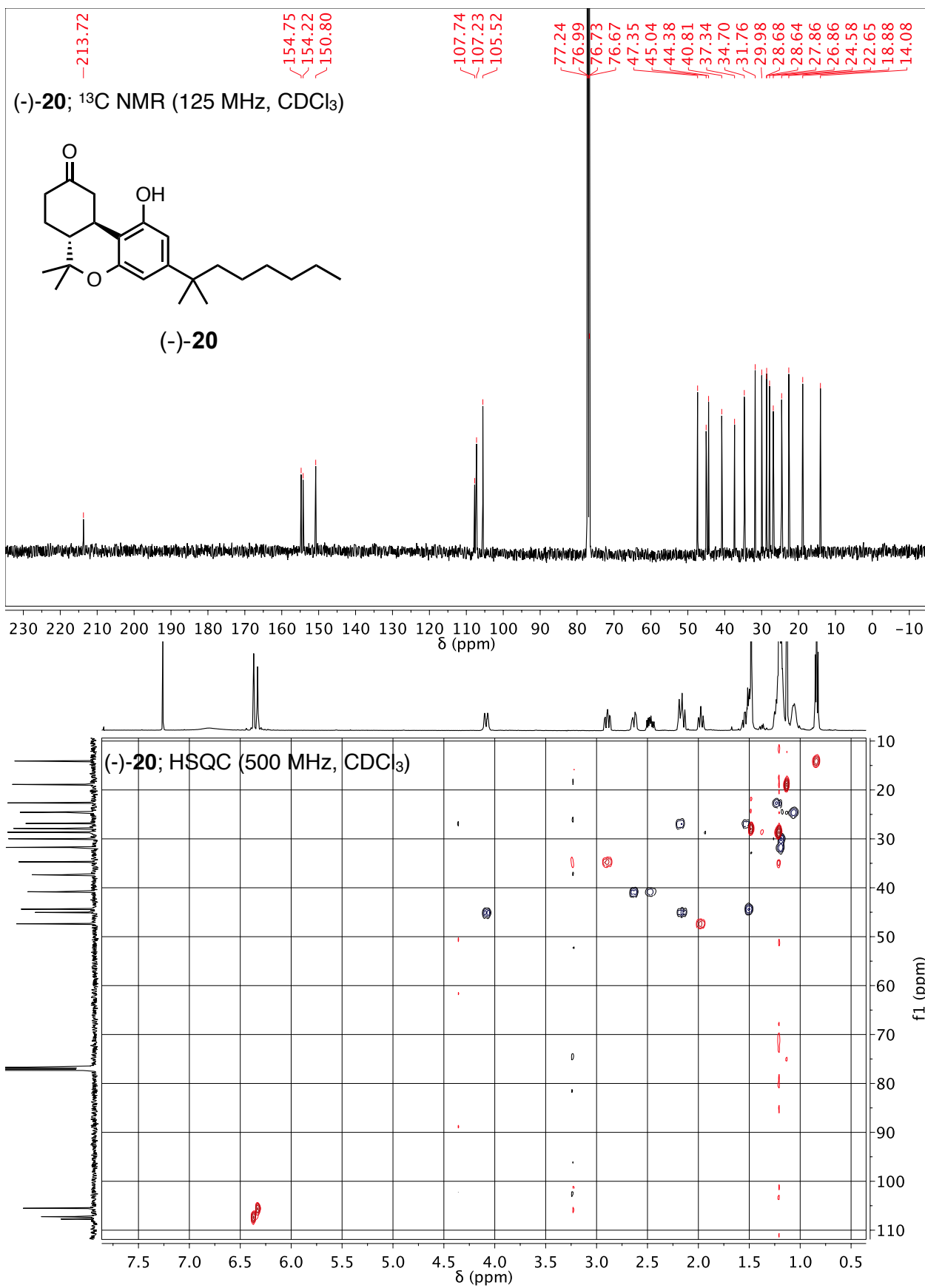


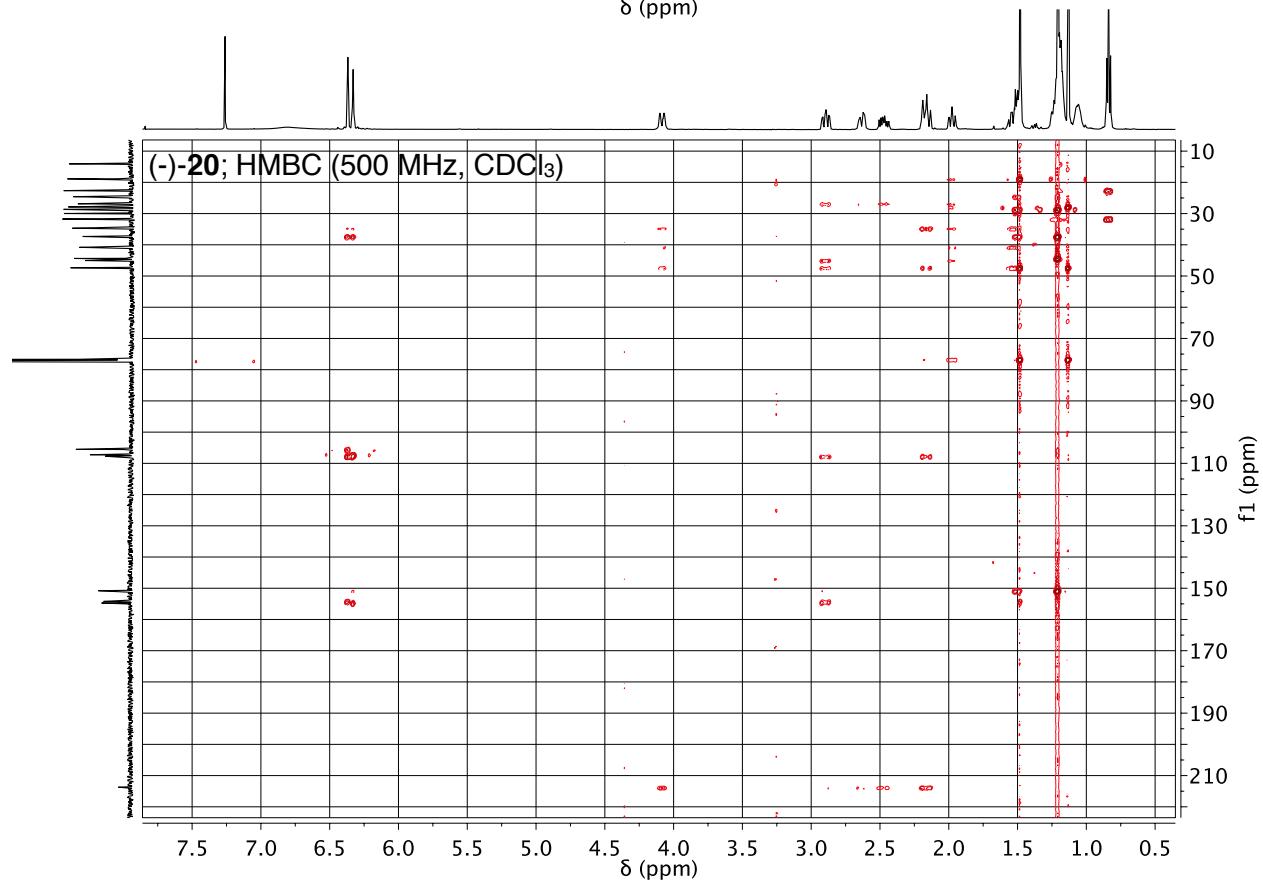
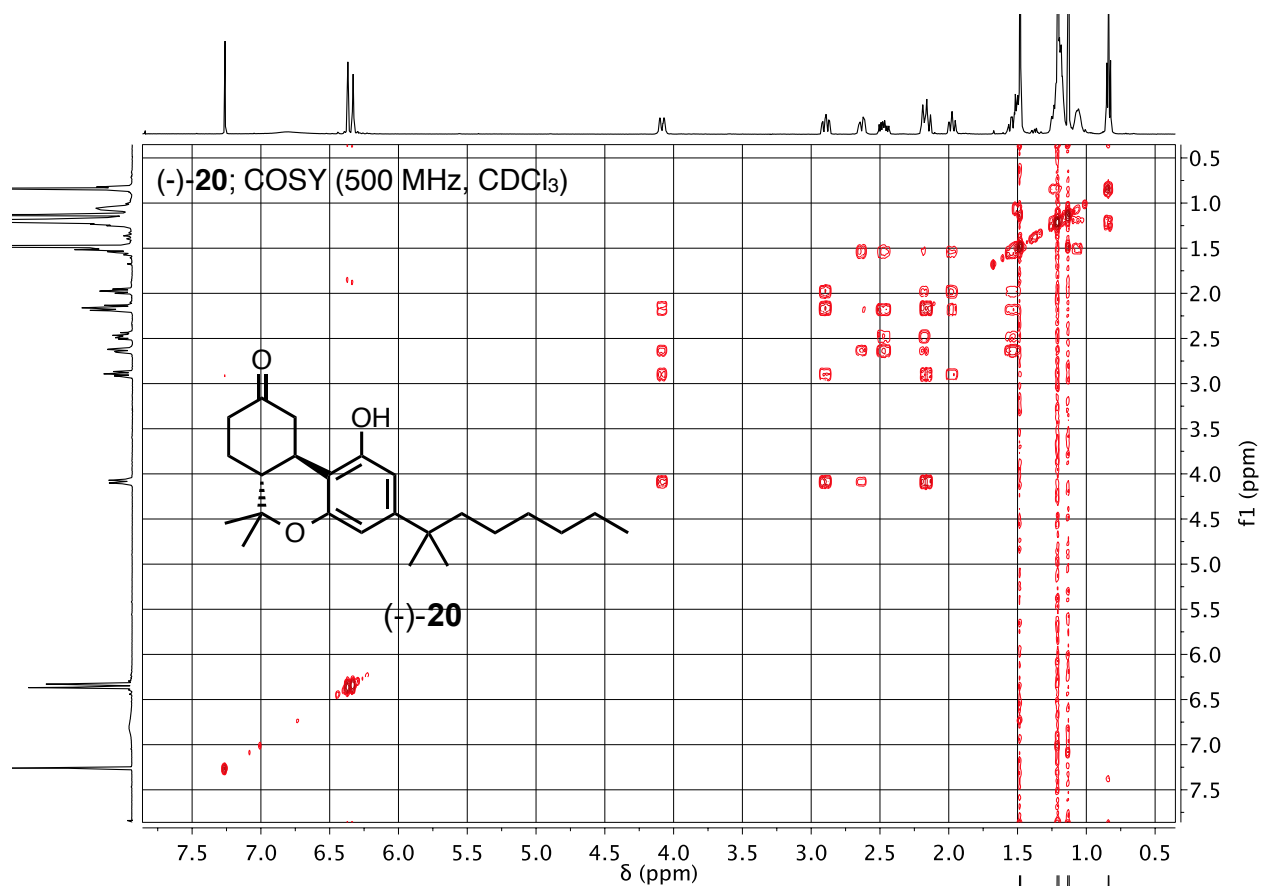
(-)-**20**



(-)-**20**; ^1H NMR (500 MHz, CDCl_3) **Expansions**







Appendix II

References and Notes

1. **canna** \ˈka-nə\ *n* [NL, genus name, fr. L, reed — more at CANE]..., and **bis** \ˈbis\ *adv* [L, fr. OL *dvis*; akin to OHG *zwiro* twice, L *duo* two — more at TWO]... Merriam-Webster's Collegiate Dictionary, 11th Ed. Springfield. **2008**.
2. Merlin, M. D. Archeological Evidence for the Tradition of Psychoactive Plant Use in the Old World. *Econ. Bot.* **2003**, 57, 295–323
3. Li, H. L., An Archeological and Historical Account of Cannabis in China, *Econ. Bot.* **1974**, 28, 437–448
4. (a) Retting; present participle of *ret.* verb, to soak to loosen the fiber from the woody tissue.
(b) For a comprehensive examination of past, present and future use of industrial hemp, read the chapter “Hemp: A New Crop with New Uses for North America” in *Trends in New Crops and New Uses*; Purdue University Press: Purdue. **2002**.
5. Abel, E. L., *Marihuana, the First Twelve Thousand Years.*; Plenum Press: New York, **1980**.
6. (a) Herer, J., *The Emperor Wears No Clothes*, 11th ed.; Ah Ha Publishing: Van Nuys, **2007**
(b) Frydl K. J., *The Drug Wars in America, 1940-1973.*; Cambridge University Press: Cambridge, **2013**.
7. Russo, E. B.; Jiang, H.; Li, X.; Sutton, A.; Carboni, A.; Bianco, F. D.; Mandelino, G.; Potter, D. J.; Zhao, Y.; Bera, S.; Zhang, Y.; Lu, E.; Ferguson, D. K.; Hueber, F.; Zhao, L.; Liu, C.; Wang, Y.; Li, C., Phytochemical and Genetic Analyses of Ancient Cannabis from Central Asia. *J. of Exp. Bot.* **2008**, 59, 4171–4182.
8. Medical History of British India, Report of the Indian Hemp Drugs Commission **1894-1895**, Vol III, 247-251.
9. Touw, M. J., The Religious and Medical Uses of Cannabis in China India and Tibet, *Psychoactive Drugs* **1981**, 13, 23–34.
10. Crawford, A. C., Notes on “Physiological Testing”, *Am. J. Pharm.* **1908**, 80, 321-335
11. (a) McMeens, R.R., *Report to the Ohio State Medical Committee on Cannabis Indica*, Transactions of the Fifteenth Annual Meeting of the Ohio State Medical Society, White Sulphur Springs, Ohio, June 12-14, **1860**, pp.75-100. (b) O'Shaughnessy, W.B., Case of Tetanus, Cured by a Preparation of Hemp (the Cannabis indica.), *Transactions of the Medical and Physical Society of Bengal* 8, **1838-40**, 462-469 (c) Clendinning, J., Observations on the Medical Properties of Cannabis Sativa of India, *Med. Chir. Trans.* **1843**; 26, 188–210 (d) Bell, J.; Derry N. H., On The Haschisch or Cannabis Indica, *The Boston*

- Medical and Surgical Journal*, **1857**; 16 April, 209-216, and 23 April, 229-236 (e) Hamilton, H. C.; Lescohier, A. W.; Perkins, R. A., The Physiological Activity of Cannabis Sativa, *J. Am. Pharm. Assoc.* **1913**, 2, 322-323
12. McPartland, J. M.; Russo, E. B., Cannabis and Cannabis Extracts: Greater Than the Sum of Their Parts? *J. Cann. Therap.* **2001**, 1, 103-132
 13. Wood, T. B., Cannabinol, Part I., *J. Chem. Soc.* **1899**, 75, 20–36.
 14. Gertsch, J.; Pertwee, R. G.; Di Marzo, V., Phytocannabinoids beyond the *Cannabis* plant – do they exist? *British J. of Pharm.* **2010**, 160, 523-529.
 15. (a) Oliver, J., On the action of Cannabis Indica. *The British Medical Journal* **1883**, 1, 905-906 (b) Wallich, G. C., Cannabis Indica, *The British Medical Journal* **1883**, 1, 1224.
 16. Opium as an international problem : the Geneva conferences by Willoughby, Westel Woodbury **1925** Publisher Baltimore : The Johns Hopkins press Pages 1-618 Chapter XIX p. 374
 17. Cahn, R. S., Cannabis indica resin, Part III. The Constitution of Cannabinol. *J. Am. Chem. Soc.* **1932**, 1342–1353.
 18. Levine, J., Origin of Cannabinol, *J. Am. Chem. Soc.* **1944**, 66, 1868–1870
 19. (a) Marshall, C. R., A contribution to the pharmacology of Cannabis indica. *J. Am. Med. Assoc.* **1898**, 31, 882–891. (b) Fraenkel, S., Chemie und Pharmakologie des Haschisch. *Arch. Exp. Pathol. Pharm.* **1903**, 49, 266–284.
 20. (a) Jacob, A.; Todd, A. R., Cannabis indica. Part II. Isolation of Cannabidiol from Egyptian Hashish. Observations on the Structure of Cannabinol. *J. Chem. Soc.* **1940**, 649–653. (b) Ghosh, R.; Todd, A. R.; Wilkinson, S., Cannabis indica, part V. The Synthesis of Cannabinol. *J. Chem. Soc.* **1940**, 1393–1396. (c) Adams, R.; Baker, B. R.; Wearn, R. B., Structure of Cannabinol. III. Synthesis of Cannabinol, 1-hydroxy-3-*n*-amyl-6,6,9-trimethyl-6-dibenzopyran. *J. Am. Chem. Soc.* **1940**, 62, 2204–2207. (d) Adams, R.; Wolff, H.; Cain, C. K.; Clark, J. H., Structure of Cannabidiol. V. Position of the Alicyclic Double Bonds. *J. Am. Chem. Soc.* **1940**, 62, 2215–2219. (e) Adams, R.; Baker, B. R., Structure of Cannabidiol. VII. A Method of Synthesis of a Tetrahydrocannabinol which Possesses Marihuana Activity. *J. Am. Chem. Soc.* **1940**, 62, 2405– 2408.

21. (a) Eckler and Miller, *J. Am. Pharm. Assoc.* **1917**, 6, 872 (b) Hamilton, *J. Am. Pharm. Assoc.* **1917**, 6, 875. (c) Marshall, *Pharm. J.* **1909**, 81, 418 (1909). (d) Chopra, "Indian Medical Research Memoirs" (Memoir No. 31, July, **1939**)
22. Gaoni, Y.; Mechoulam, R., Isolation, Structure, and Partial Synthesis of an Active Constituent of Hashish. *J. Am. Chem. Soc.* **1964**, 86, 1646–1647.
23. Gaoni, Y.; Mechoulam, R., A Total Synthesis of *dl*- Δ^1 -Tetrahydrocannabinol, the Active Constituent of Hashish *J. Am. Chem. Soc.* **1965**, 87, 3273–3275.
24. Mechoulam, R.; Braun, P., A stereospecific synthesis of (-)- Δ^1 and (-)- $\Delta^{1(6)}$ Tetrahydrocannabinols. *J. Am. Chem. Soc.* **1967**, 89, 4552–4554
25. Comprehensive Drug Abuse Prevention and Control Act of **1970**. 91-513, **1970**, 1239-1296.
26. (a) Gieringer, D. H., Review of Human Studies on Medical Use of Marijuana. **1996** NORML (b) Mikuriya, T. H., Cannabis substitution. An adjunctive therapeutic tool in the treatment of alcoholism. *Medical Times*, **1970**, 98, 187-191 (c) Hepler, R. S., Frank, I. R., Marihuana Smoking and Intraocular Pressure. *JAMA* **1971**, 217, 1392 (d) Hill, S. Y., Schwin, R., Goodwin, D. W., Powell, B., Marihuana and Pain, *J. Pharmacol. Exp. Ther.* **1974**, 188, 415-418. (e) Dunn, M., Davis, R., The Perceived Effects of Marijuana on Spinal Cord Injured Males, *Paraplegia* **1974**, 3, 175. (f) Tashkin, D. P., Shapiro, B. J., Frank, I. M., Acute Effects of Smoked Marijuana and Oral Δ^9 -tetrahydrocannabinol on Specific Airway Conductance in Asthmatic Subjects, *American Review for Respiratory Diseases* **1974**, 109, 420-428. (g) Flom M. C., Adams, A. J., Jones, R. T., Marijuana Smoking and Reduced Pressure in Human Eyes: Drug action or Epiphenomenon? *Invest. Ophthalmol.* **1975**, 14, 52-55. (h) Consroe, P. F., Wood, G. C., Buchsbaum, H., Anticonvulsant Nature of Marihuana Smoking. *JAMA* **1975**, 234, 306-307 (i) Noyes, R. Jr., Brunk, S. F., Baram, D. A., Canter, A., Analgesic Effect of Δ^9 -tetrahydrocannabinol. *J. of Clin. Pharm.* **1975**, 15, 139-143 (j) Sallan, S.E., Zinberg, N.E., Frei III, E., Antiemetic Effect of Δ^9 -tetrahydrocannabinol in Patients Receiving Cancer Chemotherapy. *N. Engl. J. Med.* **1975**, 293, 795-797 (k) Staquet, M., Gantt, C., Machin, D., Effect of a Nitrogen Analog of Δ^9 -tetrahydrocannabinol on Cancer Pain. *Clin. Pharmacol. Ther.* **1978**, 23, 397-401. (l) Herman, T. S., Einhorn, L. H., Jones, S. E., Nagy, C., Chester, A. B., Dean, J. C., Furnas, B., Williams, S. D., Leigh, S. A., Dorr, R. T., Moon, T. E., Superiority of Nabilone over Prochlorperazine as an Antiemetic in Patients Receiving Cancer Chemotherapy. *N. Engl. J. Med.* **1979**, 300, 1295-1297.
27. U.S. Dept. of Justice. Drug Enforcement Administration. Marijuana Scheduling Petition; Denial of Petition. *Federal Register*, v. 54, no. 249, December 29, 1989. p. 53767.

28. In *Cannabinoids. Handbook of Experimental Pharmacology*, Pertwee, R. G., Ed.; Springer-Verlag: Heidelberg, **2005**; Vol. 168, pp 719–756.
29. (a) Pertwee, R. G., Cannabinoid Pharmacology: The first 66 years. *Br. J. Pharmacol.* **2006**, 147, 163–171. (b) Pertwee, R. G., The Central Neuropharmacology of Psychotropic Cannabinoids. *Pharmacol. Ther.* **1988**, 36, 189–261.
30. (a) Howlett, A. C.; Fleming, R. M., Cannabinoid Inhibition of Adenylate Cyclase Pharmacology of the Response in Neuroblastoma Cell Membranes. *Mol. Pharmacol.* **1984**, 26, 532–538. (b) Howlett, A. C., Cannabinoid Inhibition of Adenylate Cyclase Biochemistry of the Response in Neuroblastoma Cell Membranes. *Mol. Pharmacol.* **1985**, 27, 429–436. (c) Howlett, A. C.; Qualy, J. M.; Khachatrian, L. L., Involvement of G_i in the Inhibition of Adenylate Cyclase by Cannabimimetic Drugs. *Mol. Pharmacol.* **1986**, 29, 307–313. (d) Howlett, A. C., Cannabinoid Inhibition of Adenylate Cyclase: Relative Activity of Constituents and Metabolites of Marihuana. *Neuropharmacology*, **1987**, 26, 507–512.
31. Devane, W. A.; Dysarz III, F. A.; Johnson, M. R.; Melvin, L. S.; Howlett, A. C., Determination and Characterization of a Cannabinoid Receptor in Rat Brain. *Mol. Pharmacol.* **1988**, 34, 605–613.
32. Gerard, C. M.; Mollereau, C.; Vassart, G.; Parmentier, M., Molecular Cloning of a Human Cannabinoid Receptor which is also Expressed in Testis. *Biochem. J.* **1991**, 279, 129–134.
33. Munro, S.; Thomas, K. L.; Abu-Shaar, M., Molecular Characterization of a Peripheral Receptor for Cannabinoids. *Nature*, **1993**, 365, 61–65.
34. (a) Burns, H. D.; Van Laere, K.; Sanabria-Bohórquez, S.; Hamill, T. G.; Bormans, G.; Eng, W.; Gibson, R.; Ryan, C.; Connolly, B.; Patel, S.; Krause, S.; Vanko, A.; Van Hecken, A.; Dupont, P.; De Lepeleire, I.; Rothenberg, P.; Stoch, S. A.; Cote, J.; Hagmann, W. K.; Jewell, J. P.; Lin, L. S.; Liu, P.; Goulet, M. T.; Gottesdiener, K.; Wagner, J. A.; de Hoon, J.; Mortelmans, L.; Fong, T. M.; Hargreaves, R., [^{18}F]MK-9470, a positron emission tomography (PET) tracer for in vivo human PET brain imaging of the cannabinoid-1 receptor, *J. Proc. Natl. Acad. Sci. U. S. A.* **2007**, 104, 9800–9805 (b) Slavik, R.; Grether, U.; Müller Herde, A.; Gobbi, L.; Fingerle, J.; Ullmer, C.; Krämer, S. D.; Schibli, R.; Mu, L.; Ametamey, S. M., Discovery of a High Affinity and Selective Pyridine Analog as a Potential Positron Emission Tomography Imaging Agent for Cannabinoid type 2 Receptor, *J. Med. Chem.* **2015**, 58, 4266–4277.
35. (a) Marciniak, G.; Charalambous, A.; Shiue, C.-Y.; Dewey, S. L.; Schlyer, D. J.; Makriyannis, A.; Wolf, A. P., ^{18}F -Labeled tetrahydrocannabinol: Synthesis and PET studies in a Baboon, *J. Label. Compd. Radiopharm.* **1991**, 30, 413–415. (b) Charalambous, A.; Marciniak, G.;

- Shiue, C.-Y.; Dewey, S. L.; Scldyer, D. J.; Wolf, A. P.; Makriyannis, A., PET Studies in the Primate Brain and Biodistribution in Mice using (-)-¹⁸F- Δ^8 -THC, *Pharm. Biochem. Behav.* **1991**, *40*, 503–507. (c) Stempel, A. V.; Stumpf, A.; Zhang, H. Y.; Ozdogan, T.; Pannasch, U.; Theis, A. K.; Otte, D. M.; Wojtalla, A.; Racz, I.; Ponomarenko, A.; Xi, Z. X.; Zimmer, A.; Schmitz, D., Cannabinoid Type 2 Receptors Mediate a Cell Type-Specific Plasticity in the Hippocampus, *Neuron*. **2014**, 1–15.
36. Palczewski, K.; Kumasaka, T.; Hori, T.; Behnke, C. A.; Motoshima, H.; Fox, B. A.; Le, T. I.; Teller D. C.; Okada, T.; Stenkamp, R. E.; Yamamoto, M.; Miyano, M. Crystal Structure of Rhodopsin: A G-protein-coupled receptor, *Science*, **2000**, *289*, 739–745
37. *Essentials of Cell Biology*. Unit 4. How do cells sense their environment? **2014**. Nature Education
38. (a) Howlett, A. C.; Barth, F.; Bonner, T. I.; Cabral, G.; Casellas, P.; Devane, W. A.; Felder, C. C.; Herkenham, M.; Mackie, K.; Martin, B. R.; Mechoulam, R.; Pertwee, R. G., International Union of Pharmacology. XXVII. Classification of Cannabinoid Receptors, *Pharmacol. Rev.* **2002**, *54*, 161–202. (b) Rukwied, R.; Gauter, B.; Schley, M.; Konrad, C., Cannabinoide–signal transduktion und wirkung, *Schmerz*, **2005**, *19*, 528–534. (c) Turu, G.; Hunyady, L., Signal transduction of the CB1 Cannabinoid Receptor, *J. Mol. Endocrinol.* **2010**, *44*, 75–85.
39. Hilal-Dandan R.; Brunton L.; *Goodman and Gilman's Manual of Pharmacology and Therapeutics*. 11th ed: McGraw-Hill Companies. New York. **2008**.
40. Devane, W. A.; Hanus, L.; Brewer, A.; Pertwee, R. G.; Stevenson, L. A.; Griffin, G.; Gibson, D.; Mandelbaum, A.; Etinger, A.; Mechoulam, R., *Science* **1992**, *258*, 1946–1949
41. (a) Brown, A. J., Novel Cannabinoid Receptors. *Br. J. Pharmacol.* **2007**, *152*, 567–575. (b) Mackie, K.; Stella, N., Cannabinoid Receptors and Endocannabinoids: Evidence for New Players. *AAPS J.* **2006**, *8*, E298-E306. (c) Johns, D. G.; Behm, D. J.; Walker, D. J.; Ao, Z.; Shapland, E. M.; Daniels, D. A.; Riddick, M.; Dowell, S.; Staton, P. C.; Green, P.; Shabon, U.; Bao, W.; Aiyar, N.; Yue, T. L.; Brown, A. J.; Morrison, A. D.; Douglas, S. A., The Novel Endocannabinoid Receptor GPR55 is Activated by a Typical Cannabinoids but does not Mediate their Vasodilator Effects, *Br. J. Pharmacol.* **2007**, *152*, 825–831. (d) McHugh, D.; Hu, S. S.-J.; Rimmerman, N.; Juknat, A.; Vogel, Z.; Walker, J. M.; Bradshaw, H. B., *N*-arachidonoyl glycine, An Abundant Endogenous lipid, Potently Drives Directed Cellular Migration Through GPR18, the Putative Abnormal Cannabidiol Receptor, *BMC Neurosci.* **2010**, *11*, 44
42. Viveros, M. P.; Fonseca, F. R. De; Bermudez-Silva, F. J.; McPartland, J. M., Critical Role of the Endocannabinoid System in the Regulation of Food Intake and Energy Metabolism, with

Phylogenetic, Developmental, and Pathophysiological Implications, *Endocrine, Metab. Immune Disord. - Drug Targets*, **2008**, *8*, 220–230.

43. Cheng, Y.-C.; Prusoff, W. H., Relationship Between the Inhibition Constant (K_i) and the Concentration of Inhibitor Which Causes 50 per cent Inhibition (I_{50}) of an Enzymatic Reaction, *Biochem. Pharmacol.* **1973**, *22*, 3099–3108
44. Lazareno, S.; Birdsall, N. J. Estimation of Competitive Antagonist Affinity from Functional Inhibition Curves using the Gaddum, Schild and Cheng-Prusoff Equations, *Br. J. Pharmacol.* **1993**, *109*, 1110–1119.
45. (a) Kenakin, T., Inverse, Protein, and Ligand-Selective Agonism: Matters of Receptor Conformation, *FASEB J.* **2001**, *15*, 598–611. (b) Tikhonova, I. G.; Costanzi, S., Unraveling the Structure and Function of G protein-coupled Receptors Through NMR Spectroscopy, *Curr. Pharm. Des.* **2009**, *15*, 4003–4016. (c) Cherezov, A.; Abola, E.; Stevens, R. C., Recent Progress in the Structure Determination of GPCRs, a Membrane Protein Family with High Potential as Pharmaceutical Targets, *Methods Mol. Biol.* **2010**, *654*, 141–168.
46. Wiener, M. C.. A Pedestrian Guide to Membrane Protein Crystallization, *Methods*, **2004**, *34*, 364–372
47. (a) Zvonok, N.; Pandarinathan, L.; Williams, J.; Johnston, M.; Karageorgos, I.; Janero, D. R.; Krishnan, S. C.; Makriyannis, A., Covalent Inhibitors of Human Monoacyl Glycerol Lipase: Ligand-assisted Characterization of the Catalytic site by Mass Spectrometry and Mutational Analysis, *Chem. Biol.* **2008**, *15*, 854–862. (b) Pei, Y.; Mercier, R. W.; Anday, J. K.; Thakur, G. A.; Zvonok, A. M.; Hurst, D.; Reggio, P. H.; Janero, D. R.; Makriyannis, A., Ligand-binding Architecture of Human CB2 Cannabinoid Receptor: Evidence for Receptor Subtype-specific Binding Motif and Modeling GPCR Activation. *Chem. Biol.* **2008**, *15*, 1207–1219. (c) Mercier, R. W.; Pei, Y.; Pandarinathan, L.; Janero, D. R.; Zhang, J.; Makriyannis, A., hCB2 Ligand-interaction Landscape: Cysteine Residues Critical to Biarylpyrazole Antagonist Binding mMotif and Receptor Modulation, *Chem. Biol.* **2010**, *17*, 1132–1142.
48. Stern, E.; Lambert, D. M., Medicinal Chemistry Endeavors around the Phytocannabinoids, *Chem. Biodivers.* **2007**, *4*, 1707–1728.
49. Rinaldi-Carmona, M.; Barth, F.; Heaulme, M.; Shire, D.; Calandra, B.; Congy, C.; Martinez, S.; Maruani, J.; Neliat, G.; Caput, D.; Ferrara, P.; Soubrie, P.; Breliere, J. C.; Le Fur, G., SR141716A, a Potent and Selective Antagonist of the Brain Cannabinoid Receptor, *FEBS Lett.* **1994**, *350*, 240–244.

50. Bell, M. R.; D'Ambra, T. E.; Kumar, V.; Eissenstat, M. A.; Herrmann Jr., J. L.; Wetzel, J. R.; Rosi, D.; Phillion, R. E.; Daum, S. J.; Hlasta, D. J.; Kullnig, R. K.; Ackerman, J. H.; Haubrich, D. R.; Luttinger, D. A.; Baizman, E. R.; Miller, M. S.; Ward, S. J., Antinociceptive (aminoalkyl)indoles, *J. Med. Chem.* **1991**, *34*, 1099–1110.
51. Mauler, F.; Mittendorf, J.; Horváth, E.; De Vry, J., Characterization of the Diarylether Sulfonylester (-)-(R)-3-(2-hydroxymethylindanyl-4-oxy)phenyl-4,4,4-trifluoro-1-sulfonate (BAY 38-7271) as a Potent Cannabinoid Receptor Agonist with Neuroprotective Properties, *J. Pharmacol. Exp. Ther.* **2002**, *302*, 359–368.
52. Iwamura, H.; Suzuki, H.; Ueda, Y.; Kaya, T.; Inaba, T., In Vitro and in Vivo Pharmacological Characterization of JTE-907, a Novel Selective Ligand for Cannabinoid CB₂ Receptor, *Pharmacology*, **2001**, *296*, 420–425.
53. (a) Wiley, J. L.; Barrett, R. L.; Lowe, J.; Balster, R. L.; Martin, B. R., Discriminative Stimulus Effects of CP-55,940 and Structurally Dissimilar Cannabinoids in Rats, *Neuropharmacology* **1995**, *34*, 669–676. (b) Thomas, B. F.; Gilliam, A. F.; Burch, D. F.; Roche, M. J.; Seltzman, H. H., Comparative Receptor Binding Analyses of Cannabinoid Agonists and Antagonists, *J. Pharmacol. Exp. Ther.* **1998**, *285*, 285–292.
54. (a) Tius, M. A.; Makriyannis, A.; Zou, X. L.; Abadji, V., Conformationally Restricted Hybrids of CP-55,940 and HHC: Stereoselective Synthesis and Activity, *Tetrahedron*, **1994**, *50*, 2671–2680. (b) Tius, M. A.; Hill, W. A. G.; Zou, X. L.; Busch-Petersen, J.; Kawakami, J. K.; Fernandez-Garcia, M. C.; Drake, D. J.; Abadji, V.; Makriyannis, A. Classical/non-classical Cannabinoid Hybrids: Stereochemical Requirements for the Southern Hydroxyalkyl Chain, *Life Sci.* **1995**, *56*, 2007–2012. (c) Drake, D. J.; Jensen, R. S.; Busch-Petersen, J.; Kawakami, J. K.; Fernandez-Garcia, M. C.; Fan, P.; Makriyannis, A.; Tius, M. A., Classical/nonclassical Hybrid Cannabinoids: Southern Aliphatic Chain-functionalized C-6 β Methyl, Ethyl, and Propyl Analogues, *J. Med. Chem.* **1998**, *41*, 3596–3608. (d) Harrington, P. E.; Stergiades, I. A.; Erickson, J.; Makriyannis, A.; Tius, M. A., Synthesis of Functionalized Cannabinoids, *J. Org. Chem.* **2000**, *65*, 6576–6582 (e) Huffman, J. W.; Lu, J.; Dai, D.; Kitaygorodskiy, A.; Wiley, J. L.; Martin, B. R., *Bioorganic Med. Chem.* **2000**, *8*, 439–447.
55. (a) Edery, H.; Grunfeld, Y.; Ben-Zvi, Z.; Mechoulam, R., Structural Requirements for Cannabinoid Activity, *Ann. N.Y. Acad. Sci.* **1971**, *191*, 40–53. (b) Mechoulam, R.; Lander, N.; Varkony, T. H.; Kimmel, I.; Becker, O.; Ben-Zvi, Z., Stereochemical Requirements for Cannabinoid Activity, *J. Med. Chem.* **1980**, *23*, 1068–1072.
56. (a) Wilson, R. S.; May, E. L., Analgesic Properties of the Tetrahydrocannabinols, Their Metabolites, and Analogs, *J. Med. Chem.* **1975**, *18*, 700–703. (b) Wilson, R. S.; May, E. L., 9-Nor-9-hydroxyhexahydrocannabinols. Synthesis, Some Behavioral and Analgesic

Properties, and Comparison with the Tetrahydrocannabinols, *J. Med. Chem.* **1976**, *19*, 1165–1167.

57. (a) Lake, K. D.; Compton, D. R.; Varga, K.; Martin, B. R.; Kunos, G., Cannabinoid-Induced Hypotension and Bradycardia in Rats is Medicated by CB1-like Cannabinoid Receptors, *J. Pharmacol. Exp. Ther.* **1997**, *281*, 1030-1037. (b) Felder, C. C.; Joyce, K. E.; Briley, E. M.; Mansouri, J.; Mackie, K.; Blond, O.; Lai, Y.; Ma, A. L.; Mitchell, R. L., Comparison of the Pharmacology and Signal Transduction of the Human Cannabinoid CB1 and CB2 Receptors, *Mol. Pharmacol.* **1995**, *48*, 443–450.
58. (a) Huffman, J. W.; Liddle, J.; Yu, S.; Aung, M. M.; Abood, M. E.; Wiley, J. L.; Martin, B. R., 3-(1',1'-Dimethylbutyl)-1-deoxy- Δ^8 -THC and Related Compounds: Synthesis of Selective Ligands for the CB2 Receptor, *Bioorg. Med. Chem.* **1999**, *7*, 2905–1914. (b) Gareau, Y.; Dufresne, C.; Gallant, M.; Rochette, C.; Sawyer, N.; Slipetz, D. M.; Tremblay, N.; Weech, P. K.; Metters, K. M.; Labelle, M., Structure Activity Relationships of Tetrahydrocannabinol Analogues on Human Cannabinoid Receptors, *Bioorg. Med. Chem. Lett.* **1996**, *6*, 189–194. (c) Huffman, J. W.; Yu, S.; Showalter, V.; Abood, M. E.; Wiley, J. L.; Compton, D. R.; Martin, B. R.; Bramblett, R. D.; Reggio, P. H., Synthesis and Pharmacology of a Very Potent Cannabinoid Lacking a Phenolic Hydroxyl with High Affinity for the CB2 Receptor, *J. Med. Chem.* **1996**, *39*, 3875–3877. (d) Huffman, J. W.; Bushell, S. M.; Miller, J. R. A.; Wiley, J. L.; Martin, B. R., 1-Methoxy-1-deoxy-11-hydroxy- and 11-Hydroxy-1-Methoxy- Δ^8 -Tetrahydrocannabinols: New Selective Ligands for the CB2 Receptors, *Bio. Med. Chem.* **2002**, *10*, 4119–4129
59. Martin, B. R.; Jefferson, R. G.; Winckler, R.; Wiley, J. L.; Thomas, B. F.; Crocker, P. J.; Williams, W.; Razdan, R. K., Assessment of Structural Commonality between Tetrahydrocannabinol and Anandamide, *Eur. J. Pharmacol.* **2002**, *435*, 35–42.
60. Huffman, J. W., CB2 Receptor Ligands, *Mini Rev. Med. Chem.* **2005**, *5*, 641–649
61. (a) Papahatjis, D. P.; Nahmias, V. R.; Nikas, S. P.; Andreou, T.; Alapafuja, S. O.; Tsotinis, A.; Guo, J.; Fan, P.; Makriyannis, A., C1'-Cycloalkyl side chain Pharmacophore in Tetrahydrocannabinols, *J. Med. Chem.* **2007**, *50*, 4048–4060. (b) Lu, D.; Guo, J.; Duclos, R. I.; Bowman, A. L.; Makriyannis, A., Bornyl- and Isobornyl- Δ^8 -Tetrahydrocannabinols: A Novel Class of Cannabinergic Ligands, *J. Med. Chem.* **2008**, *51*, 6393–6399. (c) Lu, D.; Meng, Z.; Thakur, G. A.; Fan, P.; Steed, J.; Tartal, C. L.; Hurst, D. P.; Peggio, P. H.; Deschamps, J. R.; Parrish, D. A.; George, C.; Jarbe, T. U. C.; Lamb, R. J.; Makriyannis, A., Adamantyl Cannabinoids: A Novel Class of Cannabinergic Ligands, *J. Med. Chem.* **2005**, *48*, 4576–4585.

62. Busch-Petersen, J.; Hill, W. A.; Fan, P.; Khanolkar, A.; Xie, X. Q.; Tius, M. A.; Makriyannis, A., Unsaturated Side Chain β -11-hydroxyhexahydrocannabinol Analogs, *J. Med. Chem.* **1996**, *39*, 3790–3796.
63. (a) Noe, M. C.; Gilbert, A. M. *Targeted Covalent Enzyme Inhibitors*, 1st ed.; Vol. 47; Elsevier Inc. **2012**. (b) Johnson, D. S.; Weerapana, E.; Cravatt, B. F., Strategies for Discovering and Derisking Covalent, Irreversible Enzyme Inhibitors, *Future Med. Chem.* **2010**, *2*, 949–964.
64. (a) Rice, K. C.; Jacobson, A. E.; Burke, T. R., Jr.; Bajwa, B. S.; Streaty, R. A.; Klee, W. A., Irreversible Ligands with High Selectivity toward δ and μ Opiate Receptors, *Science*, **1983**, *220*, 314–316. (b) Portoghese, P. S.; Sultana, M.; Takemori, A. E. Naltrindole 5'-Isothiocyanate: A Non-equilibrium Highly Selective δ Opioid Receptor Antagonist, *J. Med. Chem.* **1990**, *33*, 1547–1548.
65. Raftery, M. F.; Mattson, M.; Jacobsen, A. E.; Rice, K. C., A Specific Acylating Agent for the [3 H]Phencyclidine Receptors in Rat Brain, *FEBS Lett.* **1986**, *181*, 318–322.
66. Allen, M. S.; Hagen, T. J.; Trudell, M. L.; Coddington, P. W.; Skolnick, P.; Cook, J. M., Synthesis of Novel 3-Substituted, β -Carbolines as Benzodiazepine Receptor Ligands: Probing the Benzodiazepine Receptor Pharmacophore, *J. Med. Chem.* **1988**, *31*, 1854–1861.
67. (a) Guo, Y.; Abadji, V.; Morse, K. L.; Fournier, D. J.; Li, X.; Makriyannis, A., (-)-11-Hydroxy-7'-isothiocyanato-1', 1'-dimethylheptyl- Δ^8 -THC: A Novel, High-Affinity Irreversible Probe for the Cannabinoid Receptor in the Brain, *J. Med. Chem.* **1994**, *37*, 3867–3870. (b) Pei, Y.; Mercier, R. W.; Anday, J. K.; Thakur, G. A.; Zvonok, A. M.; Hurst, D.; Reggio, P. H.; Janero, D. R.; Makriyannis, A., Ligand-Binding Architecture of Human CB2 Cannabinoid Receptor: Evidence for Receptor Subtype-Specific Binding Motif and Modeling GPCR Activation, *Chem. Biol.* **2008**, *15*, 1207–1219.
68. (a) Sokolovsky, M., Photoaffinity Labeling of Muscarinic Receptors, *Pharmac. Ther.* **1987**, *32*, 285–292. (b) Raymond, J. R.; Fargin, A.; Lobe, J. M.; Regan, J. W.; Senogles, S. E.; Lefkowitz, R. J.; Caron, M. G., Identification of the Ligand-binding Subunit of the Human 5-hydroxytryptamine_{1A} Receptor with *N*-(p-azido-m-[125 I] iodophenethyl)piperone, A High Affinity Radioiodinated Photoaffinity Probe, *Mol. Pharmacol.* **1989**, *36*, 15–21 (c) Nakayama, T. A.; Khorana, H. G., Orientation of Retinal in Bovine Rhodopsin Determined by Cross-Linking Using a Photoactivatable Analog of 11-cis-Retinal, *J. Biol. Chem.* **1990**, *265*, 15762–15769.
69. (a) Brunner, J., New Photolabeling and Crosslinking Methods, *Annu. Rev. Biochem.* **1993**, *62*, 483–514. (b) Bräse, S.; Gil, C.; Knepper, K.; Zimmermann, V., Organic Azides: An

Exploding Diversity of a Unique Class of Compounds, *Angew. Chemie - Int. Ed.* **2005**, *44*, 5188–5240.

70. (a) Ogawa, G.; Tius, M. A.; Zhou, H.; Nikas, S. P.; Halikhedkar, A.; Mallipeddi, S.; Makriyannis, A., 3'-Functionalized Adamantyl Cannabinoid Receptor Probes, *J. Med. Chem.* **2015**, *58*, 3104–3116. (b) Unpublished results from Go Ogawa's notebook.
71. (a) Bolla, M.; Almirante, N.; Benedini, F., Therapeutic Potential of Nitrate Esters of Commonly Used Drugs, *Curr. Top. Med. Chem.* **2005**, *5*, 707–720. (b) Thatcher, G. R. J.; Nicolescu, A. C.; Bennett, B. M.; Toader, V., Nitrates and NO Release: Contemporary Aspects in Biological and Medicinal Chemistry, *Free Radic. Biol. Med.* **2004**, *37*, 1122–1143.
72. (a) Tius, M. A., Stereospecific Cannabinoid Synthesis: The Application of New Techniques to a Classical Problem, *Stud. Nat. Prod. Chem.* **1996**, *19 (C)*, 185–244. (b) Teske, J. A.; Deiters, A., A Cyclotrimerization Route to Cannabinoids, *Org. Lett.* **2008**, *10*, 2195–2198. (c) Itagaki, N.; Sugahara, T.; Iwabuchi, Y., Expedient Synthesis of Potent Cannabinoid Receptor Agonist (-)-CP-55,940, *Org. Lett.* **2005**, *7*, 4181–4183. (d) Itagaki, N.; Kimura, M.; Sugahara, T.; Iwabuchi, Y., Organocatalytic Entry to Chiral bicyclo[3.n.1]alkanones via Direct Asymmetric Intramolecular Aldolization, *Org. Lett.* **2005**, *7*, 4185–4188.
73. (a) Schafroth, M. A.; Zuccarello, G.; Krautwald, S.; Sarlah, D.; Carreira, E. M., Stereodivergent Total Synthesis of Δ^9 -tetrahydrocannabinols., *Angew. Chem. Int. Ed. Engl.* **2014**, *53*, 13898–13901. (b) for related synthesis: Klotter, F.; Studer, A., Short and Divergent Total Synthesis of (+)-Machaeriol B, (+)-Machaeriol D, (+)- Δ^8 -THC, and Analogues, *Ang. Chem. Int. Ed.* **2015**, *54*, 8547–8550.
74. Nikas, S. P.; Thakur, G. A.; Parrish, D.; Alapafuja, S. O.; Huestis, M. A.; Makriyannis, A., A Concise Methodology for the Synthesis of (-)- Δ^9 -tetrahydrocannabinol and (-)- Δ^9 -tetrahydrocannabivarin Metabolites and their Regiospecifically Deuterated Analogs, *Tetrahedron*, **2007**, *63*, 8112–8123.
75. Archer, R. A.; Baldwin, J.E.; Blanchard, W. B.; Day, W. A.; Johnson, D. W.; Lavagnino, E. R.; Ryan, C. W., Cannabinoids. 3. Synthetic Approaches to 9-ketocannabinoids. Total Synthesis of Nabilone, *J. Org. Chem.* **1977**, *42*, 2277–2284 (b) (-)- β -pinene (**94**) was purchased from Aldrich Chemical Company: Catalog No. 11,208-9 with $[\alpha]_D^{20}$ -21° (neat) which represents a 92.5% ee. (c) Whitham, G. H., The Reaction of α -Pinene with Lead Tetra-acetate, *J. Chem. Soc.* **1961**, 2232–2236. (d) Mori, K., Synthesis of Optically Pure (+)-trans-Verbenol and Its Antipode, the Pheromone of Dendroctonus Bark Beetles, *Agr. Biol. Chem.* **1976**, *40*, 415–418. (e) In 1977, (-)-nabilone prepared from (+)-apoverbenone exhibited a specific rotation of $[\alpha]_D^{20}$ -40.2° (c 1.0, CHCl₃), resulting in the lowest optical purity reported by Archer.

Moreover, (-)-nabilone prepared from the diacetates (**97**) and dimethylheptyl resorcinol (**93**) exhibited a specific rotation of $[\alpha]^{20}_{\text{D}} -47.5^{\circ}$ (c 1.0, CHCl_3) or $[\alpha]^{20}_{\text{D}} -52.3^{\circ}$ (c 1.0, CHCl_3) following the procedure using $\text{BF}_3 \cdot \text{OEt}_2$ or the cyclization of **98** with SnCl_4 , respectively. For greater details see ref.^{75a}

76. I.Bureau W O 2010/013006 A2. IMPROVED SYNTHESIS OF HEXAHYDRODIBENZOPYRANONES, **2010**.
77. Sharma, R.; Nikas, S. P.; Guo, J. J.; Mallipreddi, S.; Wood, J. T.; Makriyannis, A., C-ring Cannabinoid Lactones: A Novel Cannabinergic Chemotype, *ACS Med. Chem. Lett.* **2014**, *5*, 400–404.
78. Dixon, D. D.; Sethumadhavan, D.; Benneche, T.; Banaag, A. R.; Tius, M. A.; Thakur, G. A.; Bowman, A.; Wood, J. T.; Makriyannis, A., Heteroadamantyl Cannabinoids, *J. Med. Chem.* **2010**, *53*, 5656–5666.
79. (a) FDA. Q3D Elemental Impurities Guidance for Industry; **2015**. (b) Cesamet® Prescribing Information. Somerset, NJ: Meda Pharmaceuticals Inc; **2009**.
80. (a) Hendrickson, J. B., Systematic Synthesis Design. III. The Scope of the Problem, *J. Am. Chem. Soc.* **1975**, *97*, 5763–5784. (b) Wender, P. A., Toward the Ideal Synthesis and Transformative Therapies: The Roles of Step Economy and Function Oriented Synthesis, *Tetrahedron*, **2013**, *69*, 7529–7550. (c) Gaich, T.; Baran, P. S., Aiming for the Ideal Synthesis, *J. Org. Chem.* **2010**, *75*, 4657–4673. (d) Wender, P. A., Toward the ildeal Synthesis and Molecular Function Through Synthesis-informed Design, *Natural Products Reports*, **2014**, *31*, 433–440.
81. (a) Fahrenholtz, K. E.; Lurie, M.; Kierstead, R. W.; June, R., The Total Synthesis of *dl*- Δ^9 -Tetrahydrocannabinol and Four of its Isomers, *J. Am. Chem. Soc.* **1967**, *89*, 5934–5941. (b) Fahrenholtz, K. E.; Lurk, M.; Kierstead, R. W., Total Synthesis of *dl*- Δ^9 -Tetrahydrocannabinol and of *dl*- Δ^8 -Tetrahydrocannabinol, Racemates of Active Constituents of Marihuana, *J. Am. Chem. Soc.* **1966**, *88*, 2079–2080. (c) Siegel, C.; Gordon, P. M.; Uliss, D. B.; Handrick, G. R.; Dalzell, H. C.; Razdan, R. K., Synthesis of Racemic and Optically Active Δ^9 -Tetrahydrocannabinol (THC) Metabolites, *J. Org. Chem.* **1991**, *56*, 6865–6872.
82. (a) Wu, M.; Huffman, J. W., Synthetic Studies Toward 9-Keto-Cannabinoids, *Kaoshiung J. Med. Sci.* **1991**, *7*, 148–150. (b) Lee, P. H.; Seomoon, D.; Lee, K., Highly Efficient 1,4-Addition of 1,3-Diesters to Conjugated Enones by In/TMSCl , *J. Org. Chem.* **2003**, *68*, 2510–2513. (c) Moore II, B. M.; Gurley, S.; Mustafa, S., Pyridine Non-Classical Cannabinoid Compounds and Related Methods of Use, U.S. Patent 8,809,373 B2, August 19, **2014**. (d) Tius, M. A.; Kannangara, K. G. S., Synthesis of 11-Nor- Δ^8 -tetrahydrocannabinol-9-carboxylic

- Acid Methyl Ester, *J. Org. Chem.* **1990**, *55*, 5711–5714. (e) Busch-Petersen, J.; Hill, W. A.; Fan, P.; Khanolkar, A.; Xie, X. Q.; Tius, M. A.; Makriyannis, A., Unsaturated Side Chain β -11-Hydroxyhexahydrocannabinol Analogs, *J. Med. Chem.* **1996**, *39*, 3790–3796. (f) Samet, A. V.; Niyazymbetov, M. E.; Semenov, V. V.; Laikhter, A. L.; Evans, D. H., Comparative Studies of Cathodically-Promoted and Base-Catalyzed Michael Addition Reactions of Levoglucosenone, *J. Org. Chem.* **1996**, *61*, 8786–8791.
83. Kosugi, H.; Ku, J.; Kato, M., Preparation of Optically Active Apoverbenone and Verbenone from Nopinone by Use of the Sulfenylation-Dehydrosulfenylation Method. Stability and Reactivity Attributable to Absolute Configuration at the Sulfur Atom in Sulfoxides, *J. Org. Chem.* **1998**, *63*, 6939–6946.
84. (a) Grimshaw, J.; Grimshaw, J. T.; Juneja, H. R., Apoverbenone. An Investigation into its Preparation by Dehydrobromination of a Sterically Hindered Bromo-ketone, *J. Chem. Soc. Perkin Trans. I*, **1972**, 50–52. (b) Toda, F.; Tanaka, K.; Watanabe, M.; Abe, T.; Harada, N. Enantiomer Resolution by Crystallization with Chiral Hosts: Application to Monoterpenes, Verbenone and Apoverbenone, *Tetrahedron: Asymmetry* **1995**, *6*, 1495–1498.
85. Tius, M. A.; Kannangara, K. G. S., Synthesis of Δ^9 -Tetrahydrocannabinol Methyl Ester Methyl Ether, *Tetrahedron* **1992**, *48*, 9173–9186.
86. Watanabe, M.; Awen, B. Z.; Kato, M., Efficient Synthesis of (1S,5S)-4-Alkyl-6,6-dimethylbicyclo[3.1.1]hept-3-en-2-ones from (1R,5S)-(+)-Nopinone and Preparation of Some Chiral Building Blocks Suitable for the Asymmetric Synthesis *J. Org. Chem.* **1993**, *58*, 3923–3927.
87. (a) Buckle, D. R., Encyclopedia of Reagents for Organic Synthesis. John Wiley & Sons, Inc; New York: 2010. 2,3-Dichloro-5,6-dicyano-1,4-benzoquinone (b) Ladziata, U., Hypervalent Iodine(V) Reagents in Organic Synthesis, *Arkivoc* **2006**, *9*, 26–58. (c) (1) Nicolaou, K. C.; Zhong, Y.; Baran, P. S., A New Method for the One-Step Synthesis of Unsaturated Carbonyl Systems from Saturated Alcohols and Carbonyl Compounds, *J. Am. Chem. Soc.* **2000**, *122*, 7596–7597. (d) Nicolaou, K. C.; Montagnon, T.; Baran, P. S.; Zhong, Y. L., Iodine(V) Reagents in Organic Synthesis. Part 4. o-Iodoxybenzoic acid as a Chemospecific tool for Single Electron Transfer-based Oxidation Processes, *J. Am. Chem. Soc.* **2002**, *124*, 2245–2258. (e) Nicolaou, K. C.; Montagnon, T.; Baran, P. S., Modulation of the reactivity profile of IBX by Ligand Complexation: Ambient Temperature Dehydrogenation of Aldehydes and Ketones to α,β -unsaturated Carbonyl Compounds, *Angew. Chemie - Int. Ed.* **2002**, *41*, 993–996. (g) Thottumkara, A. P.; Bowsher, M. S.; Vinod, T. K., *In situ* Generation of o-Iodoxybenzoic acid (IBX) and the Catalytic use of it in Oxidation Reactions in the Presence of Oxone as a Coo-oxidant, *Org. Lett.* **2005**, *7*, 2933–2936. (h) Su, J. T.; Goddard, W. A., Enhancing 2-iodoxybenzoic acid Reactivity by Exploiting a Hypervalent Twist, *J. Am. Chem.*

- Soc.* **2005**, *127*, 14146–14147. (g) Moorthy, J. N.; Senapati, K.; Parida, K. N.; Jhulki, S.; Sooraj, K.; Nair, N. N., Twist Does a Twist to the Reactivity: Stoichiometric and Catalytic Oxidations with Twisted Tetramethyl-IBX, *J. Org. Chem.* **2011**, *76*, 9593–9601.
88. Uyanik, M.; Akakura, M.; Ishihara, K., 2-Iodoxybenzenesulfonic Acid As an Extremely Active Catalyst for the Selective Oxidation of Alcohols To Aldehydes, Ketones, Carboxylic Acids, and Enones With Oxone, *J. Am. Chem. Soc.* **2009**, *131*, 251–262.
89. (a) Tsuji, J.; Minami, I.; Shimizu, I., A novel Palladium-catalyzed Preparative Method of α,β -unsaturated Ketones and Aldehydes from Saturated Ketones and Aldehydes *via* their Silyl Enol Ethers, *Tetrahedron Lett.* **1983**, *24*, 5635–5638. (b) Ito, Y.; Hirao, T.; Saegusa, T., Synthesis of α,β -unsaturated Carbonyl Compounds by Palladium(II)-catalyzed Dehydrosilylation of Silyl Enol Ethers, *J. Org. Chem.* **1978**, *43*, 1011–1013. (c) Larock, R. C.; Hightower, T. R., A Simple, Effective, New, Palladium-Catalyzed Conversion of Enol Silanes to Enones and Enals, *Tetrahedron Lett.* **1995**, *36*, 2423–2426. (d) Hiraoka, S.; Harada, S.; Nishida, A., Catalytic Enantioselective Total Synthesis of (-)-Platyphyllide and its Structural Revision, *J. Org. Chem.* **2010**, *75*, 3871–3874.
90. (a) Krohn, K.; Riaz, M.; Flörke, U., Synthesis of xyloketal, Natural Products from the Mangrove Fungus *Xylaria* sp., *European J. Org. Chem.* **2004**, *6*, 1261–1270. (b) Müller, H.; Paul, M.; Hartmann, D.; Huch, V.; Blaesius, D.; Koeberle, A.; Werz, O.; Jauch, J., Total Synthesis of Myrtucommulone A. *Angew. Chemie - Int. Ed.* **2010**, *49*, 2045–2049. (c) Krawczyk, H.; Bodalski, R., C-Alkylation of Hydroxyarenes by Michael Reaction, *J. Chem. Soc. Perkin Trans. 1*, **2001**, 1559–1565.
91. Lin, Y.; Kao, J.; Chen, C., Catalytic Conjugate Additions of Carbon-Containing Nucleophiles by Amphoteric Vanadyl Triflate, *Org. Lett.* **2007**, *9*, 5195–5198.
92. (a) Armarego, W. L. F.; Chai, C. L. L., *Purification of Organic Chemicals*; 7th Ed. p. 376; Elsevier. Oxford. **2009**. (b) Sigma-Aldrich Catalog; Product Number: Z562440 ALDRICH; <http://www.sigmaaldrich.com/catalog/product/aldrich/z562440?lang=en®ion=US>, (accessed August 19, 2016).
93. (a) Emmons, W. D.; Ferris, A. F.; McLean, K. W.; Marks, I. G., Metathetical Reactions of Silver Salts in Solution. III The Synthesis of Nitrate Esters, *J. Am. Chem. Soc.* **1953**, *75*, 4078. (b) Bordwell, F. G.; Garbisch, E. W., Nitrations with Acetyl Nitrate. I. The Nature of the Nitrating Agent and the Mechanism of Reaction with Simple Alkenes, *J. Am. Chem. Soc.* **1960**, *82*, 3588–3598. (c) Gavril, A.; Andersen, L.; Skrydstrup, T., A Convenient and Simple Procedure for the Preparation of Nitrate Esters from Alcohols Employing $\text{LiNO}_3/(\text{CF}_3\text{CO})_2\text{O}$, *Tetrahedron Lett.* **2005**, *46*, 6205–6207. (d) Fedorov, B. S.; Eremenko, L. T., Brief Communications: Nitration of Alcohols by Nitryl Fluoride, *Russ. Chem. Bull.* **1997**, *46*,

- 1022–1023. (e) Boschan, R., The Reaction of Alkyl Chloroformates with Silver Nitrate. Evidence for Stereoselective Intramolecular Formation of Nitrate Esters, *J. Am. Chem. Soc.* **1959**, *81*, 3341–3346.
94. (a) Isoda, T.; Hayashi, K.; Tamai, S.; Kumagai, T.; Nagao, Y., Efficient Synthesis of Isothiocyanates Based on the Tandem Staudinger/Aza-Wittig Reactions and Mechanistic Consideration of the Tandem Reactions, *Chem. Pharm. Bull.* **2006**, *54*, 1616–1619. (b) Kulkarni, P. M.; Kulkarni, A. R.; Korde, A.; Tichkule, R. B.; Laprairie, R. B.; Denovan-Wright, E. M.; Zhou, H.; Janero, D. R.; Zvonok, N.; Makriyannis, A.; Cascio, M. G.; Pertwee, R. G.; Thakur, G. A., Novel Electrophilic and Photoaffinity Covalent Probes for Mapping the Cannabinoid 1 Receptor Allosteric Site(s), *J. Med. Chem.* **2016**, *59*, 44–60.
95. (a) Thakur, G. a.; Bajaj, S.; Paronis, C.; Peng, Y.; Bowman, A. L.; Barak, L. S.; Caron, M. G.; Parrish, D.; Deschamps, J. R.; Makriyannis, A., Novel Adamantyl Cannabinoids as CB1 Receptor Probes, *J. Med. Chem.* **2013**, *56*, 3904–3921.
96. (a) Periasamy, M.; Thirumalaikumar, M., Methods of Enhancement of Reactivity and Selectivity of Sodium Borohydride for Applications in Organic Synthesis, *J. Organomet. Chem.* **2000**, *609*, 137–151.
97. Compton, R. G., *Comprehensive Chemical Kinetics* Vol. 5: Decomposition and Isomerization of Organic Compounds. Edited by C.H. Bamford, C.F.H. Tipper. Elsevier, Jan 1, **1971**
98. (a) Still, W. C.; Mitra, A., A Highly Stereoselective Synthesis of Z-trisubstituted Olefins via [2,3]-Sigmatropic Rearrangement. Preference for a Pseudoaxially Substituted Transition State, *J. Am. Chem. Soc.* **1978**, *100*, 1927–1928. (b) S. C. de Andrade, V.; C. S. de Mattos, M., New Reagents and Synthetic Approaches to the Appel Reaction *Current Org. Synth.* **2015**, *12*, 309-327.
99. (a) Kürti, L.; Czakó, B., *Strategic application of Named Reaction in Organic Chemistry*. 1st ed.:Academic Press; **2005**.
- 100.(a) Kim, J. N.; Ryu, E. K., A Convenient Synthesis of Isothiocyanates from Nitrile Oxides *Tetrahedron Lett.* **1993**, *34*, 8283–8284. (b) Kim, J. N.; Jung, K. S.; Lee, H. J.; Son, J. S., A Facile One-Pot Preparation of Isothiocyanates from Aldoximes, *Tetrahedron Lett.* **1997**, *38*, 1597–1598.
- 101.(a) Bhat, V.; Allan, K. M.; Rawal, V. H., Total Synthesis of N-Methylwelwitindolinone D Isonitrile, *J. Am. Chem. Soc.* **2011**, *133*, 5798–5801.

- 102.(a) Augustine, J. K.; Bombrun, A.; Atta, R. N., A practical and cost-efficient, one-pot conversion of aldehydes into nitriles mediated by 'activated DMSO', *Synlett* **2011**, 2223–2227.
- 103.(a) Kumar, V.; Kaushik, M. P. *N*-tert-butyl-*N*-chlorocyanamide: A Novel and Versatile Reagent in Organic Synthesis, *Synlett* **2007**, 2937–2951. (b) Kumar, V.; Kaushik, M. P., *N*-tert-butyl-*N*-chlorocyanamide, *EROS Encyclopedia Reagents*. **2007**, 1, 4-5
104. Grundmann, C.; Grünanger, P., *The Nitrile Oxides*. **1971**, *Organische Chemie in Einzeldarstellungen*, 13, 1-242.
- 105.(a) Bigdeli, M. A.; Mahdavinia, G. H.; Jafari, S., The Synthesis of Benzhydroximoyl chloride and Nitrile Oxides Under Solvent Free Conditions, *J. Chem. Res.* **2007**, No. 1, 26–28. (b) Minakata, S.; Okumura, S.; Nagamachi, T.; Takeda, Y., Generation of Nitrile Oxides from Oximes Using tert-BuOI and Their Cycloaddition, *Org. Lett.* **2011**, 13, 2966–2969. (c) Yoshimura, A.; Middleton, K. R.; Todora, A. D.; Kastern, B. J.; Koski, S. R.; Maskae, A. V.; Zhdankin, V. V., Hypervalent Iodine Catalyzed Generation of Nitrile Oxides from Oximes and their Cycloaddition with Alkenes or Alkynes, *Org. Lett.* **2013**, 15, 4010–4013. (d) Yoshimura, A.; Zhu, C.; Middleton, K. R.; Todora, A. D.; Kastern, B. J.; Maskae, A. V.; Zhdankin, V. V., Hypoiodite Mediated Synthesis of Isoxazolines from Aldoximes and Alkenes using Catalytic KI and Oxone as the Terminal Oxidant, *Chem. Commun.* **2013**, 49, 4800–4802. (e) Singhal, A.; Parumala, S. K. R.; Sharma, A.; Peddinti, R. K., Hypervalent Iodine Mediated Synthesis of di- and tri-substituted Isoxazoles via [3+2] Cycloaddition of Nitrile Oxides, *Tetrahedron Lett.* **2016**, 57, 719–722.
- 106.(a) Ayedi, M. A.; Bigot, Y. Le; Ammar, H.; Abid, S.; Gharbi, R. El; Delmas, M., Synthesis of Primary Amines by one-pot Reductive Amination of Aldehydes, *Synth. Commun.* **2013**, 43, 2127–2133. (b) Milligan, B. Vulcanisation Accelerator–Activator Complexes, Part 1: Amine Complexes of Zinc and Cadmium Benzothiazole-2-thiolate, *J. Chem. Soc. A Inorg., Phys. Theor.* **1966**, 34–35.
- 107.Ho, T. C. *The Total Synthesis of C1'-Azacycloalkyl Hexahydrocannabinoids, The Total Synthesis of 3-Oxadadamantyl Hexahydrocannabinoids, The Total Synthesis of Bicyclic 3-Adamantyl Cannabinoids*. PhD. Thesis, The University of Hawaii at Manoa, HI, May **2014**.
- 108.(a) Abel-Magid, A. F.; Mehrman, S., A Review on the Use of Sodium Triacetoxyborohydride in the Reductive Amination of Ketones and Aldehydes, *J. Org. Proc. Res. Devel.* **2006**, 10, 971–1031. (b) Abdel-Magid, A. F.; Carson, K. G.; Harris, B. D.; Maryanoff, C. A.; Shah, R. D., Reductive Amination of Aldehydes and Ketones with Sodium Triacetoxyborohydride. Studies on Direct and Indirect Reductive Amination Procedures, *J. Org. Chem.* **1996**, 61, 3849–3862. (c) Bhattacharyya, S., Titanium(IV) Isopropoxide and Sodium Borohydride : A

Reagent of Choice for Reductive Amination, *Tetrahedron Lett.* **1994**, 35, 2401–2404. (d)
Hutchins, R. O.; Hutchins, M. K., Reduction of CdN to CHNH by Metal Hydrides. In
Comprehensive Organic Synthesis; Trost, B. N., Fleming, I., Eds. Vol. 8; Pergamon Press:
New York. **1991**.

109.(a) Abiraj, K.; Gowda, D. C., Zinc/ammonium Formate: A New Facile System for the Rapid
and Selective Reduction of Oximes to Amines, *J. Chem. Res.* **2003**, 6, 332-334 (b)
Steward, K.; Johnson, J., Catalytic Nucleophilic Glyoxylation of Aldehydes, *Org. Lett.* **2010**,
12, 2864-2867

110.(a) Cabral, S.; Hulin, B.; Kawai, M., Lithium Borohydride: A Reagent of Choice for the
Selective Reductive Amination of Cyclohexanones, *Tetrahedron Lett.* **2007**, 48, 7134–7136.

111. The translation on page 3 was executed by Elizabeth Ka'iulani Takamori with great haste
and professionalism. In the original english, the excerpt reads: I would first and foremost
like to acknowledge the lessons I have learned over the last decade while living on the
beautiful island of O'ahu: The culture of Hawai'i is, like many sovereign nations, a complex
one but is held together by its ideals. I have tried my best to incorporate the virtues of pono,
kuleana, and aloha into my daily life and I am so grateful for the many teachers who have
helped me understand how to do so; The spirit of the Hawaiian islands is one that holds love
above all else. Love for the land, love for your friend and family, and love for yourself. My
friends and family have given me a great deal of love during my time in graduate school and
I hope I have shared the full extent of mine with them - my sweetheart especially; The
Hawaiian rainbow is a persistent reminder to be inclusive with one another and that nothing
of true beauty can be accomplished alone. This virtue too i will carry with me on my next
journey. Aloha.